UNIVERSITY OF NATAL

DURBAN, SOUTH AFRICA

THE SOLID STATE REDUCTION OF CHROMITE

by

NICHOLAS FINCH DAWSON (B.Sc(Eng))

Submitted in partial fulfilment of the requirements for the degree of Doctor of Philosophy in the Department of Chemical Engineering, University of Natal, Durban.

Durban

September, 1989.

I wish to declare that this whole thesis, unless specifically indicated to the contrary in the text, is my own work.

N. F. DAWSON.

ABSTRACT

High carbon ferrochromium serves as the main chromium source for almost all chromium containing steel alloys. The traditional method for the production of high carbon ferrochromium via the reduction of chromite using coke in electric arc furnaces, draws its considerable energy requirement from electrical power.

The escalation in cost of electric power in South Africa has motivated research into alternative, fuel fired, reduction processes. One such process involves the partial solid state reduction of chromite in coal fired rotary kilns at temperatures between 1200 and 1400°C, prior to electric smelting. Such processes are currently operated on a commercial scale and result in considerable savings in electrical energy, despite slow reduction kinetics and low reaction extents.

A large amount of research conducted in the past, aimed at establishing the fundamentals of the reduction process, has not provided satisfactory answers to questions regarding the mechanism of reduction. It was therefore necessary to conduct further test work on the process to establish the mechanism and factors limiting the rate and extent of reduction.

Thermodynamic analysis of the reaction system indicates that at temperatures above 1050°C reduction of the ore will proceed, and should reach an extent of approximately 90%

reduction at 1200°C. Complete reduction should be achievable at approximately 1250°C. However experimental results indicate the persistence of a stable magnesiochromite spinel under normal reducing conditions even at 1400°C. This limits the degree of chromium reduction to approximately 65%.

Kinetic data from thermobalance studies and electron microscope examination of the reduction product showed independent reduction of iron and chromium. The rate of iron reduction was found to be relatively rapid and to go to completion, compared to that of chromium where the formation of a relatively inert picrochromite- spinel solid solution ($MgO(Cr,Al)_2O_3$) at the surface of the grain limited the rate and extent of reduction to approximately 65% in the case of LG6 chromite.

These findings suggested that the only way in which the kinetics of the process might be improved was through the addition of a component capable of disrupting the spinel layer at the surface of the chromite grain.

In this study, fluoride containing mixtures such as CaF_2 - NaF and fluorspar- feldspar- silica were successfully used to accelerate the reaction. Such mixtures are commercially interesting and highly effective even at low additions (4-10%).

The mechanism whereby such mixtures operate was shown to involve the dissolution of all the spinel components in the liquid flux phase. Following dissolution, rapid

recrystallization of spinel ($Mg.Al_2O_4$) occurs, simultaneous to the transport of Fe^{2+} and Cr^{3+} ions through the liquid to a site where reduction can take place. The main effect of this is to increase the rate and extent of chromium reduction to the point where virtual total reduction can be achieved in less than 90 min at temperatures as low as 1200°C.

Although the reduction kinetics in the presence of such solvent flux phases are still largely limited by the rate of solid state diffusion, the disruption of the surface enables faster overall diffusion rates to be achieved. Ultimately as the particle size and separation between oxide and reductant is increased, the rate of dissolution and transport through the flux phase become rate limiting.

ACKNOWLEDGEMENTS

I would like to express my sincere appreciation to Professor R.I. Edwards, M.F. Dawson, D.W. Wright and L.A. Andrews for their support, encouragement and helpful suggestions.

I would also like to thank the workshop and academic staff of the department of Chemical Engineering, and the staff of the E.M. unit for their assistance.

CONTENTS

LIST OF TABLES

LIST OF FIGURES

LIST OF PLATES

CHAPTER ONE : GENERAL INTRODUCTION

The highly desirable properties of chromium, chromium alloys and chromium chemicals place this element in a strategic position among the World's raw materials (ref 198,120) However, the refractory nature of chromium bearing ores (chromites) forces a high price to be paid in energy terms for its recovery from the ore.

The traditional method used in the production of chromium containing alloys involves smelting chromite together with coke and fluxes in large electric arc furnaces. The alloy produced, usually a medium to high carbon ferrochromium (3-8% carbon), is then used as the basic chromium containing component in further alloying and refining operations for stainless steel production.

Approximately 65% of all chromium ore mined is used for metallurgical purposes and is converted into one or other of the various grades of ferrochromium or into ferro-silico chrome.

The increase in demand for chromium containing alloys over the last three decades has resulted in a rapid increase in ferrochromium production throughout the World. Foremost in growth during the major expansionary period of 1960-1980 was the South African industry, with a growth rate of slightly over 20% per annum giving rise to a production of over 510 000 tons in 1978 (Minerals Bureau, 207).

The rapid growth of the local industry is seen as a reflection of two key factors. First was the ready availability of chrome ore and the then low cost of electrical power in South Africa. Second was the wide spread introduction of the Argon-Oxygen-Decarburization (A.O.D.) process which operates well on the high carbon charge chrome, the typical product from smelters operating on low chromium-to-iron ratio Transvaal ores.

The arc furnace smelting process for the production of high carbon ferrochromium draws its considerable energy requirement for both heating and reduction from electrical energy.

TABLE 1.1
Energy requirements for the production of 1t of liquid ferrochromium from chromite*

Process step requirement	Energy requirement (kW.h)	energy (% of total)
Heating of raw materials	1222	39.5
Reduction reactions		
Iron oxides	298	9.6
Cr_2O_3	1157	37.4
Fusion of metal	134	4.3
Fusion of slag	225	7.3
Super heating of metal	23	0.7
Superheating of slag	35	1.1
Total	3094	100.

* assuming a chromite composition of 45% Cr_2O_3, 25% FeO, an efficiency of 100% with alloy and slag tapped at 1700°C and slag-to-alloy ratio of 1,0
(data from Kubaschewski, 92)

The specific energy requirements as shown in table 1.1 reflect the large energy requirement for heating and reduction. To this may be added the various inefficiencies of the process, namely heat losses to the surroundings and loss of chromium to the slag. Each of these imposes a restriction on efficiency of approximately 90% and result in a final gross cost in terms of electrical energy of approximately 3,8 MWh/t of ferrochromium produced (ref. 136).

World wide trends in electrical energy costs over recent years have provided the motivation for research into the possibilities of replacing at least a portion of the electrical power with energy derived directly from natural fuel.

The implementation of such a fuel fired route would typically make use of cheaper grades of coal, where locally available, as both the source of heat and reductant. Such a process could conceivably save most of the energy used for heating and reduction, amounting to some 80% of the thermodynamic energy requirement.

Though this apparent energy saving represents only a replacement of electrical energy with fuel based energy, it does represent a significant saving in production cost for the manufacturer. In real terms this saving stems from both the cheapness of solid fuel energy compared to electrical energy, as well as the potential increase in

alloy production per unit of installed electrical capacity.

Partial carbothermic reduction prior to arc furnace smelting has been successfully implemented on an industrial scale achieving major savings in electrical energy and improved chromium recovery to the alloy. Such processes involve the partial solid state reduction of chromite- carbon mixtures in coal or off-gas fired rotary kilns at temperatures between 1200 and 1450°C (e.g. Nippon Kokkan N.K.K. and locally at Consolidated Metallurgical Industries, Lydenburg ref.210,136).

Such processes are characterised by slow and incomplete pre-reduction, typically achieving only between 60 and 70% combined iron and chromium metallization over periods in excess of two hours.

These limits have prompted the research detailed in this work, aimed at answering some fundamental questions on the behaviour of chromite ore undergoing carbonaceous reduction between 1100 and 1300°C. These questions include:

a) What are the rate limiting steps at various stages during the reduction reaction?

b) What is the reason for limited chromium metallization?

c) How can the kinetics of reduction and extent of metallization be improved and what mechanisms are operative in the promoted reduction reaction?

d) How could such a promoted pre-reduction process best be implemented to derive maximum benefit?

It is believed that an improved process for the production of ferro-chromium, though of general benefit to all ferro-chromium producers, would be of particular benefit to the South African industry. It is hoped that the benefits stemming from improved efficiency and increased competitiveness with overseas ferrochromium manufacturers would stimulate local industry, particularly regarding stainless steel production, and help the industry attain a more dominant position in the world stainless steel export market.

CHAPTER TWO: LITERATURE SURVEY

2.1 CHROMITE ORE TREATMENT

2.1.1 INTRODUCTION

Methods employed in the treatment of chromites may be divided into two categories namely:

a) upgrading, where the aim is to increase the chromium to iron ratio, and

b) recovery of the chromium content of the ore either in alloy form or as a soluble chemical compound.

Prior to the wide spread introduction of the Argon-Oxygen- Decarburization (A.O.D.) process enabling the treatment of high carbon ferrochromium with low chomium-to-iron ratios, considerable effort was spent in attempts aimed at upgrading the low grade chromite ores commonly available (ref. 70,76,193). The aim of this work was to preferentially reduce and remove most of the iron content of the chromite, leaving a chromium enriched spinel with a chromium to iron ratio of approximately 6:1. However the success of the A.O.D. process has obviated the need for chromite upgrading.

Considering the recovery of the chromium content of the ore, two processes are currently in commercial use:

a) Carbonaceous reduction of chromite to form a high carbon ferro-chromium alloy (ref. 149,12c,60,115b).

b) Oxidative roasting of chromite with sodium carbonate for the production of chromium chemicals (ref. 53,47,31).

To date, these routes have been considered as being mutually exclusive in terms of application for the recovery of chromium (ref. 40). At present my interest lies entirely with reduction and the production of

ferrochromium.

It would appear from the general concepts involved in studies on alternative routes to the standard carbonaceous reduction of chromite (ref 9,23,34,49, 106,125,143,189,172 76,79,80, 95,110,112,124, 126,134, 150,165b), that carbonaceous reduction offers the only cost effective means for the efficient extraction of the chromium content of the chromite. This is particularly true for South African ores with low chromium to iron ratios.

Standard submerged arc smelting for the production of ferrochromium places several limitations on the operational efficiency and product quality. Most research conducted in the past has concentrated on improving the productivity and cost of production of ferrochromium, including arc furnace design and operation (Stąnko, 165a, 131,132,133,162,138,187,195b,203,85).

However the increasing importance of the electrical energy cost component in the manufacture of ferrochromium has resulted in attention being focused on improving the electrical energy efficiency and the cost advantages of chromite fines treatment and pre-reduction.

2.1.2 CURRENT PRE-REDUCTION PRACTICE

Pre-reduction typically involves the treatment of pelletized, composite charges of fine chromite and reductant, in rotary kilns at temperatures above 1300°C prior to electric arc smelting. The operating experiences at the Showa Denko plant, Japan (Negasawa, 130 and Ichikawa, 84), and the local experience at Consolidated Metallurgical Industries, Lydenburg (Sciaroni, 210), confirm the benefits of pre-reduction.

The advantages of such operations include:

a) A decrease in the amount of electrical energy required for smelting, providing a charge that is more easily controlled.

b) Increasing chromium recovery to the alloy.

c) The ability to use cheaper and more readily available reductants.

d) Improving the quality of alloy produced.

e) The inclusion of pelletisation as a unit operation enables the treatment of friable ores, otherwise unsuitable for normal arc furnace operation.

A typical example is the pre-reduction process developed by Showa Denko K.K. (S.D.K.), called the Solid Reduction of Chromite or S.R.C. system (Otani and Ichikawa, 136). This process involves pulverising a low grade friable chromite ore together with a low grade reductant to less than 100 micron and pelletising the mixture prior to drying and firing in a rotary kiln, and subsequent charging into an electric arc furnace.

Approximately 60% of the total chromium plus iron oxides in the ore are reduced in the kiln prior to smelting. This reduces by half the energy requirement for smelting the ore.

Ichikawa (84) states that a key ingredient in the pellet is a flux consisting of 20-45% SiO_2 and one or more of MgO, Al_2O_3 and CaO, according to the formula : $R = (1,0MgO + 0,72CaO)/1,0Al_2O_3$ where R is between 1,3 and 2,0.

The flux is applied so as to form a film coating of a specific thickness, ideally between 1,0 and 3,0 mm. The flux is added in two stages - once before roasting and

again before smelting.

The flux aids in pellet mechanical strength and accelerates the reduction reaction between iron and chromium oxides and carbon. The second coating apparently acts to reduce charge conductivity in the arc furnace.

It is claimed that during roasting the flux forms a solid solution of forsterite ($2MgO.SiO_2$) and spinel ($MgO.Al_2O_3$). Roasting at temperatures between 1350°C-1450°C in an oxidising atmosphere (fuel fired kiln, with 150-200% stoichiometric oxygen requirement) the CO produced during the reaction is immediately oxidised, and the coated flux components penetrate into the inner portions of the pellet and harden the pellet (Ichikawa,84). The reduction reaction proceeds through the presence of a reducing atmosphere that is maintained in the immediate vicinity of the chromite particles within the sintered shell of the pellet.

The apparent isolation of the pellet interior from the external atmosphere, as a result of the presence of the outer flux layer, is of interest since this lends added flexibility to the reduction operation and may enable reasonable thermal efficiency to be attained. (Though not mentioned in this work, the proximity and size of the carbon particle must play an important role in the rate of reduction of chrome and iron species in the pellet interior).

However, problems with this process include the relatively low throughput and high capital investment and operating costs, which place limitations on the profitability of such a kiln operation, particularly for small tonnages, below 60 000 tons per annum.

2.1.3 TRENDS IN THE PROCESSING OF CHROMITE

The concerted efforts being made both in this country and overseas to develop more direct and efficient routes to stainless steel may be broadly classified in two groups both designed for treating ore fines; namely:

(a) plasma technology (Barcza et. al.,16, 111,121, 209, 195a), and

(b) coal based smelting and high temperature kiln pre-reduction operations such as the KRUPP kiln and COIN type process operating at temperatures in excess of 1550°C and the KR process (Golde, 66,97, 99,190).

In the plasma field, a considerable amount of research work has been performed in recent years both locally at the Council for Mineral Technology (Mintek) and at numerous overseas establishments (notably in Sweden and Belgium). This work has established the technical feasibility of plasma smelting for ferro-chromium production. At present, the open bath and shaft furnace systems are both operated commercially upto the 20MVA scale (Slatter, 209) to accomplish metallurgical smelting reactions, including iron making and the smelting of ferro-alloys.

In the typical open bath transferred arc plasma system, ore and reductant are fed at a controlled rate so as to form an ideal single layer of solid material on top of the liquid slag surface. The high temperature plasma source acts to create a high temperature environment into which the chromite and carbon are fed and in which most of the reaction takes place.

The large extent to which the fundamental mechanism

of dissolution in the slag and reduction of the dissolved Cr^{3+} and Fe^{2+} species are dependant on local temperature, necessitates sophisticated control to maintain a well directed stable d.c. arc. In addition a complex material feeding system is required to ensure smooth operating conditions, with material feed rate accurately matched to power input.

The results obtained from operating plasma facilities indicate that this route is technically feasible, and can be used for the treatment of chromite fines with low grade reductant as is practiced at Middelburg Steel and Alloys (Slatter et al. 209).

However, drawbacks inherent in the use of plasma technology tend to limit the wide-spread introduction of this type of operation. Among the disadvantages are the requirement for sophisticated control, and plant availability compared to the conventional submerged arc process. In addition, the large electrical energy requirement places it at similar cost disadvantages to existing sub-arc furnaces.

With regard to high temperature kiln operation, the Krupp process, though not yet in commercial use, is designed principally for the pre-reduction of chromite fines using large quantities of low grade coal as reductant and energy source.

High levels of pre-reduction efficiency are claimed for this process, with degrees of metallization of between 80 and 90% (Krupp GmbH.,97,98, 200).

In this process the chromite is mixed with well in excess of the stoichiometric carbon requirement (approx. 400% excess) and usually with the addition of a silica based flux capable of melting at the reaction

temperature. This mixture (in unpelletised form) is then fed into a rotary kiln operating at temperatures in excess of 1550°C. Average residence time in the kiln is approximately 8 hours. The final product is in the form of a well reduced mixture of metal blebs (.1-5mm diameter) in a silica-spinel matrix.

The highly metallized product may then be fed from the kiln into a modified arc furnace where the final melting and slag- metal separation is performed. The original patent includes an elaborate means of physically separating the char, slag and metal components from the kiln prior to final smelting. This operation appears to be impractical and energy inefficient.

Recent developments in steel production, such as the Kohle Reduktion Prozess (or K.R. process, Golde,66), and the Coal Oxygen Injection (COIN) process aim at the use of various grades of coal, combusted with limited quantities of oxygen as the source of reductant and thermal energy for reduction and melting.

With certain modifications this type of technology could find application in the field of ferrochrome production. Problems with the adaptation of these processes are the greatly increased enthalpy requirement for chromite reduction as well as the large fraction of non-reducible oxides present after reduction. This necessitates a large well directed energy input to ensure stable operaton.

In general it may be said that the application of coal based reduction- melting technology to ferrochromium or direct stainless steel manufacture is still in the infancy stage. A great deal of development

is required before any fuel fired process for ferrochrome production becomes industrially practical. In particular, it appears essential to find a means of increasing the reduction rate of chromite ore at temperatures compatible with existing equipment (1200-1400°C).

However, before any attempt can be made on improving the pre-reduction operation, a detailed understanding must be gained of the nature of the ore itself and the reduction reactions that it undergoes.

Of specific interest in this investigation are the chromites of the Bushveld Igneous Complex which represent a major portion of the world's chromite reserves, and which tend to have a rather low chromium-to- iron ratio of approximately 1,5:1 (a comparison of the various world chromite deposits and their respective relevance in terms of world production is given by Nafziger, 124a).

2.2 THE NATURE OF CHROMITES OF THE BUSHVELD IGNEOUS COMPLEX

2.2.1 OCCURRENCE

The bushveld complex consists essentially of a mafic phase intruded above the rocks of the Pretoria group of the Transvaal super-group.

The mafic rocks cooled and solidified very slowly, enabling a high degree of magmatic differentiation, and the mafic phase of the complex assuming a distinct layered or stratiform structure with certain clearly marked zones of differing rock.

In such stratiform igneous intrusions, the chromite mineral first separated out as a liquid layer,

immiscible with the adjacent melt, and by virtue of its higher specific gravity formed into layers of droplets, separate from the parent magma, and solidified as well defined seams.

Chromites of the Bushveld Igneous Complex occur mainly in the Critical Zone, immediately below the Merensky Reef, in sheet-like bodies parallel to the igneous layering. Mostly 16-20 seams are present and contain varying amounts of other minerals, mainly pyroxenes and plagioclase. An indication of the range of compositions for chromites of the Bushveld Igneous Complex and those used in various investigations is given in appendix 1 (tables A1.1 and A1.2).

Numerous detailed works on the geology of the chromites of the Bushveld Igneous Complex have been done in terms of occurrence, composition and mineralogy (de Waal 45, Ramdohr 144). Two features evident from these works are, firstly the small regional variation in the composition of particular chromite seams from deposit to deposit and even within the same deposit (a characteristic of such stratiform deposits), and secondly the variability in the physical properties of the different chromites, with particular regard to the friability of the ore and its behaviour in arc furnaces.

It would also appear that by solidifying from a layer of droplets under no great pressure the chromite has crystallized into somewhat rounded crystals that do not fully interlock with each other, and with an appreciable amount of gangue material in the interstices. Thus these chromites are generally friable and fine grained, and such lumpy ore as is obtained is

still weak and brittle compared with the hard lumpy ore obtained from podiform deposits.

2.2.2 MICROSTRUCTURE

Chromite is a complex, mixed-crystal system, expressable as $(Fe,Mg)(Cr,Al,Fe)_2O_4$, with small quantities of Mn,Ti,V and Zn included in the crystal structure, arranged in a face centred cubic spinel lattice matrix (41, 114,144), see figure 2.1.

The spinels, with end members $MgAl_2O_4$, $FeCr_2O_4$ $MgCr_2O_4$ and $FeAl_2O_4$, occur in two structural forms, namely normal and inverse, which differ in the distribution of cation between tetrahedral,A, and octahedral,B, positions. The general formulae for which are:

normal : 8 R^{2+} in A, 16 R^{3+} in B: e.g.

$MgAl_2O_4$; $FeAl_2O_4$; $MgCr_2O_4$; $FeCr_2O_4$

inverse: 8 R3+ in A, 8R2+ and 8R3+ in B: e.g.

$MgFe_2O_4$; $FeFe_2O_4$

In such structures the Fe2+ cation has the ability to exist in both octahedral and tetrahedral lattice sites, the inverse spinel being proof of this.

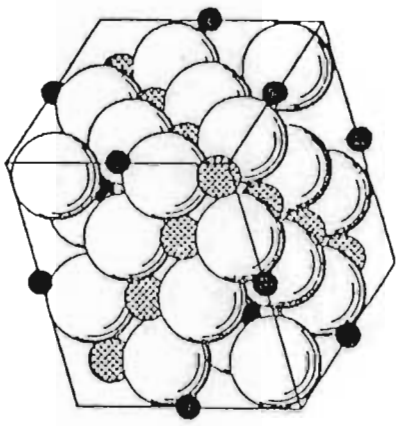

FIGURE 2.1 Perspective view of the structure of spinel. Large, spheres represent oxygen, small black spheres represent four-fold coordination positions (A) and cross-hatched spheres six-fold positions (B)

Ref Deer Howie and Zussman(41)

2.3 REDUCTION BEHAVIOUR OF CHROMITE ORES

2.3.1 BACKGROUND

The industrial importance of ferro-chromium has provided the motivation for numerous studies into the mechanism and kinetics of reduction.

Some general observations are common in all experimental work on chromite reduction with carbon at temperatures between 1100 and 1400°C, namely:

a) Metallic phases occur only at the grain exterior and in micro-cracks extending in towards the grain centre on large grains, and never interstitially located throughout the grain (Rankin , 154; Searle and Finn, 160 and Treffner, 184).

b) The scarcely altered appearance and dimensions of the chromite grains, even after considerable reduction has taken place, indicate that no breakup of the grain occurs, but merely a recrystallization of the various components within the chromite grain (Lisnyak et al.,105).

c) A limited extent of reduction is achieved, even at temperatures as high as 1400°C, where the reduction reaction would appear to halt at an extent of approximately 80% overall reduction for an LG6 type ore, as shown in figure 2.2 (Algie and Finn, 3).

It has been found that chromite composition, reductant type and the presence of carbon monoxide and hydrogen, as well as the obvious parameters of ore particle size and temperature exert an influence on reaction kinetics. Brief consideration is given to the effect of ore composition and reducing agent on the reaction in order to gain a better understanding of the reduction reaction.

2.3.2 THE EFFECTS OF ORE COMPOSITION ON THE REDUCTION RATE

The marked effect that ore composition has on the reaction rate is typified by the results of Barnes and Finn (12b) on relatively similar ores as shown in figures 2.2 and 2.3. Similar results have been observed by numerous other workers (77,45c,3, 12a,116).

Hunter and Paulson (77) postulated that the ease of reducibility and hence reduction kinetics were related to such parameters as the Fe^{2+}/Fe^{3+} ratio, the Cr/Fe ratio and Al_2O_3 content. Subsequent work has shown that while these parameters do have an influence, they can not be used as the sole basis for a reduction model.

The absence of any accurate mechanistic model describing the effect of ore composition on the reduction reaction, prompted the analysis performed in this work, based on results available in the literature.

Various published results (22,24) showed an interesting correlation over a wide composition and temperature range (1200-1450°C), between the quantity of MgO in the spinel in excess to that required for spinel formation with Al_2O_3 (i.e. formation of $MgAl_2O_4$), and the fraction of Cr_2O_3 remaining in the spinel after reduction. The correlation between the Cr_2O_3 content of the residual spinel and the formation of $MgCr_2O_4$ is shown in table 2.1.

This correlation suggests that the limited chromium recovery from the ore is associated with the formation of a stable picrochromite- spinel solid solution ($MgCr_2O_4$,$MgAl_2O_4$).

Further indication of the implications associated with the formation of the magnesiochromite- spinel solid solution is given by the increase in apparent activation energy for the

	CP	CW	Winterveld
Chemical (constituents)			
SiO_2, %	3,08	3,31	4,7
Al_2O_3, %	17,2	15,6	14,1
Cr_2O_3, %	42,5	42,15	42,9
Fe_2O_3, %	9,61	10,65	7,9
MgO, %	10,3	10,4	12,4
FeO, %	17,9	17,8	16,8
CaO, %	0,38	0,19	0,5

FIGURE 2.3

Comparison of reduction rates for two different ores of similar composition.

ref. Barnes and Finn(10)

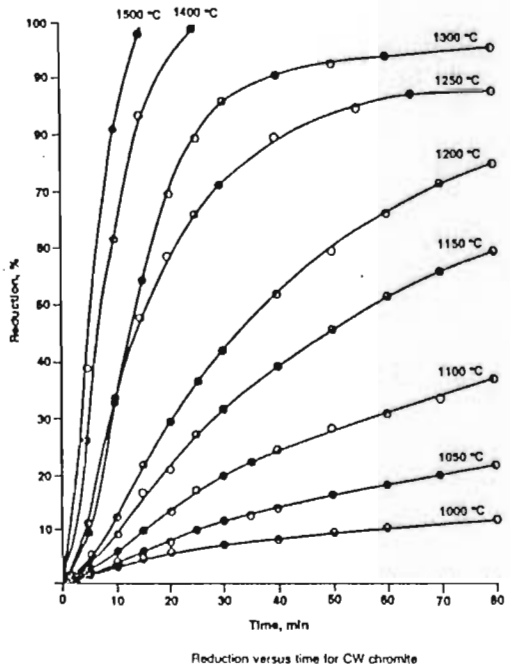

Reduction versus time for CW chromite

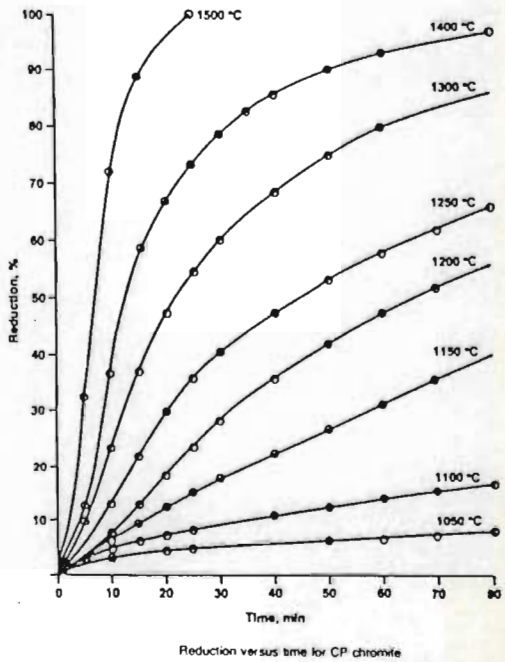

Reduction versus time for CP chromite

FIGURE 2.3

FIGURE 2.2

THE EXISTENCE OF A REACTION LIMIT IN THE REDUCTION OF CHROMITE(LG6)

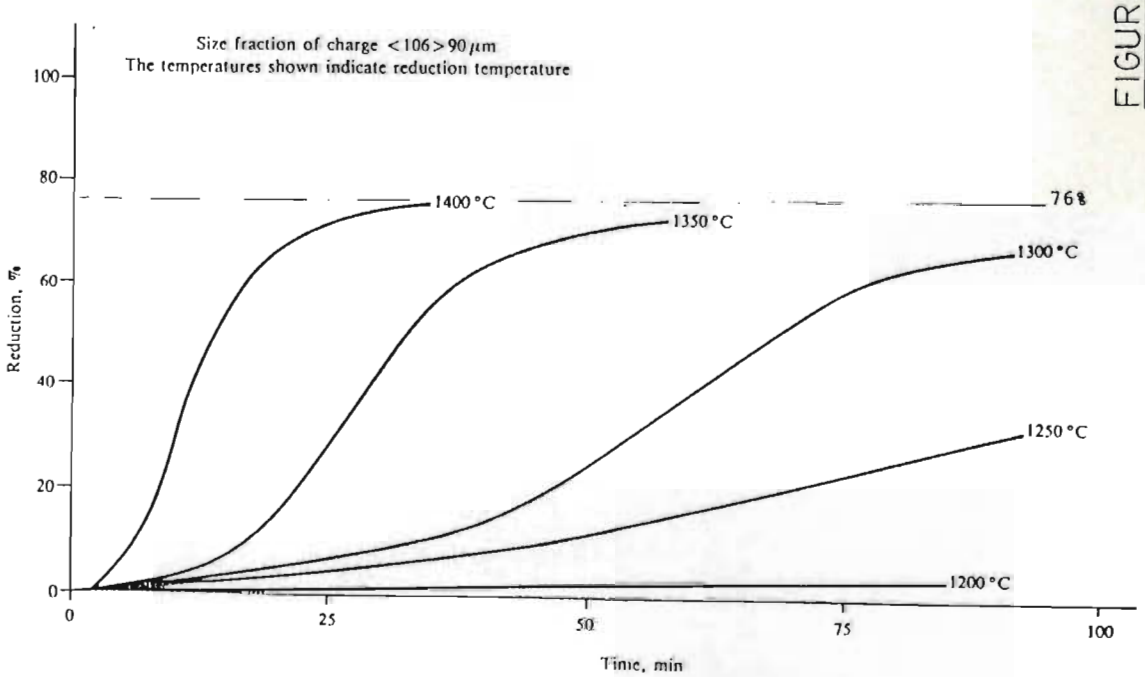

FIGURE 2.2

ref Algie (3)

TABLE 2.1 Comparison of ore and final product composition.

Component	DAVIS	SEIAD	ANTELOPE	BEN BOW	UG2	CHROME SAND
Al_2O_3	18,0	4,8	26,0	18,2	17,81	14,20
MgO	9,40	10,3	13,0	12,9	9,87	10,10
Fe_2O_3	1)	1)	1)		10,79	8,34
FeO	27,4	23,6	24,4	24,0	21,0	18,46
Cr_2O_3	37,9	52,8	36	41,3	41,3	46,92
SiO_2	1,9	1,97	6	1,6	1,24	0,84
Cr/Fe	1,22	1,97	1,3	1,5	1,183	1,59
Al_2O_3/MgO	1,91	0,47	2,0	1,41	1,80	1,41
Estimated residual Fract of Cr_2O_3 (%)	22,72	60,0	28,50	52,08	25,83	36,05
Cr_2O_3 fract. found in residue	2) 23,91	2) 67,72	3) 25,6	4) 41,0	5) 26	6) 36,18

Component	DAVIS	SEIAD	ANTELOPE	BEN BOW	UG2	CHROME SAND
REF	BOERIKE 22	BOERIKE 22	BOERIKE 22	BOERIKE 22	SEARLE & FINN 160	CHROED DATA. THIS WORK
COMMENTS	1) total Fe as FeO 2) Max. recovery shown at T = 1300°C		3) Recovery after reduction at T = 1300°C Max. recov 21% Cr_2O_3 residual	4) Max recovery at T = 1400°C	5) Recov. estimated f m results at T = 1400°C	6) ave recovery at temps upto 1200°C

TABLE 2.2

ANALYSIS OF RESULTS PUBLISHED BY BARCZA et al (14)

SAMPLE	F 524	F 596	F 604	F 652
FeO	12,0	24,40	6,90	8,3
total Fe as FeO	4,38	52,09	20,15	13,67
Cr_2O_3	44,87	15,24	46,22	48,76
Al_2O_3	13,7	6,20	8,80	9,40
MgO	11,80	3,43	11,82	17,64
SiO_2	2,55	2,92	3,77	3,28
gangue	4,40	-	8,10	7,0
Al_2O_3/MgO	1,16	1,81	0,74	0,53
est. % Cr_2O_3 res.	53,64	24,22	68,04	> 80 (1)
E KJ/mol	185,80	106,6	241,3	260,6
A $time^{-1}$	6,50	3,30	12,0	23,3

(1) The balance on this particular spinel requires more 3+ cationic species than can be supplied by the Chrome and alumina contents. Accordingly the value of Cr_2O_3 estimated in the residue is put at more than 80%: the reduction of the balance of the chromium being a result of a kinetic imbalance between the rate of reduction and the formation of $MgCr_2O_4$

FIGURE 2.4(a)

The effect that the formation of magnesiochromite in the residual spinel has on the reducibility of a chromite ore (expressed here in terms of the apparent activation energy required for reduction to take place.)
(Data originally from Barcza,14)

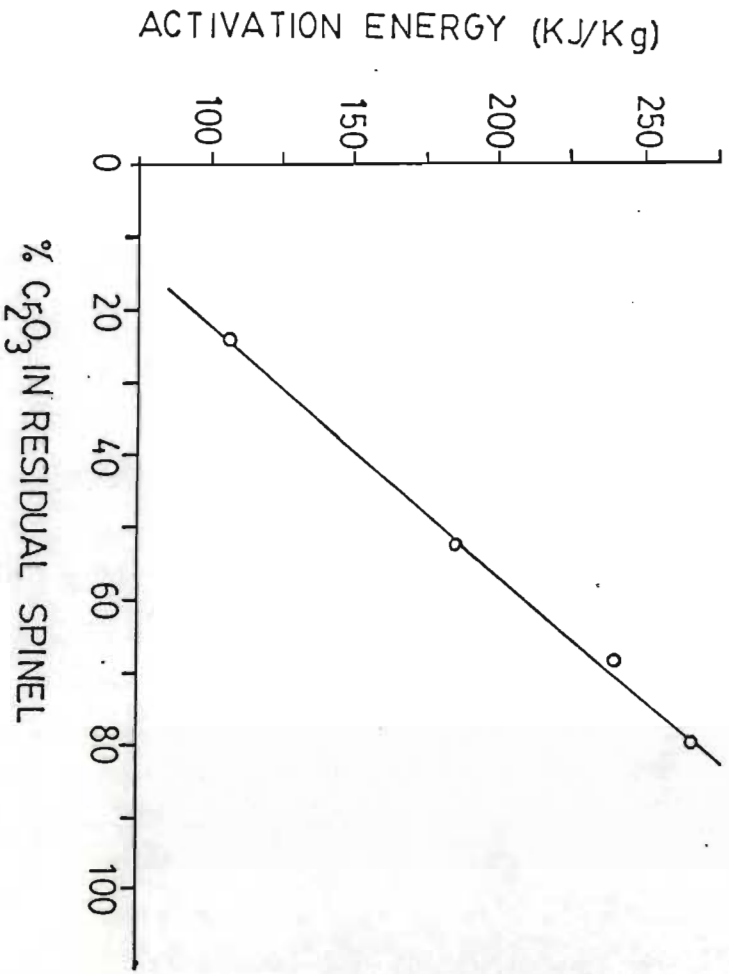

FIGURE 2.4(b)

Reduction curves for LG6 chromite with similarly sized reductant at 1300°C.
Indication of the effect of particle size on the reduction ceiling suggests the possibility that kinetic factors play a role in determining this ceiling (data from Algie and Finn,3).

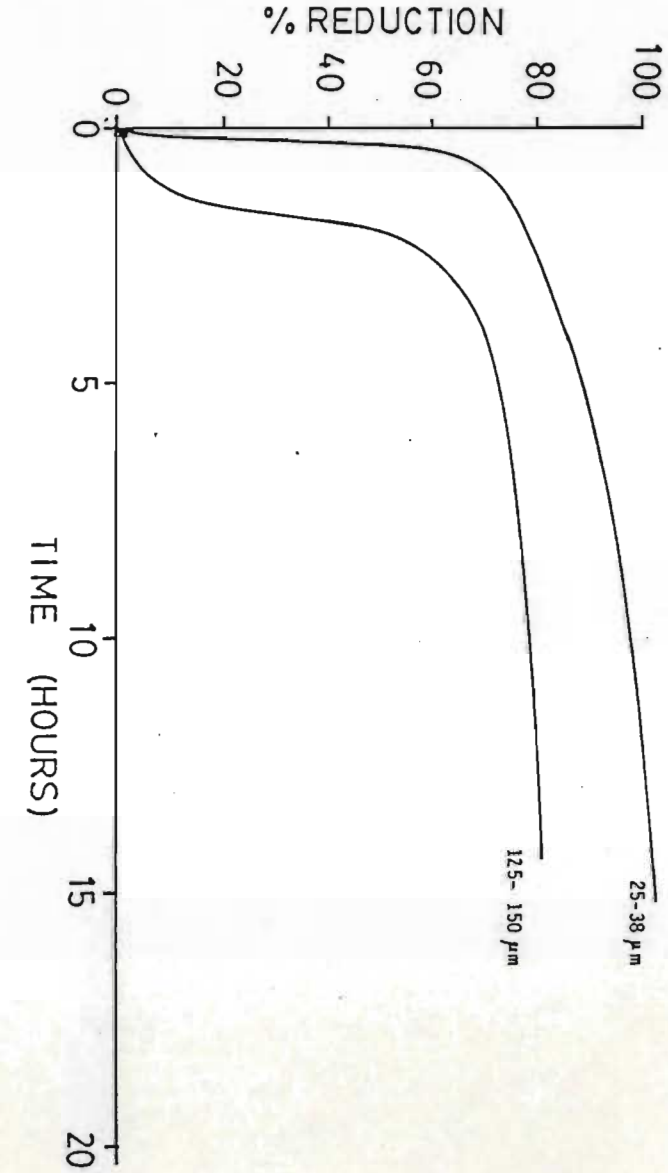

reduction of such ores as shown in table 2.2 and figure 2.4(a) (Barcza et al.,14). The increase in apparent activation energy with increasing MgO and Cr_2O_3 content, corresponding to the formation of $MgCr_2O_4$, supports the possibility that a stable phase, most likely a magnesiochromite- spinel solid solution, is being formed during the reduction reaction. The formation of this phase would tend to inhibit chromium reduction both because of its thermodynamic stability and possibly through the formation of a refractory layer on the surface of the grain which would act to retard the transport of chromium and iron species and hence reduce reaction kinetics.

It is interesting to note the influence of particle size on the reduction limit at 1300°C as shown in figure 2.4(b), taken from the results of Algie and Finn (3). This result suggests that the apparent reaction ceiling commonly encountered in experimental work has a kinetic origin rather than being purely the result of a thermodynamic limit.

Such a kinetic limit has considerable implications since it suggests that an improvement in reaction kinetics could lead to an improvement in overall extent of reaction. These aspects will be considered in detail in the following chapters.

When comparing the iron-chromium metallization curves obtained by various workers (McRae,115a,115b,Algie,3; Boerike,22,23) on different ores over a range of temperatures as shown in figure 2.5, it becomes evident that ore composition has a significant effect on the individual rates of iron and chromium reduction and hence on the overall rate of reduction of the ore.

This aspect has not been considered in previous works, largely because of the uncertainty of the relationship between ore composition and reduction kinetics. Thus any model of the reduction kinetics should include the relationship between ore composition and the respective iron and chromium reduction rates.

FIGURE 2.5

The influence of ore composition on the iron- chromium metallization curve (see table 2.1 for details on ore composition).

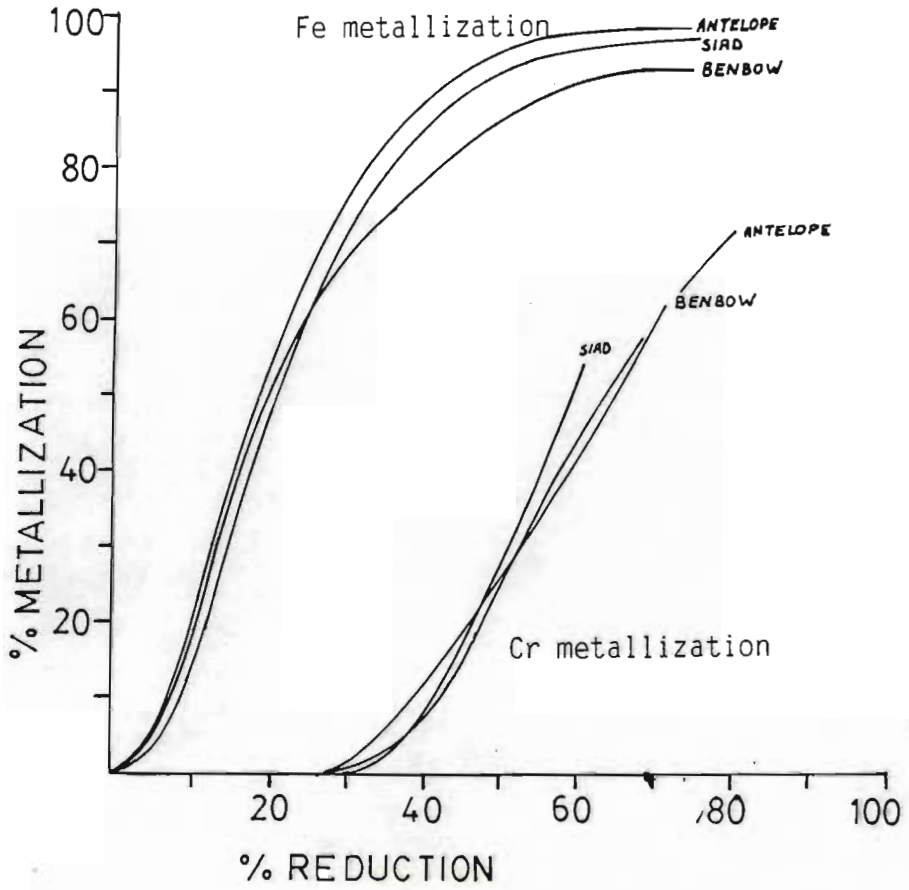

(data from Boerike, 22)

FIGURE 2.6

COMPARISON OF REDUCTION RATES OF HEMATITE ILMENITE AND CHROMITE

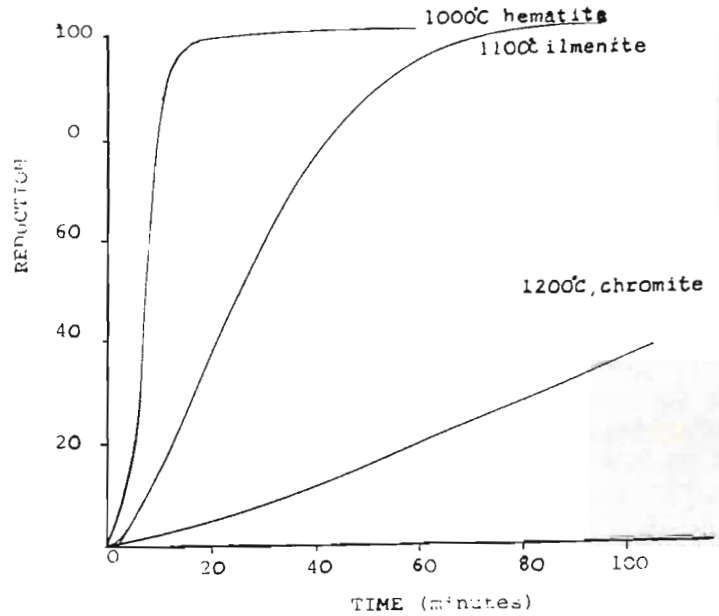

ref 43,175,11

FIGURE 2.6

2.3.3 THE EFFECT OF REDUCING AGENTS ON THE REDUCTION REACTION

Early work by Boerike and Bangert (22) showed that the quantity of reductant has an effect on reduction extent and kinetics. Increasing the quantity of reductant in excess of the stoichiometric requirement was found to increase the quantity of acid soluble material after a similar reduction period. Further, it was found that reducing the carbon addition only affects the metallization curve when the reductant addition is reduced to below that required for reduction of the iron and chromium alone, and not the formation of carbides. This supports the findings of Barcza (14) that carbides and carbon dissolved in the metal phase can act as the reductant, though reduction kinetics were slow.

Carbon grain size was also found to have an effect though much smaller than that of chromite particle size. Results showed an increased reaction rate with decreasing carbon particle size.

Investigation into the effect of reductant type (Dewar 46, and Koursaris91) revealed no differences in the mode of reduction with different reducing agents, though distinct differences in reduction rate and extent were noticed with different reducing agents over the same period of time at the same temperature. These differences were attributed to variations in fixed carbon content and reactivity of the reducing agent towards carbon dioxide.

Fremont-Lamourant et. al. (56) investigated the reactivity of carbons with respect to solid oxides (Cr_2O_3 in particular) and found significant variation in kinetics resulting from variations in carbon reactivity. In all cases the most micro-porous carbons were found to be the most reactive and gave rise to the fastest reduction rates.These results suggest an

interaction between the surface of the reductant and the oxide, a proximity effect that has an influence on reaction kinetics though it is not necessarily rate determining in itself.

Algie and Finn's results (3) indicated the beneficial effect of carbon addition in excess of the stoichiometric requirement. They postulated that reaction rates could be accelerated at extents below 50% metallization by the inclusion of volatile compounds in the charge which would act to increase the initial concentration of the reducing agents at the surface of the chromite grain.

The possible beneficial effect of volatiles present in the reductant is supported by the claims made in a recent patent filed by the Kawasaki Corporation (99). In the patent, claims are made that C3-C8 hydrocarbons may be effectively used at temperatures as low as 800°C for the reduction of chromite. However, no comment is offered on the action of the coal volatiles, and will be considered below.

Barcza (15) investigated the role of carbon monoxide (CO) as a reducing agent for chromite, and concluded that carbon monoxide was ineffective on its own as a reductant at temperatures of 1200-1300°C. This finding was supported by Ossin (131).

Subsequently, Rankine (156) showed that in theory CO could be used as a reductant at temperatures above 1200°C, though very high CO/CO2 ratios were required for reduction to proceed (over 250 at 1100°C). Experiments (156) showed that reduction with carbon monoxide as reductant could proceed at temperatures of 1200°C and above, showing the same sequence of reduction as with carbon.

The reducing action of CO on chromite in the presence of carbon at temperatures in the region of 1300°C is supported by the work of Barnes and Finn (12a), who postulate a mathematical model with CO as the major reducing species. This arises as a

result of the limited contact between carbon and chromite particles, implying that only a limited extent of reduction could take place through direct contact. It is postulated that this however is sufficient to produce a CO envelope around the chromite particle which continues the reduction reaction.

The very high CO/CO_2 ratios required to support the reduction of chromite mean that any minor CO_2 contamination in the gas stream could shift the CO/CO_2 ratio to a point where it was no longer thermodynamically possible for reduction to occur. The situation is made worse by the geometry of the reaction system i.e. a packed bed of fine powder, where removal of the CO_2 produced is hindered and can result in an accumulation of this species and a cessation of the reduction reaction (Rao, 151). It is believed that minor variations in the level of CO_2 in the reducing atmosphere is the major reason for the apparent contradiction of these results.

The sensitivity to the PCO/PCO_2 ratio increases as temperature is decreased and the difference between the PCO/PCO_2 ratio required for reduction and the limit set by equilibrium with solid carbon narrows. However, the presence of carbon in intimate association with the oxide will result in reduction of the CO_2 reaction product and the maintenance of highly reducing conditions at the surface of the oxide particle (ref 145a, 145b)

Considering the effect of other gaseous reducing agents, Read (150) Bibb (20) , and Ossin (132), showed the catalytic effect of hydrogen on the reduction of chromites in the presence of carbon. However, hydrogen alone was not found to be a good reductant, requiring exceptionally high H_2/H_2O ratios for the reduction reaction to occur and thus suffers from the same problems as considered with carbon monoxide. Reduction was found to occur 100-150°C lower in hydrogen containing atmospheres than in either inert or CO containing atmospheres.

The introduction of carbon monoxide together with hydrogen was found to inhibit the beneficial effect of hydrogen (132, 150). This effect is expected as a result of the equilibrium of the water gas reaction, where the addition of CO would limit the removal of H_2O from the atmosphere surrounding the particle and hence inhibit the hydrogen promoted reduction reaction.

Algie and Finn (3) showed that apart from kinetic enhancement achievable through the use of hydrogen, an amount of metallic product could be found located in microcracks extending into the chromite particle. The appearance of metal within the grain represents a significant difference to that encountered with a solid carbonaceous reductant, where metallization occurs only at the grain exterior. This indicates a shift in reaction mechanism, though the limit in final extent of reduction achieved (approximately 83% for the UG2 ore used) was still encountered. It is likely that the ability of the hydrogen molecule to migrate through the spinel and penetrate fine cracks in the lattice is responsible for the enhanced reaction kinetics and the appearance of metal extending into the grain.

In the Kawasaki patent application (99), claims are made that propane and butane are particularly effective in promoting the reduction reaction. Similar results were published by Quayyam (143). The Kawasaki patent suggested that reduction would occur at temperatures as low as 800^{o}C, and a process was proposed for the reduction of chromite in a fluidised bed using gas rich in C3 and C4 hydrocarbons as the reductant. No disclosure was made regarding the mechanism of reduction by the hydrocarbons. A likely possibility is that the hydrocarbons crack at the reduction temperature, depositing a layer of highly reactive carbon on the surface of the chromite particle and thus in intimate association with the oxide, which then acts as the reductant.

In summary it may be concluded that within a limited temperature range (1100- 1300°C) the reduction reaction appears to be relatively sensitive to the nature and proximity of the solid reducing agent. This in turn will influence the sensitivity of the reaction to the external atmosphere. In cases where excess fine reductant is maintained in close proximity to the surface, the external atmosphere is not expected to show a significant effect on the reduction reaction.

2.3.4 PROMOTION OF THE REDUCTION REACTION

Having considered the influence of various parameters on the reduction reaction it is of interest to consider the effect of various promoters on the reaction kinetics.

In this case, interest is focused on the promotion of reduction at moderate temperatures between 1200 and 1400°C. Not much work has been performed in this area, largely due to the lack of understanding of the mechanisms involved in pre-reduction.

However, it has been found that small quantities of alkali and alkali-earth metal oxides and halides exert a strong accelerating effect on the carbon monoxide reduction of wustite and iron (Khallafella and Weston,99). The extent of the reaction rate enhancement is found to be proportional to the ionic radius and electronic charge of the promoter additive. It was found that increasing the promoter concentration caused an acceleration in reaction kinetics to a maximum, beyond which no further increase in reduction rate occurred.

The effect of chlorides (NaCl,KCl) has also been considered (10,168) stemming from work on laterites (ref. 25,36), and it has been shown that chloride is effective in promoting the rate of reduction, particularly in the case of iron reduction, where vapor phase transport of the volatile chloride to the surface of the reductant takes place, and a rapid rate of reduction

results.

The use of various promoters on chromite reduction has been attempted and some degree of success has been achieved (Katayama et al. 87 Barnes, 12a), where borates and chlorides were found to have a significant effect in promoting the carbonaceous reduction of chromium ores. The results generally suggested that promotion occurred with borates through the promotion of the reduction reaction with CO (ref 87).

The use of reduction promoters appears to have been limited to those that will have an influence on external reactions, while little attention has been paid to the possibility of providing a locally altered environment in which the reduction can take place. This is particularly important in the case of chromium where it would appear that the stability of the spinel phase presents severe problems with regard to reaction rate and extent. This aspect will be considered in greater detail in chapter 6.

2.4 MODELLING OF THE REDUCTION PROCESS

2.4.1. BACKGROUND

A large amount of work has been performed on the analysis of reactions in metal oxide- carbon mixtures (96,108,178). These studies have usually concentrated on the iron oxide system because of its economic importance in D.R.I. applications. Rate equations have been developed to take into account the rate of reduction as controlled by carbon-CO_2 oxidation (i.e. carbon gasification rate controlled), and by diffusive and viscous flow of the CO and CO_2 reaction products through packed beds (Tien and Turkdogan; 177,181, 182,183, 180a, 180b).

In the case of iron oxide reduction, in the absence of diffusional resistance through the boundary layer surrounding the particle, the overall process is controlled by the rate of reaction at the interface between reduced and unreduced layers (Themelis and Gauvin, 175). In the case of hematite ores, it is usually pore diffusion which is rate limiting, and in the extreme case of very porous ore types where pore diffusion is not rate limiting, it is found that the chemical reaction rate limits the overall rate of reduction. These rates are however several orders of magnitude greater than those found in chromite reduction as shown in figure 2.6.

In the case of chromite reduction, major differences are found in the form of the reaction product as shown in figure 2.7. With iron ore (hematite), the material that is formed after reduction is porous, regardless of the density or condition of the original oxide species. This contrasts sharply with the appearance of the chromite reduction product, which shows no

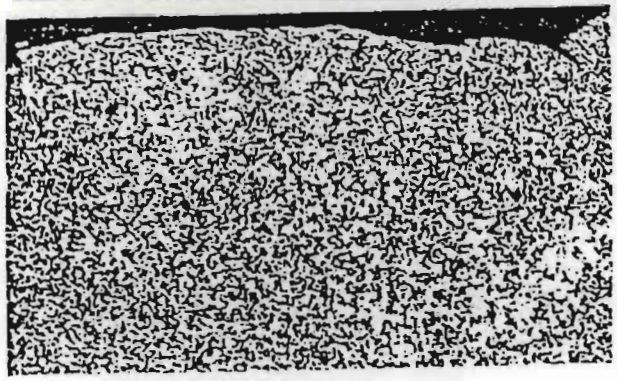

100% H_2

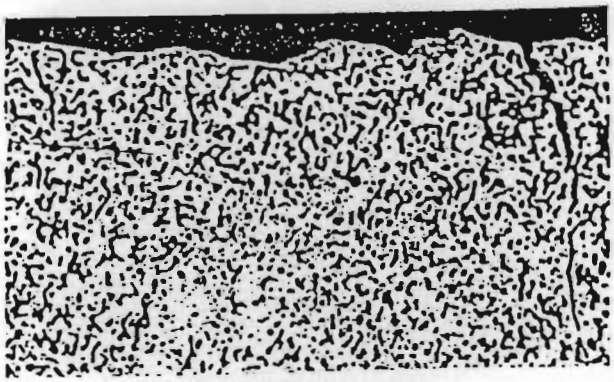

90% CO - 10% CO_2

100 μm

—Polished sections showing network of pores in the iron formed by H_2 or CO-reduction of dense wustite at 1200°C.

ref. Turkdogan et al.(181a,b), and below, chromite reduced with carbon black at 1200C, the central region representing altered spinel with a reduced iron content, the metal on the grain exterior showing no porosity.

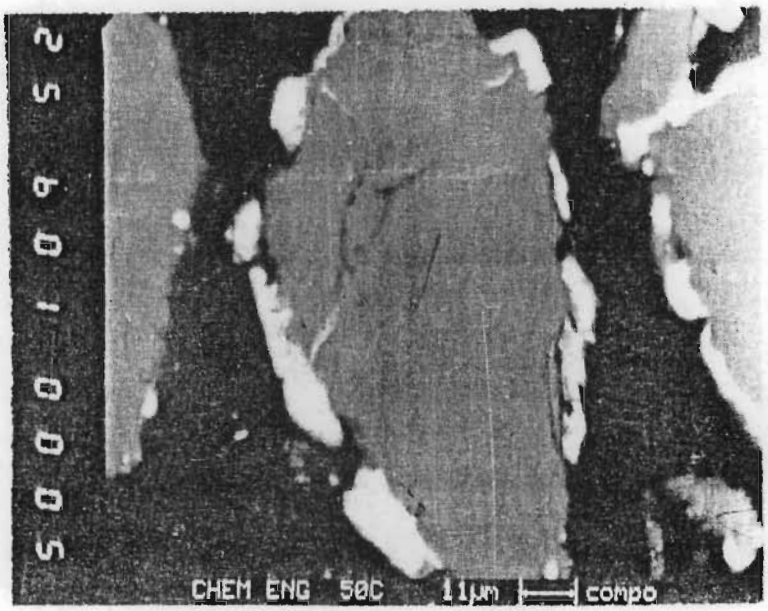

FIGURE 2.7 COMPARISON OF REDUCTION PRODUCT MORPHOLOGY OF CHROMITE AND DENSE WUSTITE.

porosity in the grain bulk, and metallization occurs only at the grain exterior.

In the case of ilmenite reduction, where it is found that iron reduction occurs rapidly at relatively low temperatures (~1000°C), the form of the reduction product is very different, with the metallic iron nucleating and growing at various sites evenly distributed within the ilmenite grain, in a shrinking core manner (den Hoed, 43; Barksdale, 13).

The obvious differences between the behaviour of chromite and these other ores may be ascribed to the presence of the considerable nonreducible oxide fraction of the spinel lattice. The presence of this stable component renders penetration of gases to the particle interior impossible, limits electron transfer and slows diffusion rates within the particle, resulting in a reduction mechanism that is inherently slower, with a far larger number of factors exerting an influence on the reaction kinetics.

These contrasts suggest that a model for chromite reduction would have to reflect the nature and composition of the spinel to a far greater degree compared to models of iron ore reduction.

2.4.2 CONCEPTUAL MODEL FOR CHROMITE REDUCTION

Investigation into the reduction behaviour of synthetic chromites ($FeCr_2O_4$) by carbon (Katayama, 87; Lisnyak,105), revealed that metallic products were formed in the following order:

austenite-> austenite+ $(Fe,Cr)_3C$ -> $(Fe,Cr)_3C$ +$(Cr,Fe)_7C_3$ -> $(Cr,Fe)_7C_3$

This sequence suggests the formation of an iron rich metal phase with gradually increasing chromium and carbon content, as

would be expected from the shape of the iron-chromium metallization curve described earlier (figure 2.5).

Lisnyak et al.(105), showed the initial step in the reduction sequence to be the reduction of tri-valent iron to di-valent iron within the spinel lattice, followed by total reduction of iron and chromium at the exterior of the grain at temperatures greater than 1050-1200°C.

This may be summarized in two stages:

a) first stage

Reduction of $FeCr_2O_4$ component (with FeO and Cr_2O_3 reduced simultaneously at temperatures in excess of 1150C, the reduction of FeO only proceeding at lower temperatures)

b) second stage

The reduction of $MgCr_2O_3$ component started at 1200°C and proceeded rapidly at temperatures higher than 1250°C.

The description of the second stage suggests the importance of the magnesium and aluminium components of the spinel in determining the final extent as well as the kinetics of reduction.

Searle and Finn (160) proposed that reduction first occurs at the points of contact between the solid reductant and the chromite particles.The reaction products are metal and carbon monoxide. The carbon monoxide surrounds the chromite particle and continues to act as the the main reducing agent.

The more recent works of Searle, Kucukkaragoz et al. (3,93, 160) define the sequence as:

1) the initial rate of chromite reduction is governed by the initial generation of CO at points of contact between particles of carbon and chromite.

2) metal nucleation occurs after essentially all the

ferric ion has been reduced to the ferrous state.

3) four distinct regimes of rate control operate sequentially.

a) direct control by generation of CO

b) other rates governed directly by the form of the reduced metallic product and as the supply of the gaseous reducing agents is limited, metallization is confined to the surface.

4) reduction up to an extent of 50% could be accelerated by the incorporation of volatile compounds in the charge, which would increase the initial concentration of the reducing agent, and of compounds that would assist the nucleation of iron.

5) If carbon is the reductant; metallization must be confined substantially to the exposed surfaces of the chromite.

6) The fourth stage at an extent above approx. 50% is controlled by the solid state diffusion of Cr^{3+} ions to the carbon saturated reduction point.

No reference is made in either of these works to the apparent reduction limit encountered even at temperatures as high as 1400°C, as shown in figure 2.2.

Searle and Finn (160) and Kucukkaragoz (93) draw the conclusion that the increase in carbon content of the metal phase with increased degree of reduction indicated a state of equilibrium between the metal and oxide phases. It was concluded from this that the rate of carbon supply was rate limiting to the reduction reaction.

These conclusions are however not consistent with concentration profiles of iron and chromium found within the chromite grain (12a,154,94). In addition, the increase in carbon content of the metal is a reflection of the changing metal

composition and hence local metal- carbon equilibrium, rather than that involving the oxide.

2.4.3 SPECIFIC MODELS OF THE REDUCTION PROCESS

Most recent models of the reduction process are based on some form of diffusion mechanism for reduction. There is however no general agreement on the rate determining process nor consequently on the effect of parameters such as ore composition and particle size.

The model proposed by Barcza (14) was based on the conclusion that the mechanism of reduction of chromite ores by solid carbon over the temperature range 1000 to 1500°C was consistent with three dimensional diffusion of the reactants through a reaction product layer. It was postulated that diffusion of carbon to the surface of the chromite grain through the metallic product layer was rate limiting. Spherical symmetry was assumed, and a model presented based on the equation:

$$1 - 2/3X - (1-X)^{2/3} = kt$$

where X = degree of reduction, K = rate constant, t = time

Three modes of diffusion were listed, namely, surface diffusion, grain boundary diffusion and volume diffusion, each of which could play a significant role at different stages of the reduction reaction.

It was suggested that the overall reduction rate was initially governed by volume diffusion into the bulk of the chromite grain. The subsequent break-up of the chromite grain at higher extents of reduction and the formation of interconnected metal lathes offering communication between the surface and the grain interior enabled higher reduction rates to be achieved through the reduced distances for carbon diffusion in the spinel and the more rapid diffusion of carbon in the alloy.

Several aspects of this model appear to be contradictory.

Firstly, the absence of metal formation within the grain interior until relatively high extents of reduction at relatively high temperatures (+80%,+1400°C), is not consistent with the postulated volume diffusion of carbon into the grain interior, in which case a regular distribution of metal nuclei would be expected throughout the chromite grain interior.

Secondly, the rate limitation of carbon supply suggests that there should not be any concentration gradient of species within the chromite grain. This is not consistent with the findings of Algie et al.(3,93,94), who show definite concentration gradients for different species within the grain.

Urquhart et al.(186) investigated the smelting mechanisms associated with the production of high carbon ferrochromium. It was found that the equations that came closest to fitting the results obtained from numerous tests were based on the solid-state diffusion of the reacting species through a product layer. It was concluded that although the reduction of iron from the chromite ore satisfies a topochemical reaction, the reduction of chromium from the ore does not follow an unique mechanism over the temperature range.

An expression of the form:

$$X = A + B.t + C.t^2 + dt^3.(\exp(\frac{-E}{RT}))$$

describing a topochemical reaction starting simultaneously on the faces of cubic crystals was used to describe the reduction of iron.

Searle's model (160), was based on a Fickian diffusion model for the combined iron and chromium species. The mathematical form of which, assuming spherical symmetry, was simplified to:

$$\log (100-R/100) = (- \pi^2.D.t/2,303.r^2)$$

where R= reaction extent; D= lumped diffusion coefficient and r= particle radius.

Plots of $\log(100-R/100)$ versus t/r^2 at 1200°C and 1300°C were

found to be relatively linear over a region corresponding to reduction up to approximately 75%, from which it was concluded that the reduction reaction is controlled by the diffusion of iron and chromium species up to a point corresponding to approximately 75% reduction. However,the change in the slope of these lines, corresponding to changes in the diffusion coefficient with changing particle size, suggest that this model has inaccuracies, probably stemming from the lumping of both chromium and iron reduction.

The subsequent model by Kucukkaragoz (94) described above, defines an earlier reaction period involving the formation and growth of metal nuclei; where the rate of metal formation is proportional to the interface:

$2(m)^{1/2} = kt$, with m representing the amount of metal formed (i.e. combined iron and chromium). Following this the standard diffusion mechanism is assumed to be rate controlling at extents exceeding 50%, with a rate form similar to that of Searle et al. described above.

Although this last model does make some attempt at describing the individual processes occurring during chromite reduction, it is still only in very general terms, and no attempt has been made to describe the individual rates of iron and chromium reduction, or any dependence that the reaction sequence might have in terms of rate or extent on the chromite ore composition.

More recently, Perry (176) developed a complex model based on the results of Searle and Finn (160). Perry describes chromite reduction in terms of a spinel unit cell model, where changes in the spinel are expressed in terms of changes in the spinel unit cell composition.

Based on a single analysis where a phase of sesquioxide type composition ($(Cr,Al)_2O_3$) was found, Perry postulates the widespread presence of this phase, and proposes that the Cr^{2+} species is present in this phase, in sufficient quantity to act as a vital charge carrying component. Perry postulates that the presence of the Cr^{2+} cation enables the

reduction of iron from the partly altered chromite, even when separated from the reductant by the sesquioxide phase.

The general occurrence of such sesquioxide phases during the reduction of fine chromite with excess carbon has not been described in the literature and it is presumed that in this case it was as a result of improper mixing of the relatively coarse reductant and oxide.

Subsequently Soykan (169) proposed a similar model. However, in the absence of finding any sesquioxide phase at temperatures of 1416°C and above, Soykan's model omits the role of sesquioxide formation but retains the action of Cr2+ as charge carrier.

Though the presence of Cr^{2+} is certainly possible (29,122a,147,155,208), the conditions under which significant quantities of the Cr^{2+} species could be present in the context of solid state reduction, as presently under consideration, are not well defined.

Since this species cannot be detected other than by the use of highly sophisticated equipment, together with the fact that in neither of the above two works is any positive experimental evidence of the presence of this species given, the role of Cr2+ cations in the reduction reaction (certainly within the region of interest in this work) is assumed to be negligable.

In summary it may be said that the previous attempts made at describing the reduction mechanism have failed principally on two accounts:

Firstly they have failed to gain a sufficiently comprehensive picture of the events taking place during the standard carbonaceous reduction of chromite ores and to explain the interaction of these parameters.

Secondly they have failed to define any difference in iron and chromium reduction rate or mechanism.

The detailed approach used in this investigation is aimed at resolving these problems.

CHAPTER THREE : THE THERMODYNAMICS OF CHROMITE REDUCTION

3.1 INTRODUCTION

The chromite reduction reaction is a kinetic process, proceeding from a specific starting point towards an end point or final thermodynamic equilibrium. In order to fully describe the reaction mechanism, a knowledge is required of the starting and ending points of the reaction, the pathway followed by the reaction and the rate of progress along the pathway.

Previous investigations into the reduction behaviour of chromite spinels have provided little insight into either the thermodynamic or kinetic limitations on the reduction reaction. This is of particular importance with regard to the apparent reaction ceiling encountered at approximately 75% reduction as considered in the previous chapter.

In addition, the conclusion drawn by Kucukkaragoz et al. (93), that the metal reduction product is in a state of near equilibrium with the partially reduced spinel suggests that the iron chromium metallization curve (itself an indication of the progress of the reaction) is in fact representative of a set of equilibrium stages between metal and oxide.

This conclusion has profound implications in terms of the mechanism and rate limitations applicable to the reduction reaction. The implication of a state close to thermodynamic equilibrium between metal and oxide suggests

that the rate determining process lies external to the chromite grain. This is contrary to the indications gained from most work as discussed in the previous chapter, which point towards factors internal to the chromite grain being rate controlling.

In order to resolve this issue, and gain further insight into the overall reduction mechanism, consideration is given in this chapter to the progress of the reduction reaction in terms of an equilibrium pathway. That is, the progress of the reaction is examined in terms of the equilibrium between metal and oxide phases during the course of the reaction, as a function of oxygen partial pressure, up to the point where equilibrium in the presence of solid carbon is achieved.

Considering briefly Rankin's analyis of chromite reduction (154), particular attention was paid to reactions involving carbon monoxide as the prime reductant (based on the works of Kolchin, 89 and Krupkowski,96). Chromite reduction is described in terms of the two reactions:

$$2FeCr_2O_4 + 80/7CO = 2Fe + 4/7\ Cr_7C_3 + 68/7\ CO_2 \quad \text{--- (3.1)}$$

and

$$C + CO_2 = 2CO \quad \text{--------- (3.2)}$$

Comparison of the equilibria of these reactions and that of the CO/CO_2 equilibrium in the presence of solid carbon (figure 3.1) suggests that reduction should proceed at temperatures in excess of approximately 1060°C at 1 atmosphere pressure.

However this simple approach does not indicate any thermodynamic limitations on reaction extent above this temperature, nor does it provide any information on the effect of ore composition on either the reaction extent or

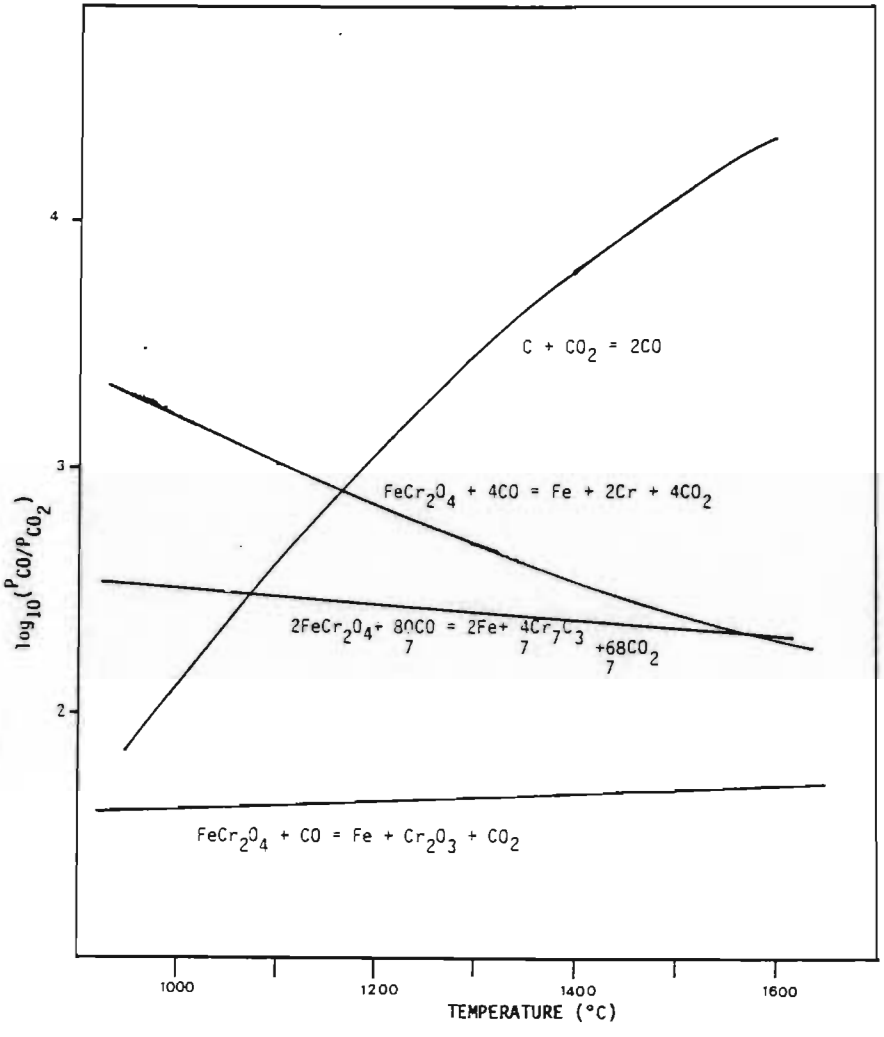

FIGURE 3.1 Equilibrium reactions for the reduction of chromite ($FeCr_2O_4$), assuming unit activity for all solid species.
(after RANKIN, 149)

FIGURE 3.2

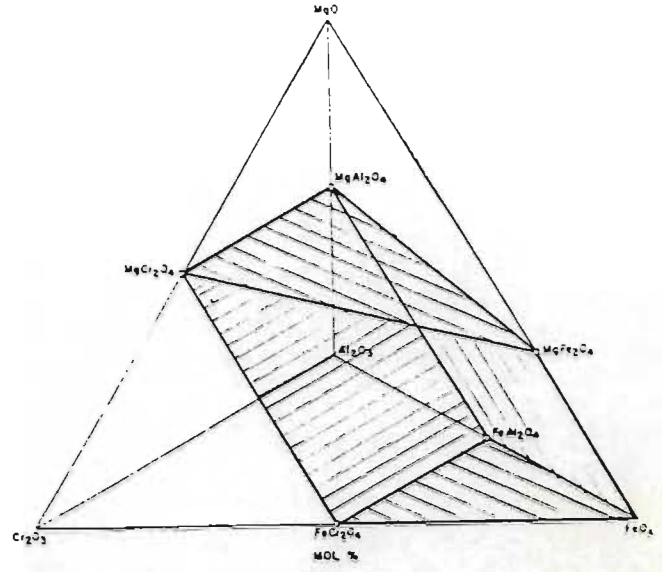

Tetrahedron used to represent main constituents of chromium-containing spinels, slightly modified after ULMER (1969). The 'spinel volume' is the distorted trigonal prism $MgCr_2O_4$–$MgAl_2O_4$–$FeAl_2O_4$–$FeCr_2O_4$–$MgFe_2O_4$–FeO_x

ref MUAN, 122b

the nature of products formed. Clearly a more detailed model is required if these aspects are to be considered.

Cognisance must be taken of the fact that naturally occurring chromite spinel is a complex solid solution of oxide species. The large compositional variations typically experienced by a spinel undergoing reduction, together with known miscibility gaps in the various binary systems of the oxide species that constitute the spinel, suggest non ideal behaviour of this oxide solid solution.

In addition, the effect of carbon on the solid solution of iron and chromium that constitute the metal phase, and the possible formation of carbides is expected to have a significant influence on the thermodynamics of the metal phase and hence on the system as a whole.

As a first step in modelling the thermodynamics of chromite reduction, consideration is given to the solution behaviour of both oxide and metal species and a means of describing their behaviour.

3.2 REVISED APPROACH

3.2.1 Solution behaviour of the oxide and metal species.

Neglecting the effects of components present only in very minor quantities such as TiO_2 and MnO, the chromium containing spinels encountered during the major part of the reduction sequence fall within the composition volume highlighted in figure 3.2.

The number of components in this system, and the complexity of their interaction makes accurate analysis difficult. As a first step, brief consideration is given to some of the subsolidus binary and ternary phase relationships.

In the $MgO-Al_2O_3$ system appreciable solid solution is expected between Al_2O_3 and $MgAl_2O_4$, the only binary compound (Warshaw, 196). At the liquidus temperature, up to 86 mol% Al_2O_3 can exist in solid solution, but this decreases to 66% at 1400°C. In contrast however, while it is known that the composition range for homogeneous spinels extends beyond MOM_2O_3 stoichiometry, the margin on the MO side is relatively small. This is particularly true for MgO with only 6mol% excess at 2000°C, decreasing rapidly to zero below 1400°C (Alper, 5b).

In the $MgO-Cr_2O_3$ system, only one binary compound is found($MgCr_2O_4$), and it is not expected to form solid solutions with an excess of either MgO or Cr_2O_3 (Wilde and Reese, 197).

Introduction of Al_2O_3 into the $MgO-Cr_2O_3$ system was found to result in complete solid solution between end members $MgCr_2O_4$ and $MgAl_2O_4$ which remained stable to below 510°C (Warshaw, 196).

However, mixtures in the $MgOCr_2O_3-Al_2O_3$ system at 1400-1600°C were found to result in a twin phase system composed of Cr_2O_3 - Al_2O_3 sesquioxide and a spinel solid solution ($MgCr_2O_4$ - $MgAl_2O_4$) confirming that the join is not binary (ref. 8).

It would appear from the wide composition ranges obtainable in homogeneous spinels that additional stabiliy is achieved in the multicomponent system, presumably stemming from the flexibility in oxidation state and site location of the numerous components. The stability field for spinel is not limited to the join corresponding to

stoichiometric spinels but extends into areas where the ratio of trivalent to divalent species is variable and in excess of 1 (Ulmer et al. 185 a,b ; Woodhouse et al. 205).

The dependence of the $\Sigma O/\Sigma Fe$ ratio on composition in the MgO-FeO- Fe_2O_3- Cr_2O_3 system indicates that the $\Sigma O/\Sigma Fe$ ratio tends to assume a value which keeps the whole composition within the homogeneity range.

The shift in the conjugation lines in the two phase area in figure 3.3, which steepen rapidly with increasing temperature at constant oxygen partial pressure, indicates such a shift in oxidation state in order to maintain homogeneity (Woodhouse, 205).

A similar effect is to be expected under isothermal conditions with decreasing oxygen partial pressure, where a fair portion of iron might be expected in the trivalent state (figure 3.4).

Similarly stoichiometric $FeCr_2O_4$ - $MgCr_2O_4$ spinels and those towards the Cr_3O_4 join can be expected at temperatures in the region of 1300°C under sufficiently reducing conditions (Ulmer and White, 185).

The ability of both iron and chromium species to change oxidation states, enabling the presence of Fe^{3+} and Cr^{2+} under highly reducing conditions (Ulmer 185a,b and Stubican et al.170), suggest that a homogeneous spinel is likely to be maintained in practice throughout the reduction reaction.

In addition, the results of Stubican indicate the formation of an $(Mg_{8-x}\ Cr^{2+}_{x})^{iv}\ (Cr^{3+}_{16})^{vi}\ O_{32}$ spinel under reducing conditions at 1300°C. This has considerable implications regarding the stability of a spinel undergoing reduction beyond the point where sufficient chromium remains in the spinel to maintain a balanced spinel with the remaining

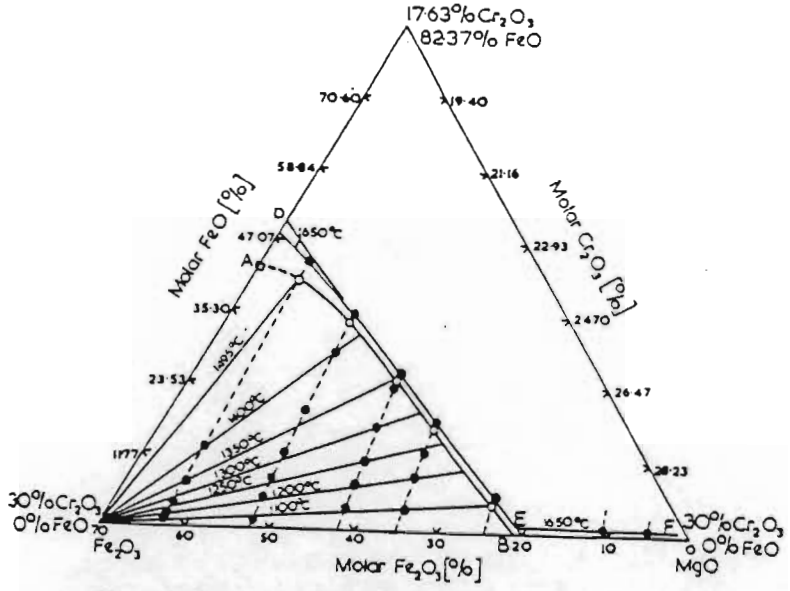

Phase relationships in section of system MgO–FeO–Fe_2O_3–Cr_2O_3, containing dissociation paths of mixtures containing initially 30 molar % Cr_2O_3. Dissociation paths shown dashed. Composition isotherms shown as thin continuous lines with temperatures alongside. Phase boundaries shown as thick lines

ref WOODHOUSE, 205

FIGURE 3.3

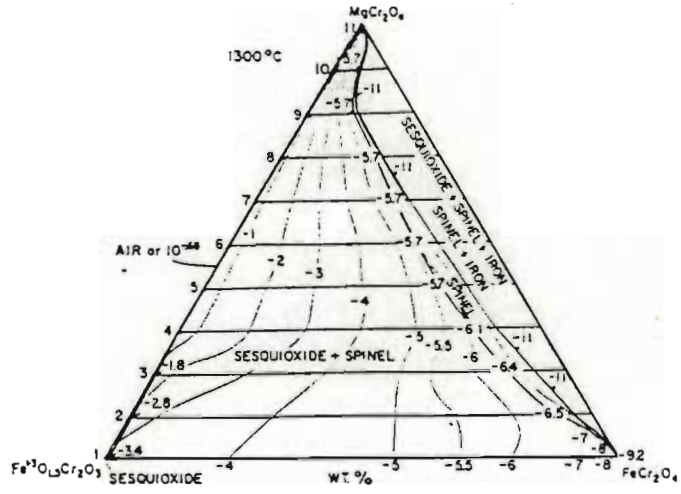

Diagram showing phase relations in magnesium–iron chromites at 1300°C, ref: ULMER (185)

FIGURE 3.4

magnesia and alumina (assuming negigable iron remains at this point). Under such conditions the spinel might be expected to remain as a single phase, where otherwise exsolution of MgO might be expected.

Considering the metal phase, a large amount of work has been published describing the iron- chromium system and the effect of carbon and the formation of carbides on this system (Chipman et al. 27 a,b,c, 63,61 , 78,90,59,68,67,28,18,42,54,147,153)

In general the iron chromium binary may be considered to be Raoultian and reasonably ideal (Reese et al. 158,27b,191,208,148,166) However the presence of carbon, having a strong interaction with chromium means the ternary system cannot be treated as ideal.

Since in the region of interest the major carbide formed is an M_7C_3, containing upto 45% iron, an initial simplified approach would be to consider the metal phase as a solution of Fe and M_7C_3.

A more elaborate approach was also investigated based on the works of Healy (58), Darken and Chipman (27b) and Wada (191) and (204), where the change in activity of chromium and iron from the ideal binary case due to the presence of carbon at near saturation levels was calculated. However the effect on overall oxide- metal equilibrium results was found to be very small and the simpler initial method was thus generally used.

3.2.2 Thermodynamic model for chromite reduction.

The system of interest comprises in its simplest form of seven species, namely Mg^{2+}, Fe^{2+}, Fe^{3+}, Cr^{3+}, Al^{3+}, O and C. The thermodynamic model proposed is based on a set of equilibrium reactions describing the overall reduction reaction together with a set of assumptions regarding the

solution behaviour of the oxide and metal phases.

The 'thermodynamic' path that the reduction might be expected to follow was investigated in terms of the equilibrium between metal and oxide phases at specified oxygen partial pressures (or CO/CO_2 ratios) up to a point corresponding to the equilibrium CO/CO_2 ratio obtainable in the presence of a solid carbon phase.

In the calculations it is implicitly assumed that all the components in the oxide, metal and gas phases are in intimate contact and that the equilibrium state is applicable throughout each phase in the system.

Initial calculations were based on the assumption that the spinel could be treated as an ideal solution of spinel end member components (namely Fe_3O_4, $FeCr_2O_4$, $MgCr_2O_4$ and $MgAl_2O_4$).

The following set of equations was used to describe the reduction system:

$$Fe_3O_4 + 4CO = 3\,Fe + 4\,CO_2 \quad \text{----------} \quad (3.3)$$

$$2\,FeOCr_2O_3 + 80/7\,CO = 2\,Fe + 4/7\,Cr_7C_3 + 68/7\,CO_2 \quad -(3.4)$$

$$7\,MgOCr_2O_3 + 33\,CO = 7\,MgO + 2\,Cr_7C_3 + 27\,CO_2 \quad ---(3.5)$$

Based on the assumption of ideality in the spinel and metal phases, mass balance relationships were formulated and activities of the species described in terms of the extent of each of the above reactions (appendix 3). A set of nonlinear , independent equations was formulated and solved at each specified P_{O_2} for the extents of each reaction.

The results obtained are summarised in figure 3.5. Though the metallization curve obtained is similar in form to the results expected as discussed in the previous chapter (figure 2.5), the model still only crudely approximates the experimental results as shown

FIGURE 3.5(b) Equilibrium P_{O_2} - Reduction profile calculated assuming ideal metal and spinel end member solutions.

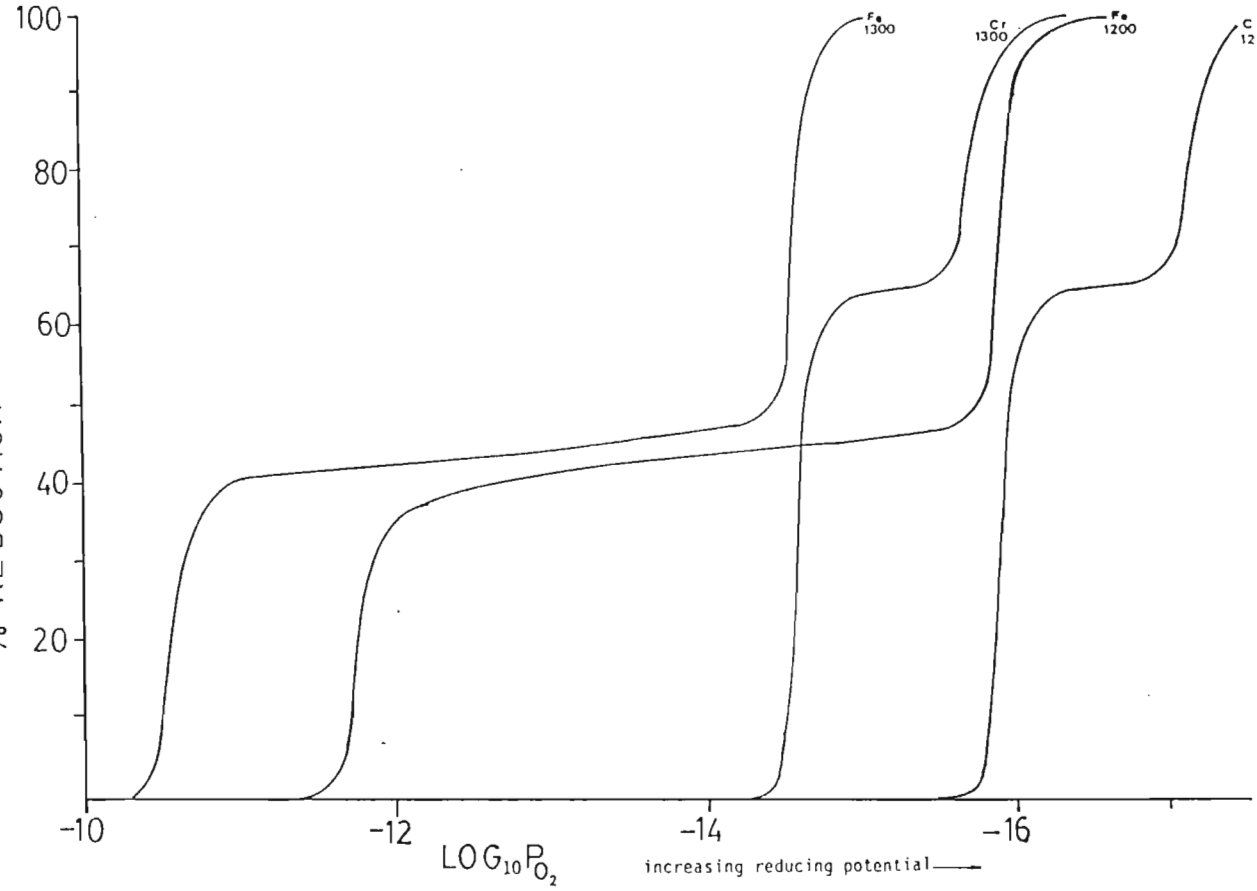

FIGURE 3.5(a) Calculated equilibrium metallization curve for LG6 chromite assuming ideal metal and spinel end member solutions.

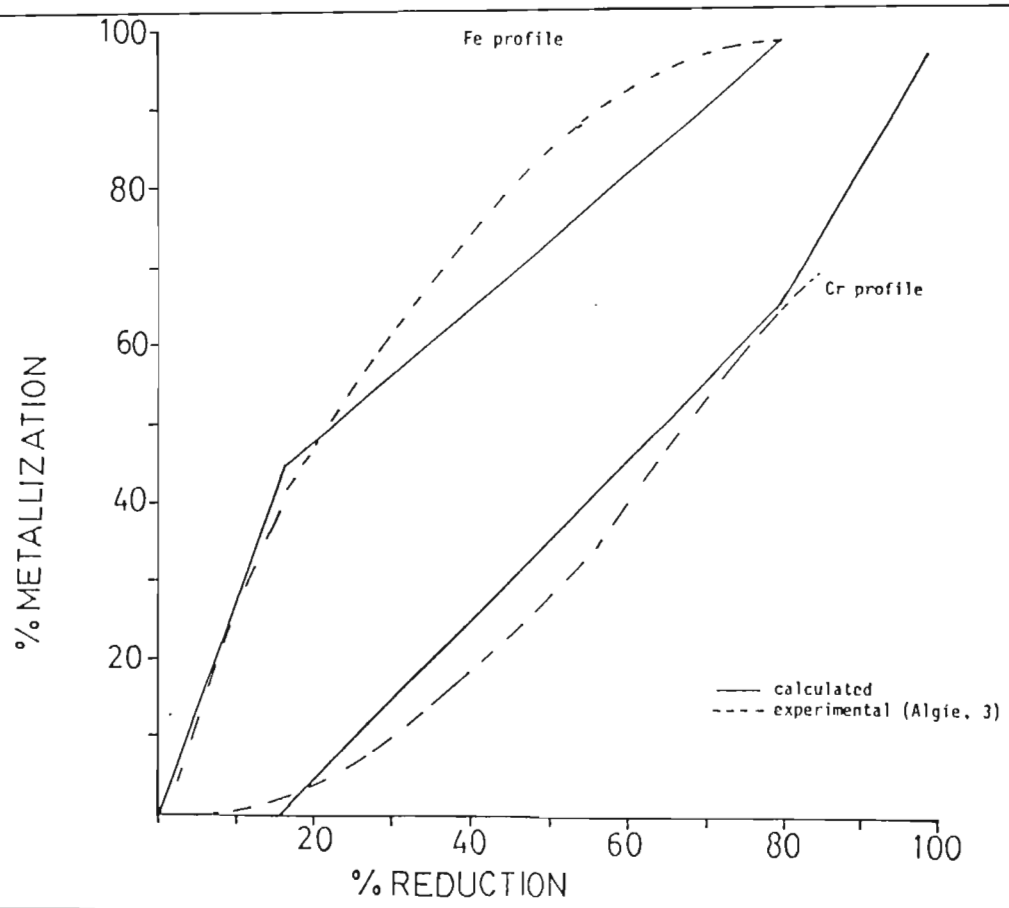

by the angular nature of the metallization curve and very sharp changes in the P_{O_2} - reduction profile. A further restriction is the fixed Cr/Fe reduction ratio specified over the major portion of the reaction in terms of equation 3.4. Accordingly several improvements to the model were considered.

Treating the spinel as an ideal solution of essentially two spinel species, $(Fe,Mg)M_2O_4$, and $(M)(Cr,Al)_2O_4$, with the ability to accept any surplus M_2O_3 into solid solution to form a sesquioxide phase in solid solution with the spinel, the reduction was expressed in terms of the equations :

$$Fe_2O_3 = 2\ FeO + 1/2\ O_2 \quad \text{---------- (3.6)}$$

$$FeO = Fe + 1/2\ O_2 \quad \text{---------- (3.7)}$$

$$FeCr_2O_4 = Fe + Cr_2O_3 + 1/2\ O_2 \quad \text{--- (3.8)}$$

$$MgCr_2O_4 = MgO + Cr_2O_3 \quad \text{---------- (3.9)}$$

$$Cr_2O_3 = 2\ Cr + 3/2\ O_2 \quad \text{---------- (3.10)}$$

$$Cr + 3/7\ C = 1/7\ Cr_7C_3 \quad \text{---------- (3.11)}$$

Solutions to this set of equations in terms of individual extents of reaction (e_i) were obtained as a function of oxygen partial pressure (or CO/ CO_2 ratio) using a similar technique to that employed previously.

The results, summarised in terms of the reduction metallization curve (figure 3.6) and P_{O_2} - reduction profiles (figure 3.7) bear a close resemblance to the experimental results published by Kucukkaragoz (93), and suggests that although still fairly crude, the assumptions made regarding the behaviour of the spinel are reasonable.

Results obtained using the model indicate that temperature has a marked influence on the P_{O_2} - reduction profile , with relatively little influence on

Comparison of experimental and calculated equilibrium reduction- metallization curves for LG6 and UG2 ores (1200- 1300°C).

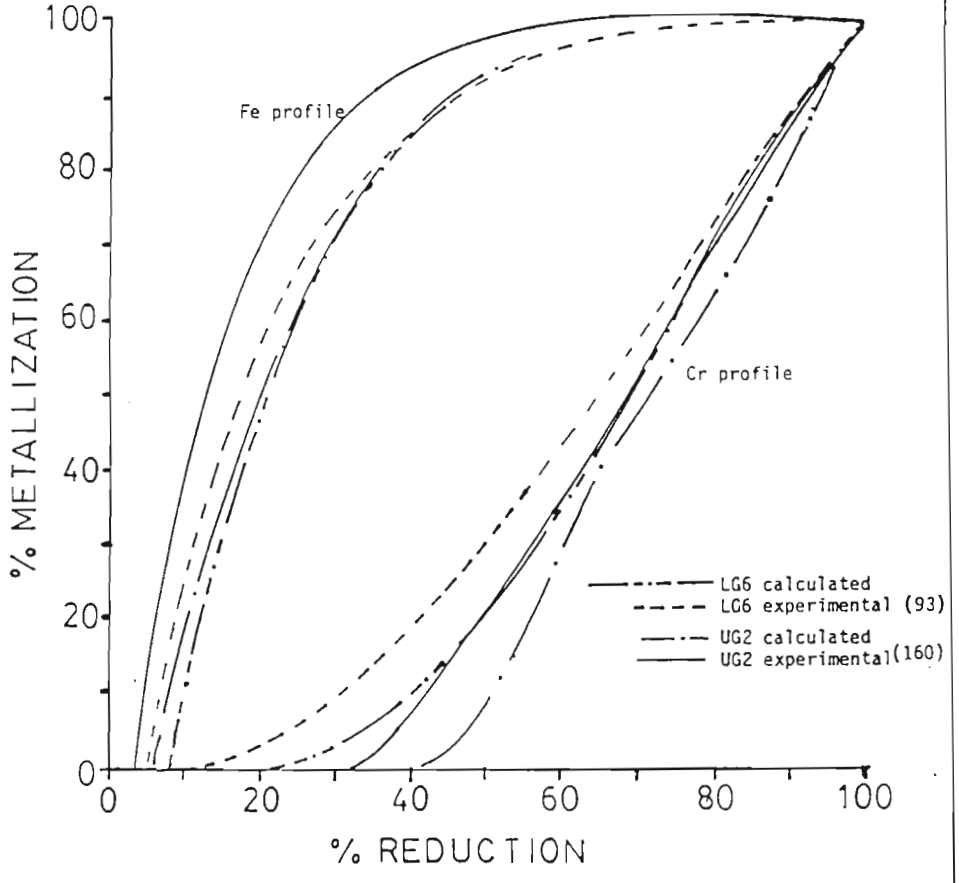

FIGURE 3.6 Reduction- metallization curve for LG6 ore at 1200°C, calculated assuming equilibrium between metal and spinel-sesquioxide phases.

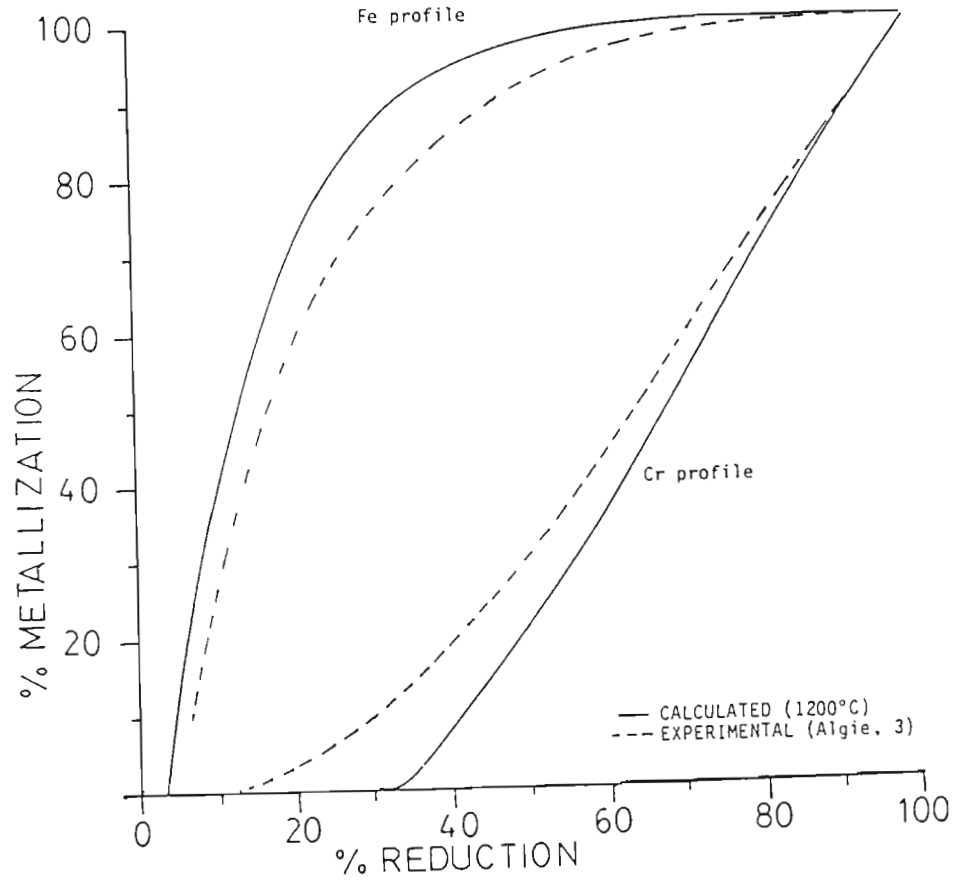

FIGURE 3.7(a) Calculated equilibrium P_{O_2} - reduction profile for LG6 ore at 1200°C

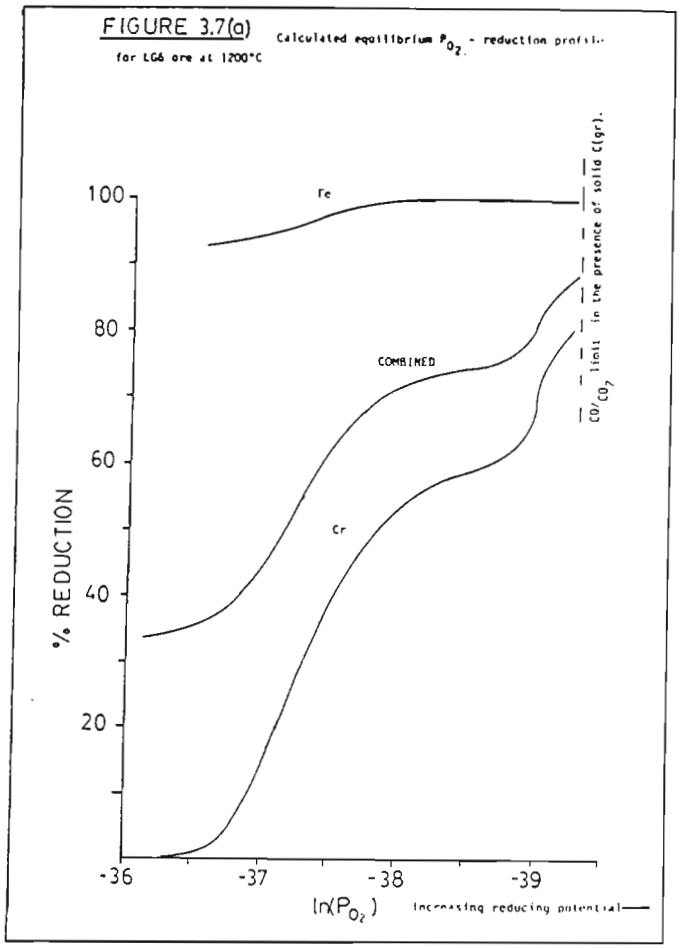

FIGURE 3.7(b) Calculated equilibrium P_{O_2} - reduction profile for LG6 ore at 1250°C.

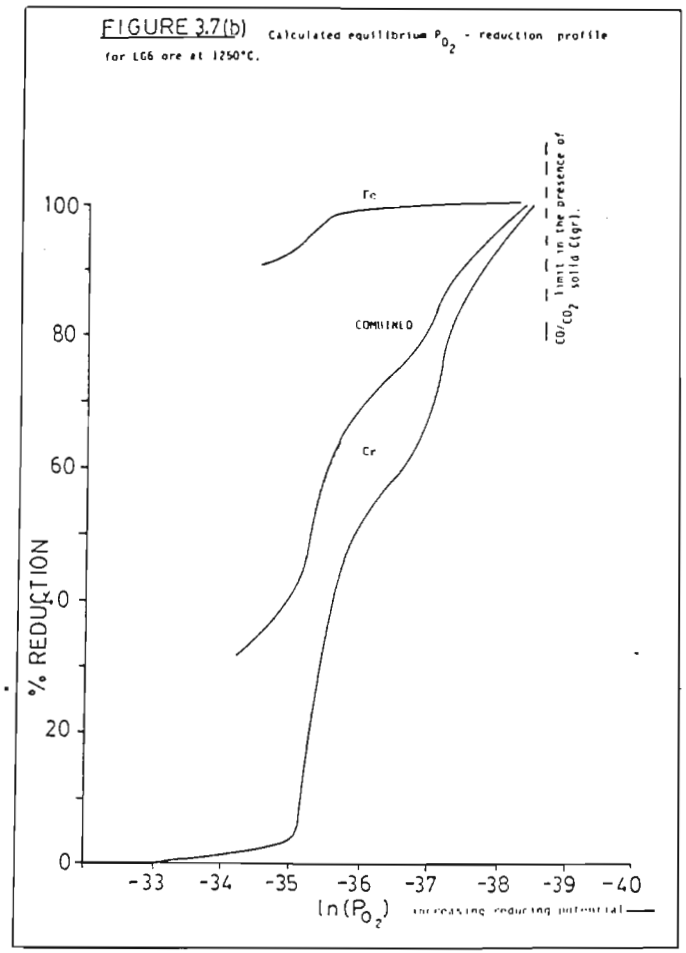

FIGURE 3.7(c) Calculated equilibrium P_{O_2} - reduction profile for LG6 ore at 1300°C.

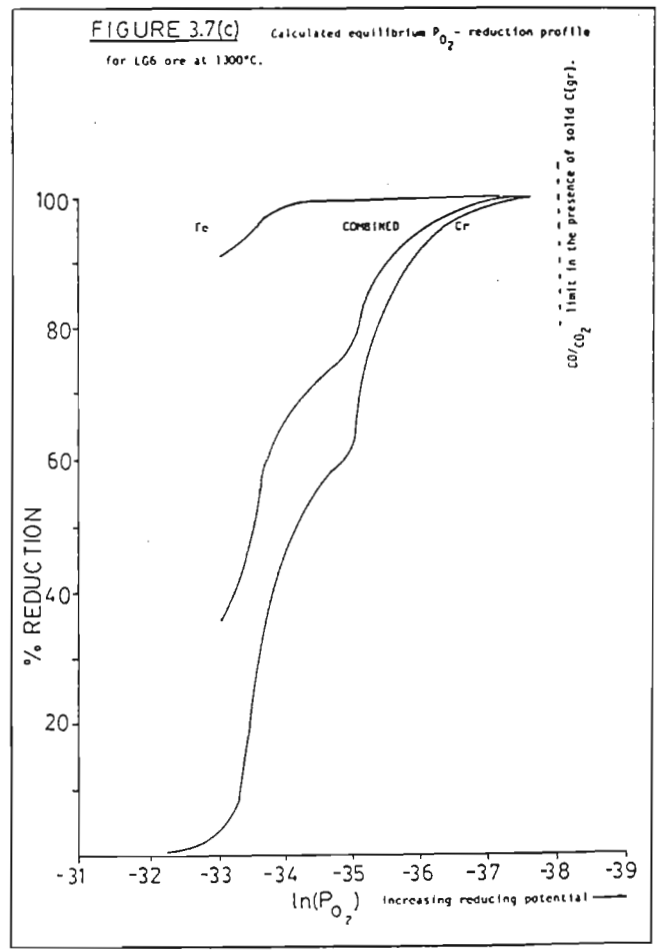

the metallization curve. However, composition is found to have a very marked effect on the metallization curve as shown in figures 3.6, 3.7 and 3.8).

Calculation of the equilibrium point for LG6 ore in the presence of solid carbon, indicates that in excess of 85% reduction should be achievable at 1200°C. This limit is found to be very temperature sensitive and by 1250°C complete reduction might be achieved (figure 3.7).

This calculated thermodynamic equilibrium limit is found to be much higher than the reaction ceiling found experimentally at approximately 75% reduction.

The low level of the experimental limit, and its relative insensitivity to temperature in the range 1200- 1400°C, compared to the value of over 88% reduction and sensitivity of the calculated limit to temperature, suggests that the limit encountered experimentally is not a thermodynamic limit.

It is conceivable that the marked changes which occur in the composition and structure of the spinel towards the end of the reduction could cause a severe slowing of the reaction kinetics. Such changes are suggested by the sharp drop in Cr_2O_3 activity at approximately 75% reduction as calculated using the model (figure 3.9). If representative of the actual spinel, such a change could result in the slowing of the overall reaction rate to the extent where it appeared as a thermodynamic reaction limit.

3.3 CONCLUSIONS

The thermodynamic model proposed above is fairly

crude, and the results obtained are extremely sensitive to the accuracy of the thermochemical data used as shown by the P_{O_2}- reduction profiles in figure 3.10.

Such sensitivity places limitations on the model and any conclusions based on the model. However two key aspects have been highlighted by this model that are of considerable importance in defining the chromite reduction reaction.

Firstly, the apparent reaction limit commonly experienced in experimental work in the range 1200 -1400°C appears to be kinetic in origin, and a far higher degree of reduction should be achievable. This conclusion is supported by the apparent influence of particle size on the reaction ceiling as indicated in chapter 2 (figure 2.4b).

Secondly, although the metallization curve calculated closely resembles the experimental results (figure 3.6); the sensitivity to composition (figure 3.8) and the implicit assumption of uniformity throughout the spinel and metal phases suggest that the calculated equilibrium curve need not be representative of the actual reduction reaction.

The possible kinetic dependence inherent in the actual metallization curve and the likely existence of compositional variations across the chromite grain during reduction suggest that the system may be far from equilibrium but still yield a metallization curve similar to that calculated assuming equilibrium conditions.

This contradicts the conclusion drawn by Kucukkaragoz et al. (93), that the reaction system is in a near equilibrium state. Certainly any compositional

FIGURE 3.9 Calculated change in component activity in the spinel during reduction, assuming equilibrium between metal and spinel phases (1200°C).

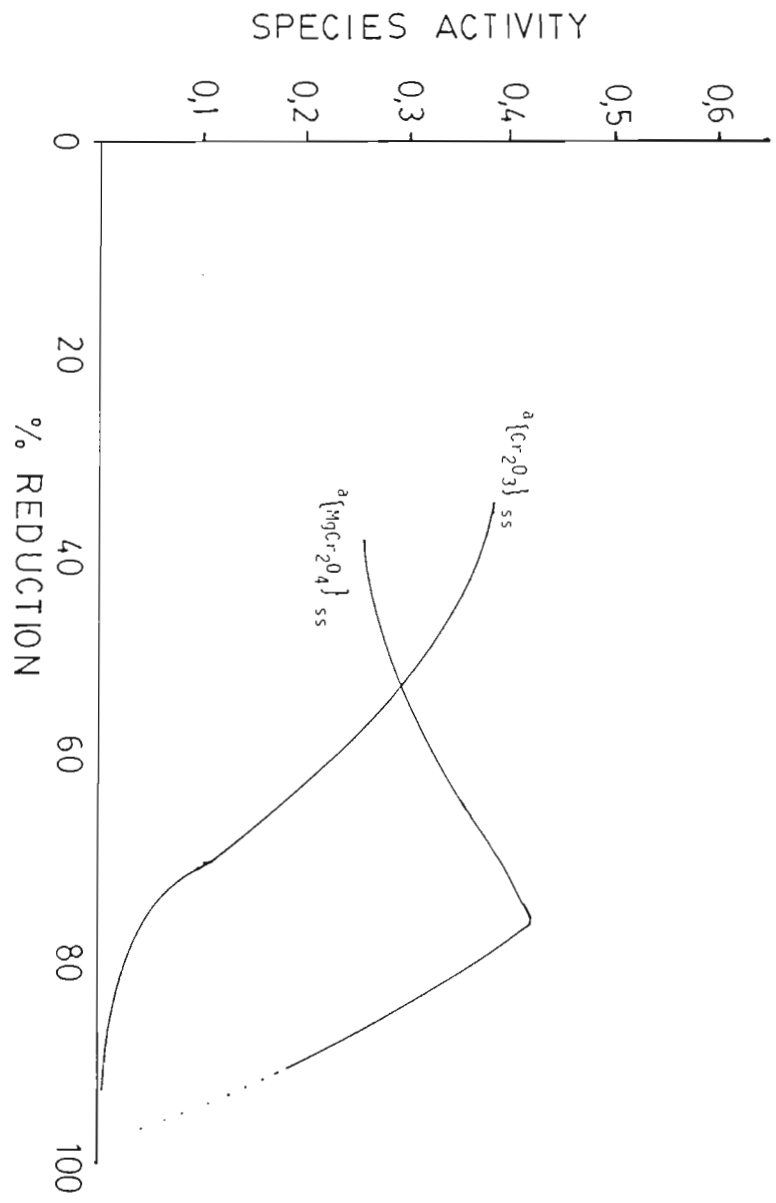

FIGURE 3.10 Calculated variation in the P_{O_2} - reduction profile for LG6 ore caused by a ± 1% variation in Gibbs free energy for the reduction reaction (3.6-3.11) at 1200°C.

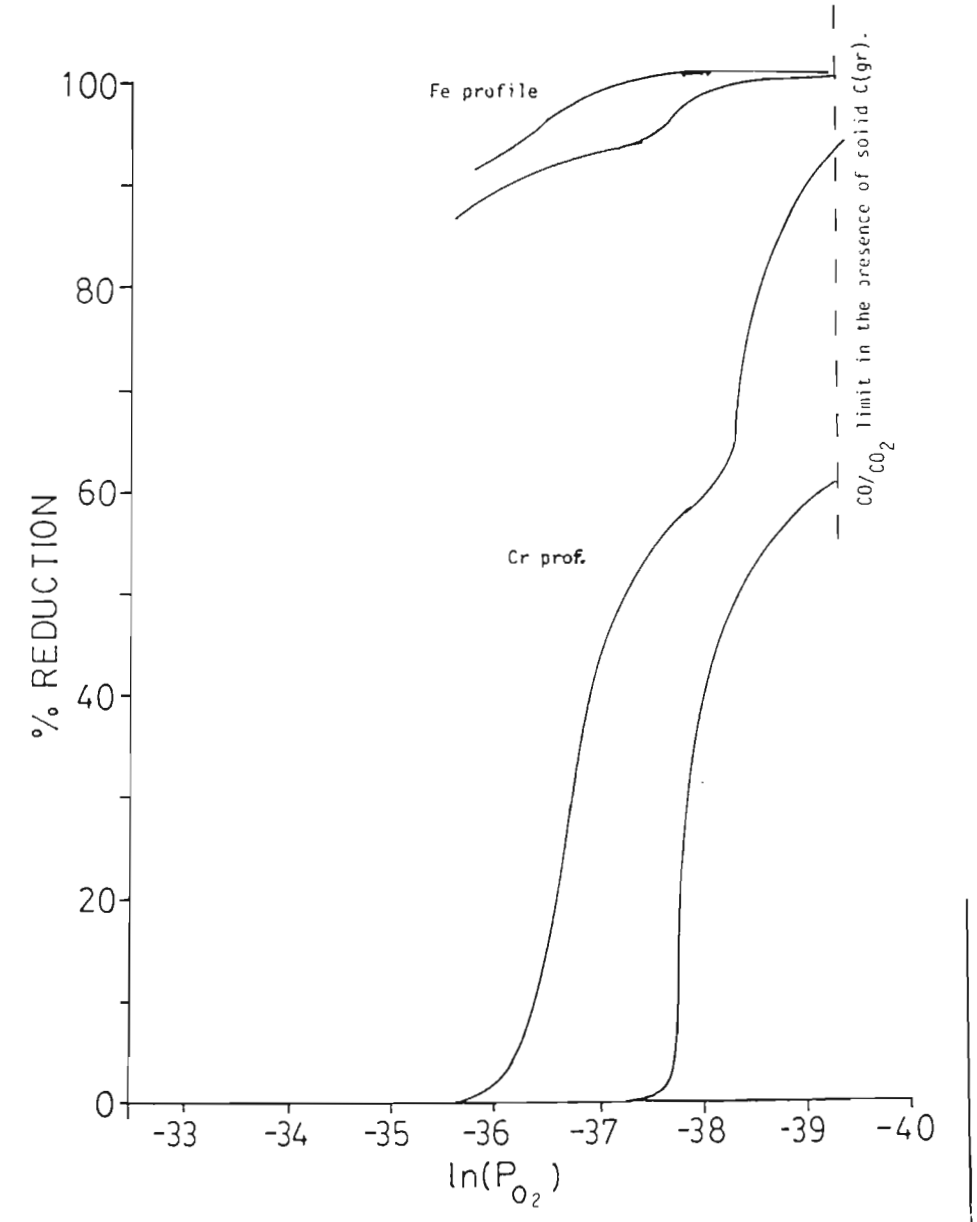

variation across the chromite grain during the reaction would suggest a non equilibrium condition, and support the hypothesis that the metallization curve has a measure of kinetic dependence.

Based on the thermodynamic analysis it would appear that a far higher degree of metallization should be obtainable than is achieved under normal experimental conditions, with complete reduction achievable certainly at 1300°C. It is thus concluded that the reaction is largely controlled by kinetic factors, though detailed analysis of the reaction kinetics are required in order to support these conclusions.

CHAPTER FOUR: EQUIPMENT AND SCOPE OF EXPERIMENTAL INVESTIGATION

4.1 EXPERIMENTAL PHILOSOPHY

In order to perform a detailed experimental investigation of chromite reduction, a technique was required for continuously monitoring the changes occurring within the sample while it was maintained under closely controlled conditions in terms of atmosphere and temperature. It was decided to use thermogravimetric analysis (TGA) as the basic tool for investigating the reduction reaction (Blazec,21; 48).

A limited number of experiments within the spectrum of those described in the literature were performed with the aim of establishing the reliablity of the equipment and the broad nature of the reduction process. Experimentation was then started according to a systematic schedule, aimed at establishing the reaction mechanism in both the unpromoted standard reduction and solvent phase promoted reduction cases.

In the following discussion, the term solvent phase is applied to certain fluoride based fluxing agents that were added in relatively small quantities of between 5 and 20% of the chromite mass. These solvent phases were not found to take part in the reduction reaction. Instead, such fluxes were found to form a discrete liquid phase at the reaction temperature,

which underwent little compositional change, but played a significant role in promoting a particular aspect of the reaction, affecting both the kinetics and extent of reduction.

In a final series of experiments, where greater quantities of a liquid phase of similar composition were present, the reduction was found to occur as a slagging type reaction. In such cases, the liquid phase became part of the reaction system undergoing considerable compositional change during the course of the reaction.

4.2. EQUIPMENT DETAILS

4.2.1. THE THERMOBALANCE APPARATUS

Most of the test work was performed on a low temperature thermobalance, capable of operating at temperatures of 1200°C under isothermal test conditions. Loosely packed powder charges of 10-50g were used, contained in an ALSINT sintered alumina crucible. The crucibles had an i.d. of 35mm, height of 60mm and wall thickness of 2mm. The charges were all premixed to achieve as high a degree of homogeneity in the sample as possible (ref. 137).

Data gathering was performed using a computerised data gathering and display system comprising a Mettler PC2000 electronic balance coupled to an Apple IIC microcomputer for data logging. The digital (serial) output from the Mettler balance was received by an Apple microcomputer through a serial interface, and matched to a time from an on- board clock. The time elapsed from the start of the experiment and the mass

change since the previously recorded reading were then calculated and the results shown on the text screen in the form of a continuously updated table. If the mass change over this time was found to be greater than a user specified sensitivity criterion, then the sample mass and time were recorded onto floppy disk, and displayed on a graphics screen in the form of a mass loss versus time plot.

This method of recording mass and time enabled easy data recall and analysis. The results were then produced in hard copy either in the form of a direct listing of mass, time and rate of mass loss or graphically displayed (details in appendix 4). The latter allowed for simplified analysis of the actual reaction rate, and description in terms of the individual rates of chromium and iron reduction as will be discussed later.

The apparatus as shown in figure 4.1 (details in appendix 4) was found to be both reliable and accurate. The accuracy of the equipment was monitored from time to time using the well known decomposition of limestone reaction equilibrium. The equipment was always found to be within the design specification of T+/- 5^{o}C.

Tests were performed at regular intervals to check for oxygen leaks in the system. This was done by replacing the standard chromite and carbon charge with a pure carbon charge maintained at a temperature of 1000^{o}C while the mass was monitored over a period of between 12 and 20 hours in a standard nitrogen atmosphere. The apparatus was never found to have any detectable oxygen leaks as shown by the zero mass loss recorded.

FIGURE 4.1

OUTLINE OF THE LOW TEMPERATURE THERMOBALANCE SYSTEM.

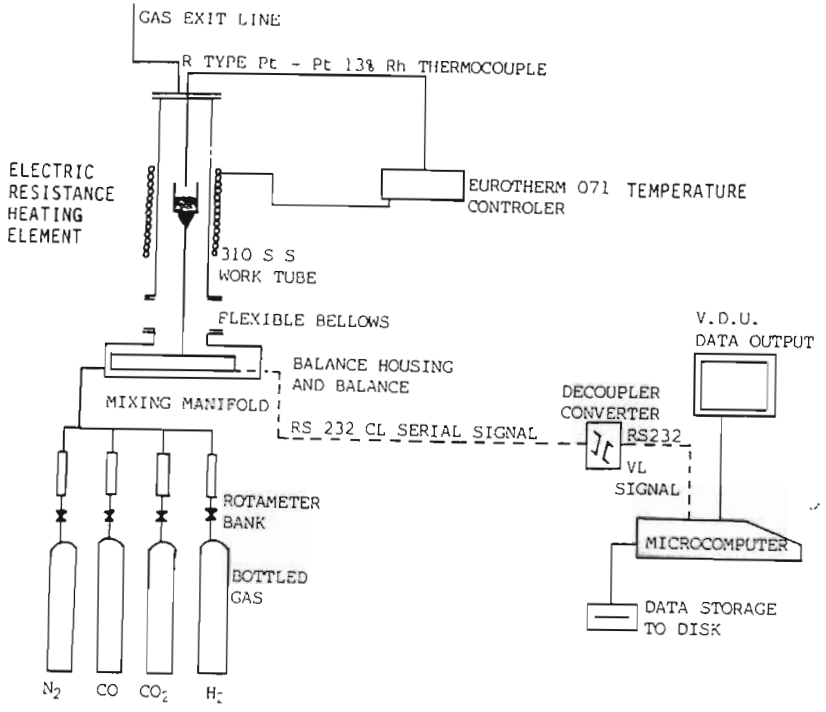

NOTES

1) SAMPLE IN RAISED POSITION. (BELLOWS COMPRESSED)

2) ELECTRICAL RESISTANCE HEATING ON WORK TUBE.

3) DETAILS OF THERMOBALANCE IN APPENDIX 4

FIGURE 4.2

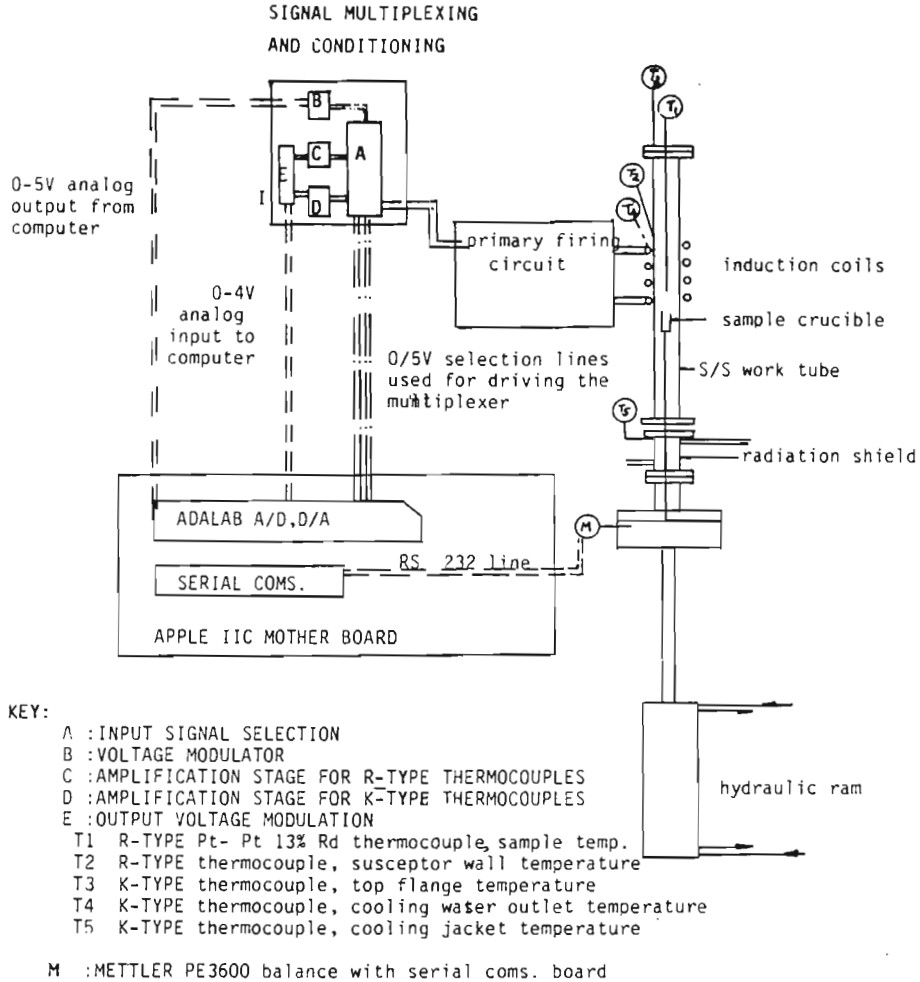

KEY:

A :INPUT SIGNAL SELECTION
B :VOLTAGE MODULATOR
C :AMPLIFICATION STAGE FOR R-TYPE THERMOCOUPLES
D :AMPLIFICATION STAGE FOR K-TYPE THERMOCOUPLES
E :OUTPUT VOLTAGE MODULATION
T1 R-TYPE Pt- Pt 13% Rd thermocouple, sample temp.
T2 R-TYPE thermocouple, susceptor wall temperature
T3 K-TYPE thermocouple, top flange temperature
T4 K-TYPE thermocouple, cooling water outlet temperature
T5 K-TYPE thermocouple, cooling jacket temperature

M :METTLER PE3600 balance with serial coms. board

FIGURE 4.2 OUTLINE OF THE INDUCTIVELY HEATED THERMOBALANCE APPARATUS USED IN THE INVESTIGATION OF REACTION KINETICS AT 1300°C AND AT HIGHER TEMPERATURES.

In addition, a 3kW inductively heated thermobalance was designed for T.G.A. work in the region of 1200-1350°C. Computerised control and data capture were included in the design. The basic outline of the system is shown in figure 4.2. The work tube was designed to act as both atmospheric container and as susceptor for the induction heating. All temperature readings and conversions were performed on the microcomputer.

4.2.2 THERMOBALANCE DATA HANDLING

Various computer programmes were developed for data capture and display. The programmes were designed for general use incorporating moving average and stability analysis. Further programmes were developed for data recall and data handling. Such programs included the ability to calculate derivatives of the raw data as well as to perform analyses on smoothed data fitted to cubic spline approximations (detailed in appendix 4). This method of data gathering and analysis was found to be fast, reliable and accurate.

4.2.3 REACTANT SPECIFICATION

Before discussing specific results it is important to state the nature of the reactants and the basis on which reagent addition was calculated.

(i) All additions are quoted as a fraction of the chromite mass present in the sample at the start of the reaction.

(ii) All test work described in this chapter,

unless specifically stated refers to work performed on CHROME SAND, a commercially available LG6 chromite ore, with the composition shown in table 4.1.

This chromite has undergone a certain amount of preliminary beneficiation to remove excess gangue material. Because of the low gangue contaminant level and constant composition of CHROMESAND, no further upgrading of the ore was performed. Where tests were performed on material with a reduced particle size, the milling was performed using a batch ball mill or PALLA vibratory mill (details in appendix 2)

In the kinetic studies performed, discrete particle size ranges were used, with the individual fractions between 7,8 and 106 micron as defined in table 4.2. Individual particle size fractions were analysed and no compositional variation across the ranges was found.

In most of the kinetic and mechanistic studies the source of carbon was in the form of Phillips lampblack. The ultrafine particle size of carbon black, together with its very high purity (no volatile or ash content) was found to be beneficial in aiding the reproducibility of results, which depend to a large extent on the uniformity of mixing and the absence of segregation in the sample. To achieve the maximum possible degree of homogeneity in the sample, a small addition of a wetting agent, namely methanol was used as a mixing aid. This was found to help considerably in achieving reproducible results.

The reagents used as fluxes in the experimental work

...ROCK SAND ANALYSIS. (LG6 CHROMITE)

Component	Mass %
MgO	10,10
Cr_2O_3	46,92
SiO_2	0,84
FeO	18,46
Fe_2O_3	6,36
Al_2O_3	14,20
CaO	0,16
MnO	0,19
TiO_2	0,57

TABLE 4.2

...rticle size range and code used :

dp range	ave. dp.
75-105	88,74
53-75	63,05
38-53	44,88
26,9-38	31,97
20,3-26,9	23,37
14,5-20,3	17,16
10,5-14,5	12,34
7,9-10,5	9,11

: The cyclosizer cut points were determined using a mean chromite density of $4,5 \times 10^3$ kg/m^3

TABLE 4.3

CHEMICAL ANALYSIS OF REAGENTS USED

COMPONENT	IMPURITIES	MAX. LIMIT MASS %	SUPPLIER
CaF2 (AnalR)	chloride (Cl^-)	0,005	B.D.H chemicals
	iron (Fe)	0,005	
	lead (Pb)	0,005	
	silica (SiO_2)	0,05	
	sulphate (SO_4^{2-})	0,01	
NaF (AnalR)	chloride (Cl^-)	0,01	B.D.H. chemicals
	sulphate (SO_4^{2-})	0,05	
	NaF >99%		
NITROGEN GAS	O2	0,05	Union Liquid Air
	CO2	0,002	
	H2O	0,001	
HYDROGEN GAS	CO2	0,002	Union Liquid Air
	H2O	0,0005	

on the kinetics and mechanism were always of the highest quality analytical grade, and very fine particle size, usually d50< 5 micron. A full specification is given in table 4.3.

In subsequent larger scale test work involving pelletized feed, ground and sized metallurgical graphite and char were used as reductants. The chemical analyses and sizing of these materials are given in tables 4.4 and 4.5.

4.2.4 EXPERIMENTAL METHOD

The experimental method developed was standard for all thermobalance runs.

Work performed on the mechanism and kinetics of chromite reduction was done using discrete particle sizes as specified (table 4.2). The reactants were thoroughly mixed, where necessary a small amount of methanol was used as a wetting agent to promote mixing.

The sample was sealed in the low temperature thermobalance, with the flexible bellows expanded, and a constant flow of nitrogen established. The temperature in the centre of the hot zone, as measured by a thermocouple positioned with the tip immediately above the final sample position, was raised from its standard temperature of 500^{o}C to the desired reaction temperature, with the desired atmosphere flowing over the sample. Once the hot zone had reached the desired temperature for the isothermal reaction, the sample was raised into the hot zone without a change in atmosphere.

At termination of the experiment, the sample was lowered from the hot zone into the cool zone below,

TABLE 4.4

PROXIMATE ANALYSIS OF REDUCTANTS USED

SOURCE	% FIXED CARBON	% VOLS.	% ASH	% P	% S
LAMP BLACK	> 99.95	0,00	BALANCE	--	--
CHAR	78,8	5,0	16,2	0,003	0,40
ELECTRODE	98,92	0,00	1,08	--	--
GRAPHITE COKE	81,0	1,0	18,0	0,03	0,85

TABLE 4.5(a)

SIZE ANALYSIS OF COARSE ELECTRODE GRAPHITE

Size/µm	% (M/M)	% Passing
+600	9,20	90,80
+425	7,85	82,95
+300	18,77	64,18
+212	26,25	37,93
+150	18,97	18,96
+106	8,81	10,15
+75	4,79	5,36
+53	2,87	2,49
-53	2,49	

TABLE 4.5(b)

GRAPHITE PARTICLE SIZE DISTRIBUTION: SELECTED SIZE FRACTION 53 - 300µm

Size/µm	% (M/M)	% Passing
+300	1,85	98,15
+212	29,12	69,03
+150	26,57	42,46
+106	17,54	24,92
+75	14,38	10,54
+53	9,35	1,19
-53	1,19	

under an inert nitrogen atmosphere and the temperature of the hot zone reduced to 500°C. At this point the bellows could be decoupled and the sample could be retrieved. This method allowed rapid sample cooling to take place and prevented the worktube and sample from excessive oxidation experienced at the higher reaction temperatures.

In the case of the high temperature thermobalance, the sample was raised into final position and sealed. An inert nitrogen atmosphere was established and heating at maximum rate initiated. Once the sample temperature had reached a predetermined value (typically 1100°C), heating according to a chosen profile could be maintained till a final control setpoint had been reached.

Analysis of the reduction products from all experimental tests were comprehensive as described below.

4.3 ANALYTICAL PROCEDURES AND ACCURACY

4.3.1. WET CHEMICAL AND A.A. ANALYSIS

A fraction of each reduced sample was taken and leached in a constant boiling solution of hydrochloric acid (~21%HCl) for periods in excess of 5 hours (HCl solution initially consisted of a 50%vol. of analytical grade HCl). The filtered and diluted leach liquor was then analysed using a Varian model 1433 A.A. analyser. The dried and weighed filtered residue was preserved for microscopic and S.E.M. analysis and peroxide fusion.

Complete mass balance checks were performed on most

samples. These checks involved peroxide fusion of the acid leach residue and A.A. analysis of the solubilised product. These checks gave mass balance closures to within 5%. In addition, microscope analysis of the leach residue was performed to confirm completeness of leach.

Inaccuracies incurred through improper leaching and general A.A. inaccuracy were considered to be less than 10%.

4.3.2 OPTICAL MICROSCOPY, S.E.M. AND MICROPROBE ANALYSIS

Samples of typical reaction products and acid leach residues from various experiments were taken for S.E.M. and micro probe analysis.

Polished mounts of these samples were made and after preliminary optical investigation, detailed structural and compositional analyses were performed using the S.E.M. and microprobe.

The aim of this work was to establish the chemical composition and morphology of the different phases formed at various times during the reaction sequence, under differing conditions.

The instruments used were :

S.E.M. : JEOL JSM-35 with KEVEX 7077 EDS microanalysis system

E.M.P.A. : CAMECA computer driven microprobe and a Cambridge instruments GEOSCAN mk V with off line data correction.

Despite the use of chromite standards for microanalytical work, results on oxide phases obtained using the S.E.M. tended to be of a semi-quantitative

nature only (details specified in Appendix 4.3).

Because of the semiquantitative nature of the results obtained from the E.D.S. system, in the results and discussion that follow, the graphical representation of various E.D.S. spectra have been included for purposes of comparison. In this case, peak height corresponds to element concentration without ZAF correction.

4.3.3 X.R.D. ANALYSIS

X-Ray diffraction work was conducted on various reaction products with the aim of obtaining more detailed structural and compositional information. This work was performed using a Phillips model 7000 instrument with goniometer attachment.

This instrument is believed to be accurate to within 1% in terms of angle, enabling the calculation of unit cell dimensions. No quantitative analytical work was performed because of the lack of suitable reference standards.

The examination of powders and pellets required uniform treatment of material. Accordingly samples were taken and milled to fine particle sizes using a laboratory pulverizer and the fine powder product was then compacted in a perspex holder for analysis.

A Cr-Cu lamp was used, with 20kV excitation, (λ CuKα = 1,5418Å). Peak calibration was done using an internal quartz standard, d= 26,67Å.

The information obtained enabled the identification of phases present in the sample, as well as enabling the calculation of spinel lattice dimensions.

CHAPTER FIVE

RESULTS, DISCUSSION AND INTERPRETATION: THE STANDARD REDUCTION REACTION

5.1 INTRODUCTION

The results of numerous reduction experiments on LG6 chromite ore are presented and discussed in this chapter. In addition, some of the results obtained by other workers in the field (notably Finn et al. 3,11,160) are presented for comparison and discussion.

The effects of the most important variables in terms of reaction kinetics, namely the particle size of ore and reductant, temperature and spinel composition were investigated.

The aim of this work was to establish a realistic mechanism and model for the standard reduction process, and to provide a reference case for comparison with the solvent phase promoted reduction considered in the following chapter.

5.2 SUMMARY OF EXPERIMENTAL RESULTS

5.2.1 TYPICAL REDUCTION CURVES

The influence of ore particle size, temperature and reduction atmosphere on the reduction behaviour of LG6 chromite at temperatures between 1100 and 1300°C was

found to be in accordance with results as discussed in chapter 2. These results may be briefly summarised as follows:

a) Reduction rate is strongly influenced by chromite particle size as shown in figures 5.1 and 5.5. 5. . Detailed investigation showed an approximate inverse square relationship between reduction rate and particle size.

b) Temperature was found to have a very significant (exponential) effect on the reduction rate as shown in figure 5.2.

c) A reduction limit of approximately 78% was encountered at temperatures between 1100°C and 1300°C. This limit was not found to be sensitive to either temperature or particle size within the range investigated. Analysis of the reaction product showed it to be composed of an $MgCr_2O_4$ -$MgAl_2O_4$ solid solution (figures 5.2 and 5.3).

d) The bulk reaction atmosphere was not found to have any significant effect on reduction kinetics. Variation in gas flow rate and carbon monoxide partial pressure in the nitrogen gas stream were found to have little effect at temperatures in the region of 1200°C.

e) The nature and quantity of reductant were found to have an effect on the rate of reduction. The reaction rate was found to increase with increased carbon addition up to a certain point, beyond which no further increase was noted (figures 5.4 and 5.5).

FIGURE 5,1

COMPARISON OF THE REDUCTION RATES OF CHROMITE PARTICLES OF DIFFERENT SIZES

CONDITIONS:
TEMPERATURE : 1200°C (isothermal)
REDUCTANT : CARBON BLACK (25% addition)
CHROMITE : LG 6 (CHROME SAND)

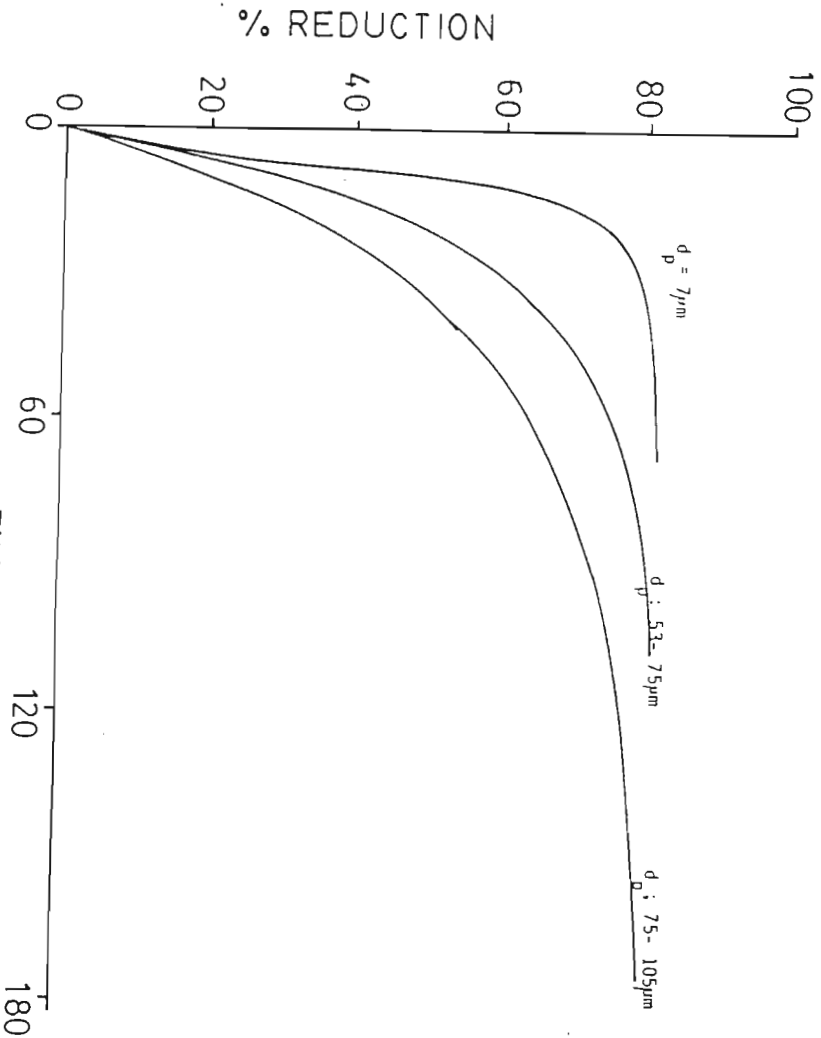

FIGURE 5,2

Comparison of the effect of temperature and particle size on the reduction rate of LG-6 chromite.

CONDITIONS:
REDUCTANT : CRABON BLACK
CHROMITE : LG 6 (chrome sand)
REDUCTION UNDER ISOTHERMAL CONDITIONS

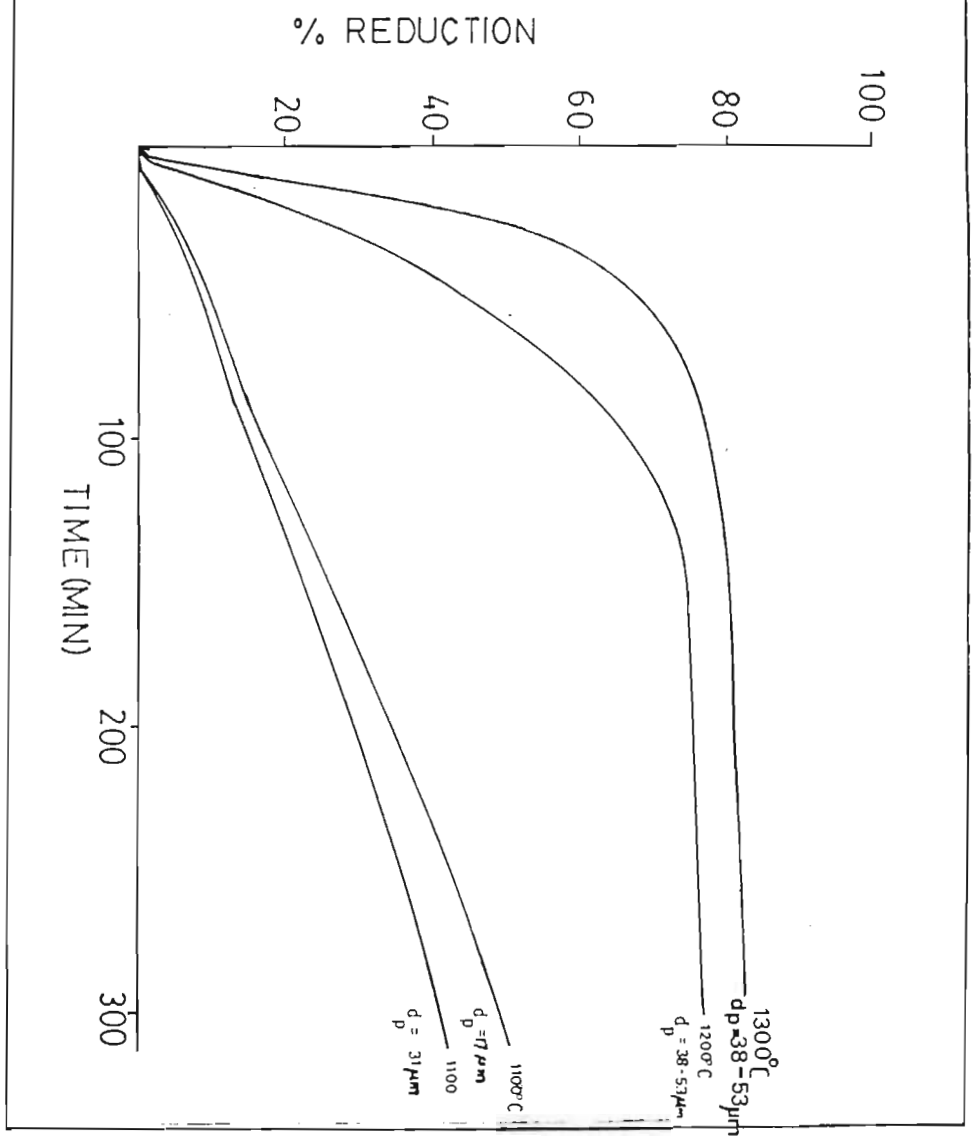

FIGURE 5.4

Comparison of the effect of varying carbon addition on the reduction rate of fine LG-6 chromite ore.

CONDITIONS: temperature = 1200C (isothermal)
chromite particle size: d_{50} = 7µm
carbon black reductant.

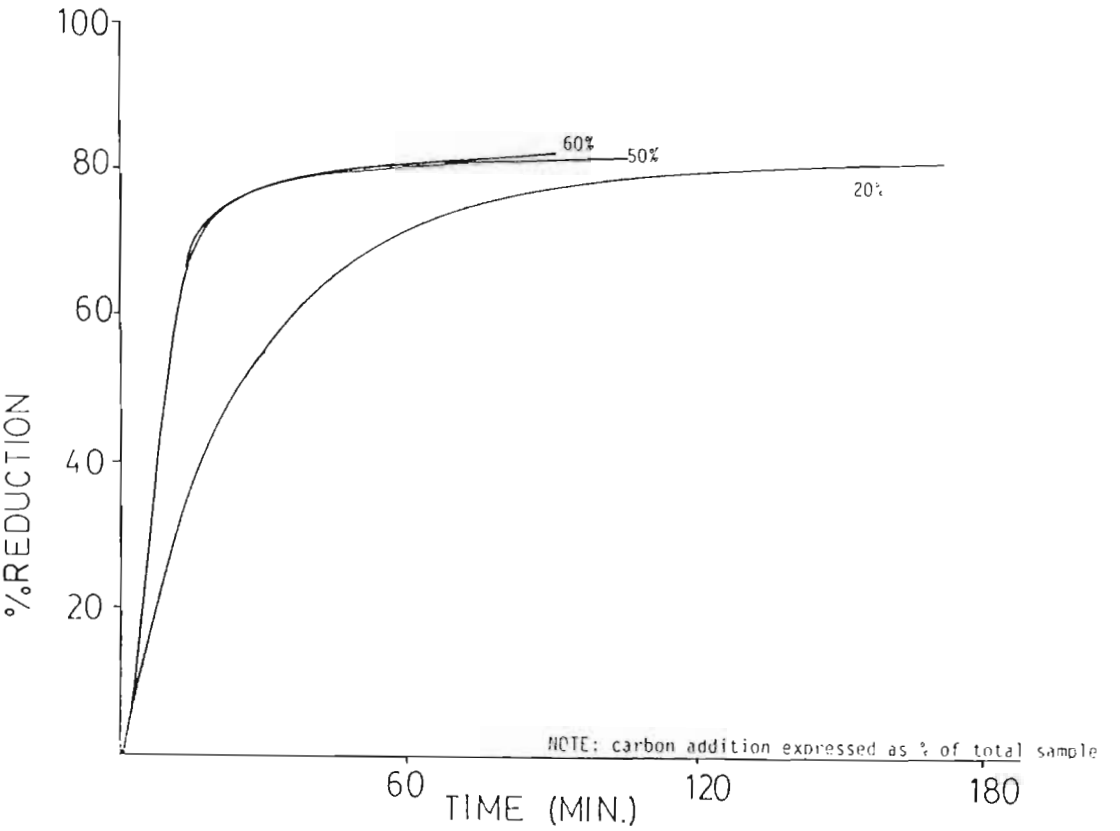

Reduction results obtained across a wide range of ore particle sizes and temperatures, indicating the existence of a reduction limit or ceiling.

CONDITIONS:
CHROMITE : LG 6 (chrome sand)
REDUCTANT: LAMP BLACK
ISOTHERMAL REDUCTION CONDITIONS

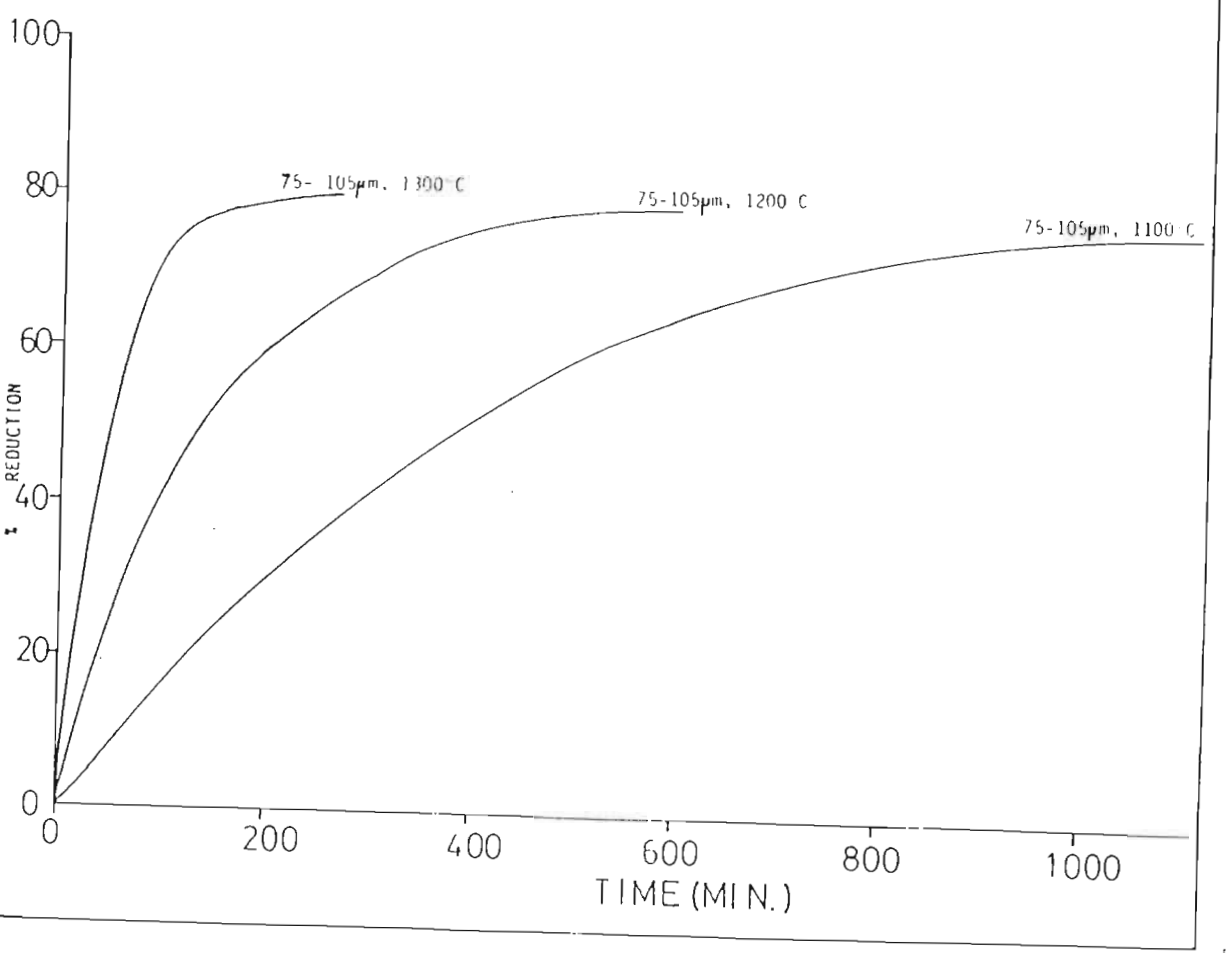

FIGURE 5.5

The effect of chromite particle size at high carbon addition
CONDITIONS: temperature 1200°C (isothermal)
reductant; carbon black
reductant addition = 50% of total charge mass.

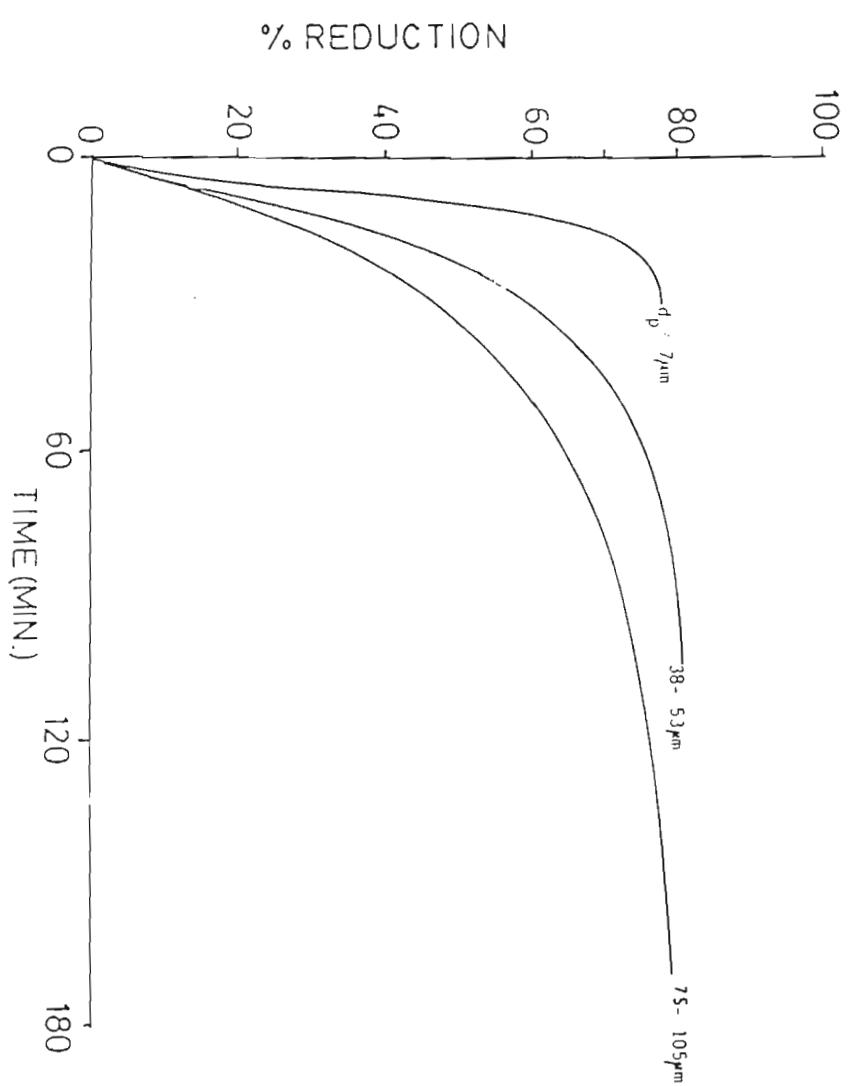

FIGURE 5.6

Schematic representation of features typical of a chromite grain undergoing reduction in the temperature range 1100°C- 1300°C.

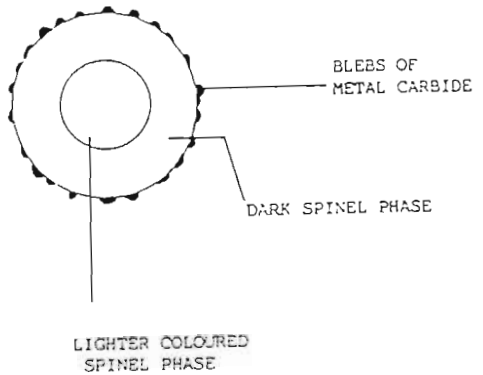

NOTES

1. DARK SPINEL PHASE HAS REDUCED IRON CONTENT
2. COLOUR MOST APPARENT IN BACK SCATTERED ELECTRON IMAGING MODE WHEN COMPOSITIONAL DIFFERENCES ARE HIGHLIGHTED

5.2.2 MINERALOGICAL INVESTIGATION OF REACTION PRODUCTS

Polished sections of chromite having undergone various degrees of reduction were studied under the optical microscope and S.E.M.,with the aim of establishing the sequence of events taking place during reduction. These samples all showed certain standard characteristics as indicated in figure 5.6.

Sections through particles sized between 53 and 75 micron diameter after reduction for varying lengths of time at 1200°C are shown in plates 5.1 through 5.5.

Some of the outstanding features are:

a) The competence of the chromite grain throughout the reduction reaction and even during the final stages of reduction.

b) The appearance of metal only at the grain exterior.

c) Rapid shrinkage of the iron rich core followed by a gradual lowering of the residual chromium and iron concentration throughout the grain.

The compositional changes taking place during the reaction, measured using E.D.S. and W.D.S. techniques, are summarised in table 5.1. Both these results and those obtained from the E.D.S. spectra of samples at various stages of reduction (figure 5.7), show a change in iron content in the outer rim of the grain while the core composition remains fairly static. Analysis of core and rim regions at subsequent stages during the reduction (figure 5.8) shows the composition of the core and rim regions to remain approximately constant

MINERALOGICAL SEQUENCE IN THE UNPROMOTED REDUCTION

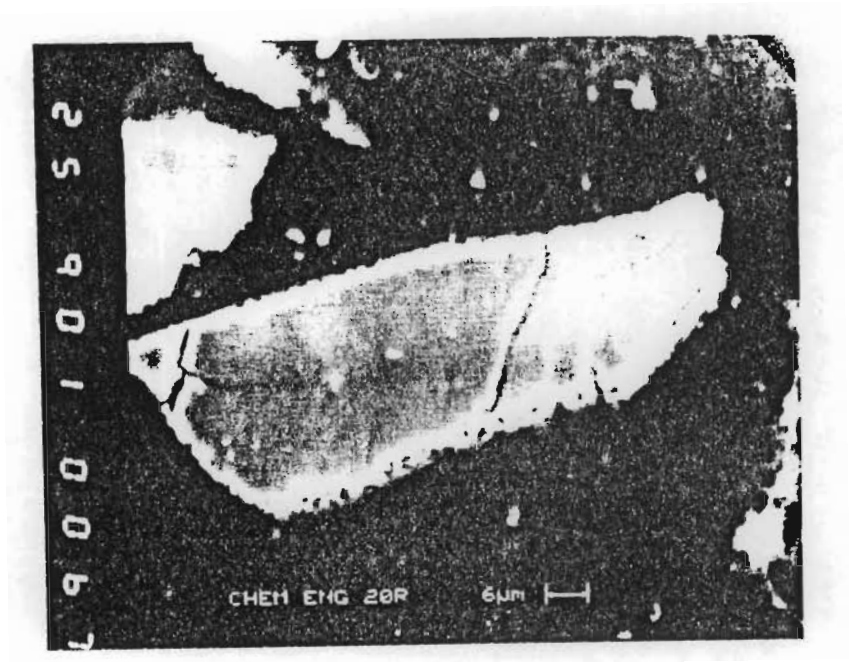

PLATE 5.1

The general appearance of a chromite grain after 20% reduction has taken place.

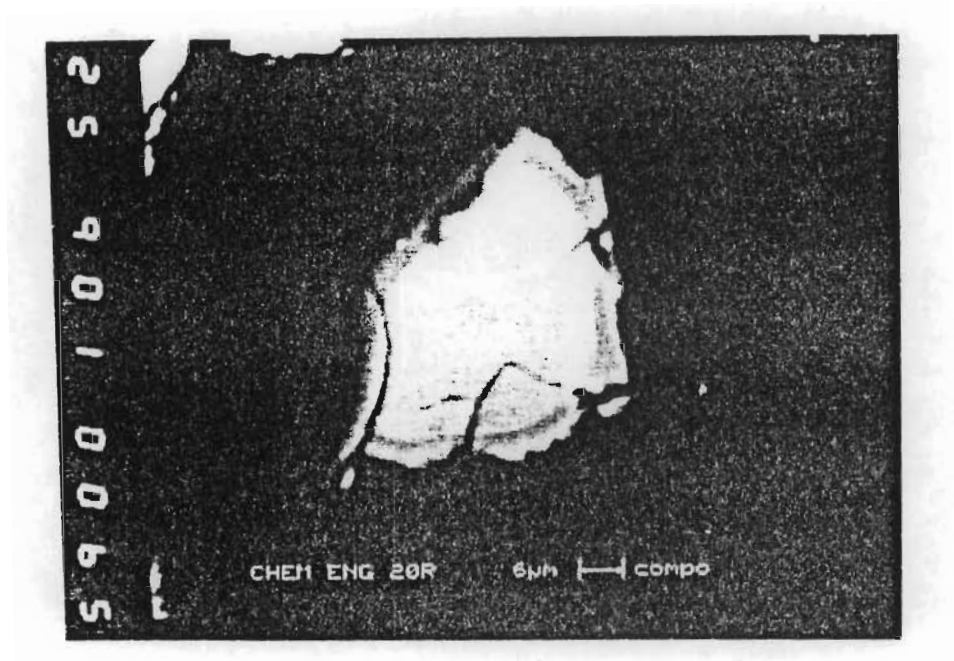

PLATE 5.2

Compositional S.E.M. photograph (or B.E.I.) of the material shown above at 20% reduction, showing the large core of different composition. (The cracks seen across the grain are a result of polishing)

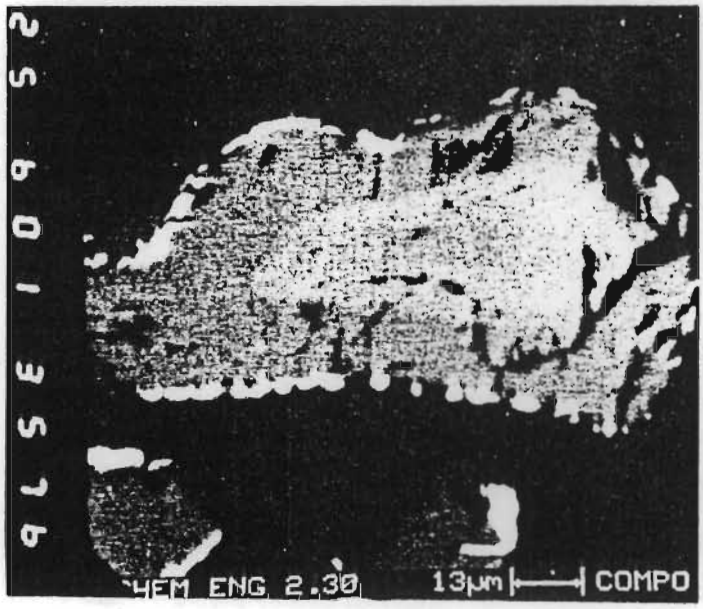

PLATE 5.3

Chromite grain at 30% reduction, showing the shrinking core and metal blebs evenly distributed around the grain perimeter.

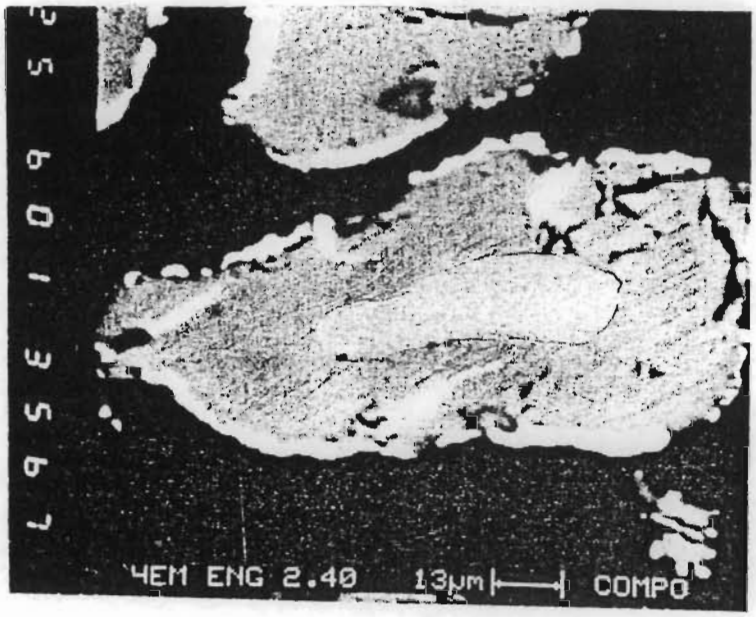

PLATE 5.4

Chromite grain at 40% reduction, with greatly reduced central core region (BEI)

MINERALOGICAL SEQUENCE IN THE UNPROMOTED REDUCTION

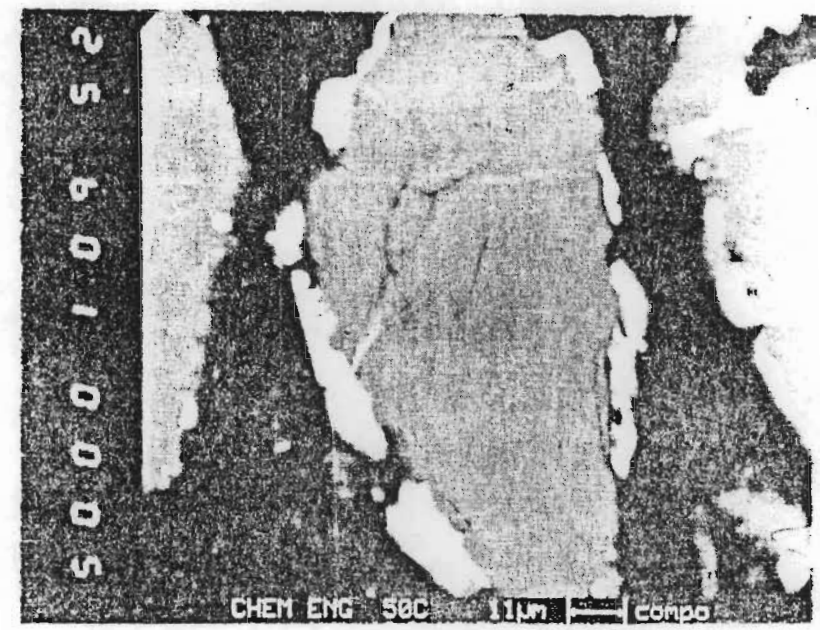

PLATE 5.5

Grain at 50% reduction (BEI), with no remaining core region visible.

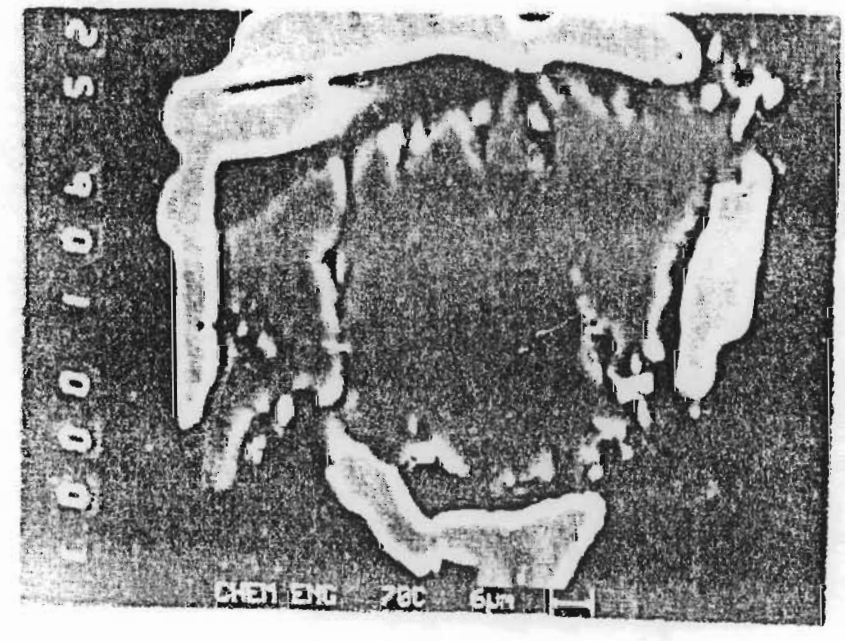

PLATE 5.6

Grain at 70% reduction (BEI), showing uniform composition and texture

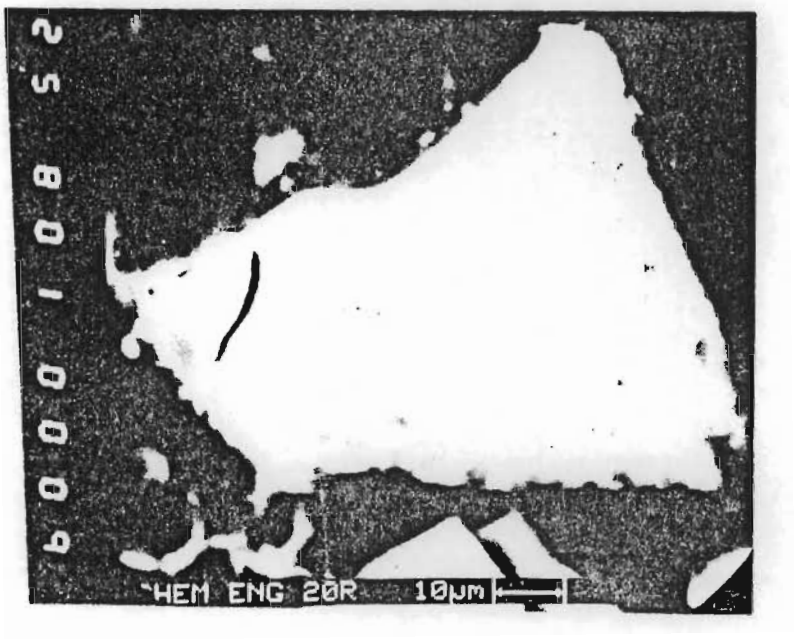

PLATE 5.7

Comparison between SEI (plate A) and BEI (plate B) imaging of the same grain under the SEM. - Highlighting the compositional and structural variations within the grain.

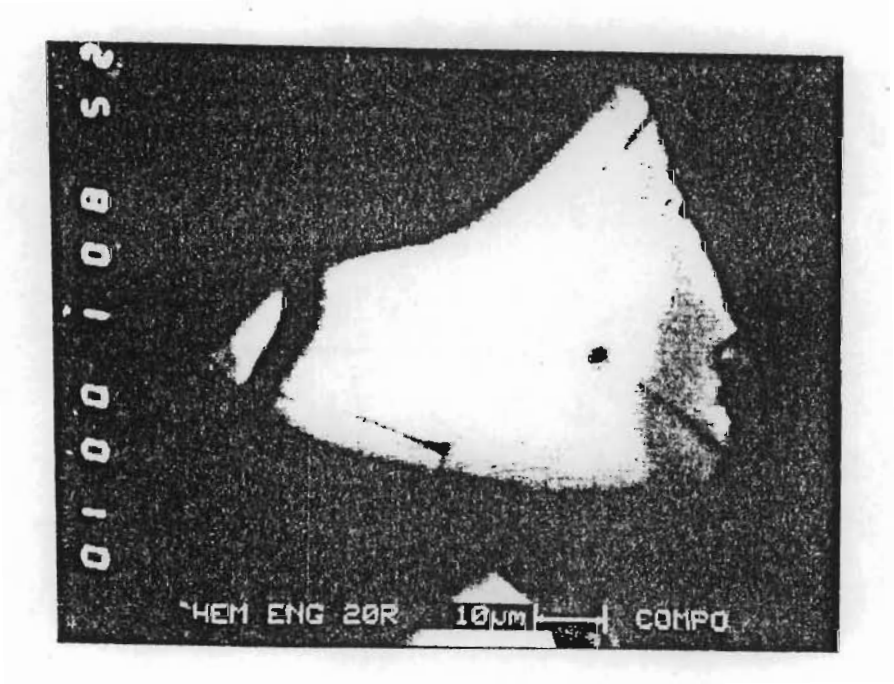

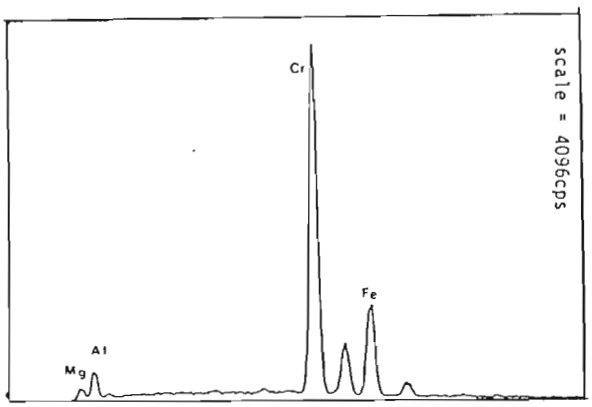

20% REDUCTION: GRAIN EDGE

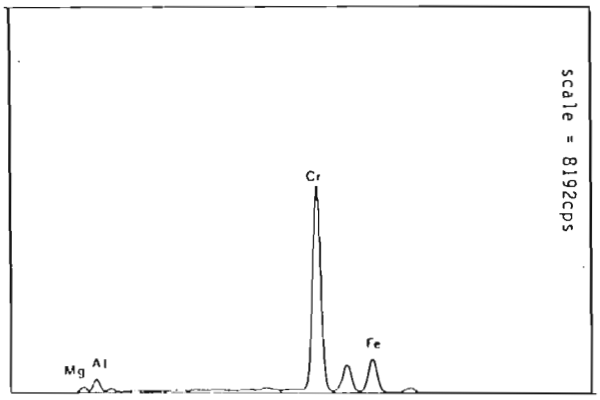

40% REDUCTION: GRAIN EDGE

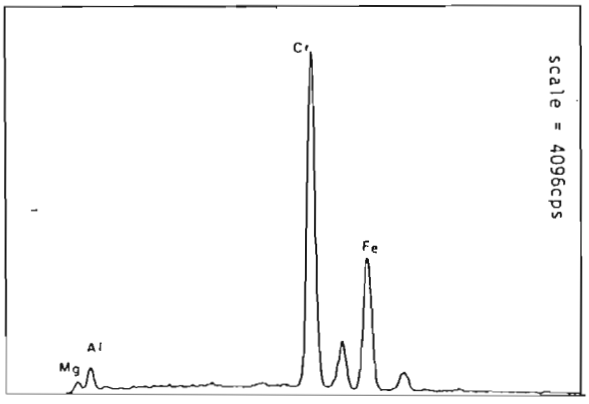

20% REDUCTION: GRAIN CORE REGION

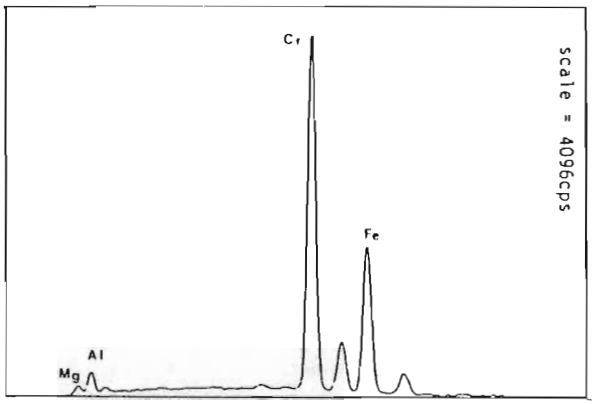

40% REDUCTION: GRAIN CORE REGION

FIGURE 5.7

Comparison of the E.D.S. spectra of the core and edge regions of chromite grains at 20% and 40% reduction.

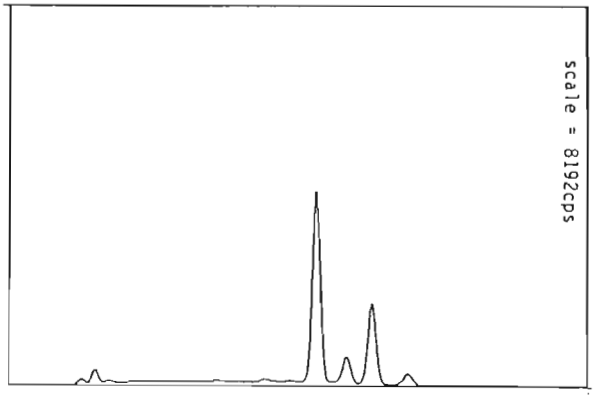

30% REDUCTION: GRAIN CORE REGION

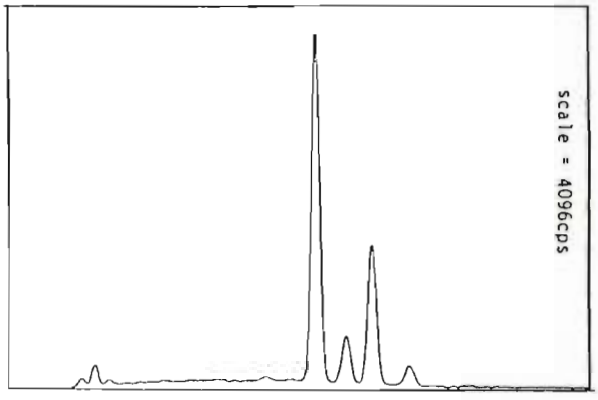

40% REDUCTION: GRAIN CORE REGION

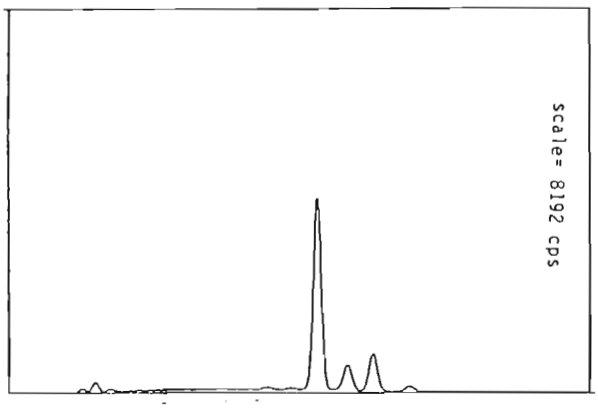

30% REDUCTION: GRAIN EDGE REGION

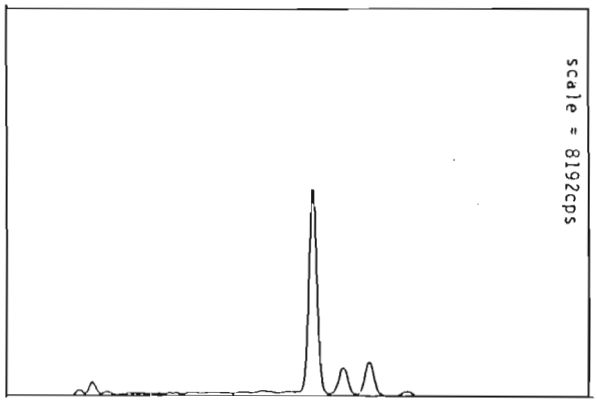

40% REDUCTION: GRAIN EDGE REGION

FIGURE 5.8

Comparison of core and edge regions of grains at 30% and 40% reduction showing the reasonably constant compositions maintained in these regions as the core is shrinking.

Comparison of E.D.S. spectra of metal, rim and core regions of a chromite particle at 40% reduction.

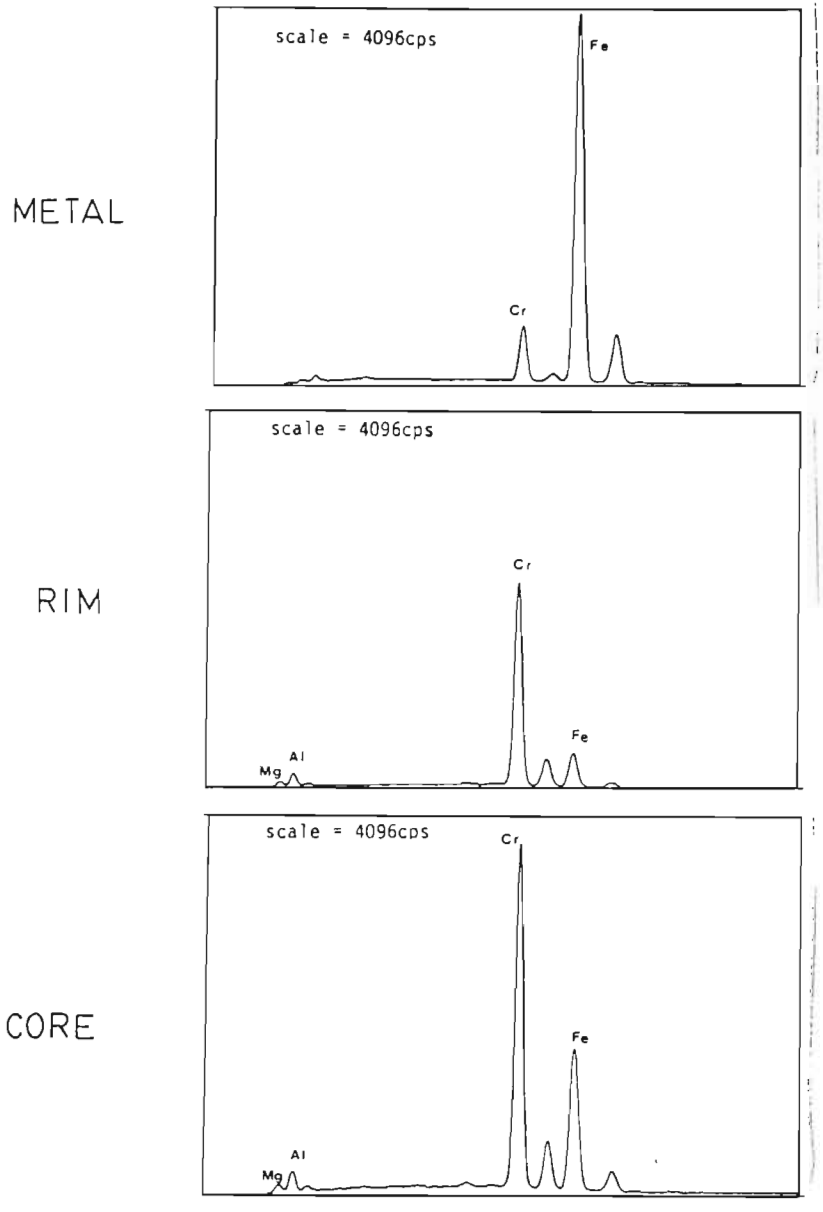

Comparison of the E.D.S. spectra of the metal, rim and core regions of a chromite grain at 50% reduction.

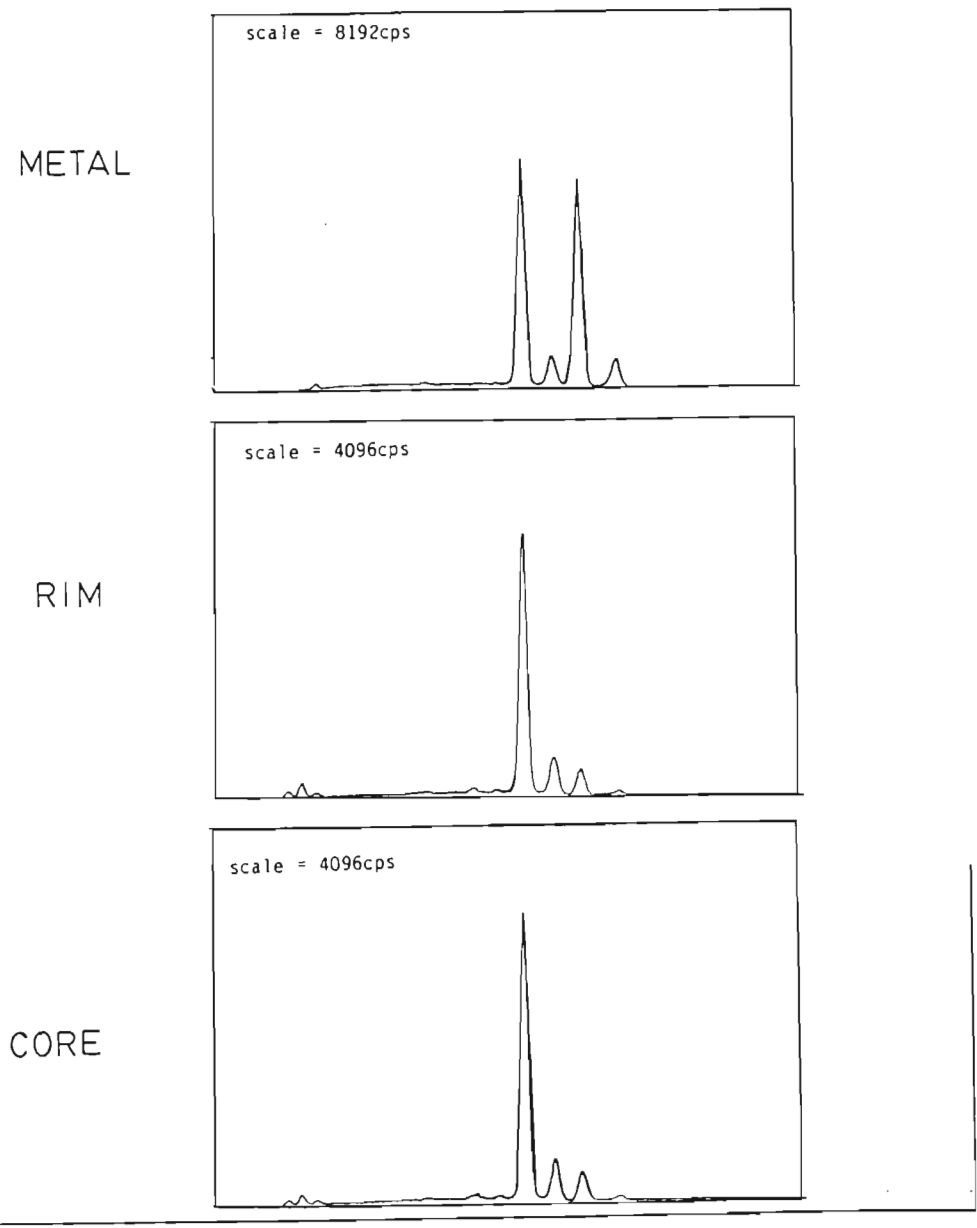

FIGURE 5.11(a)

Comparison of the E.D.S. spectra of the metal, rim and core regions of a chromite grain at 70% reduction showing the uniformity in composition across the grain cross- section.

RIM

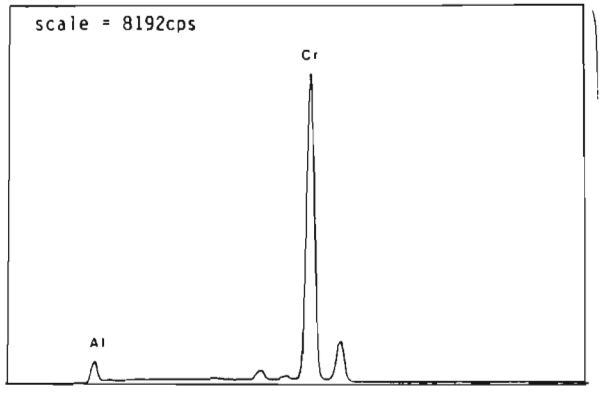

CORE

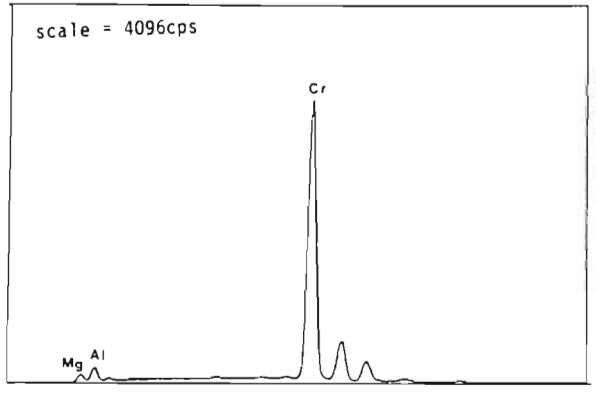

CORE

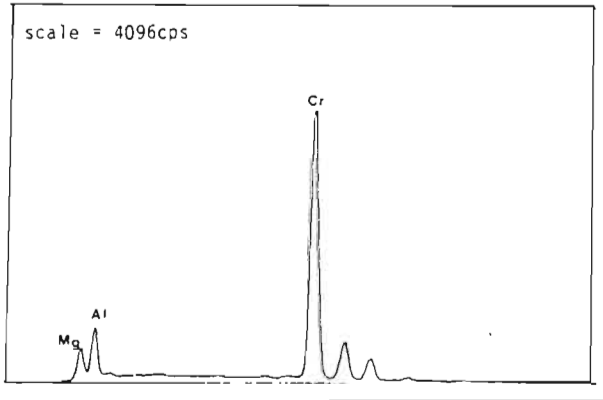

FIGURE 5.11(b)

Microprobe rate meter trace across a grain at approximately 74% reduction.

CONDITIONS: LG6 chromite ore, 53- 75 micron particle size
temperature = 1200°C isothermal
reductant = lampblack (carbon black)

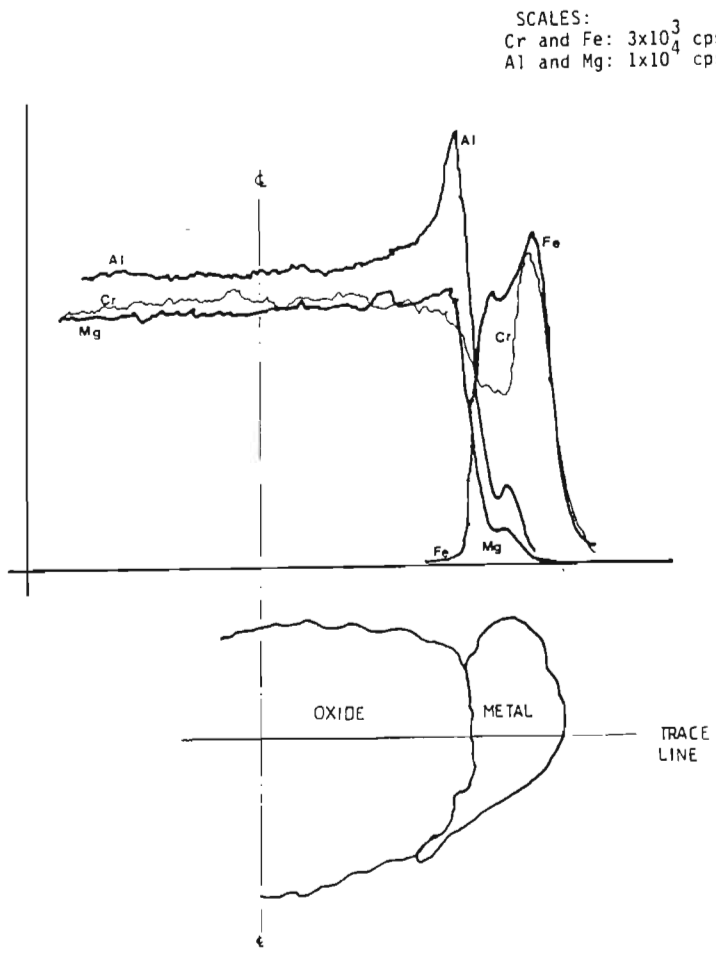

FIGURE 5,12

SCHEMATIC REPRESENTATION OF VARIATION IN COMPOSITION ACROSS SPINEL GRAIN.

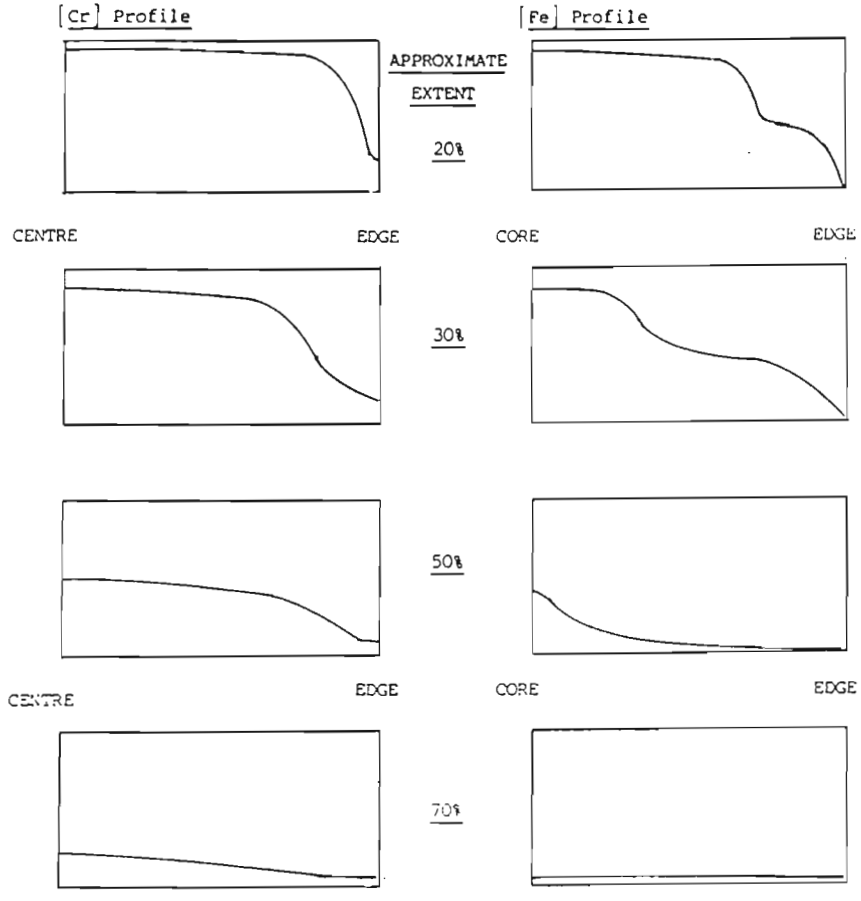

NOTES

1) CONCENTRATION SHOWN IN ABSOLUTE TERMS RELATIVE TO THE INITIAL SPECIES CONCENTRATION

2) STEP CHANGE IN [Fe] COINCIDENT WITH SHRINKING CORE

TABLE 5.1

S.E.M. Analysis of the different phases present in Chromite undergoing standard reduction.

% Redn.	$\overline{Cr}$ (Wt%)	$\overline{Fe}$ (Wt%)	$\overline{Mg}$ (Wt%)	$\overline{Al}$ (Wt%)	area
20	4,92	95,08	---	---	Metal
20	48,09	28,18	10,28	13,45	Rim
20	45,79	30,76	10,34	13,11	Core
30	14,74	85,26	---	---	Metal
30	52,36	24,04	9,71	13,89	Rim
30	49,63	28,37	9,38	12,63	Core
40	15,95	84,05	---	---	Metal
40	58,43	16,21	11,41	13,96	Rim
40	46,22	30,68	9,56	13,54	Core
50	40,50	59,50	---	---	Metal
50	73,80	9,88	7,95	8,37	Spinel Core
70	45,83	54,17	---	---	Metal
70	69,08	5,54	15,79	9,59	Spinel Core
75+	40,47	1,74	24,76	33,02	Spinel

while the core is shrinking.

The relative composition of the core, rim and metal regions (figure 5.9) indicates reduction of iron from the grain forming the expanding rim region and a metal phase composed of virtually pure iron. The change in iron composition between core and rim regions was found to correspond approximately to the removal of the trivalent iron content of the spinel.

Core extinction was found to occur at between 40% and 50% reduction, at which point the grain is found to have a fairly uniform composition through the cross-section (i.e. no compositional difference between core and rim regions, figure 5.10).

From the point of disappearance of the core, both the remaining iron and chromium concentrations were found to start decreasing, particularly near the edge of the chromite grain. The chromium content of the metal phase was found to increase in response to the removal of chromium from the spinel.

Towards the end of the reduction the grain was found to have a uniform composition in cross- section with a fairly high residual chromium content (figure 5.11).

The final spinel composition was found to be uniform throughout the grain and to correspond in analysis to an $Mg(Cr,Al)_2O_4$ spinel i.e. a solid solution of $MgCr_2O_4$ and $MgAl_2O_4$.

Changes in spinel composition may be summarised in terms of the concentration profiles for iron and chromium across the grain shown schematically in figure 5.12.

5.2.3 THE INFLUENCE OF EXTRANEOUS FACTORS ON THE REDUCTION RATE

As discussed in the literature survey, several other factors have been found to influence the reduction kinetics, in particular carbon type and proximity.

In the experimental work performed, efforts were made to minimize these effects through the use of ultra fine reductant added in quantities sufficient to ensure good mixing and optimum carbon- ore contact.

Additional assumptions made in interpreting the kinetic data were:

i) There is no significant degree of gangue contamination of the chromite particles.

ii) The carbon-chromite particle contact is assumed to be the same irrespective of ore particle size (i.e. assuming all chromite particles are evenly coated in reductant).

5.3 ANALYSIS OF EXPERIMENTAL RESULTS

5.3.1 THE IRON - CHROMIUM METALLIZATION CURVE

The reduction curves obtained in T.G.A. test work as shown in figures 5.1-5.5, represent the simultaneous occurrence of both iron and chromium metallization.

In order to perform an accurate analysis of the kinetics it is essential to separate the reduction curve, and perform the analysis in terms of the individual iron and chromium metallization rates.

Separation of the iron and chromium metallization rates is done using the iron- chromium metallization curve described in chapters 2 and 3.

In this instance an accurate metallization curve for LG6 chromite (figure 5.13), was established experimentally by halting the reduction reaction prematurely at different points and analysing the reaction products for the quantity of iron and chromium metallized.

Comparison of the experimental metallization curve with various other published results (figure 5.14) shows that the metallization curve obtained in this work is typical of a variety of similar ores.

These results indicate that the shape of the

FIGURE 5.13

Iron - chromium metallization curve for LG-6 chromite in the temperature range 1100°C - 1300°C.
(all experiments were performed with a 25% addition of carbon black as the reductant)

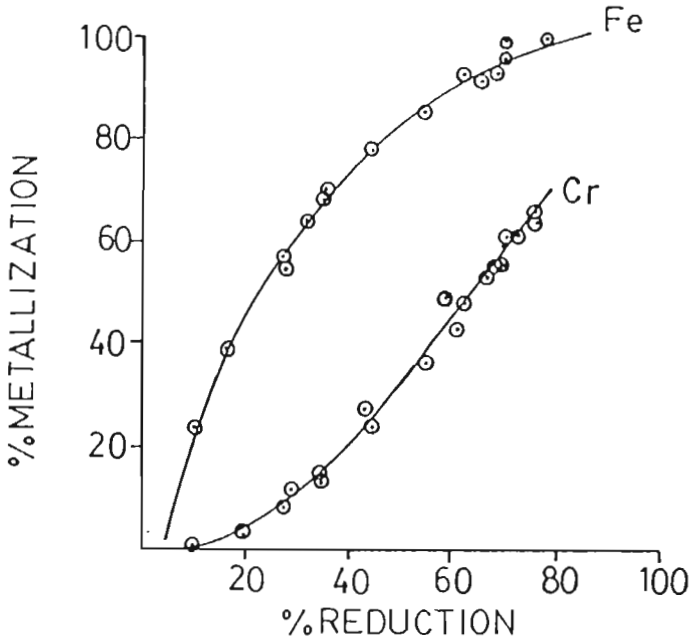

Comparison of the iron - chromium metallization curves for various ores at different temperatures.
A) UG-2 ore at 1100°C - 1200°C (reference 160)
B) UG-2 ore at 1300°C (references 12a and 160)
C) LG-6 and LG-5 ores at 1100°C - 1200°C (references 3,94,116 and this work)

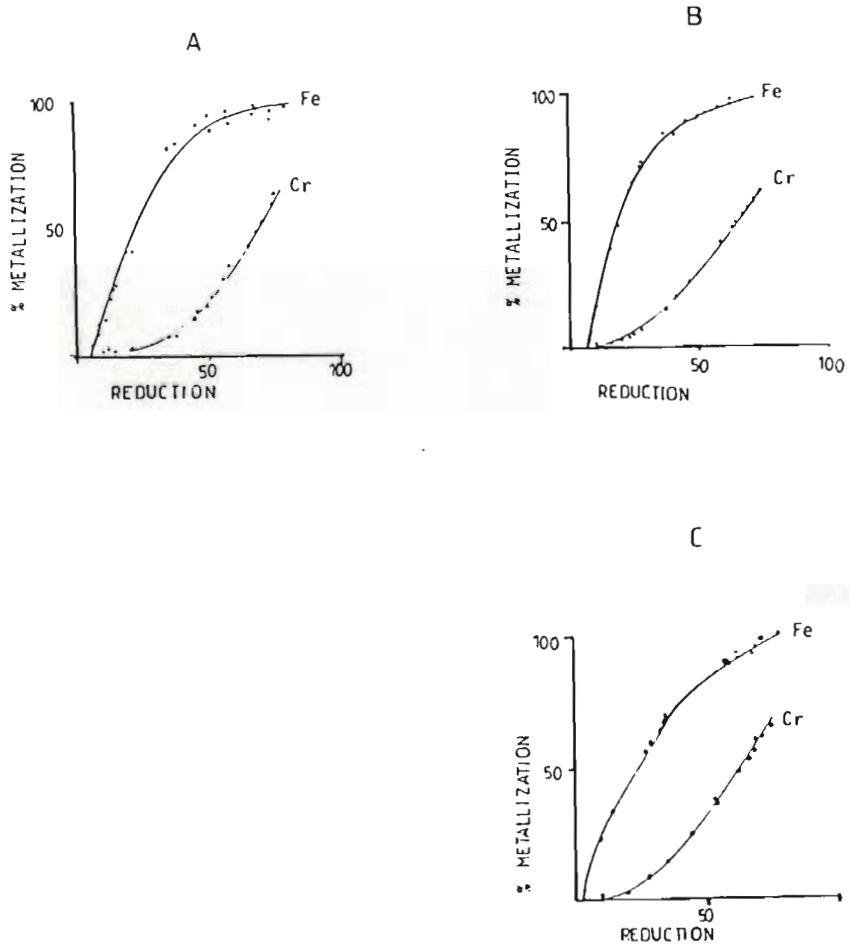

metallization curve is relatively insensitive to temperatures in the range 1100- 1300°C, but that ore composition does have a significant effect on the shape of the curve. Thus within the accuracy of the experimental results and the narrow range of particle size, temperature and reductant addition investigated, a single metallization curve can be used to describe the relationship between overall extent of reduction and the individual extents of iron and chromium metallization for a particular type of ore.

However, despite the close similarity found between the metallization curve determined from experimental results and that calculated assuming equilibrium between metal and oxide phases, the presence of sharp concentration profiles across the grain during the reduction reaction clearly indicate that the metal and oxide are not in equilibrium as suggested by Kucukkaragoz (93). It is concluded that the actual relationship between overall extent of reduction and the individual extents of iron and chromium metallization has a measure of kinetic dependence inherent in it.

The fact that the calculated 'equilibrium' curve mimics the actual experimental reduction curve is an indication of the complex relationship between the kinetic behaviour of the individual species participating in the reaction and the thermodynamic activity (or chemical potential) of these species.

The postulated kinetic dependence inherent in the metallization envelope is of particular significance with respect to the reaction limit encountered at approximately 76% reduction (in terms of the

metallization curve this limit is shown up as an incomplete metallization envelope).

The results obtained in this work show this limit to be relatively insensitive to temperature, a result atypical of any thermodynamic limitation. Such a kinetic dependence has the implication that manipulation of the reaction kinetics (e.g. increasing them), could result in a variation in the metallization curve. Most importantly, a possible closing of the metallization envelope implying a higher degree of metallization might be attained.

However, before considering this aspect in any detail (chapter 6), consideration is first given to the kinetics of the standard chromite reduction reaction in terms of the individual rates of iron and chromium metallization.

5.3.2 RESULTS IN TERMS OF THE INDIVIDUAL CHROMIUM AND IRON METALLIZATION RATES

Having established the metallization curve for LG6 ore, this curve can be used to translate the extent of reduction measured at a particular time using the T.G.A., into the individual extents of iron and chromium metallization at that point.

Thus a standard reduction curve (figure 5.1) can be represented in terms of the individual extents of iron and chromium metallization as shown in figure 5.15, the latter giving a more detailed image of the reduction reaction on which to perform any kinetic analysis.

The effects of parameters such as particle size, reaction temperature and ore composition on the individual iron and chromium reduction rates can now be

FIGURE 5.16

The effect of carbon addition on the individual iron and chromium reduction rates.

CONDITIONS: LG-6 chromite, 53- 75micron size
temperature = 1200°C (isothermal)

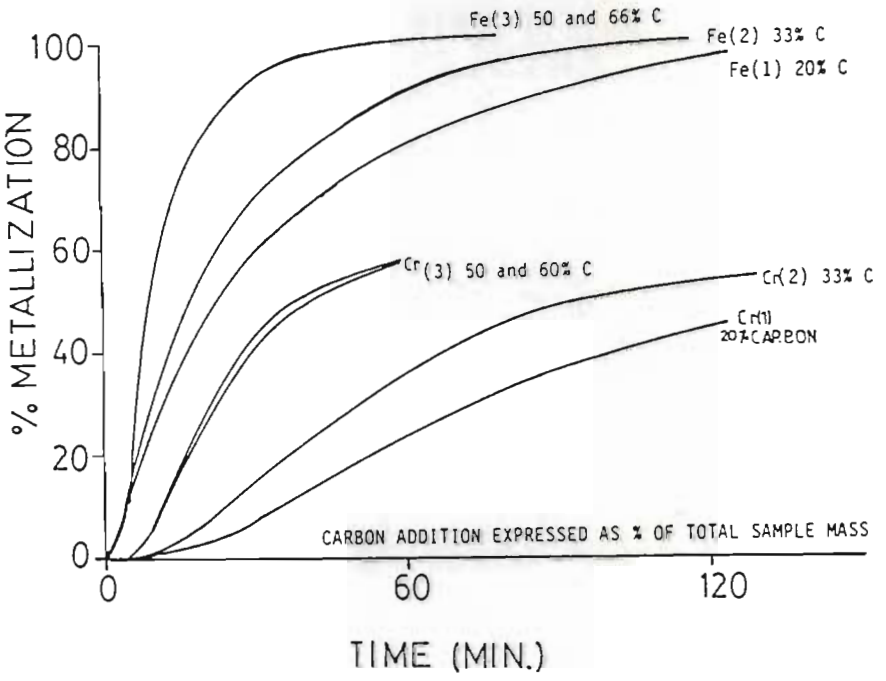

FIGURE 5.15

Description of the standard composite reduction rate in terms of the individual iron and chromium reduction rates using the metallization curve shown in figure 5.13.

CONDITIONS: LG-6 chromite , 53-75 micron in size
carbon black as reductant (25% addition)
temperature = 1200°C (isothermal)

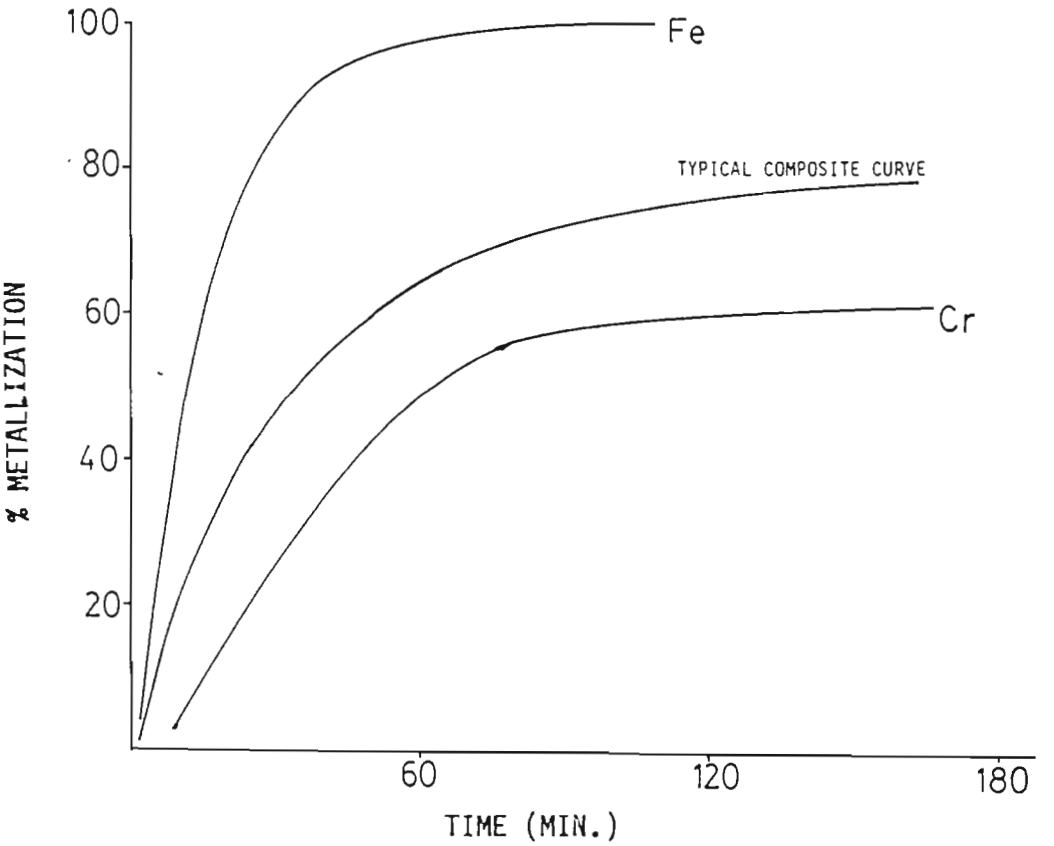

analysed as shown in figures 5.16 and 5.17.

These curves clearly indicate that the limit found in practice at approximately 76% reduction, corresponds to a limit only in terms of the extent of chromium reduction of approximately 65%.

Mineralogical examination of samples at this stage of the reaction shows the residual oxide phase to be an $MgOCr_2O_3$- $MgOAl_2O_3$ solid solution containing insignificant quantities of iron, in agreement with the results calculated in chapter 3.

Comparison of the chromium metallization profiles at different temperatures (figure 5.17b), indicates that the limit experienced in chromium metallization is temperature sensitive in the range 1100-1300°C. Relatively small particle sizes and relatively long reaction times at high temperatures (1300°C and above) are required to achieve higher extents of chromium reduction (Algie, 3).

From the results presented above, it would appear that the kinetic inhibition experienced during the latter portion of the reduction reaction stems from the formation of a picrochromite- spinel solid solution at the surface of the chromite grain.

The formation of this refractory layer covering the grain would act to retard the reaction kinetics by hindering the movement of species, particularly chromium across it. It is believed that this isolation of the grain interior leads to a very rapid decrease in reaction kinetics, giving rise to the apparent reaction ceiling commonly experienced in experimental work.

The importance of factors internal to the chromite grain, such as composition and particle size, compared to factors external to the chromite grain such as the

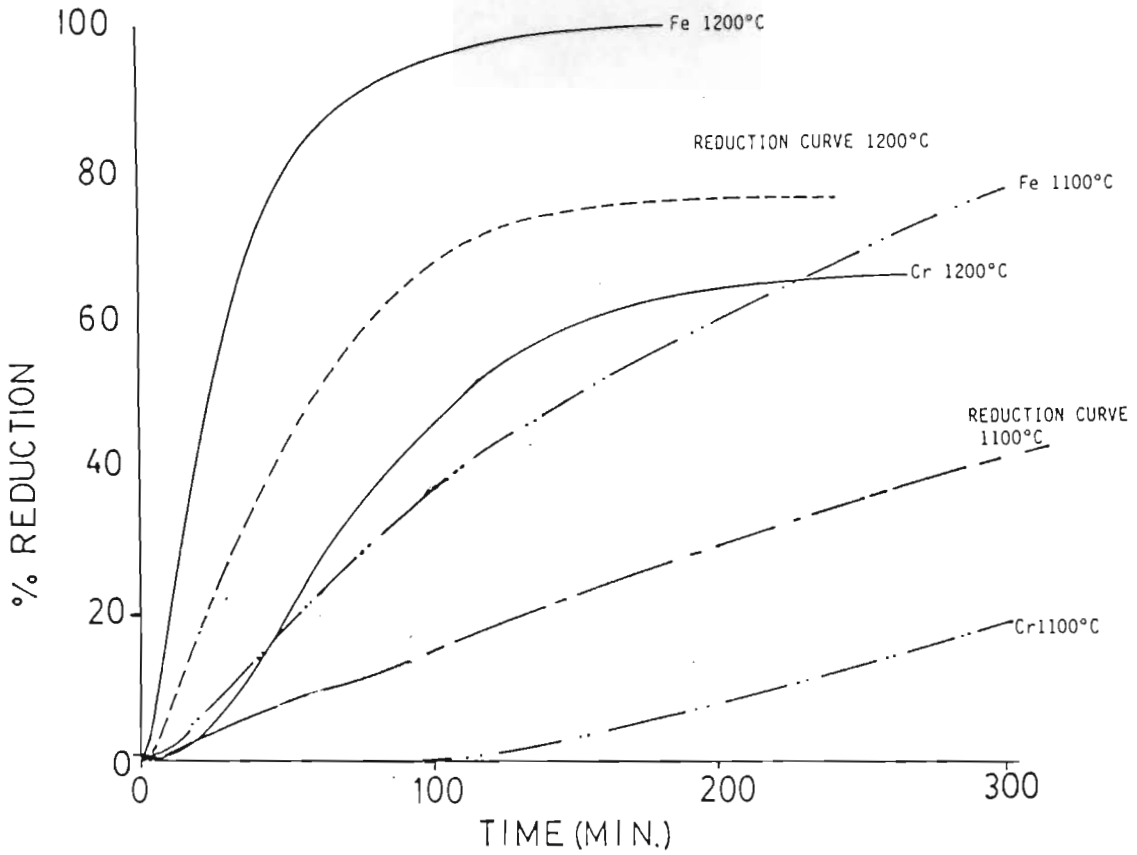

The effect of temperature on the individual rates of iron and chromium reduction. A dramatic decrease in the rate of chromium reduction is seen below 1200°C.

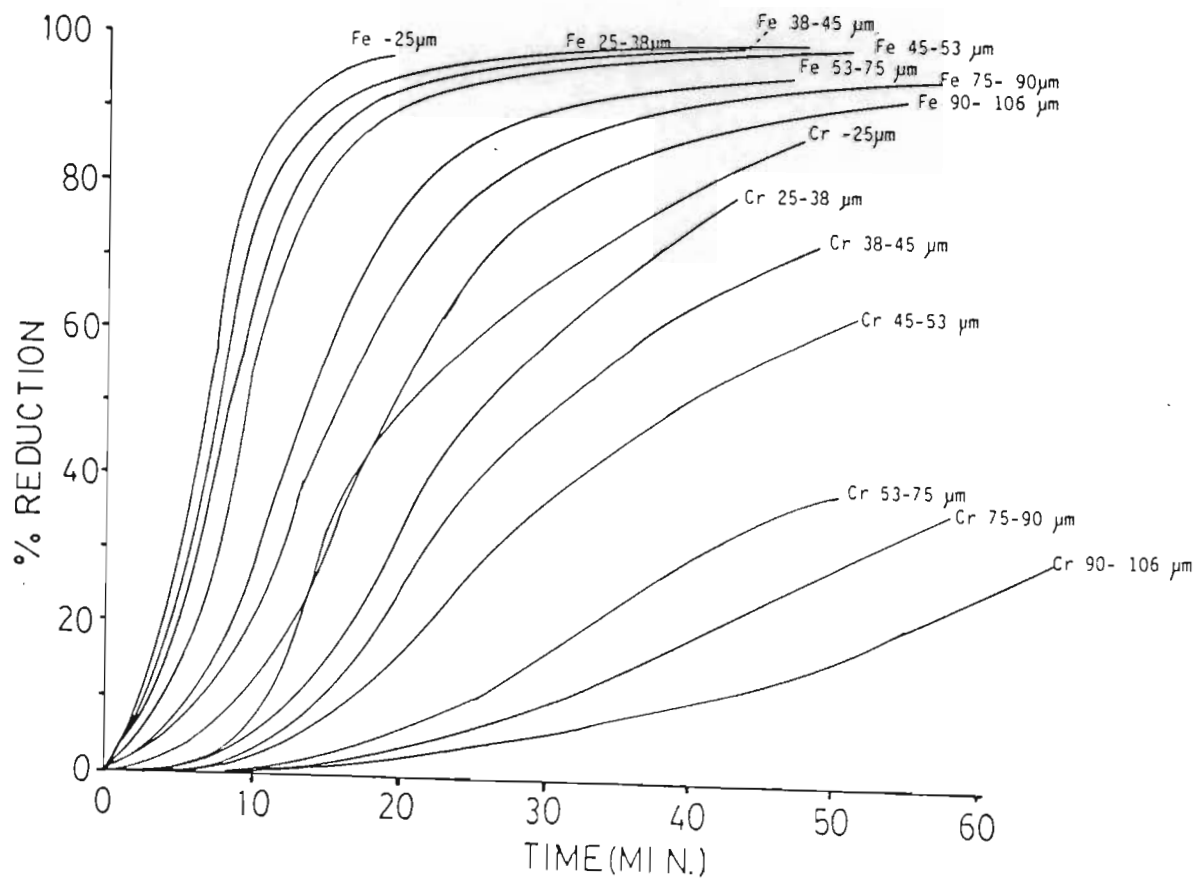

for different particle sizes of UG2 ore at 1300°C. (Original data from Searle and Finn, 160).

composition of the gas atmosphere, indicates that factors internal to the chromite grain are largely responsible for overall rate control.

Examining the various possible rate limitations that could apply to the reduction reaction in the light of the kinetic and mineralogical data gathered, the possibilities exist that one or more of the following limitations may govern reduction kinetics at some stage during the reaction:

a) Mass and heat transport in the fluid phase.

b) Reaction initiation and product nucleation.

c) Surface reaction kinetics.

d) Solid state diffusion.

As regards mass transfer, inter particle diffusion of carbon monoxide is known to be rate limiting in the extreme cases of rapid reduction of iron oxides where normal pore diffusion limitations have been eliminated through the use of very fine particles (Themelis et al., 175). However, no significant bulk diffusion limitations are encountered in the case of hematite reduction with fine carbon black (Rao, 145), or in the case of the kinetically slower reduction of ilmenite (den Hoed, 43).

In comparison, the slow nature of chromite reduction, and the small response to variations in bulk gas flow rate and gas composition (CO partial pressure in the nitrogen gas stream), suggest that this form of rate limitation is not likely to dominate either iron or chromium reduction kinetics for the duration of the reduction reaction.

A similar conclusion is reached regarding the possibility of heat transfer to the ore sample as being

rate limiting. The small charge mass and volume, unhindered radiation path and gas flow around the sample ensure a relatively rapid rise in sample temperature (~ 4 minutes) compared to the duration of the reaction (~ 4 hours). This makes it unlikely for heat transfer limitations to dominate reaction kinetics over any significant part of the reaction.

Algie et al. (3) suggested that metal nucleation may play an important part in determining reduction kinetics. Again, the relative duration of the period of metal nucleation compared to that required for the entire reduction reaction makes it unlikely for such a process to dominate the kinetics over any extended period of the reaction. Further, the suggestion that nucleation takes place at specific sites on the chromite surface, dependent on crystallographic orientation, giving rise to a porous structure are not supported by the S.E.M. investigations performed in this work. The approximately uniform distribution of reduction sites around the periphery of the grain, independent of grain size or shape; contrast sharply with the results of Algie et al. (3), and is most likely a reflection of the closer contact and more even distribution of carbon and chromite obtained in this work by using carbon black.

Possibly the most significant feature of the reduction reaction is the marked iron concentration profiles found in the first half of the reduction reaction.

The presence of this profile clearly indicates a rate limitation internal to the chromite particle, and since this profile is present during the first and most rapid

stage of reduction the same factor might be expected to dominate reduction kinetics throughout the reduction reaction.

The existence of an internal rate limitation together with the fact that migration of the iron and chromium species towards the surface of the grain must have taken place makes solid state diffusion the most likely rate limiting process.

Should solid state diffusion specifically be rate limiting in the case of either chromium or iron, a number of the following characteristics would be expected:

a) Concentration profiles for iron and chromium within the grain.

b) A marked dependence of reduction kinetics on particle size.

c) A marked dependence of reduction kinetics on temperature.

d) A relative insensitivity of reaction kinetics to external factors including gas composition and flow rate.

All of these features are found in the T.G.A. results obtained on both LG6 and UG2 ore.

It is concluded that within the temperature and particle size range investigated in this work, the kinetics of both iron and chromium reduction are controlled by the rate of diffusion of these species through the chromite spinel.

5.4 DIFFUSION IN THE CHROMITE SPINEL

The obvious importance of diffusion within the chromite spinel in terms of the overall reaction

kinetics prompts a closer analysis of the diffusion process.

The close packed structure of the spinel and the relative size of ionic species and interstices suggest that diffusion of the iron and chromium species will take place largely by means of a vacancy mechanism. Thus the diffusion of these species would be governed by the availability and mobility of vacancies within the spinel.

The large compositional variation experienced within the spinel during the course of reduction implies that significant deviation from stoichiometry within the spinel is likely. The changing composition and stoichiometry is likely to result in changing concentrations of vacancies on particular lattice sites and thus in diffusion coefficients for the various species.

The changes occurring within a control volume* of the spinel during reduction were analysed in terms of the ratio of trivalent to divalent cations within the spinel.

Based on the assumption that the metallization curve described above (figure 5.13) is applicable to the control volume, a balance can be performed on the residual spinel, expressed in terms of the cation ratio $\Sigma 3+/\Sigma 2+$, as a function of the extent of reduction (figure 5.18).

A clear deviation from stoichiometry within the spinel is found, implying relatively high concentrations of defect vacancies until the point is reached at which a balanced spinel structure is reached at approximately 75% reduction.

*(A volume that is small enough to remain uniform)

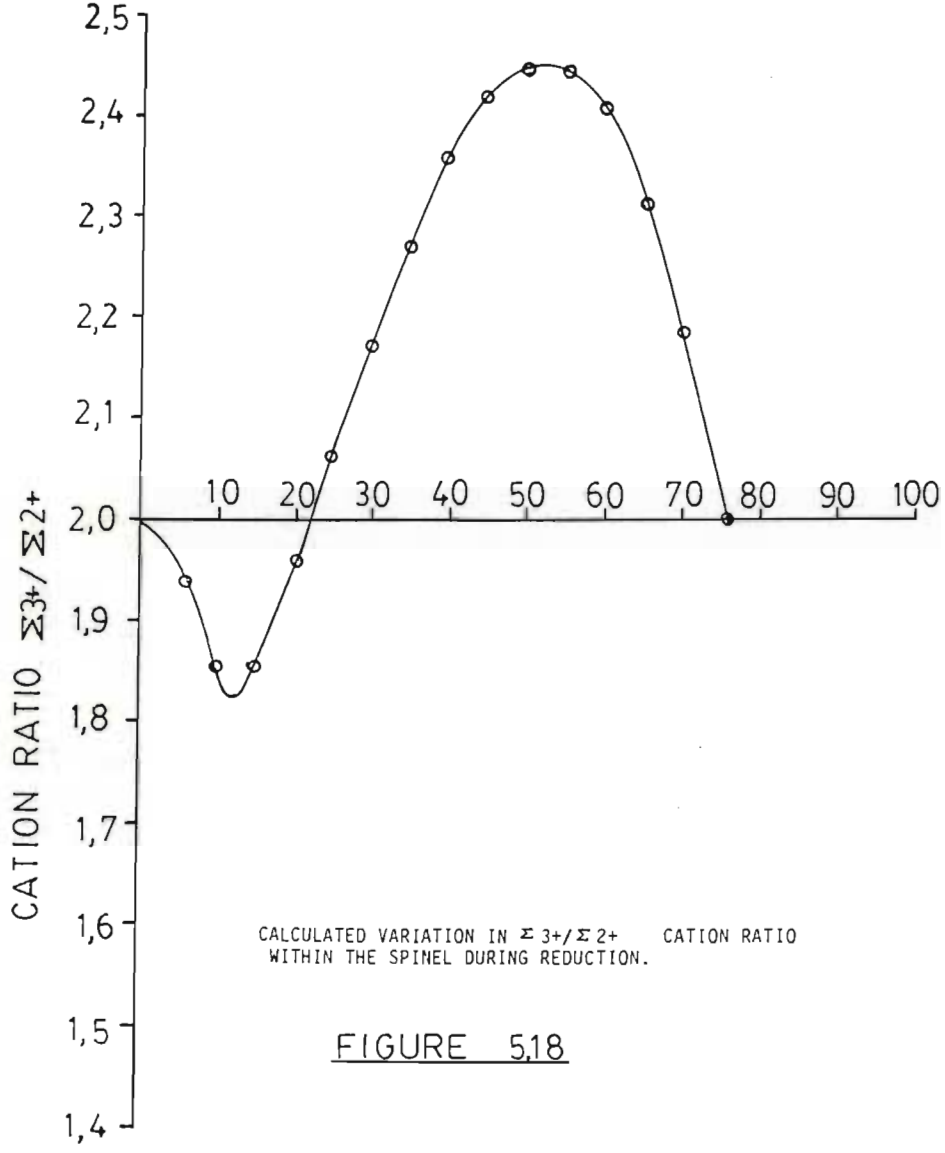

CALCULATED VARIATION IN $\Sigma 3+/\Sigma 2+$ CATION RATIO WITHIN THE SPINEL DURING REDUCTION.

FIGURE 5.18

FIGURE 5.19 Schematic representation of the reduction model.

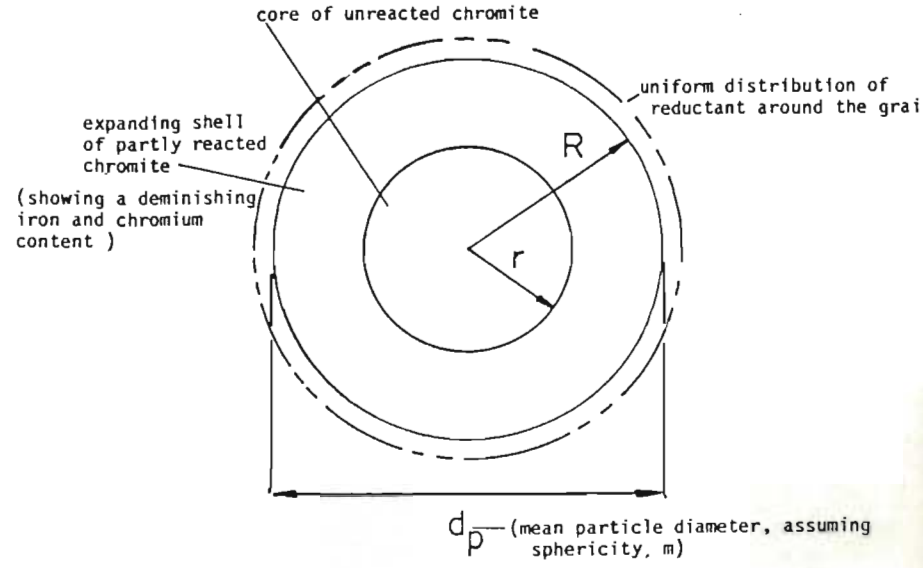

r = core radius, m
R = particle radius, m $(=d_p/2)$

The shape of this curve shows three distinct stages in the reduction sequence:

a) Negative deviation in the $\Sigma 3+/\Sigma 2+$ ratio (relative to the balance point of 2 for a normal spinel), caused by reduction of the Fe^{3+} species.

b) A strong positive deviation caused by reduction of the Fe^{2+} species.

c) A strong negative deviation caused by reduction of the Cr^{3+} species.

The significance of these results lies in the relative concentration of specific site defects indicated by the change in $\Sigma 3+/\Sigma 2+$ ratio.

The experimental data and discussions presented above, and the non rigorous analysis of the diffusion behaviour of species in the spinel during the reduction reaction (as detailed in appendix 5), suggests that the reduction reaction is controlled by the solid state diffusion of species through the spinel lattice to the surface of the grain.

The diffusion of iron and chromium species in the spinel is expected to be similar to the diffusion behaviour typical of a ceramic oxide showing intrinsic nonstoichiometric behaviour. Principally one diffusing species is expected to be dominant at any point during the reaction, and that the entire reduction reaction would thus be characterised by a sequence of major diffusing species.

A relatively high diffusion coefficient is expected for the iron component originally located in octahedral lattice sites, with significantly smaller coefficients for the remainder of the iron and particularly the chromium species. A significant decrease in the

chromium diffusion coefficient is expected towards the end of the reduction reaction, at a point equivalent to that where the formation of a picrochromite- spinel solid solution is encountered in practice (i.e. after approximately 76% reduction has taken place). This is considered to be the principal reason for the apparent reduction ceiling encountered in experimental work.

Though temperature must have an exponential effect on the absolute values of the individual diffusion coefficients, it is expected that their relative magnitudes would be affected to a much smaller extent. As a result the metallization curve would be expected to remain fairly constant over a range of temperatures.

In contrast the composition of the chromite spinel, in terms of the relative quantities of cationic species and hence vacancies, is expected to have a much more significant effect on the individual iron and chromium diffusion coefficients and hence a correspondingly significant effect on the shape of the metallization curve as seen in practice.

Having outlined in some detail a postulated mechanism for chromite reduction, an indication of the accuracy of the model can be gained by comparing the results obtained from a mathematical expression of this model with actual experimental results.

5.5 A KINETIC MODEL FOR CHROMITE REDUCTION

5.5.1 BASIS FOR THE MODEL

Consider a single chromite particle, assumed to be spherical with a specific diameter, undergoing isothermal reduction with an abundance of carbon at its

surface (figure 5.19).

From the discussion above, the formation of vacancies, stemming from the progressive removal of cations from the spinel would result in a growing shell rich in vacancies, through which the cations would have to diffuse. This condition is expected to persist up to the point where the spinel composition at the surface of the grain reaches a relatively high extent of reduction, and effective isolation of the grain interior takes place. The latter condition resulting in the apparent reaction limit at approximately 76% reduction.

Such a system can be simply expressed in mathematical terms using a shrinking core type model, with diffusion through an altered shell layer as being rate determining (Yoon et al. [206]; Levenspiel, [103], see appendix 6). Assuming that iron and chromium reduce independently, the extent of reduction of species i, at any time t, may be simply expressed as:

$$t/\tau = 1-3(1-x)^{2/3} + 2(1-x) \quad \text{----- (5.1)}$$

where Ti is the time taken for complete reaction of species i ($\tau = R^2/6\,D_i$) and D_i is the effective diffusion coefficient for species i through the partially reacted spinel.

The net extent of reduction can then be calculated by adding the individual extents of iron and chromium reduction in proportion to their occurrance in the ore.

Initially the results of Searle and Finn (160) on UG2 ore at 1300°C, together with the appropriate metallization curve, were used to establish values of τ_i and D_i over a range of particle sizes.

Values of τ were found to be relatively linear in R^2,

but a distinct y intercept was found (figure 5.20), implying the existence of an additional limitation i.e.

$$\tau_i = R^2/6D_i + C_i \quad \text{------ (5.2)}$$

However, since insufficient data were available to meaningfully define the nature of this additional limitation any further, values of τ_i obtained from experimental results were used according to equation 5.2 to define values of C_i and D_i for a particular ore type under specific conditions.

Results obtained using this model were found to closely match experimental results as shown in figures 5.21 and 5.22.

In addition the iron- chromium metallization curve obtained using this model bears a close resemblance to the metallization curves established experimentally (figure 5.23). This provides a clear indication that the postulated mechanism of reduction closely approximates the actual reduction reaction.

The values of D_i and C_i calculated from experimental results (as shown on the figures) were found to be sensitive to the nature of the reducing environment (including carbon type and addition) as well as ore type and temperature. Values of D_i were found to decrease and of C_i to increase with decreasing temperature as expected. However it must be emphasised that the values of D_i and C_i obtained represent effective values and are not intrinsic to the system.

Apart from the work described in this thesis, the only other attempt to calculate the diffusion of cationic species in a naturally occurring chromite spinel was that performed by Soykan (169), who published a value of $2{,}63.10^{-9}$ m^2s^{-1} for D_2. However, close examination of the method employed shows several inaccuracies, and substitution of more appropriate

FIGURE 520(a) Analysis of the variation in time to complete reduction of the Fe^{2+} species (τ_1) with particle size.

UG 2 ORE, 1300°C

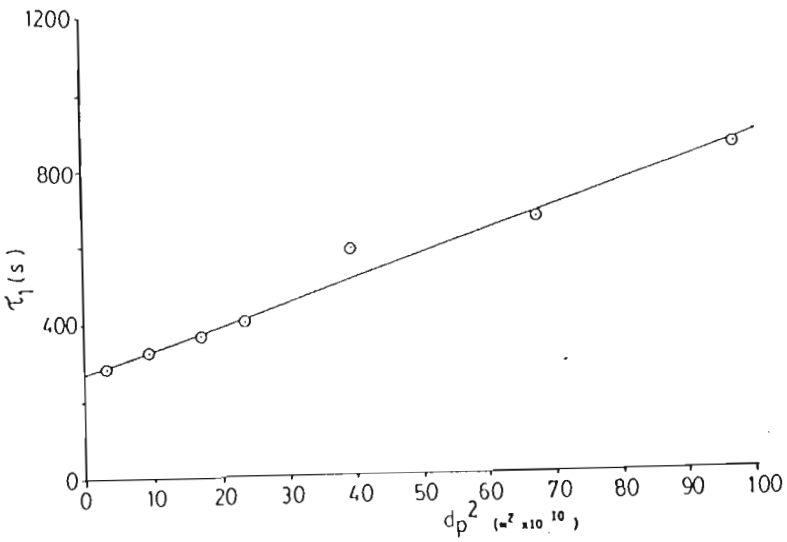

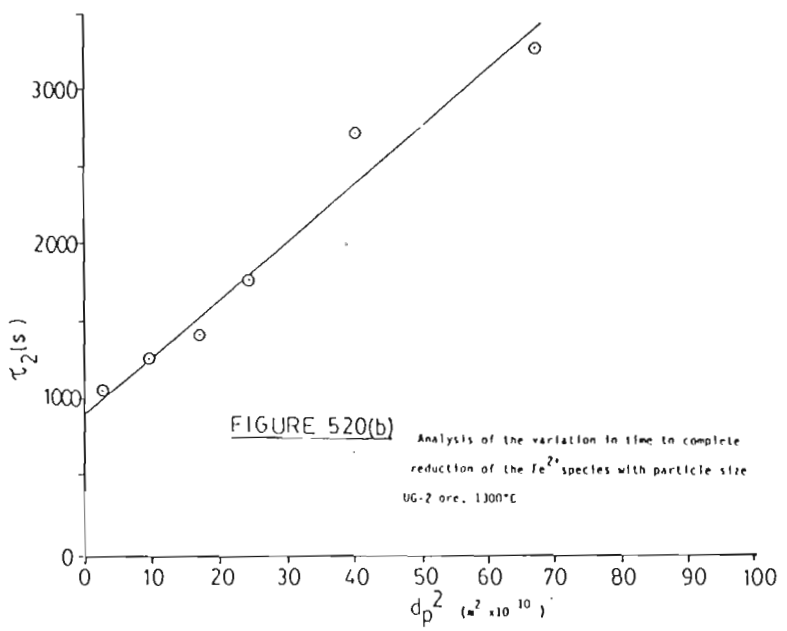

FIGURE 520(b) Analysis of the variation in time to complete reduction of the Fe^{2+} species with particle size

UG-2 ore, 1300°C

FIGURE 5.20(c) Analysis of the variation in time to complete reduction for the Cr^{3+} species (τ_3) , with particle size. UG-2 ore, 1300°C

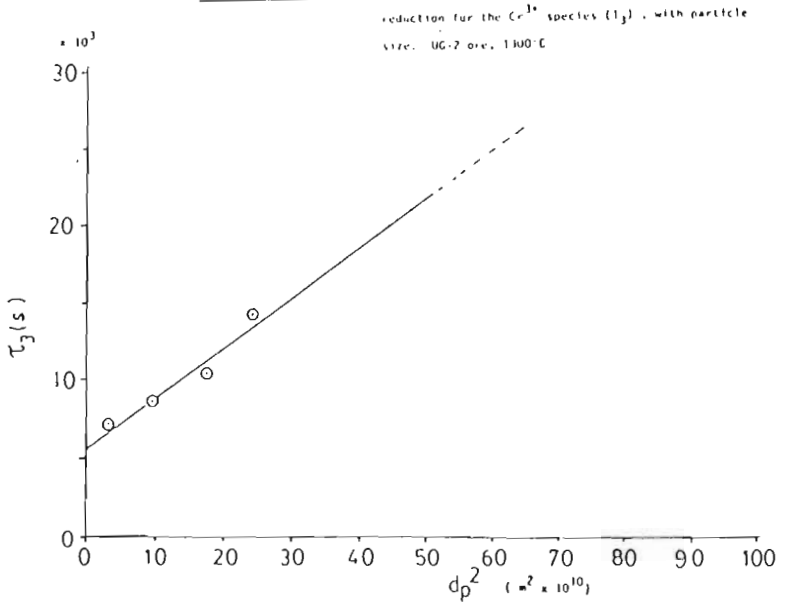

FIGURE 5.21(b)

Comparison of experimental and predicted results using a shrinking core model to simulate the reduction of UG2 ore at 1200°C

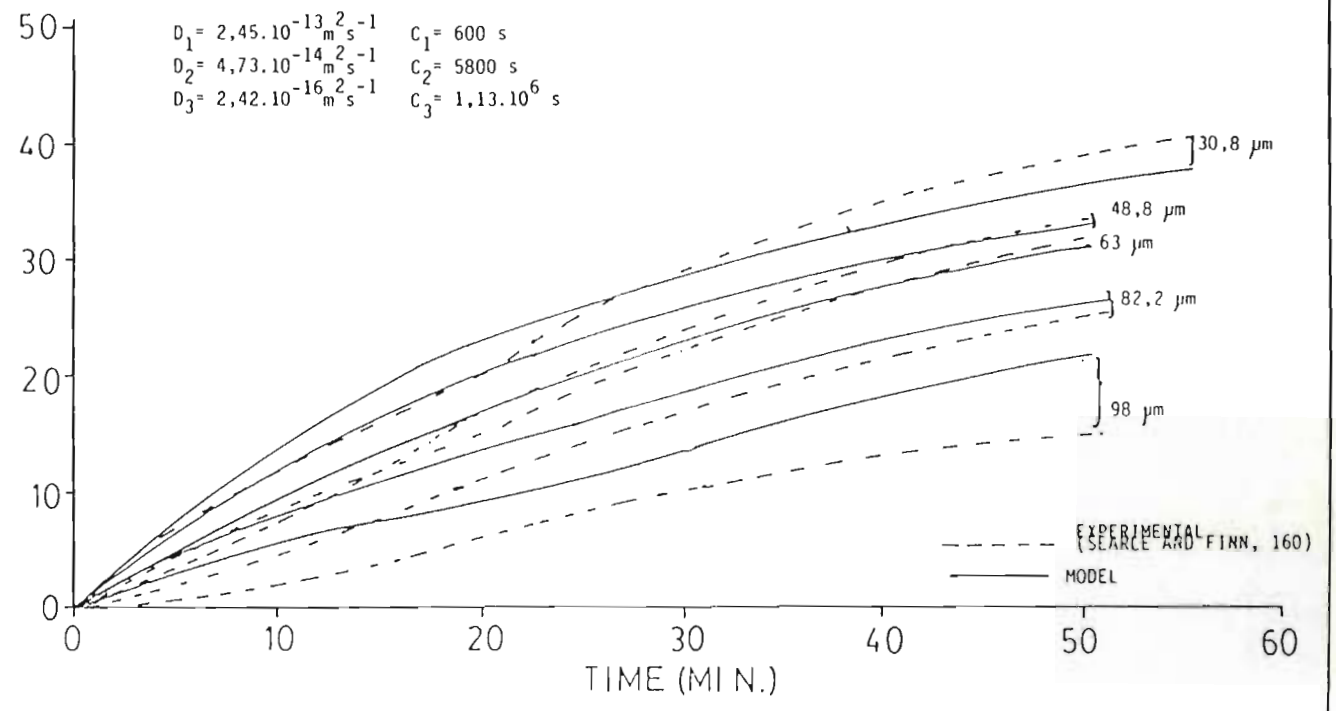

Comparison of experimental and predicted results using a shrinking core model to simulate the reduction of UG2 ore at 1300°C.

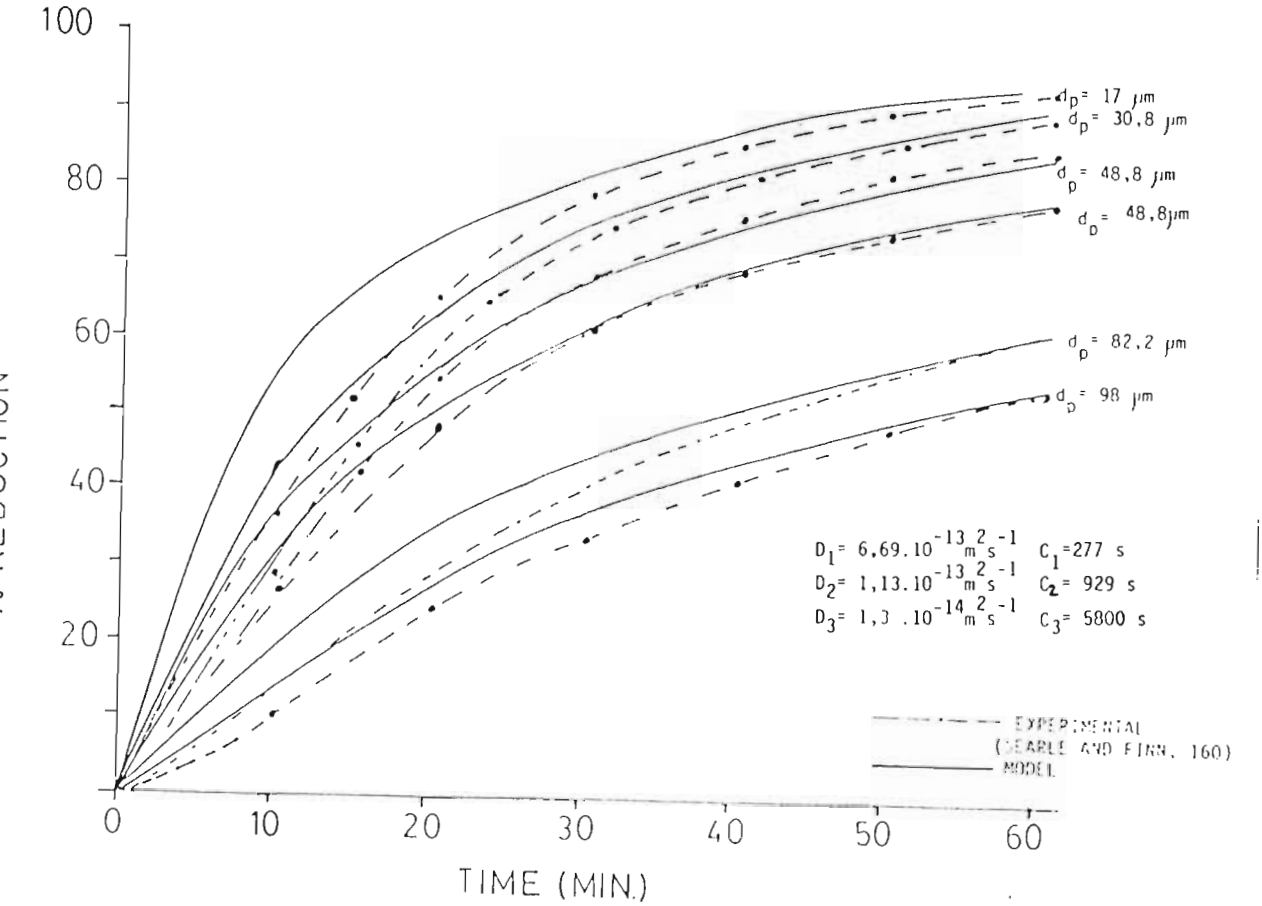

Comparison of experimental and predicted results using a shrinking core model to simulate the reduction of LG6 chromite ore at 1200°C with very high carbon addition (= 100% of chromite mass)

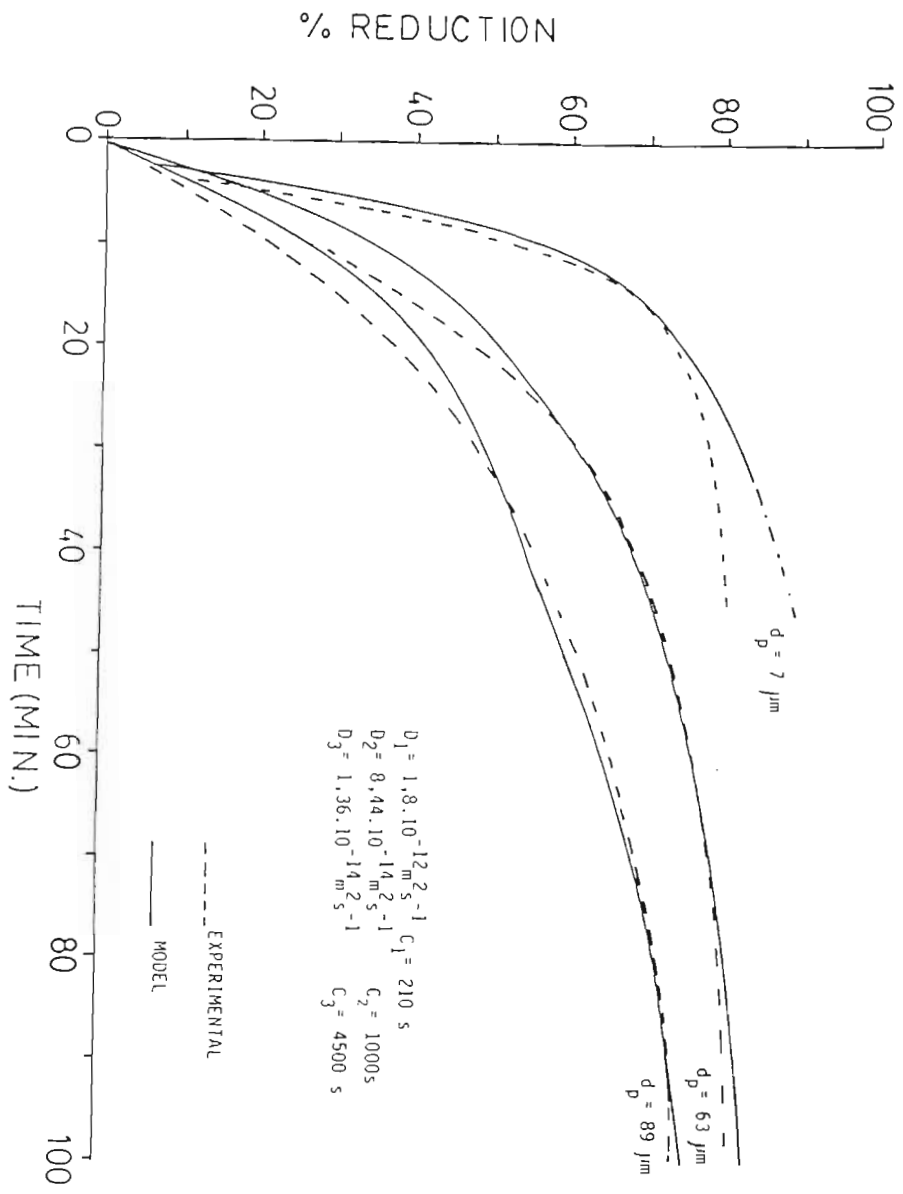

FIGURE 5.23

Comparison of the iron and chromium metallization curves calculated using the kinetic shrinking core model with the curves established experimentally.

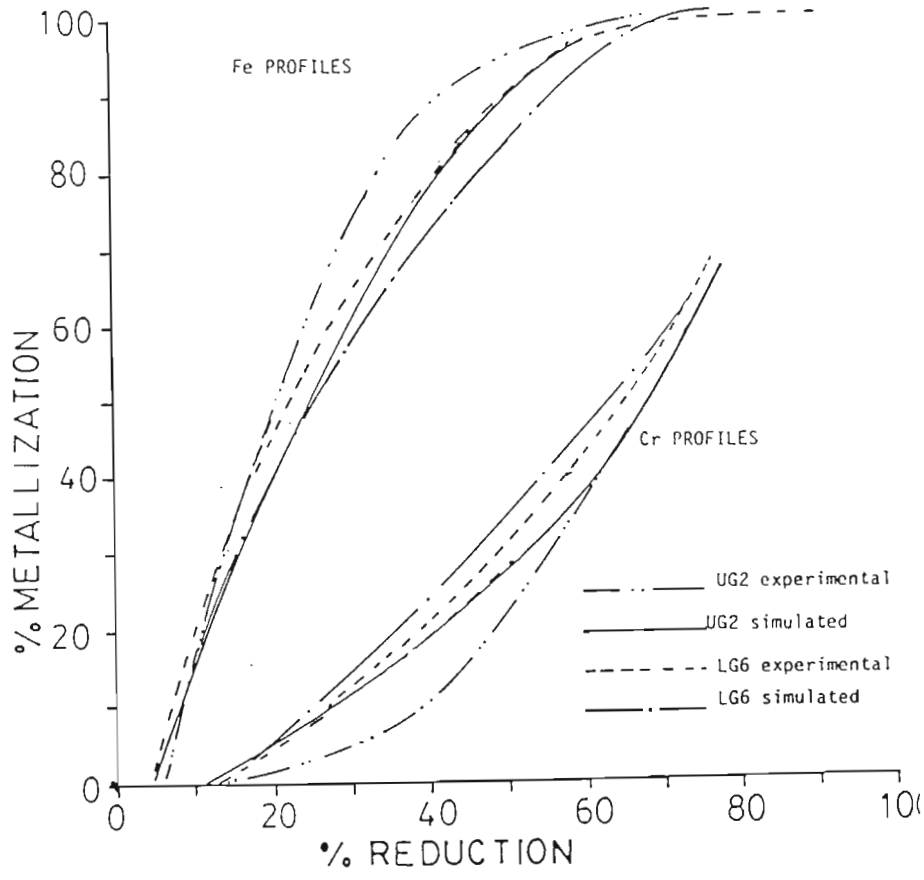

values for the constants used in Soykan's calculation yields a value of approximately $1,9.10^{-15}$ m^2s^{-1} at 1416°C. This is considerably different from the value originally calculated, and much closer to the value of $8,44.10^{-14}m^2s^{-1}$ calculated for D_2 in this work.

It is obvious that further refinement of these coefficients and the model as a whole could be (ref.30,141) performed. However, in terms of supporting the validity of the proposed reduction mechanism, this model is considered adequate, and the coefficients suitable for comparison with other ores under similar conditions of reduction.

5.5.2 CONCLUSIONS CONCERNING THE KINETICS OF CHROMITE REDUCTION

The general close agreement obtained between experimental results and those obtained using the model described above supports the assumptions made regarding chromite reduction as a diffusion rate limited process, certainly within the range of experimental conditions covered in this work.

The existence of a kinetic barrier, stemming from a marked reduction in vacancy concentration beyond the point where a balanced spinel structure ($\Sigma 3+/\Sigma 2+ = 2$) is achieved, is expected to persist well beyond the point where thermodynamic limitations are applicable. Under such conditions the reduction rate would be limited by the rate of transport of iron and chromium species through the refractory spinel layer at the surface of the chromite grain. Though this itself does not set a limit on the extent of reduction achievable,

it would appear that the rate of migration of species through the outer layer may become so slow as to impose an effective kinetic limit on the extent of reduction achievable.

From the form of the reaction product it would appear that the kinetics of reduction could be enhanced by the progressive removal or disruption of the inhibiting surface layer. This would be expected to lead to enhanced reduction rates, depending on the rate of removal of this layer, and to improved chromium recovery to the metal.

Thus if a means could be found of progressively removing the refractory spinel surface layer at a rate commensurate with that of reduction, a significant increase in the overall reduction rate and extent could be expected.

CHAPTER SIX : CHROMITE REDUCTION IN THE PRESENCE OF PROMOTERS

6.1 INTRODUCTION

6.1.1 OBSERVED ACTION OF KNOWN PROMOTERS

As shown in the previous chapters, the reduction of chromite with a carbonaceous reductant is slow and does not achieve thermodynamic equilibrium even at temperatures of 1300°C. Such limitations have prompted investigations into means of enhancing the reduction kinetics and extent where possible.

In this work consideration was initially given to the action of gaseous (H_2,CH_4); alkali halide (NaCl) and carbonate (Na_2CO_3) promoters. The action of these agents was investigated under the same conditions as those used in the analysis of the standard reduction reaction in chapter 5.

Of the gaseous agents, only hydrogen was found to cause any significant degree of kinetic enhancement as shown in figure 6.1.

Small additions (~10%) of NaCl were found to cause a degree of kinetic enhancement, though better results were obtained using Na_2CO_3 as shown in figure 6.2.

Larger additions of Na_2CO_3 were found to produce rapid reduction rates at relatively low temperatures (1000- 1100°C). Analysis of the product showed that selective reduction of the iron component of the spinel had occurred together with substantial changes in product morphology. Four distinct product phases were

FIGURE 6.1

The effect of hydrogen addition on the reduction rate .
CONDITIONS:
Temperature= 1150°C (isothermal)
LG-6 chromite ore, d_p = 30 micron
Reductant: Carbon black

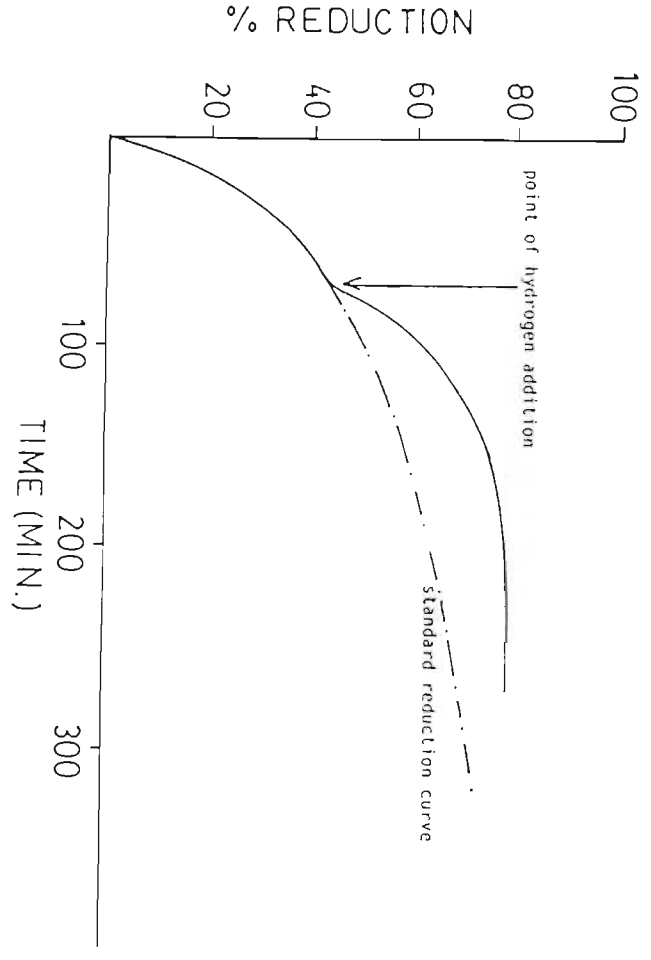

FIGURE 6.2

The effect of various reaction promoters on the reduction rate.

CONDITIONS:
LG-6 chromite d_p = 40 micron
Temperature = 1150°C
Reductant: Carbon black

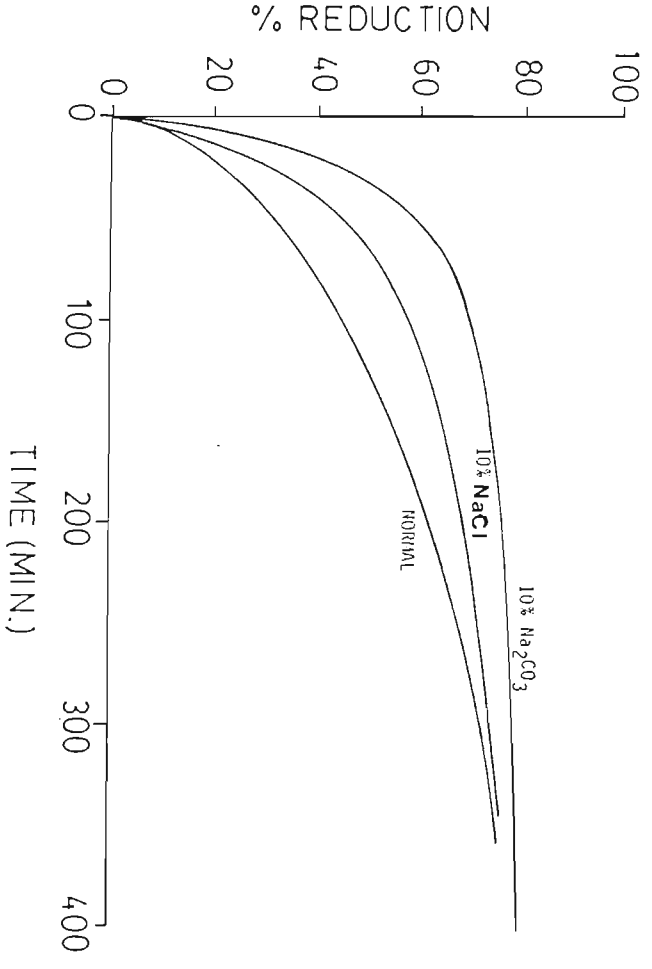

found.

i) An iron rich metallic phase containing minimal amounts of chromium.

ii) A water soluble sodium aluminate phase

iii) A magnesia rich phase, soluble in weak acid

iv) An acid insoluble residual oxide phase rich in Cr_2O_3.

(The composition of these phases is detailed in table 6.1)

The increase in reduction rate caused by addition of Na_2CO_3 was concluded to be a result of the disruption and partial dissolution of the chromite spinel. The addition of hydrogen into the gas stream was seen to further increase the reduction rate, suggesting the complementary action of these promoters.

In summary, the action of these promoters appears to be one of disrupting the chromite spinel and increasing communication between the grain interior and the reductant.

6.1.2 INVESTIGATION OF A LIQUID PHASE REDUCTION PROMOTER

As shown in the previous chapter, the formation of a refractory spinel layer at the surface of the chromite grain acts to retard the rate and extent of the reduction reaction. Effective promotion of reduction thus requires disruption of the stable reaction product formed at the surface of the chromite grain.

One way in which such a disruption can be achieved is through the presence of a quantity of liquid phase at the surface of the chromite grain in which the partly reacted chromite spinel is soluble.

TABLE 6.1

THE EFFECT OF Na_2CO_3 ON SELECTIVE REDUCTION

id	Na_2CO_3 Addition %	% Red (MET)	Recovery Cr(A)	Fe(A)	Al(W)	Mg(A)	% Cr_2O_3 in RES
101	20	38,47	14,37	77,02	16,02	1,44	54,43
102	50	51,60	24,04	95,70	19,56	77,98	70,71
104	75	43,60	13,57	91,64	37,50	98,13	78,31
103	100	41,22	7,91	95,00	61,03	98,41	86,10

A = Leach in weak HCl solution

W = Water leach

FIGURE 6.3

The NaF - CaF_2 system.

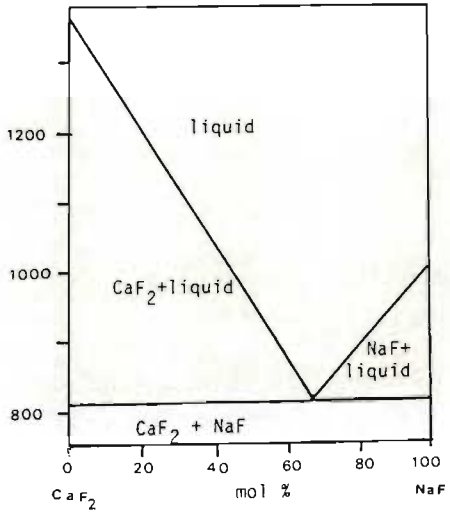

(data from Levin et al. 102)

It might be expected that an optimum would be achieved with a liquid phase in which the spinel was only slightly soluble, and which did not experience any significant change in physical properties with dissolution of the spinel.

In the design of such a solvent phase, a simple eutectic phase relationship is required between the solvent flux phase and the various spinel components, with the eutectic valley lying close to the pure solvent axis. In addition several physical characteristics would appear important, among them low viscosity, melting point and low volatility at high temperature.

In this investigation it was decided to concentrate on a traditional fluxing agent, calcium fluoride, known to exhibit aggressive behaviour towards various spinels, and having most of the desired physical characteristics.

Because of the relatively high temperatures required (~1300°C) to obtain a calcium fluoride rich melt phase containing minor quantities of spinel components, it was concluded that better results could be obtained with the addition of a second component together with the CaF_2 , aimed at reducing the liquidus temperature.

The NaF- CaF_2 system as shown in figure 6.3 appeared suitable, offering a simple eutectic relationship at 810°C (65 mol% NaF). Based on the effect of NaF on several other systems, it was assumed that NaF addition would result in a lowering of the eutectic temperature in the flux- MgO- Al_2O_3 system, together with a possible shift in composition with more Al_2O_3 and MgO in solution (though still below 10%).

Initial experimentation was thus conducted using various mixtures of CaF_2 and NaF as a solvent flux phase capable of disrupting the refractory spinel surface layer.

Once in solution, the spinel components were expected to show non-ideal behaviour. Based on the work of Hawkins and Davies (72) it was expected that particularly the iron and chromium species would show strong positive deviations from ideality. The resultant higher activities of these species in the melt phase are conducive to improved transport in the flux phase and good recovery to the metal.

Oxygen partial pressure was also expected to play an important role, governing the oxidation state of the iron and chromium species in solution and hence affecting the physical characteristics of the melt phase.

These effects suggest that low oxygen partial pressure and close carbon proximity are required with this type of flux phase in order to achieve rapid and effective removal of the iron and chromium species once in solution.

Two main aspects of the flux promoted reduction were investigated, namely

i) The degree of enhancement obtainable with the limited use of different types of promoter

ii) An analysis of rate controlling mechanisms during the reduction in the presence of a fluxing agent.

6.2 SUMMARY OF EXPERIMENTAL RESULTS USING A FLUX PROMOTER

6.2.1 THE EFFECT OF LIMITED FLUX ADDITION

The dramatic effect that even a small quantity of flux has on the reduction rate is clearly shown in figure 6.4. Increasing the flux addition from 5 to 20% of the chromite mass is seen to result in a progressive increase in reduction rate as shown in figure 6.5.

The composition of the flux phase was also found to have a significant effect on the reduction rate as shown in figure 6.6. It was found that the lower the liquidus temperature and viscosity of the flux the greater the increase in reduction rate.

The effect of temperature on the reduction rate is indicated in figure 6.7(a). Temperature was found to have a dual effect, with increased temperature causing an increased rate of reduction as in the absence of any promoter, as well as causing changes in the physical properties of the flux phase, such as increasing the solubility of the spinel components and lowering the viscosity (both resulting in increased reduction rates). An indication of this effect is given in figure 6.7(b) where the sharp response to temperature change (more pronounced than in the standard reduction) is accentuated by the melting point of the flux at approximately 1000°C.

Chromite particle size was found to have a significant effect as shown in figures 6.8 and 6.9. The effect of flux addition appeared to be amplified to a certain extent for large particle sizes of ore and reductant (figure 6.9).

In the case of ultra- fine lampblack and fine

The dramatic effect that a small quantity of eutectic fluoride flux has on the reaction rate of chromite ore.

CONDITIONS:
LG-6 chromite ore, d_p = 53- 75 micron.
temperature = 1200°C (isothermal)
reductant = carbon black.
flux addition: 5% of a NaF- CaF_2 eutectic composition.

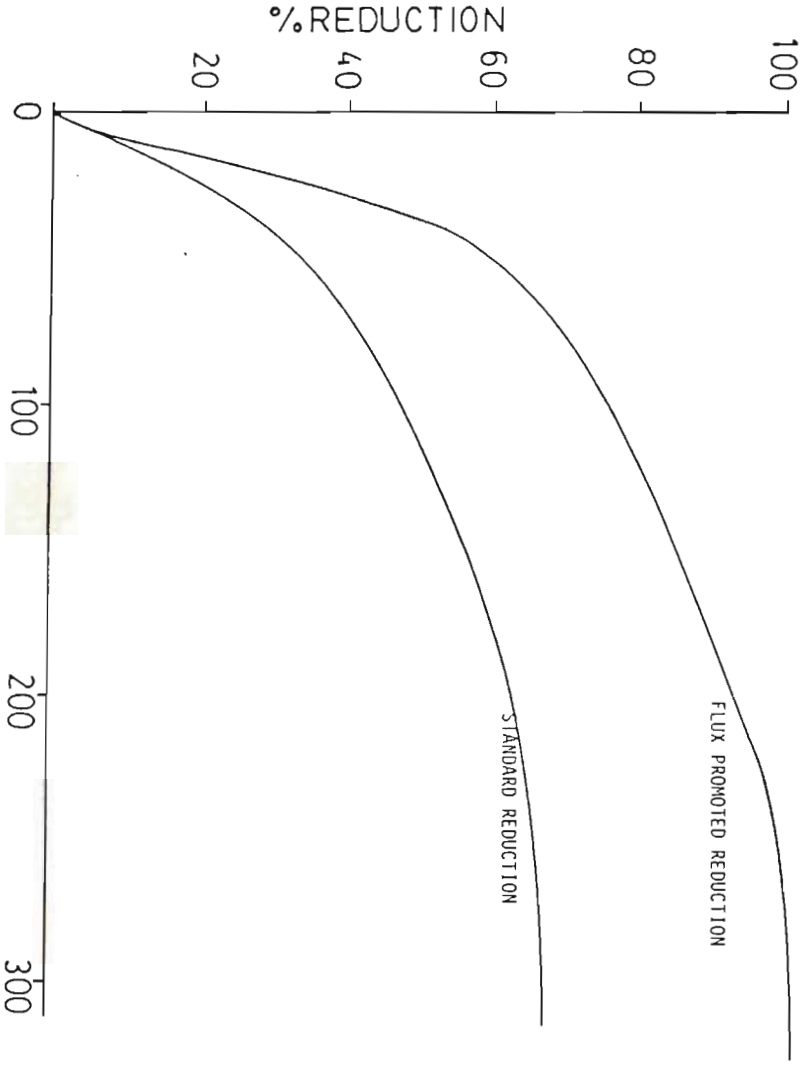

FIGURE 6.5

The effect of progressive flux addition on the reduction reaction in comparison to the standard reaction without flux addition.

CONDITIONS:

LG-6 chromite , d_p = 53- 75 micron.

Temperature= 1200°C (isothermal)
Reductant: carbon black.
Flux addition: percent of chromite mass of a eutectic NaF-CaF_2 mixture.

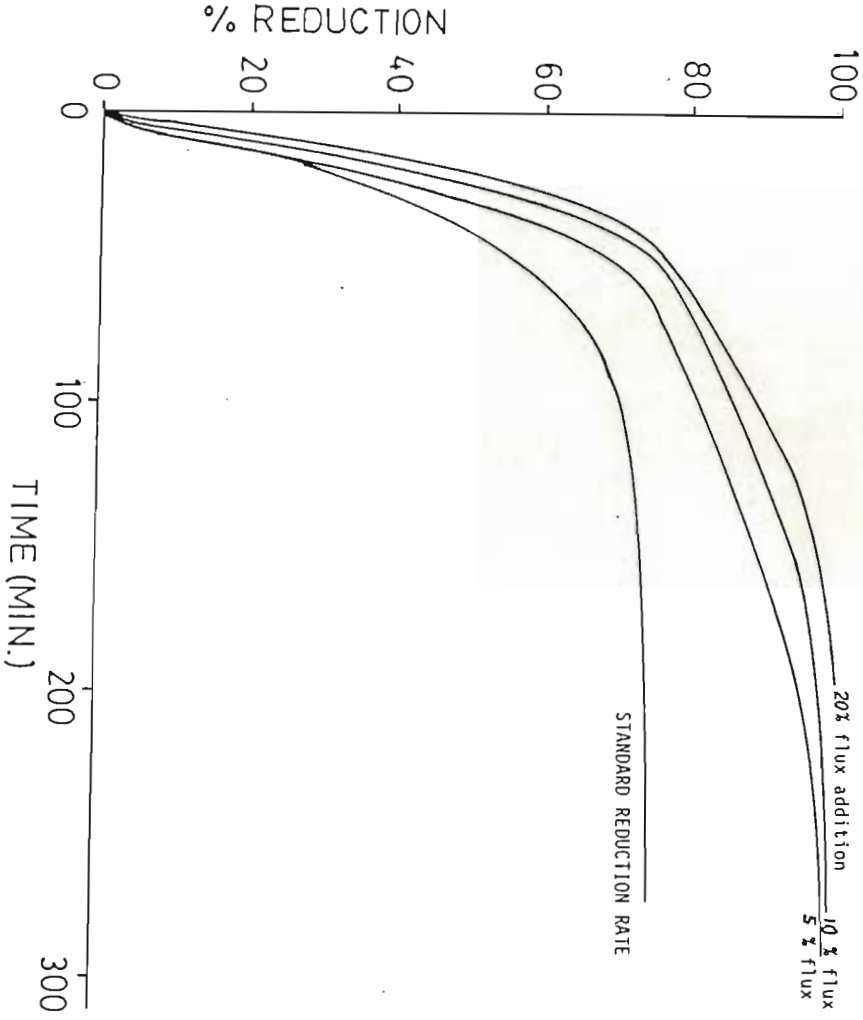

FIGURE 6.8

The effect of particle size on reduction rate in the presence of a flux phase.

CONDITIONS:
TEMPERATURE : 1100°C (isothermal)
ORE : LG6 CHROME SAND
REDUCTANT : LAMPBLACK
FLUX : 10% CaF_2 2% NaF

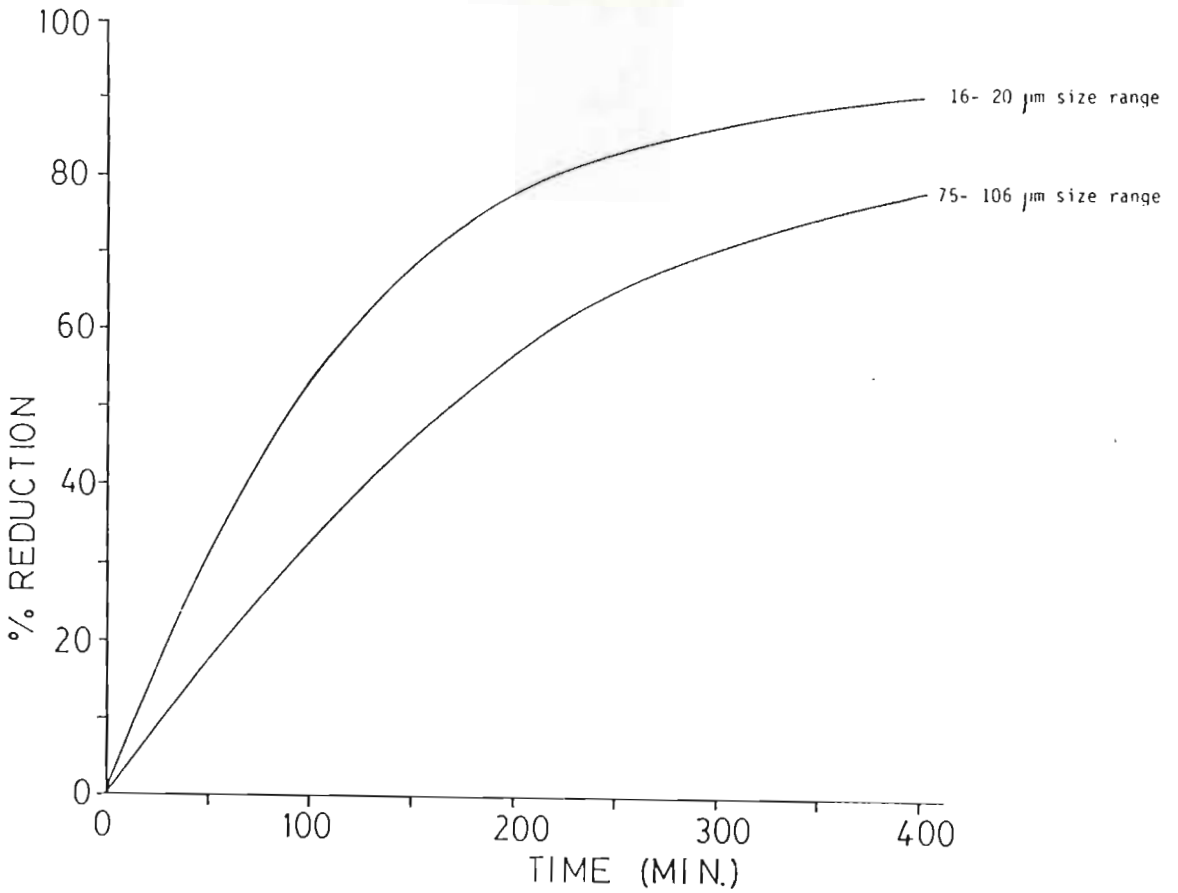

FIGURE 6.6

THE EFFECT OF FLUX COMPOSITION ON THE OVERALL REDUCTION RATE

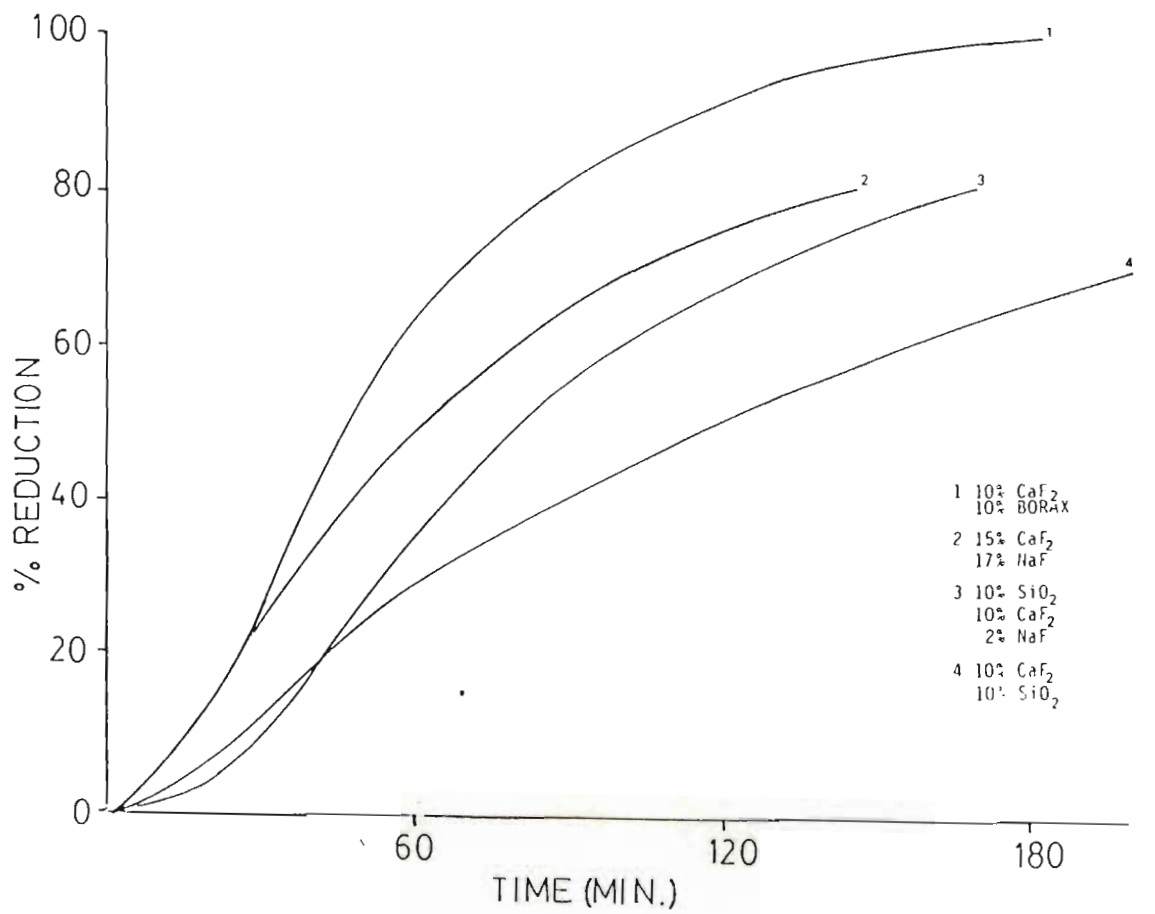

FIGURE 6.7(b)

The time-temperature response of the reduction reaction in the presence of a fluoride flux.

CONDITIONS:
REDUCTANT : LAMPBLACK
ORE : LG6 CHROME SAND
ORE SIZE : d_{50} = 7um
FLUX : 10% CaF_2, 2% NaF

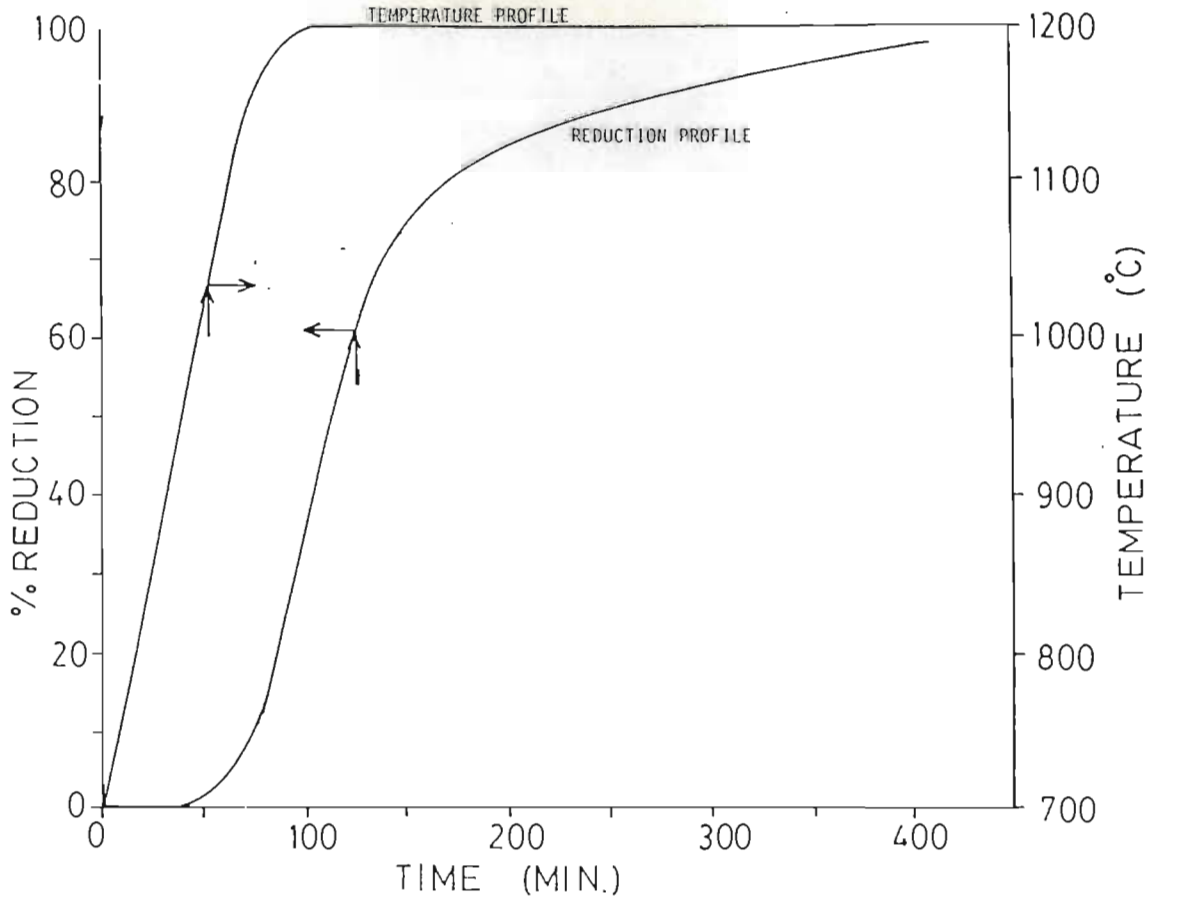

FIGURE 6.7(a)

The effect of temperature on the reduction rate in the presence of a fluoride flux phase.

CONDITIONS:
REDUCTANT: LAMPBLACK
ORE : LG6 CHROME SAND
PARTICLE SIZE: 53- 75 um
FLUX: 10% CaF_2, 2% NaF

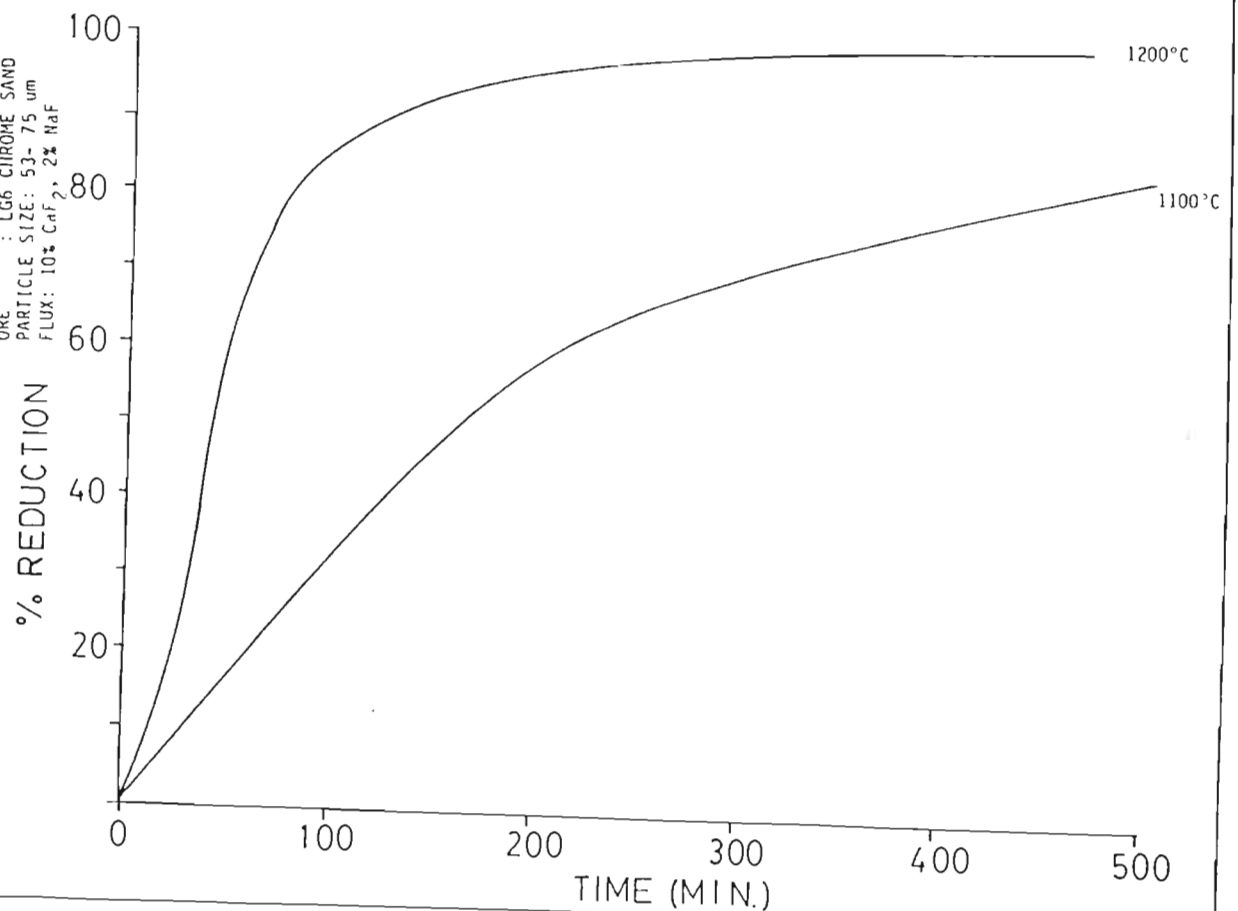

FIGURE 6.10

The effect of carbon addition on the reaction rate with fine chromite and carbon particle sizes.

CONDITIONS:
TEMPERATURE: 1200°C (isothermal)
CHROMITE : LG-6, d_p = 63 micron
REDUCTANT : carbon black
FLUX ADDITION: 10% CaF_2, 2% NaF

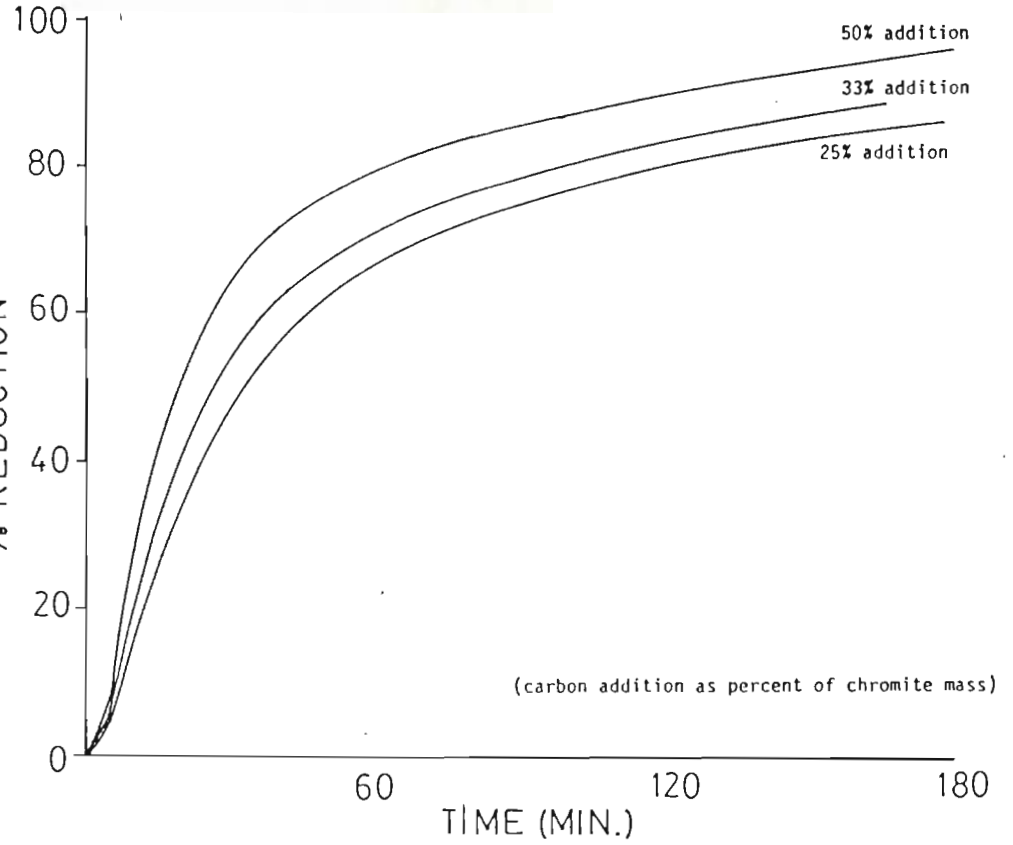

FIGURE 6.9

The effect of coarse particle sizing on the reduction rate in the presence of a flux.

CONDITIONS:
TEMPERATURE :1300°C (isothermal)
REDUCTANT : CHAR (same particle size as ore)
ORE : LG6 CHROME SAND
FLUX : 5% CaF_2 , 10% SiO_2

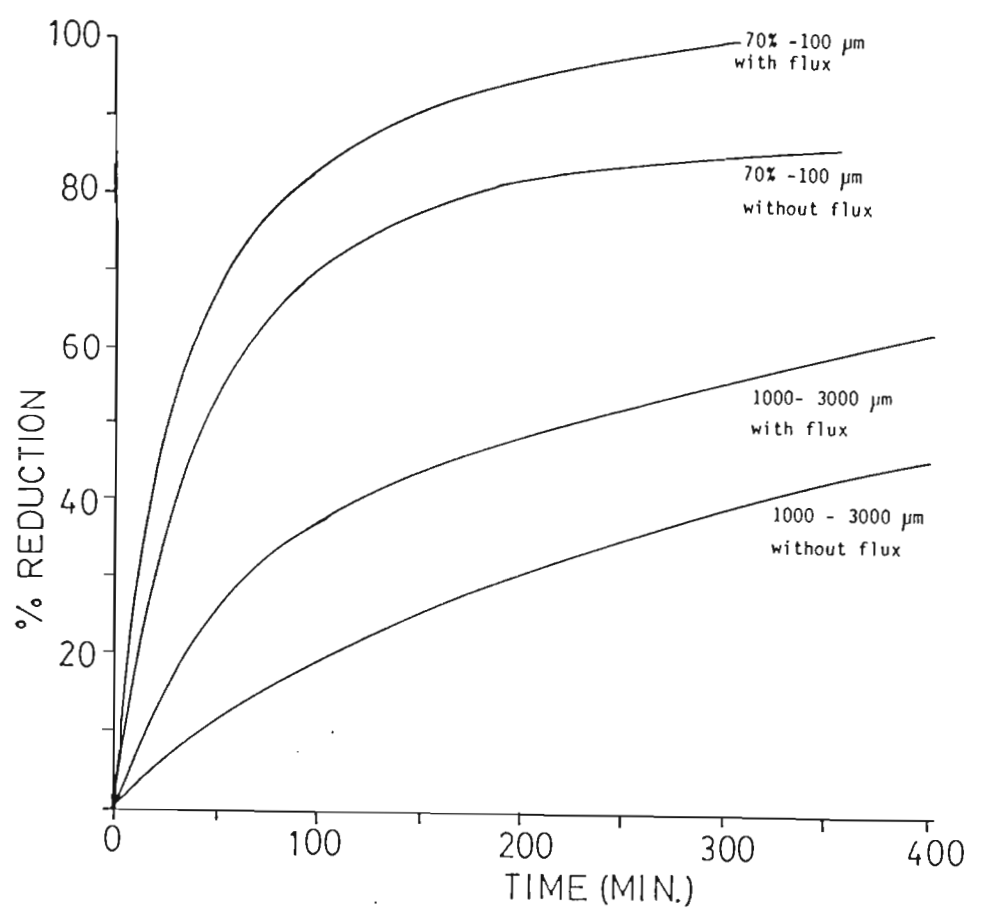

FIGURE 6.11

The effect of carbon addition in excess to the stoichiometric requirement with large carbon and chromite particles, where transport through the fluid flux phase plays an important part in the overall reaction rate.

CONDITIONS:
TEMPERATURE= 1300°C (isothermal)
CHROMITE: LG-6, 200- 500 micron size range
REDUCTANT: metallurgical graphite 200- 300 micron size range

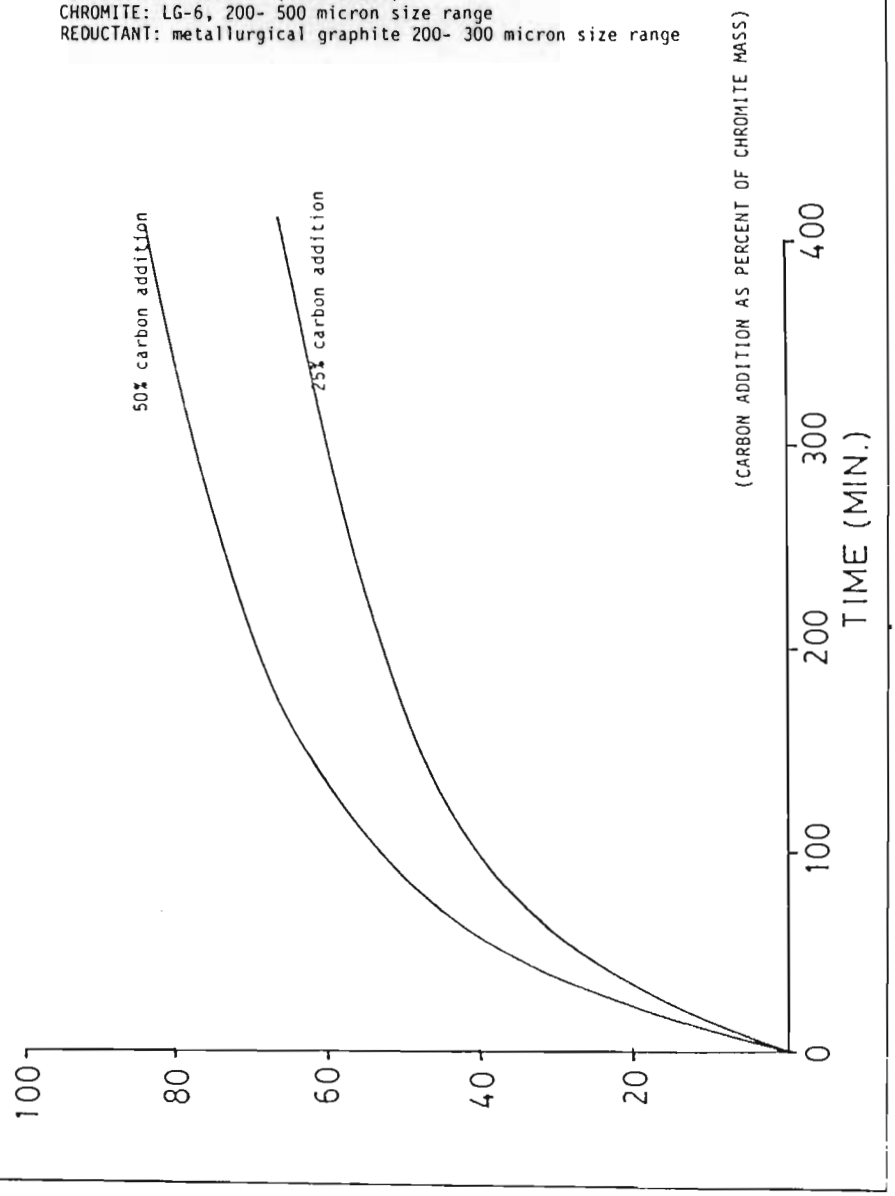

chromite particles (7-75 micron), addition of carbon in excess to the stoichiometric requirement was found to cause a slight increase in reduction rate up to a certain point (figure 6.10). The effect is similar though not as dramatic as in the absence of flux.

However, with coarser discrete particles of carbon, the results were dramatically different to that experienced in the absence of any flux. With carbon particles 30-100 micron in size, the reaction rate was found to be slightly slower than with lampblack, though the major difference was the appearance of the reduced metal product at the surface of the carbon grain, instead of the chromite grain surface. This suggested that the presence of discretely sized reductant had caused a significant change in the reduction mechanism.

With large chromite and carbon particle sizes, in the range 300- 3000 micron, the rate was found to be particularly sensitive to carbon addition (figure 6.11). In such cases, the rate curve tended to show a more linear form at the lower carbon additions, underlining the shift in rate controlling mechanism; from solid state diffusion as shown in the previous chapter, to one where factors external to the chromite grain (such as the physical characteristics of the flux) play a far more important role.

6.2.2 MINERALOGICAL INVESTIGATION

As before, samples of reaction product were analysed in detail using the S.E.M. and microprobe. Characteristics typical of a chromite grain after reduction in the presence of a solvent flux phase are shown in figure 6.12.

The appearance of samples after treatment with the standard flux indicated that the flux had melted to form small pools of melt phase on the grain surface. This is indicated by the dark mixed phase region at the surface of the grain (plate 6.1). With continued reduction the flux is found to penetrate into the grain as shown in plate 6.2.

Investigation of the acid leach residue of a chromite sample having undergone reduction in the presence of a solvent phase revealed the distinct porous nature of the grain exterior. Comparison of plates 6.3(a) and (b), before and after acid leaching, shows removal of metal from the grain exterior and the metallized region that surrounds the bright centrallized core. The disrupted nature of the outer ring of residual spinel is shown up by the removal of the acid soluble flux component located in this region prior to acid leaching.

Detailed examination of this outer spinel region on numerous unleached samples revealed that it was a composite region, consisting of recrystallized spinel and virtually unaltered solvent flux phase in intimate association.

The central region, seen as a uniform bright phase

FIGURE 6.12

SCHEMATIC REPRESENTATION OF CHROMITE GRAIN AFTER REDUCTION IN THE PRESENCE OF A FLUORIDE SOLVENT PHASE

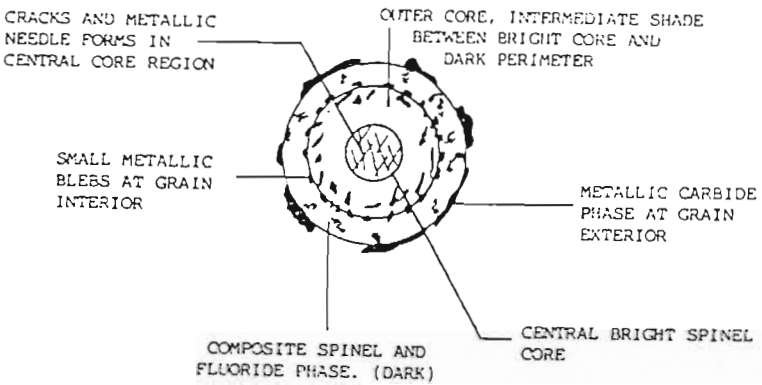

NOTES

1) THE COMPOSITE SPINEL AND FLUORIDE PHASE USUALLY APPEAR AS A SINGLE HOMOGENOUS PHASE

2) SHADE OF PHASE GIVES AN INDICATION OF CHROMIUM AND IRON CONTENT.

3) GRAIN AS SHOWN ABOVE IS REASONABLY WELL REDUCED (80 - 90 % OF Cr + Fe METALLISED)

TABLE 6.2 S.E.M. AND PROBE ANALYSES OF THE VARIOUS REGIONS WITHIN THE CHROMITE GRAIN AFTER REDUCTION IN THE PRESENCE OF A FLUORIDE BASED FLUX PHASE.

REGION IN THE GRAIN	MASS % OXIDE COMPONENT						DELTA [1]
	MgO	Al2O3	Cr2O3	FeO	CaO	SiO	
CENTRAL CORE (A)	10,86	14,23	44,71	25,51	---	---	4,69
CENTRAL CORE (A)	12,09	13,03	46,32	23.25	---	---	5,31
OUTER CORE (A)	17,49	18,90	49,15	9,27	---	---	5,19
OUTER CORE (B)	17,41	19,09	53,37	7,18	(0,27)	(1,13)	2,95
GRAIN EDGE (A)	27,65	45,00	15,77	0,32	(4,00)	(0,64)	7,06
GRAIN EDGE (B)	32,81	50,49	4,63	0,37	(5,50)	(1,39)	4,81
GRAIN EDGE (B) COMPOSITE	26,27	52,82	5,24	0,66	(10,51)	(2,38)	2,12

NOTES:

A = a typical grain at a low state of reduction (10-30%)

B = a typical grain at a higher state of reduction (40+ %)

[1] non normalised results are shown, DELTA = 100% - sum of oxides

grain edge analyses tend to be an average of two finely dispersed phases- one a pure flux phase and the other a relatively pure, recrystallised spinel ($MgOAl_2O_3$).

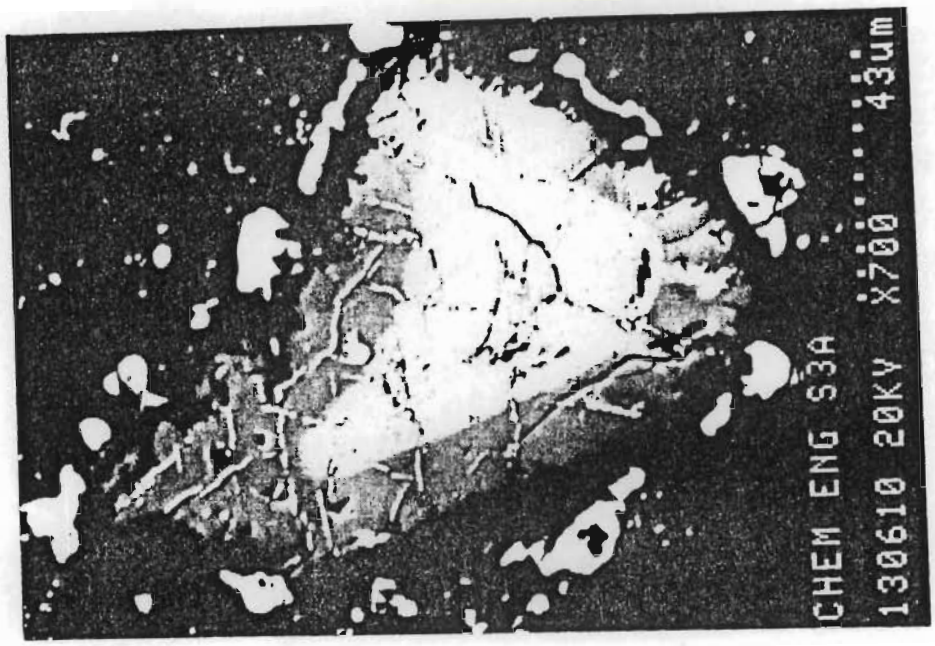

PLATE 6.1 A chromite grain undergoing reduction in the presence of a solvent flux phase (this is a B.E.I. image that emphasises the compositional differences across the grain.)

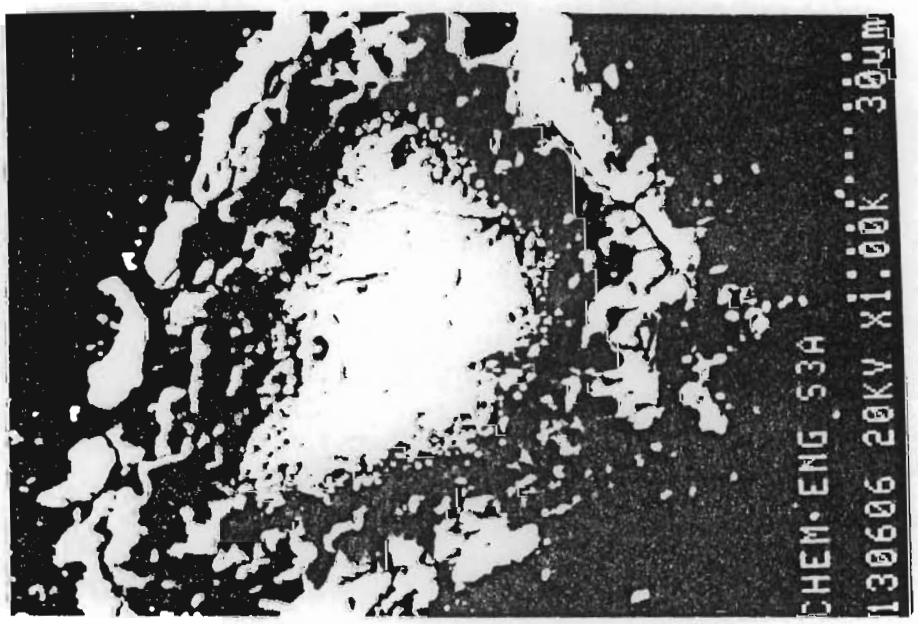

PLATE 6.2 A chromite grain at a more advanced degree of reduction (approx. 80%) showing a very small central core. This is also a B.E.I. image.

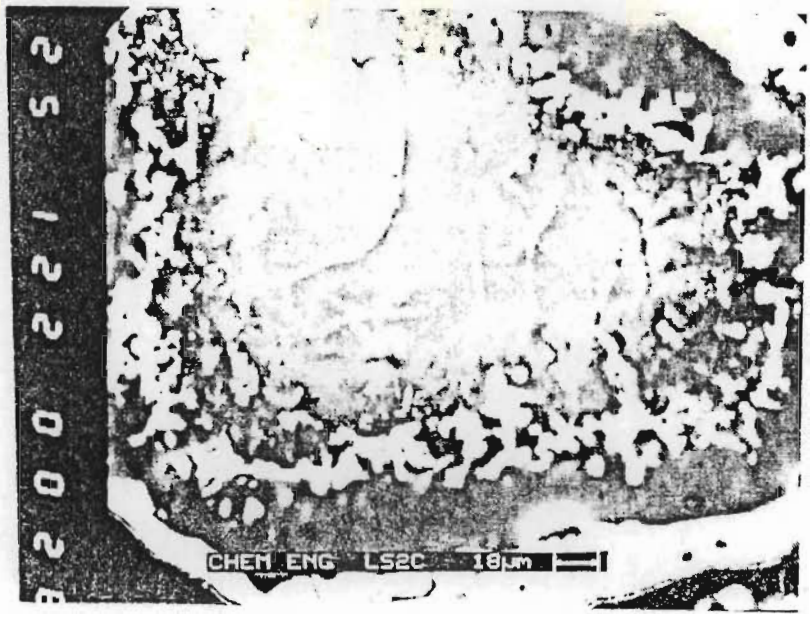

PLATE 6.3 (A) A chromite grain at an advanced state of reduction prior to acid leaching.

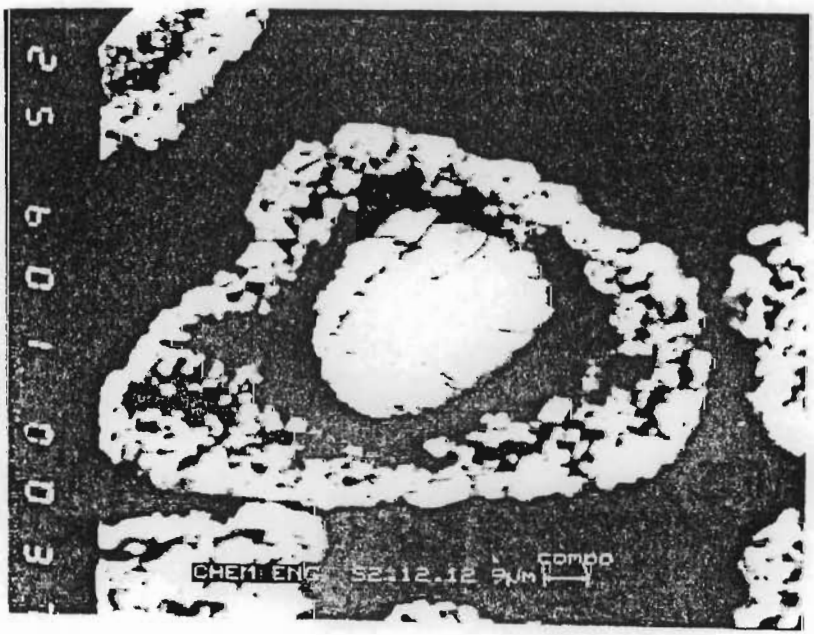

PLATE 6.3 (B) A chromite grain from the same sample after acid leaching to remove metal and flux phases.

particularly evident in plates 6.2 and 6.3(b) was found to be rich in chromium, but with very little residual iron. This indicates the formation of a refractory chromium rich $MgCr_2O_4$ - spinel core.

In the latter stages of the reduction (plate 6.3(a)), the central core region of the grain undergoes severe attack, becoming disrupted, with beads of metal forming a ring around the central core, and along cracks extending through the core.

From these plates it would appear that the flux phase acts to partially dissolve oxide components from the spinel, resulting in a gradual ingress of the flux towards the centre of the grain. The limited solubility of magnesia and alumina in the flux encourages precipitation of these components to form a pure spinel phase around the grain periphery.

Metallization is found to occur initially at the grain exterior, and as the reaction proceeds, the ingress of flux towards the grain centre and resultant breakup of the grain enables metallization to take place within the original grain boundary.

The appearance of twin concentric cores (plate 6.1) is evident from fairly early in the reduction sequence (~30%), and was not previously encountered in the standard reduction reaction. Analysis of these cores (table 6.2), showed the central core to be rich in chromium and iron (effectively unaltered chromite, similar to the central core discussed in chapter 5). The outer core is found to be rich in chromium, but depleted in iron. The grain rim is found to have no residual chromium or iron. The progressive development of these cores is summarised in figure 6.13, with the

FIGURE 6.13

SCHEMATIC REPRESENTATION OF THE COMPOSITIONAL VARIATION ACROSS A CHROMITE GRAIN UNDERGOING REDUCTION IN THE PRESENCE OF A SOLVENT FLUX PHASE.

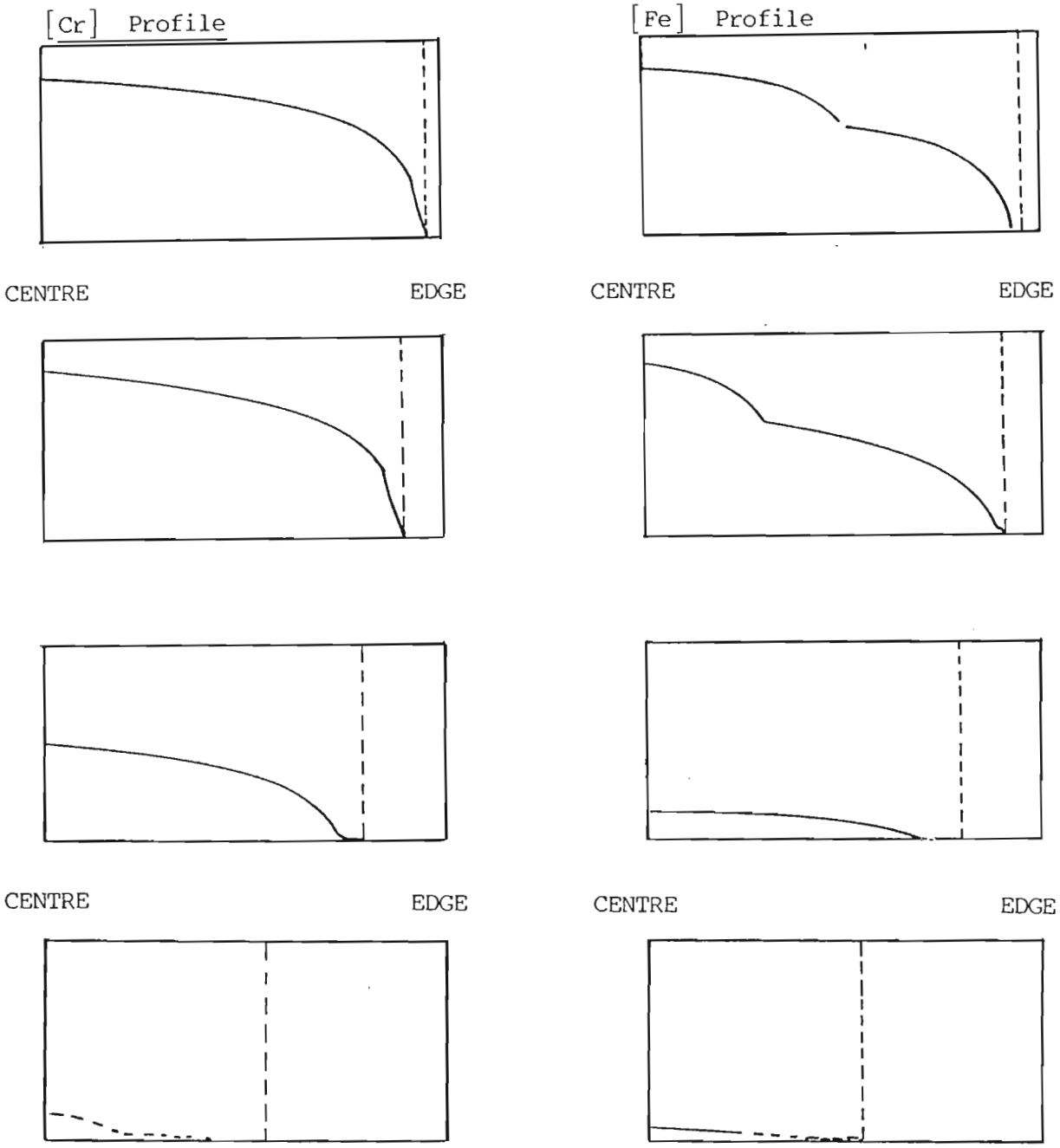

NOTES

1) DIAMETER OF GRAIN (ASSUMING SPHERICITY) IS ASSUMED NOT TO SHRINK APPRECIABLY WITH INCREASE IN REACTION EXTENT.
2) DASHED LINE INDICATES COMPOSITE REGION OF RECRYSTALLIZED SPINEL AND FLUX PHASE.

relative iron and chromium contents summarised in figures 6.14 and 6.15. The limited flux additions were found to result in a small amount of metal phase growth compared to reduction in the absence of any flux (d_{50} increasing from ~5 to ~10 micron).

However, the morphology of the metal phase formed in the presence of a flux promoter differed considerably from that found in the unpromoted reduction reaction. Three prime differences were noted:

a) From a reaction extent of ~ 70% onwards, fine rounded metal blebs start appearing in the chromite grain interior. These blebs form an internal spherical shell, concentric to the core at a certain depth below the grain surface, dependent on grain size, flux composition and addition.

b) During the latter stages of the reduction (i.e. above 50% reduction), the central grain region becomes disrupted, and fine parallel shear planes start to appear. Metal needle forms then develop along these lines. The appearance of these needles is approximately simultaneous to the disappearance of the central iron rich core. The implication being that because of the disruption of the grain, the final quantity of iron is able to be reduced virtually in situ, resulting in an iron rich metal phase.

c) In the presence of larger reductant particle sizes (30-100 microns or larger), metallization is found to occur at the surface of the reductant rather than at the

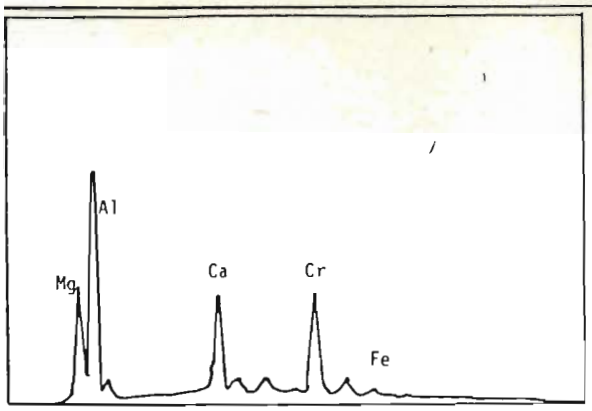

1) Outer core region with very little iron remaining and significant chromiu, depletion.

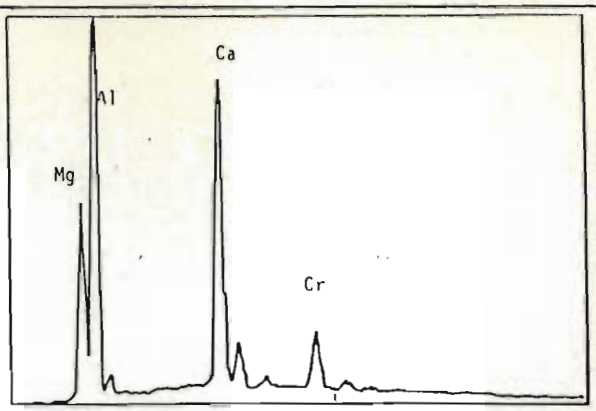

2) Grain rim region (dark spinel phase), with very little chromium or iron remaining in the spinel.

3) Dark spinel phase after acid leaching showing this phase to be virtually pure $MgAl_2O_4$ spinel.

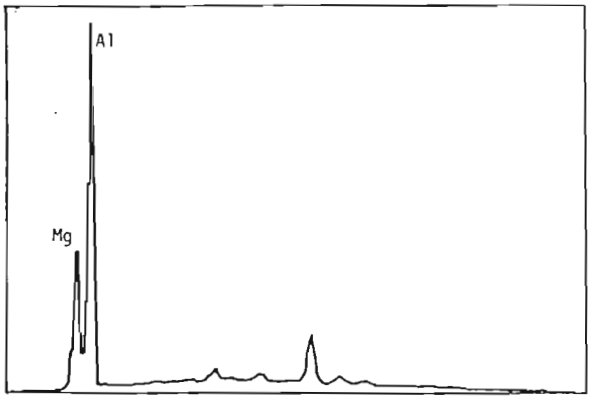

4) Spectrum from a larger portion of flux phase near the edge of the chromite grain showing it to be almost pure flux with very little contamination.

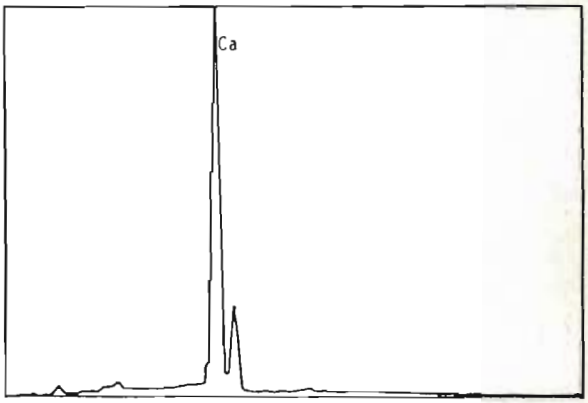

FIGURE 6.14 E.D.S. Spectra from samples after reduction in the presence of a sodium fluoride(2%), calcium fluoride (10% flux at 1200°C. Sample at approximately 30% reduction showing twin core structure.

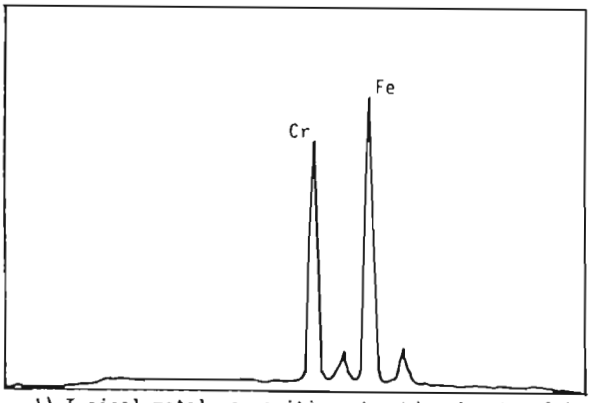

1) Typical metal composition at grain rim at a fairly low degree of reduction (50%)

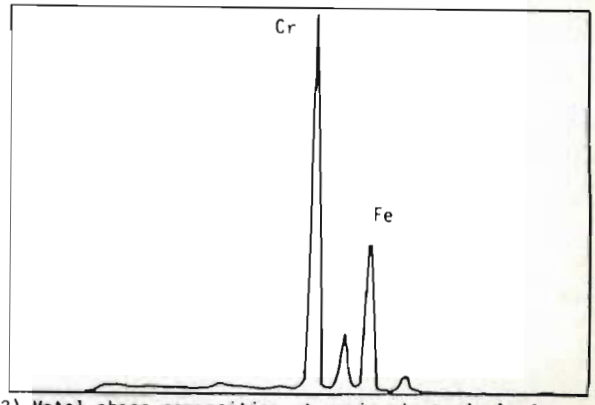

2) Metal phase composition at grain rim typical of a high degree of reduction (approx. 80- 90%)

3) Metal bleb within grain interior (approx. 70% reduction)

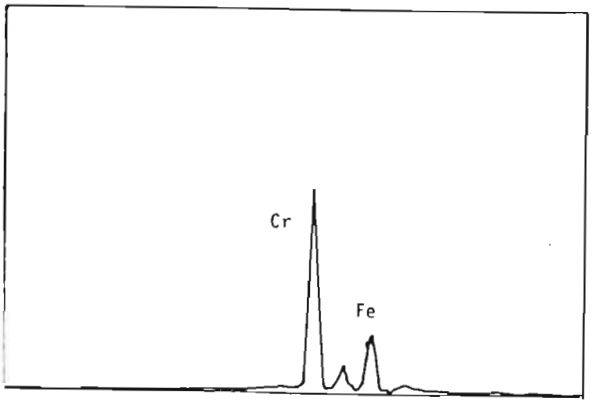

4) Metal needle form at grain interior (approx. 80%)

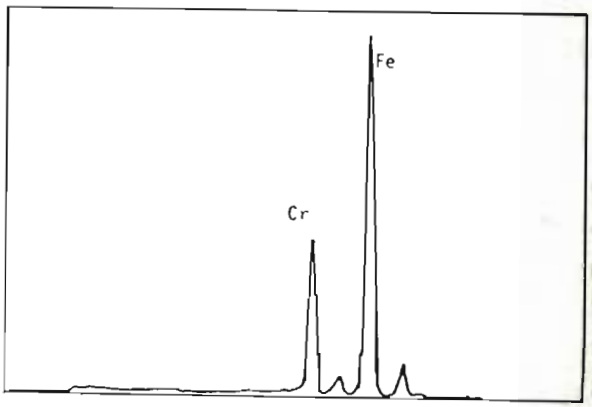

FIGURE 6.15 Comparison of the relative iron and chromium contents of metal phases formed during the flux promoted reduction of chromite at 1200°C . (Flux comp. 2% NaF, 10%CaF_2)

surface of the chromite grain, and little or no metallization is seen in the grain interior.

Each of the separate metallic regions has its own distinctive composition range (table 6.3). These results confirm that the needle form metal within the chromite grain (plates 6.2 and 6.4), is initially very rich in iron, while the surrounding spinel is virtually devoid of any iron. The chromium content of these needles does increase slightly near the end of the reaction (figure 6.15).

In general flux distribution in samples with very fine chromite (d_{50} = 7 micron), was found to be relatively uneven, with some grains showing extensive flux attack, while others appeared little affected.

With larger chromite particles in the range 20- 100 micron, a more even flux distribution was noted, with generally good penetration of the flux into the grain and disruption of the grain surface.

Analysis of samples over a wide range of particle sizes indicated that the rate of solvent penetration slows during the course of the reduction. After long reaction times with larger grains, flux ingress draws to a halt. This was shown by tests performed with chromite grains between 200 and 2000 micron diameter in a graphite crucible with a 100% addition of a eutectic CaF_2 - NaF flux. The chromite was found to react very slowly, with the reduction rate asymptoting to approximately 10% reduction after an 18 hour period. Leaching of this sample showed that only a fraction of the iron and virtually no chromium had been reduced.

Examination of the leached sample (plate 6.5) showed

TABLE 6.3 ANALYSES OF METAL PHASES FROM DIFFERENT PARTS OF THE CHROMITE GRAIN AFTER REDUCTION IN THE PRESENCE OF A METAL PHASE.

% REDUCTION	REGION	MASS% Cr	MASS% Fe	Cr/Fe	COMMENTS
40	bleb at edge of grain	40,1	60,3	0,67	small blebs, low extent of reduction
57	bleb at edge of grain	44,8	55,2	0,81	second core evident at grain edge
70	bleb at edge of grain	58,27	41,73	1,40	second core well developed, first core almost extinct
70	bleb in grain interior	60,60	35,69	1,70	small bleb inside grain rim
80	bleb at edge	63.02	37,11	1,70	large bleb at grain edge
85	bleb in grain interior	65	33	1,97	very small core remains
85	metal needle grain centre	16	84	0,19	no central core remains
96	bleb at edge of grain	61	39	1,56	smaller bleb formed later in the reaction
96	bleb in grain interior	83,67	16,30	5,12	no residual core center disrupted
96	metal needle in grain centre	28	72	0,39	no change in needle composition, with disrupted centre.

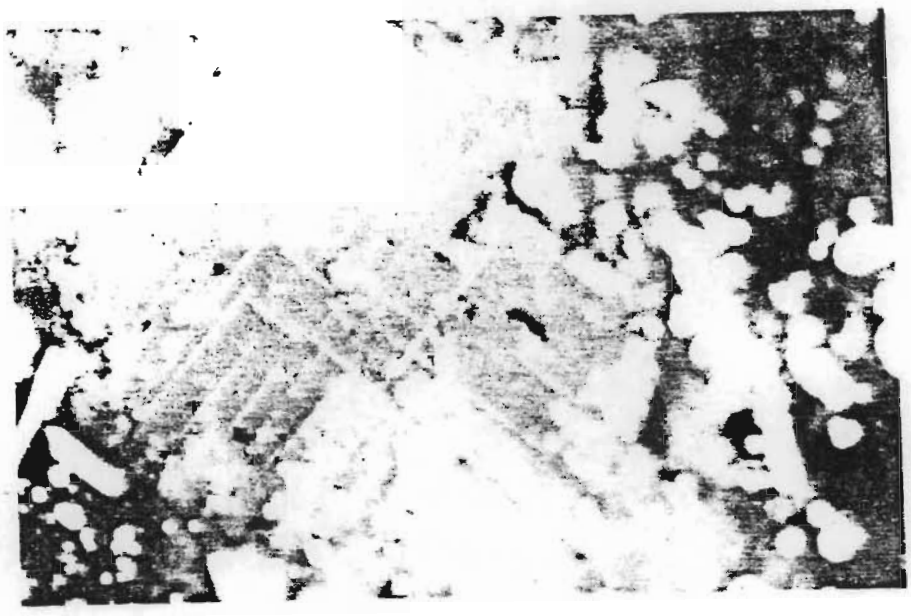

PLATE 6.4 A magnified view of the central core region of a chromite grain having undergone reduction in the presence of a solvent flux phase.

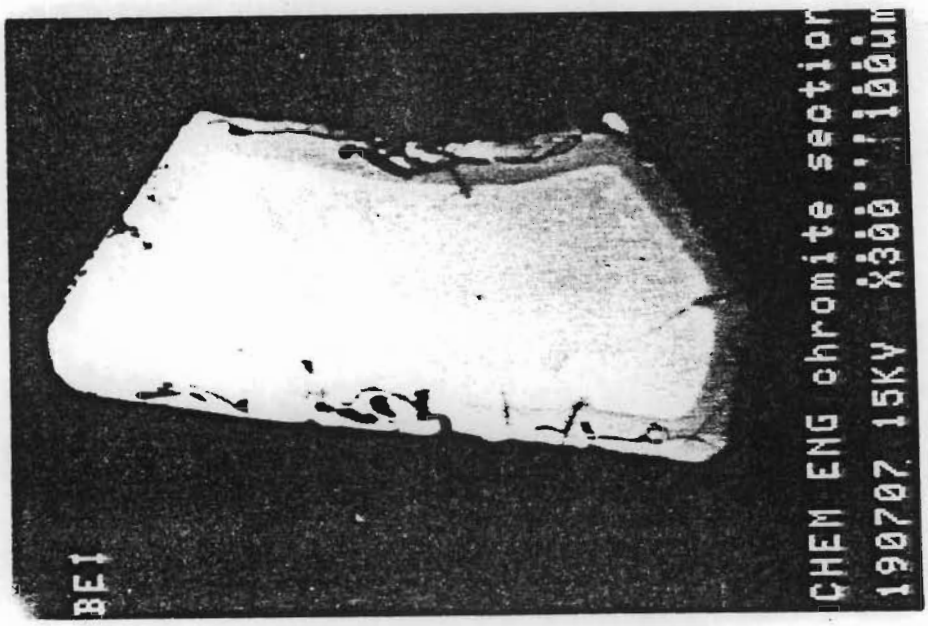

PLATE 6.5 A section view of a chromite grain after reduction in with a large quantity of flux phase and a remote carbon source, located millimetres away from the surface of the chromite grain.

the flux attack to be limited to the surface of the chromite grain, with very little penetration towards the grain interior. The interior of the grain showed an unaltered appearance with bright core, characteristic of a high iron and chromium content. Analysis of this central region showed it to be unaltered chromite.

This result underlines the importance that carbon proximity or reducing potential (Po_2) has on the physical characteristics of the flux- spinel solution. Under highly reducing conditions, part of the chromium in solution is likely to be in the divalent state. The divalent chromium in solution will act as an additional fluxing agent, reducing the viscosity of the flux and increasing the rate of spinel dissolution into the liquid phase.

Conversely, under more oxidizing conditions, the chromium in solution would be present largely in the trivalent state. This would result in a significant increase in the liquidus temperature and viscosity of the liquid phase, and severely retard the rate of spinel dissolution. Accordingly a very slow and limited rate of reduction would be expected if the carbon were to be removed from the surface of the oxide over a distance of a couple of millimetres. Thus penetration of the flux can be influenced by the nature of the reductant.

Investigation of the surface of the chromite grain (plates 6.6(a) and 6.6(b)), showed that extensive recrystallization of the spinel from the liquid phase had occurred on the surface of the grain. Analysis of this phase showed it to be mainly spinel with a small magnesio- chromite content.

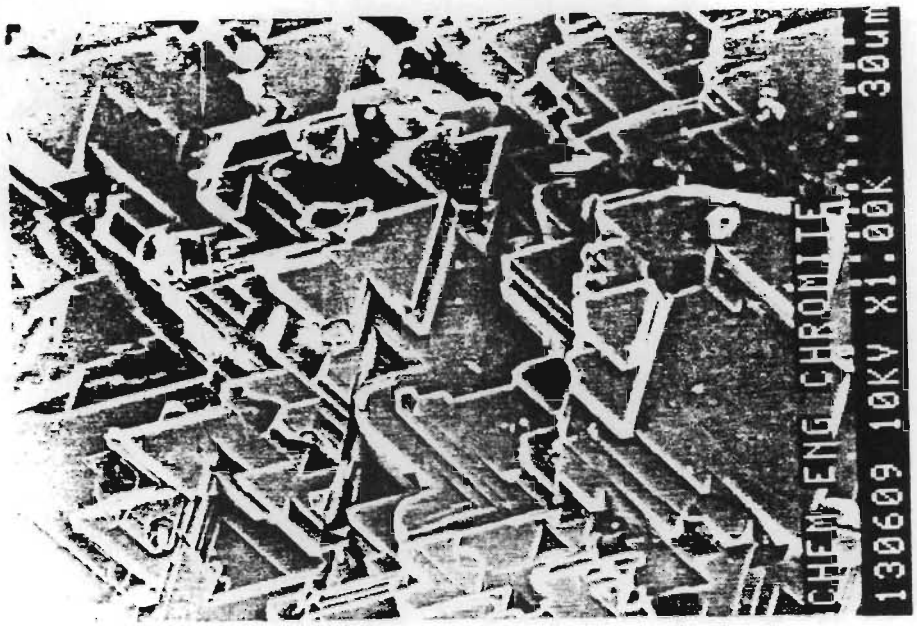

PLATE 6.6 (A) Surface detail of the chromite grain shown sectioned in PLATE 6.5.

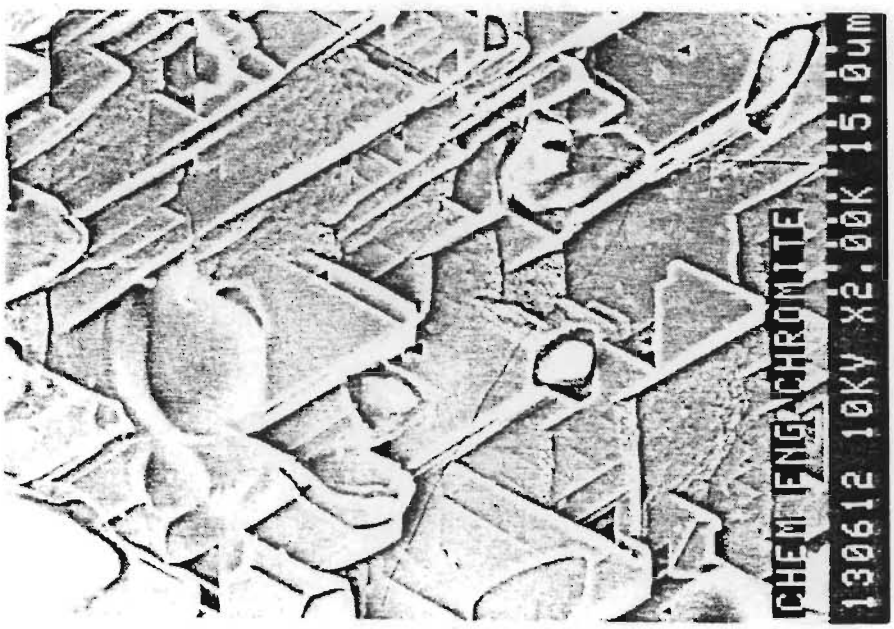

PLATE 6.6 (B) Further surface detail of the grain surface after acid leaching. The recrystallized texture covered the entire surface of the chromite grain.

This suggests that non reducible cationic species, namely magnesia and alumina, which have a very limited solubility in the flux, tend to recrystallize at the grain exterior, forming a pure spinel ($MgAl_2O_4$) phase. The formation of this phase at the grain surface, with insufficient carbon in close proximity leads to the cessation of the reduction reaction at a very low extent (similar to the inhibiting effect found in the standard reduction reaction).

Thus the limited solubility of iron and chromium species in the flux, as well as the possible formation of a refractory shell at the surface of the grain emphasises the importance of carbon proximity in ensuring rapid and complete reduction in the presence of a flux phase.

6.3 ANALYSIS OF THE SOLVENT PHASE PROMOTED REDUCTION REACTION

6.3.1 THE IRON CHROMIUM METALLIZATION CURVE

As in the case of the unpromoted reduction, the first step in a systematic analysis is to determine a relevent chromium- iron metallization curve. Additional variables that need to be considered with a flux phase present include the chemical and physical properties of the flux phase which, as indicated above, have an influence on the kinetics of the reduction reaction.

The varying degree of metallization found in samples during the typical reduction reaction with a 10% CaF_2, 2%NaF flux is shown in figure 6.16. Tests with limited additions (5-20%) of the various fluoride based fluxes

FIGURE 6.16

Experimental results in terms of the iron- chromium metallization curve obtained in the presence of a flux phase

CONDITIONS:
TEMPERATURE: 1100- 1200°C
CHROMITE : LG-6, 38- 105 micron size range
FLUX ADDITION : 10% CaF_2, 2% NaF

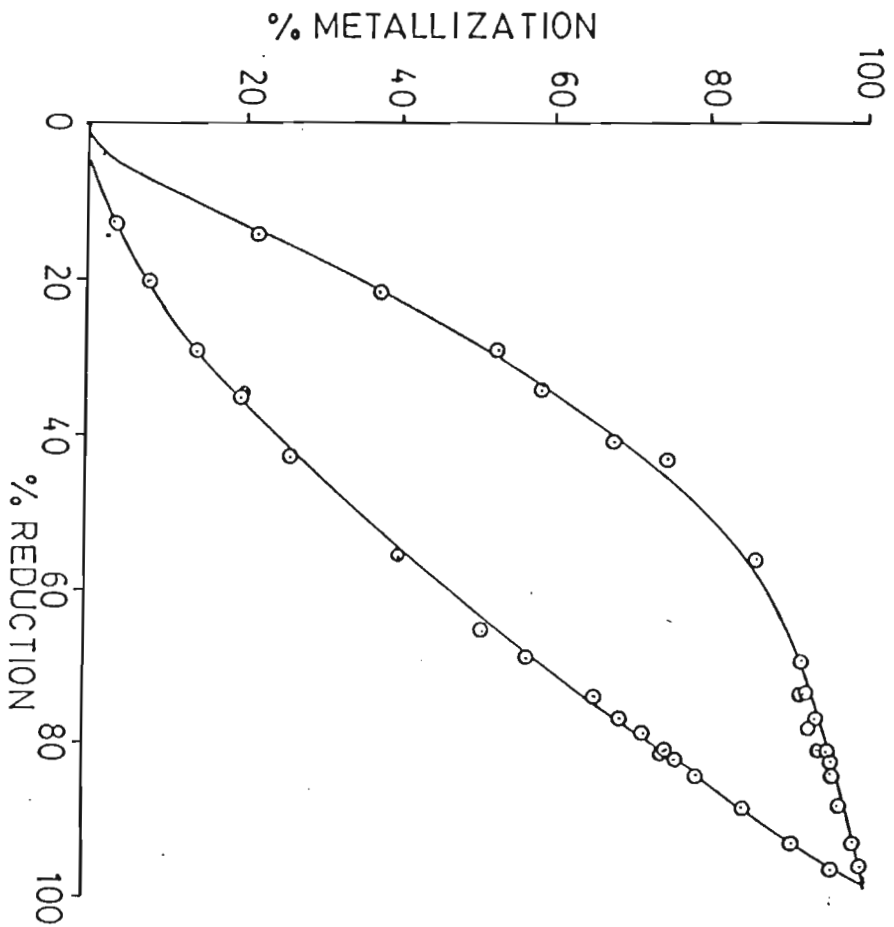

FIGURE 6.17

Comparison of the metallization envelopes obtained from experiment with and without flux.

CONDITIONS:
TEMPERATURE 1200°C (isothermal)
CHROMITE LG-6, 38- 105 micron
FLUX ADDITION 10% CaF_2, 2% NaF

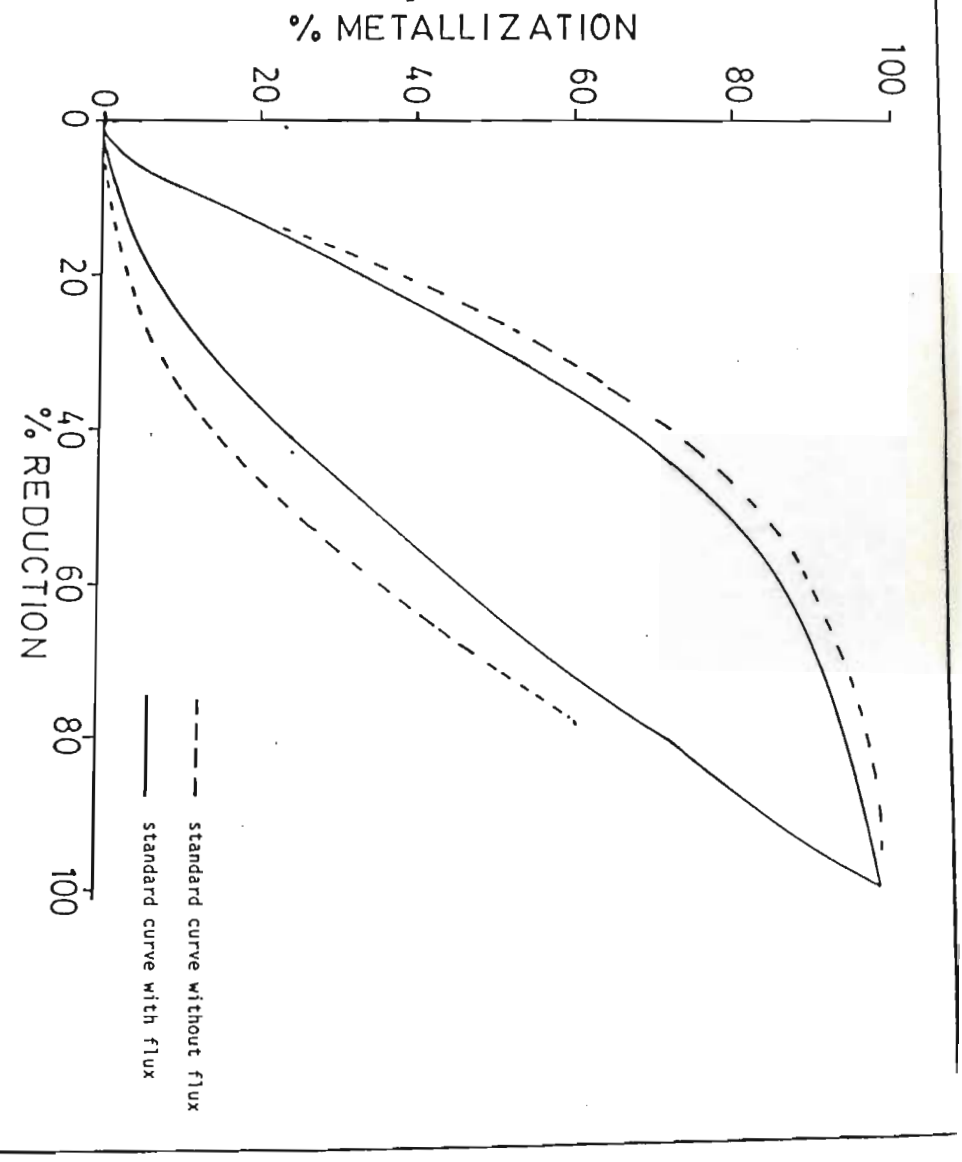

(table 6.4) in the temperature range 1100- 1300°C, were also found to give points that lay on this same curve.

It was concluded that this metallization curve was fairly typical of a reduction reaction promoted by the presence of small quantities of a fluoride based flux phase in the temperature range 1100- 1300°C.

Comparison of this metallization curve with that obtained for the standard reduction (figure 6.17) shows the flux addition to have caused a slight contraction and most important, the virtual closure of the metallization envelope.

This effect that flux addition has on the metallization curve, particularly regarding the increased extent for chromium is as expected (chapter 5) and stems from the disruption of the surface layer of the chromite grain.

6.3.2 THE KINETIC DEPENDENCE OF THE METALLIZATION ENVELOPE

Results obtained using massive additions of Na_2CO_3 (between 50 and 100% chromite mass), together with limited carbon addition (sufficient for iron reduction and very limited chromium reduction) gave rise to variations in the metallization curve.

The rapid and extensive disruption of the spinel at a relatively low temperature (1100°C) caused by the large quantities of flux addition, resulted in a progressive expansion of the metallization curve from that typical without any or only limited flux addition towards that calculated assuming a mixture of plain oxides (figure 6.18).

This change in metallization curve substantiates the

TABLE 6.4 SUMMARY OF EUTECTIC SALT MIXTURE COMPOSITIONS INVESTIGATED

Compositions expressed as mass % of chromite addition.

CaF2	NaF	SiO2	BORAX	Na2CO3	CaO
10	2	--	--	--	--
14,7	16,56	--	--	--	--
10	2	10	--	--	--
6,0	--	--	--	--	1,5
12	--	--	--	--	3,0
8,18	--	--	--	--	3,47
13,6	--	--	--	--	9,09
18	--	--	--	--	4,5
2,39	2,61	--	--	--	--
4,78	5,22	--	--	--	--
9,56	10,44	--	--	--	--
14,34	15,66	--	--	--	--

FIGURE 6.18

The effect of massive flux addition on the reduction reaction, using a Na_2CO_3 flux with carbon addition sufficient for iron reduction.

CONDITIONS:
TEMPERATURE: 1100°C (isothermal)
CHROMITE: LG-6 d_p = 10 micron
REDUCTANT: carbon black

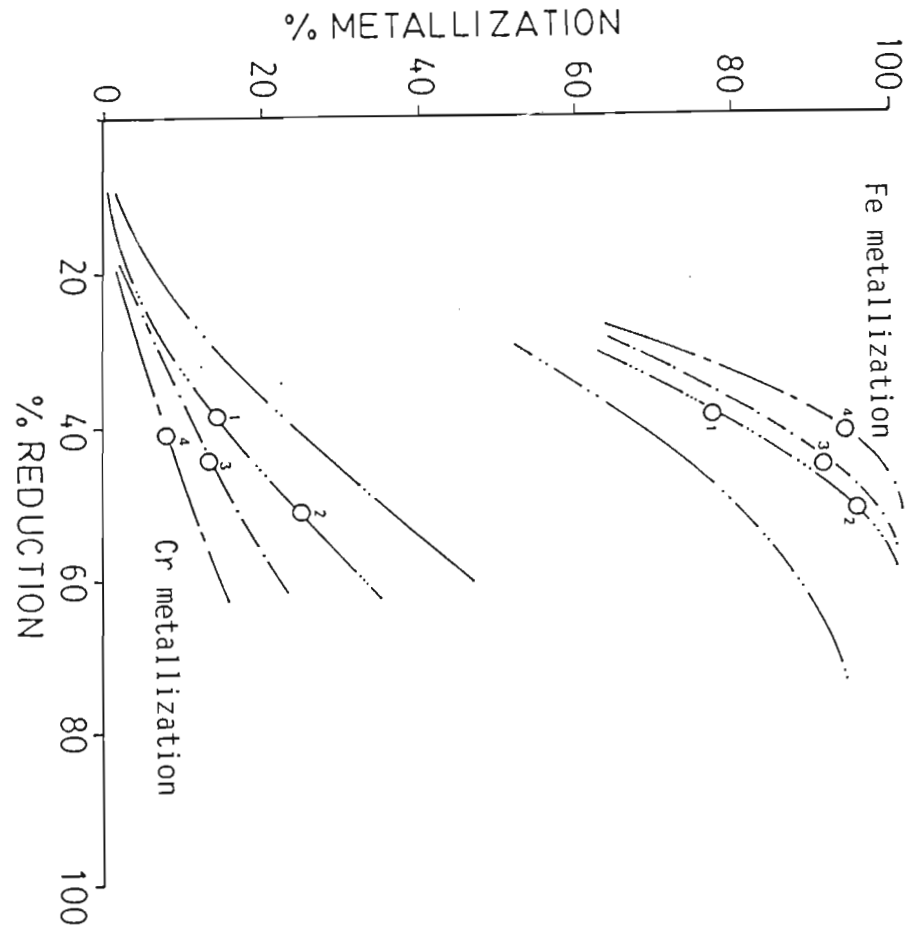

kinetic dependence inherent in the metallization curve postulated previously (chapters 3 and 5).

Under conditions of rapid and complete spinel disruption, reduction would be expected to follow a strict sequence from least stable oxide species (Fe^{3+}) to most stable oxide species (Cr^{3+}), with virtually no overlap (i.e. the spinel association of oxide phases is no longer applicable). Under such conditions the rate of reduction would be governed by factors external to the chromite grain.

However, in the case of limited flux addition, only limited disruption occurs, at a rate corresponding to the rate of reduction. Accordingly it is expected that factors internal to the chromite grain would still dominate reaction kinetics. Factors such as relative cation mobility in the spinel, and to a lesser extent in the slag, would influence the shape of the metallization curve. A narrowing of the metallization curve might well be expected in the case where the flux was particularly active in promoting the kinetics of the slower (Cr^{3+}) species. This is achieved by the disruption of the surface layer of spinel that retards chromium diffusion.

6.3.3 FUNDAMENTAL CONSIDERATIONS IN TERMS OF RATE CONTROLLING MECHANISMS

The results obtained from the mineralogical investigation, together with the information gained from the metallization curve as discussed above, indicate that a variety of factors have an influence on the reaction kinetics. The shift in relative importance

as regards rate control is summarised in figure 6.19.

Results obtained under conditions in area 1 (the focus of this work) indicated internal factors as dominating the reduction rate, with relatively little influence of external factors. However in region 2 the marked importance of reductant particle size and flux composition indicated a shift in rate controlling mechanism, with increased importance of factors external to the chromite grain.

The dramatic effect that the flux has on the reduction reaction, particularly in terms of the chromium reduction rate and extent can be clearly seen (figure 6.20).

Variables such as particle size, temperature and to a degree carbon addition have a similar effect to those experienced in the absence of any flux, though the kinetic rates are much higher, and the relatively rapid chromium reduction rate is maintained throughout the reduction reaction (figures 6.21 and 6.22).

Flux type and addition were found to affect particularly the reduction rate of chromium (figures 6.23 and 6.24). Since neither was found to have any significant effect on the metallization curve, it may be concluded that these parameters mainly affect the rate of disruption of the grain surface, doing little to alter the actual mechanism of reduction.

In terms of establishing a kinetic model of the reduction process in the presence of a limited quantity of flux phase, it would appear that the fundamental mechanism of solid state diffusion of iron and chromium species through the lattice to the surface is still rate limiting. However, the effective disruption of the

FIGURE 6.19

Schematic representation of conditions covered in the experimental investigation and summary in terms of rate controlling factors.

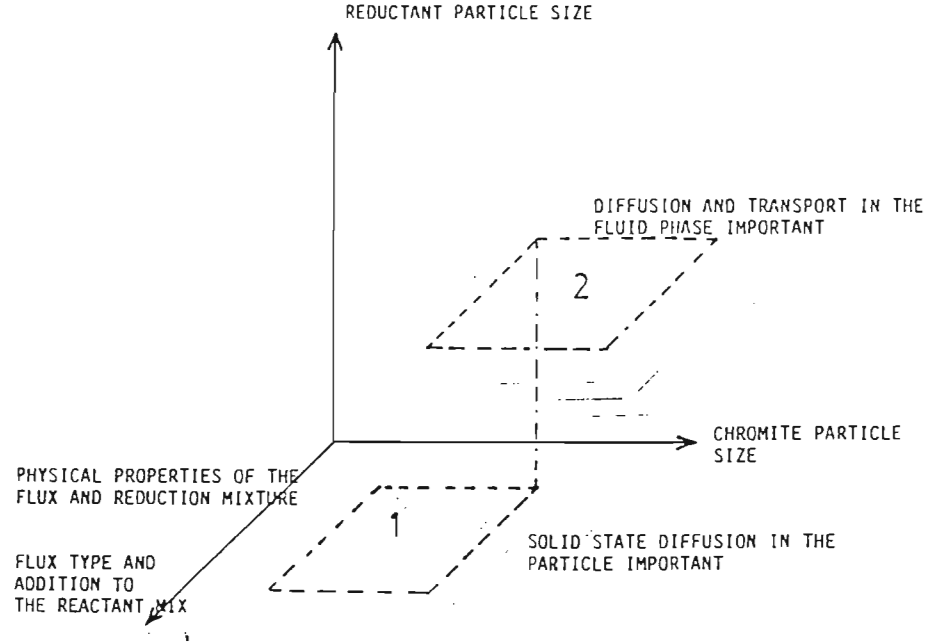

FIGURE 6.19

FIGURE 6.20

Comparison of the effect of flux addition on the individual rates of iron and chromium reduction compared with that obtained without any flux addition.

CONDITIONS:
ORE : LG6 CHROME SAND
REDUCTANT : LAMPBLACK
TEMPERATURE: 1200°C (isothermal)
FLUX : 5% addition of NaF- CaF_2 eutectic mixture.

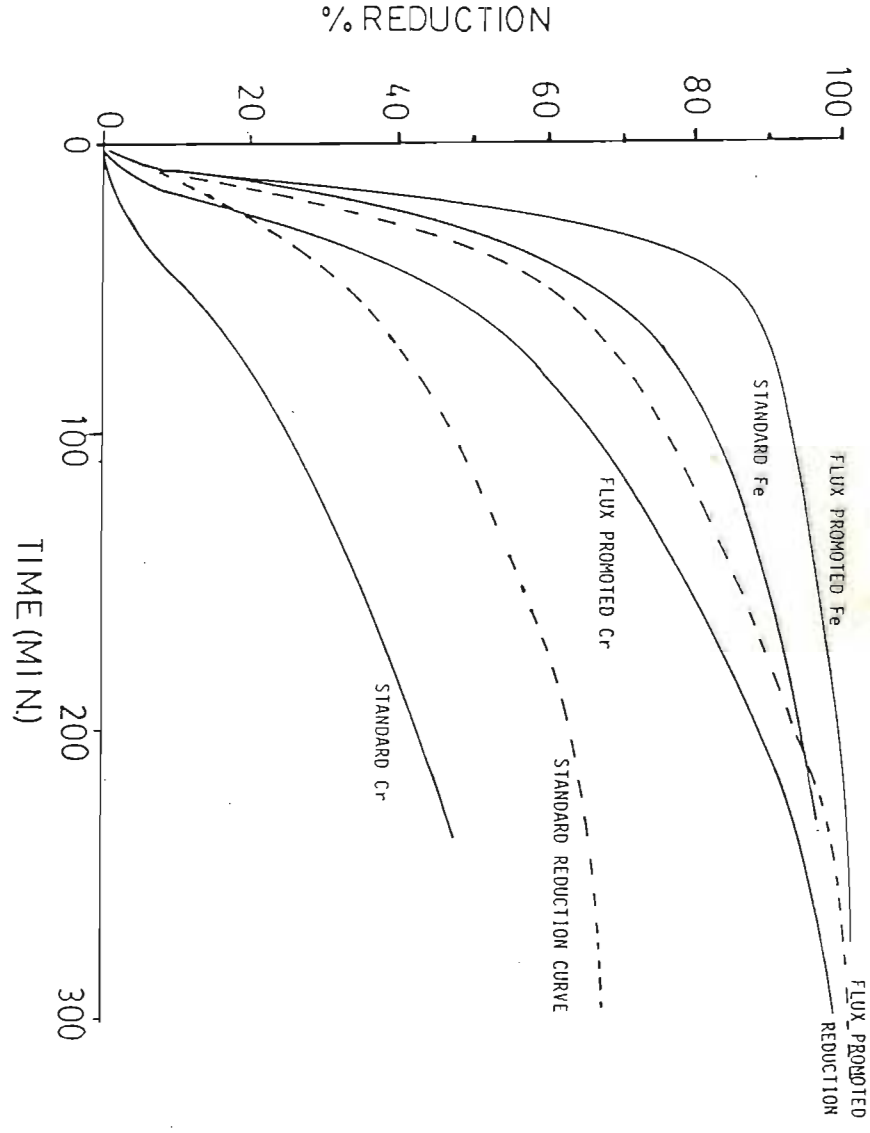

FIGURE 6.24 The effect of flux type on the individual rates of iron and chromium reduction .

CONDITIONS:

TEMPERATURE : 1200°C (isothermal)

ORE : LG6 CHROMESAND ; d_p = 10 um

REDUCTANT : LAMPBLACK

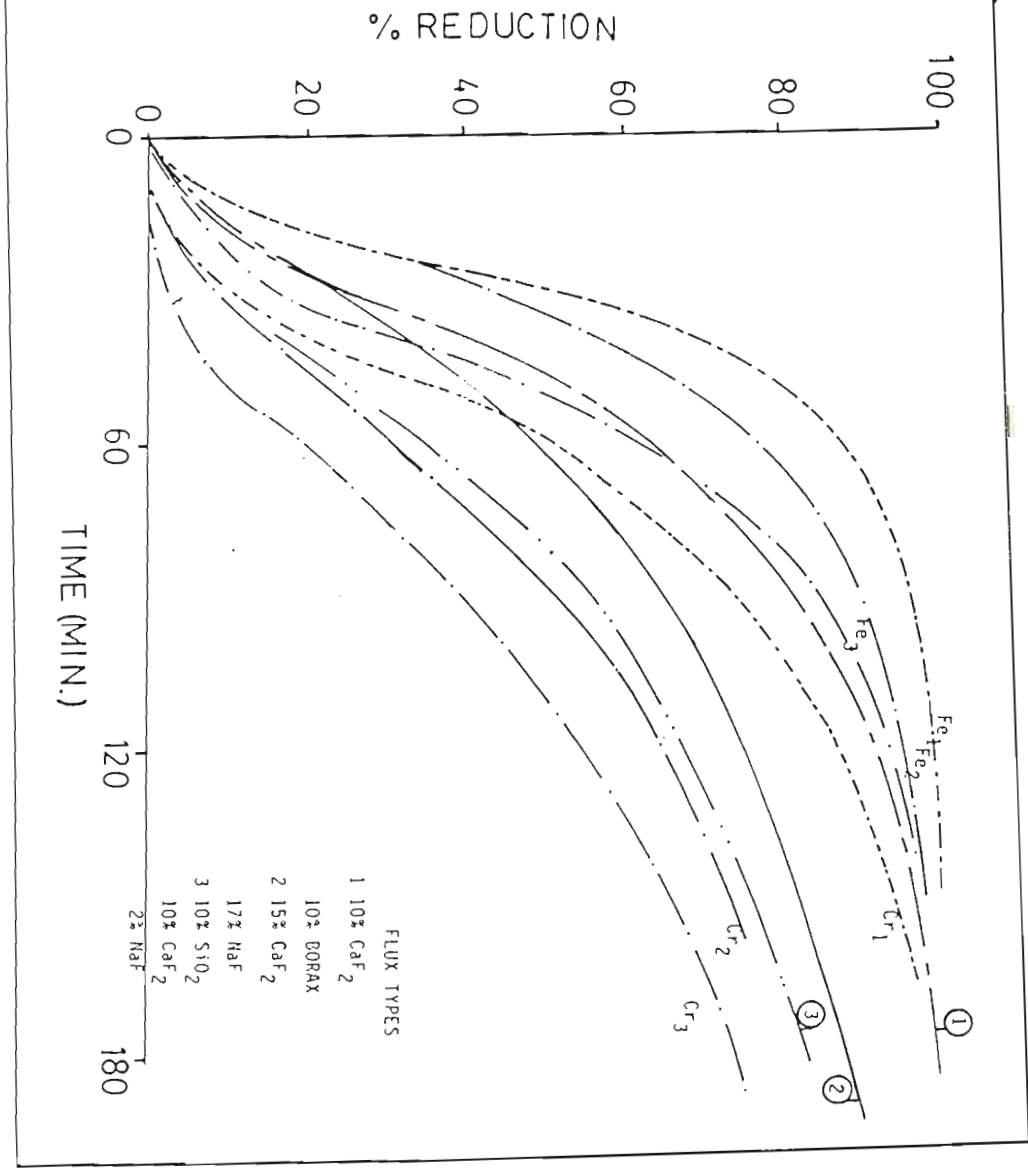

The effect of flux addition on the individual rates of iron and chromium reduction at 1200°C.

CONDITIONS:

ORE : LG6 CHROMESAND

REDUCTANT : LAMPBLACK

FLUX : 50% NaF, 50% CaF_2 mixture added as indicated (% relative to chromite mass)

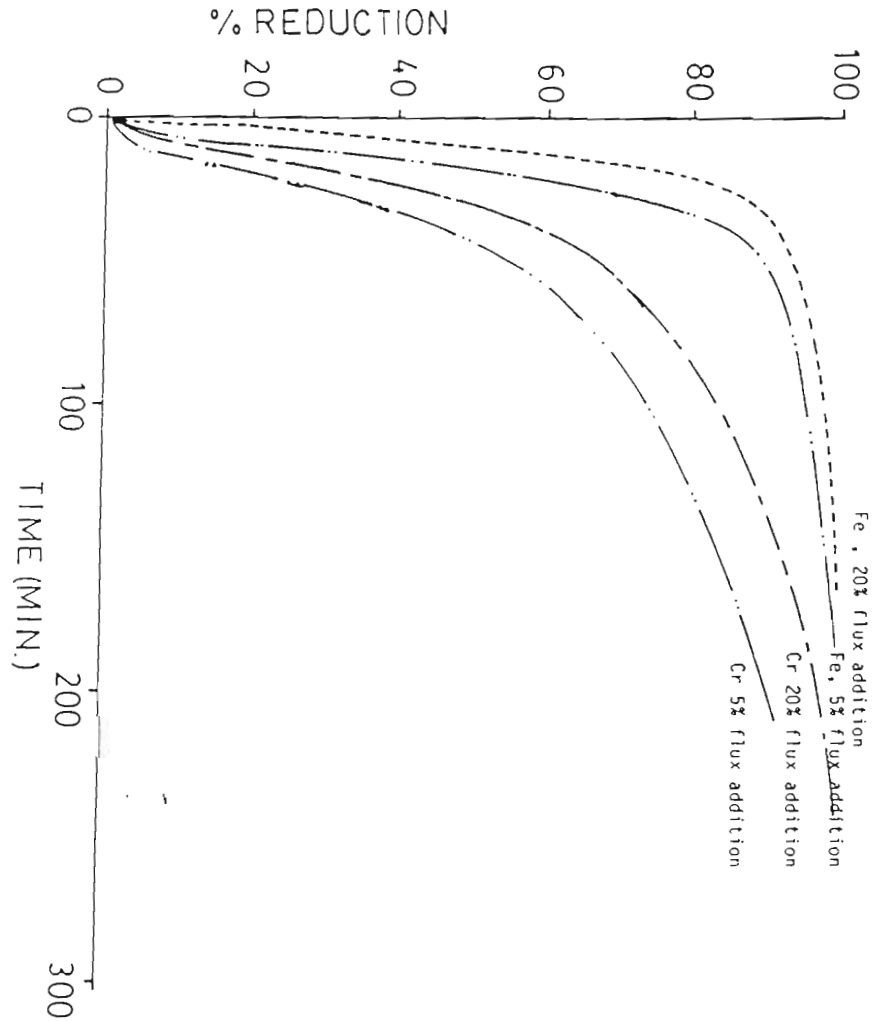

FIGURE 6.22 The effect of temperature on the individual rates of iron and chromium reduction in the presence of a flux phase.
CHROMITE: LG6 (CHROMESAND) REDUCTANT: LAMPBLACK d_p = 40 μm
FLUX : 10% CaF_2 , 10% SiO_2

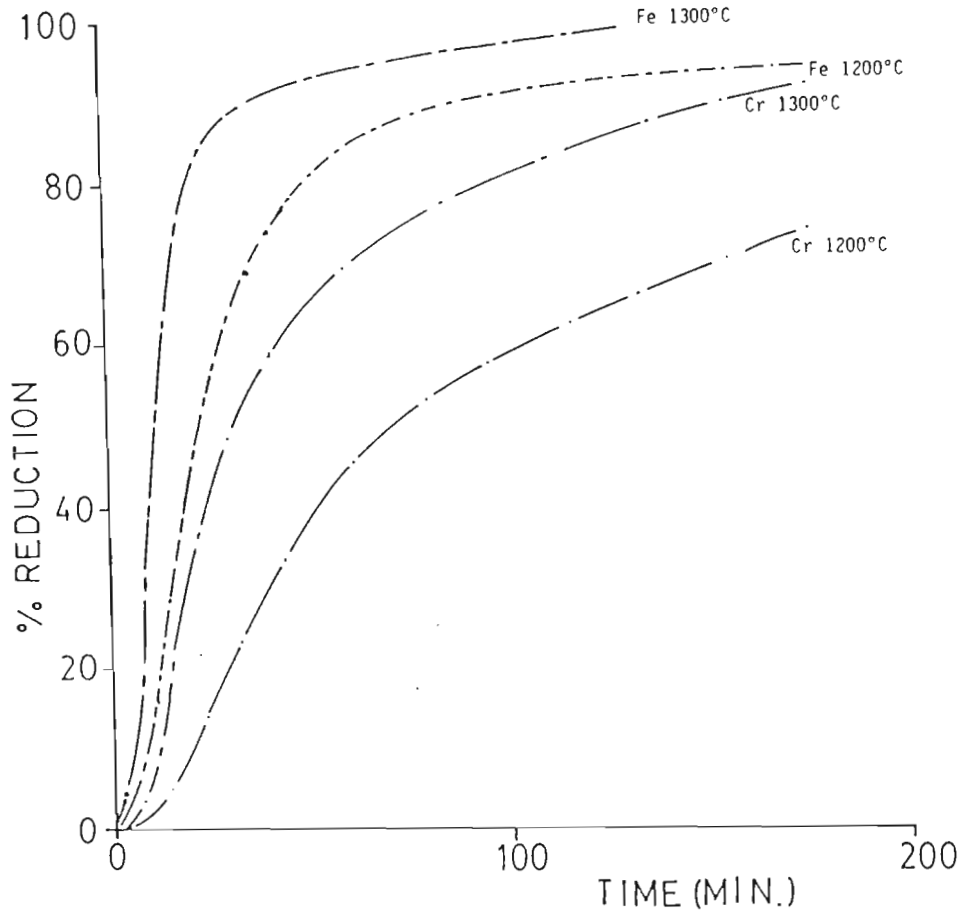

FIGURE 6.21 The effect of ore particle size on the individual rates of iron and chromium reduction in the presence of a flux phase.
TEMPERATURE = 1100°C (Isothermal) LAMPBLACK REDUCTANT FLUX: 2% NaF, 10% CaF_2
ORE : LG6 CHROME SAND

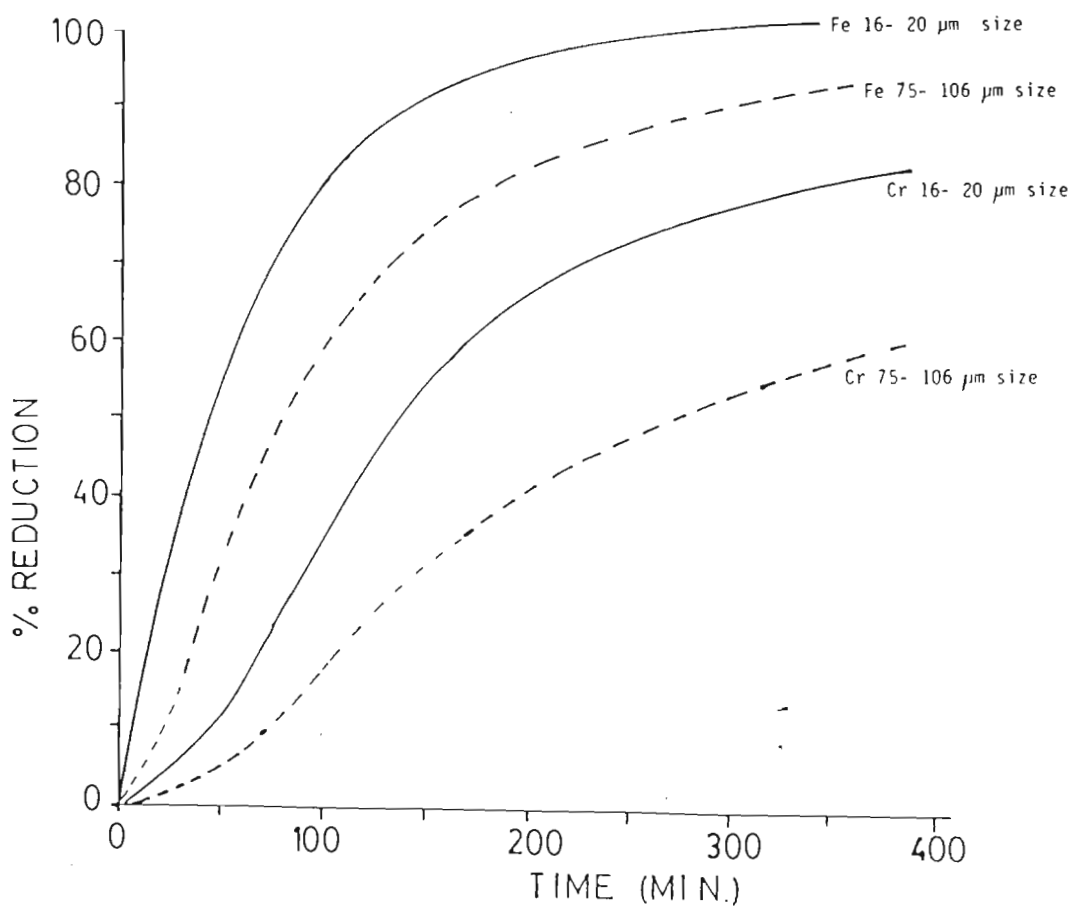

refractory surface of the grain by the flux has resulted in a significant increase in particularly the chromium reduction rate and extent. Accordingly the rate of spinel disruption will have an effect on the overall rate of reduction.

6.3.4 KINETIC MODEL FOR CHROMITE REDUCTION IN THE PRESENCE OF A FLUX PHASE

As in chapter 5, the principal reason for considering a mathematical model for the reduction reaction was to provide greater insight into the reduction mechanism; in this case in the presence of a solvent phase.

The experimental results obtained suggest that either one of three basic limitations might be applicable in the presence of a flux phase. Depending on particle size and flux addition, either solid state diffusion through the spinel, transport through the flux phase or dissolution of the chromite grain could be rate limiting.

Assuming the chromite particle to remain relatively fixed in size, consideration was given to the standard Fickian diffusion model as a means of determining the regions where solid state diffusion was likely to be the major rate limiting mechanism.

Using the expression:

$$\ln(1-R_f) = -4\pi^2 Da\,t/\,dp^2$$

(ref Searle and Finn, 160.)

where R_f is the fractional reduction of species i, Da the apparent diffusion coefficient and t the time elapsed, a linear relationship should be found between $\ln(1-R_f)$ and t/dp^2, indicating a constant diffusion coefficient.

The profiles shown in figure 6.25 indicate that with flux additions of 5 -30%, a diffusion process is applicable over the bulk of the reaction period. However the nature and quantity of flux phase has a significant effect on the apparent diffusion coefficient. The lower the melting point and the more aggressive the flux, the more rapid and complete the disruption of the surface of the chromite grain, and the greater the apparent

FIGURE 6.25(b)

The effect of flux addition on the chromium diffusion coefficient assuming a standard Fickian diffusion model for the reduction process.
(Same conditions as above.)

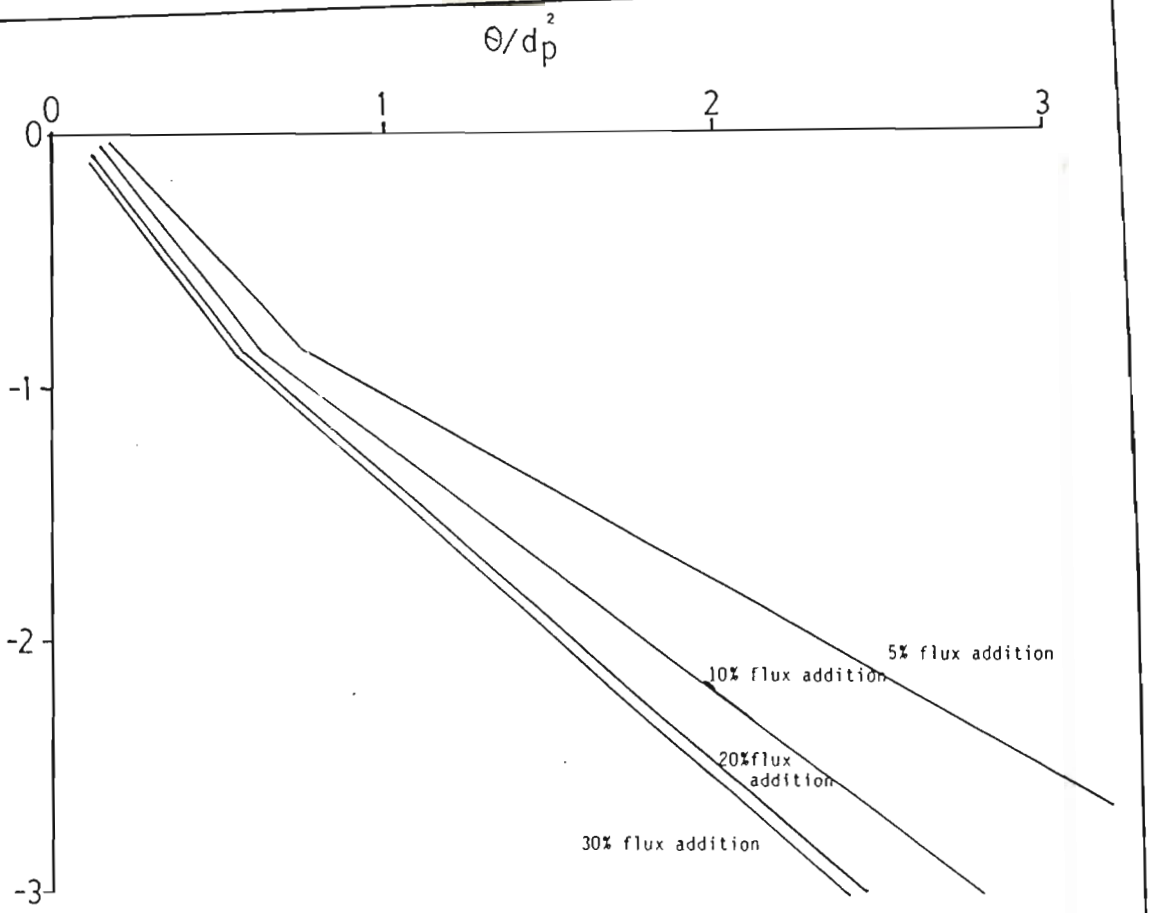

FIGURE 6.25(a)

The effect of flux addition on the Iron diffusion coefficient assuming a standard Fickian diffusion model for the reduction process.
CONDITIONS:
LG-6 chromite, d_p = 53-75 microns
Temperature = 1200°C (isothermal)
Reductant: carbon black.

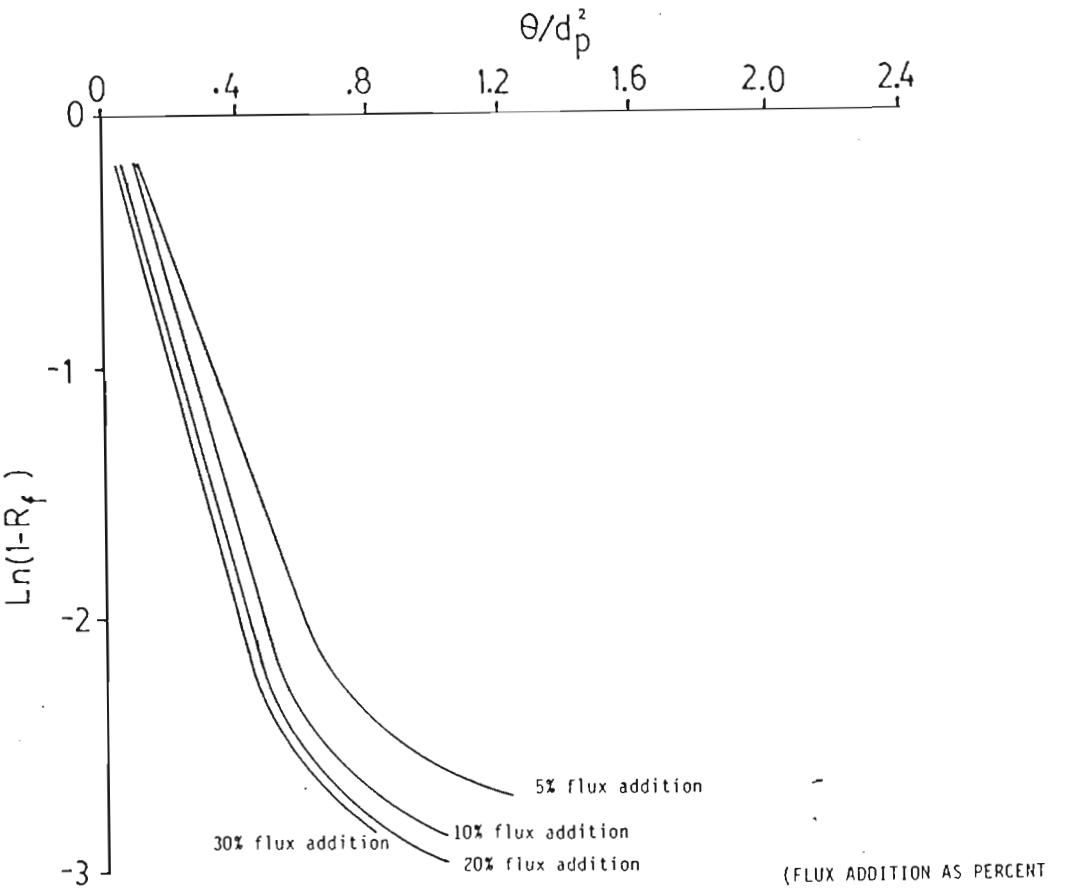

diffusion coefficient.

Because of the large number of variables, the following assumptions are implicit in the analysis:

(a) Ore particle size 20< dp< 200 microns, remaining fairly constant during the reaction.

(b) Flux (limited to CaF_2 - NaF) addition between 5 and 30% of chromite mass.

(c) Fine carbon reductant in sufficient quantity to ensure complete reduction.

(d) Temperature range (above the eutectic melting point of the flux phase) ~1100- 1300°C (Lovering,107).

In the light of diffusion still playing a dominant role in the reduction reaction, and bearing in mind the form of the reaction product, it was considered appropriate to investigate the reaction kinetics in terms of a shrinking core model as in the case of the standard reduction reaction (chapter 5).

Thus using the expression:

$t/\tau = (1-3(1-x)^{2/3} + 2(1-x))$ with $\tau = R^2/6D_i$ (ref.73,103)

analysis of the experimental results over a range of particle sizes showed reasonable linearity between τ and dp^2. However in this case the y intercept or Ci value was found to be very much smaller than in the standard reduction reaction.

In the expression $\tau_i = R^2/6D_i + C_i$, the value of C_i for chromium varied from 300- 350 seconds with 5- 10% flux addition, compared to values of 5000- 6000 seconds obtained without any flux present. This suggests that the additional rate limitation found in the standard reduction reaction is virtually removed through the presence of the flux phase.

The effective diffusion coefficients of chromium and iron were found to increase with increasing flux addition, and were generally much higher than those obtained in the unpromoted reduction.

Simulated reduction rates using the shrinking core model were found to be in excellent agreement with experimental results as shown in figures 6.26, 6.27 and 6.28.

Two important conclusions may be drawn from these results. Firstly, under conditions of limited (5-20%) flux addition, the reduction kinetics are still dominated by the solid state diffusion of iron and chromium species through the partly reacted spinel to the grain surface or flux- spinel interface.

Secondly the marked increase in chromium reduction rate and extent, mirrored in terms of the model by the increase in De and T0 values, especially for chromium, indicates the action of the flux. Under the conditions investigated, the flux is seen to slowly dissolve the surface of the chromite grain, effectively preventing the formation of the refractory spinel layer which would otherwise retard the reaction.

The observed action of the flux in disrupting the grain surface and penetrating into the grain also provides strong support for the general mechanism of chromite reduction described in the previous chapter. In particular, the reason for the apparent reaction ceiling is the formation of a relatively thin refractory shell which acts to isolate the grain interior from the reduction environment.

By adding the flux and removing this inhibiting layer, it has been clearly demonstrated that a faster and more complete reduction will ensue.

The thin nature of the inhibiting layer means that even small flux additions (5%) can be highly effective in promoting the extent of reaction achievable. Such limited flux additions have obvious potential benefits in terms of a commercial pre-reduction operation and are considered in some detail below.

FIGURE 6.27 Modelling of experimental results obtained with a 10% addition of a 50% CaF_2 , 50% NaF flux mixture.

LG 6 ORE, 1200°C, LAMPBLACK REDUCTANT.

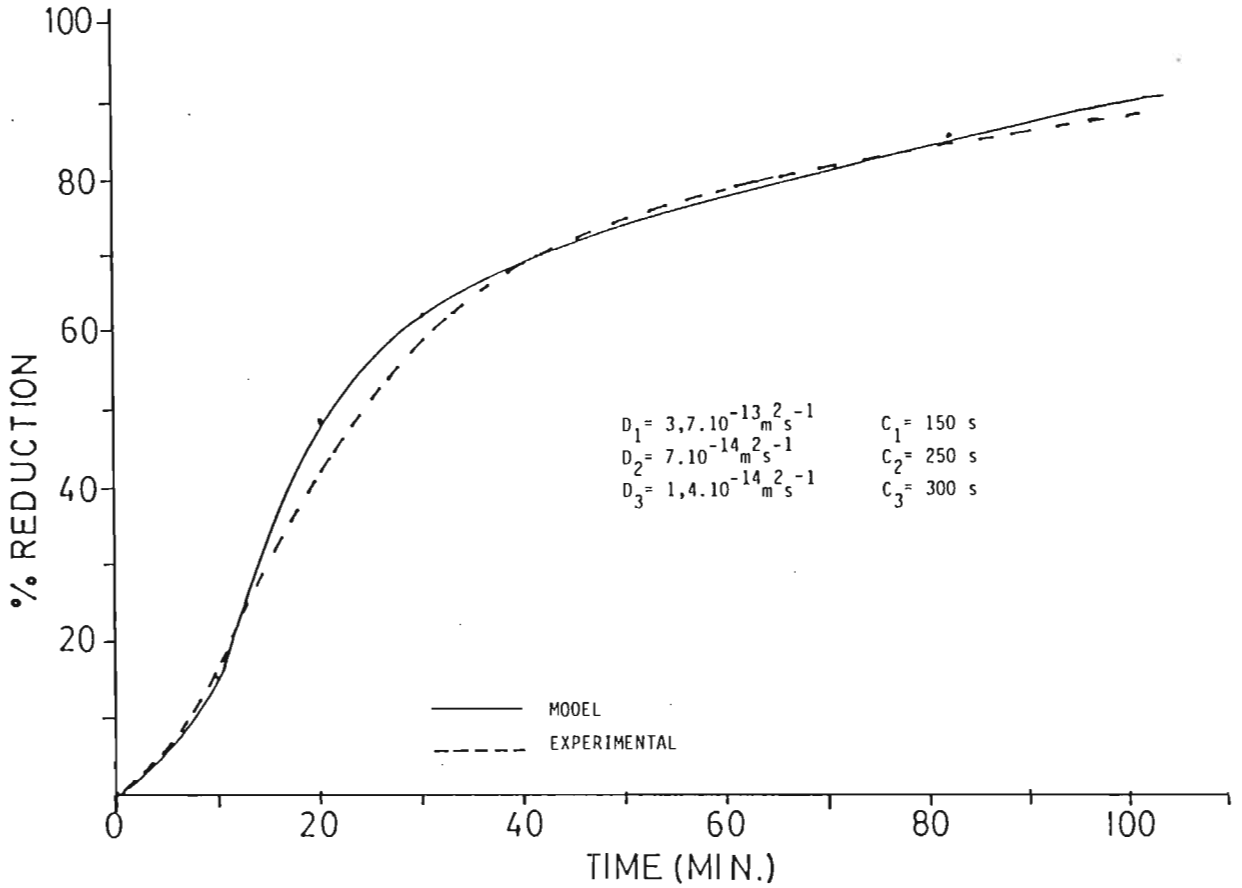

...ling of experimental results obtained with a 5% addition of a 50% CaF_2, 50% NaF flux mixture.

LG6 ore (CHROME SAND) with LAMPBLACK as reductant.
TEMPERATURE = 1200°C (isothermal)

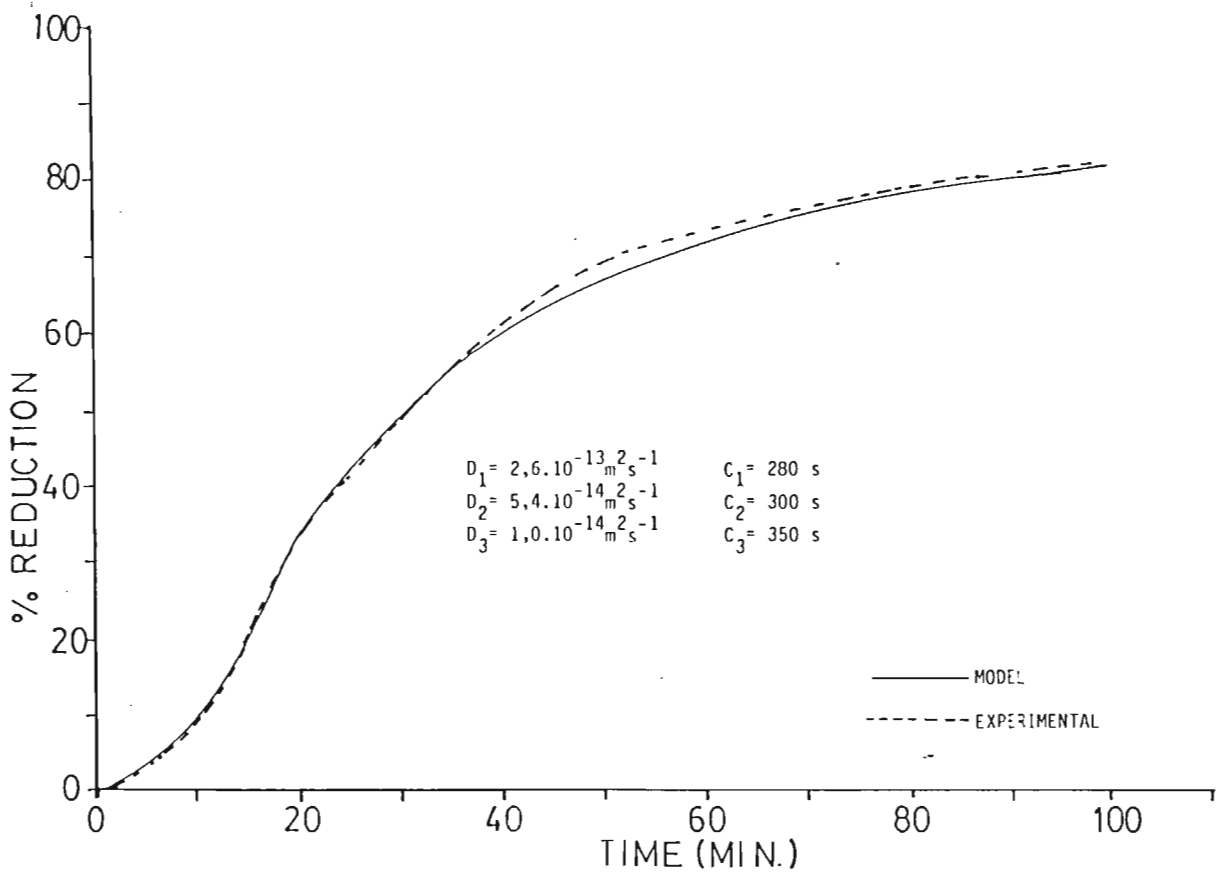

FIGURE 6.28 Modelling experimental results obtained with a 20% flux addition of a 50% NaF, 50%CaF_2 flux mixture.

LG6 ORE, 1200°C, LAMPBLACK REDUCTANT

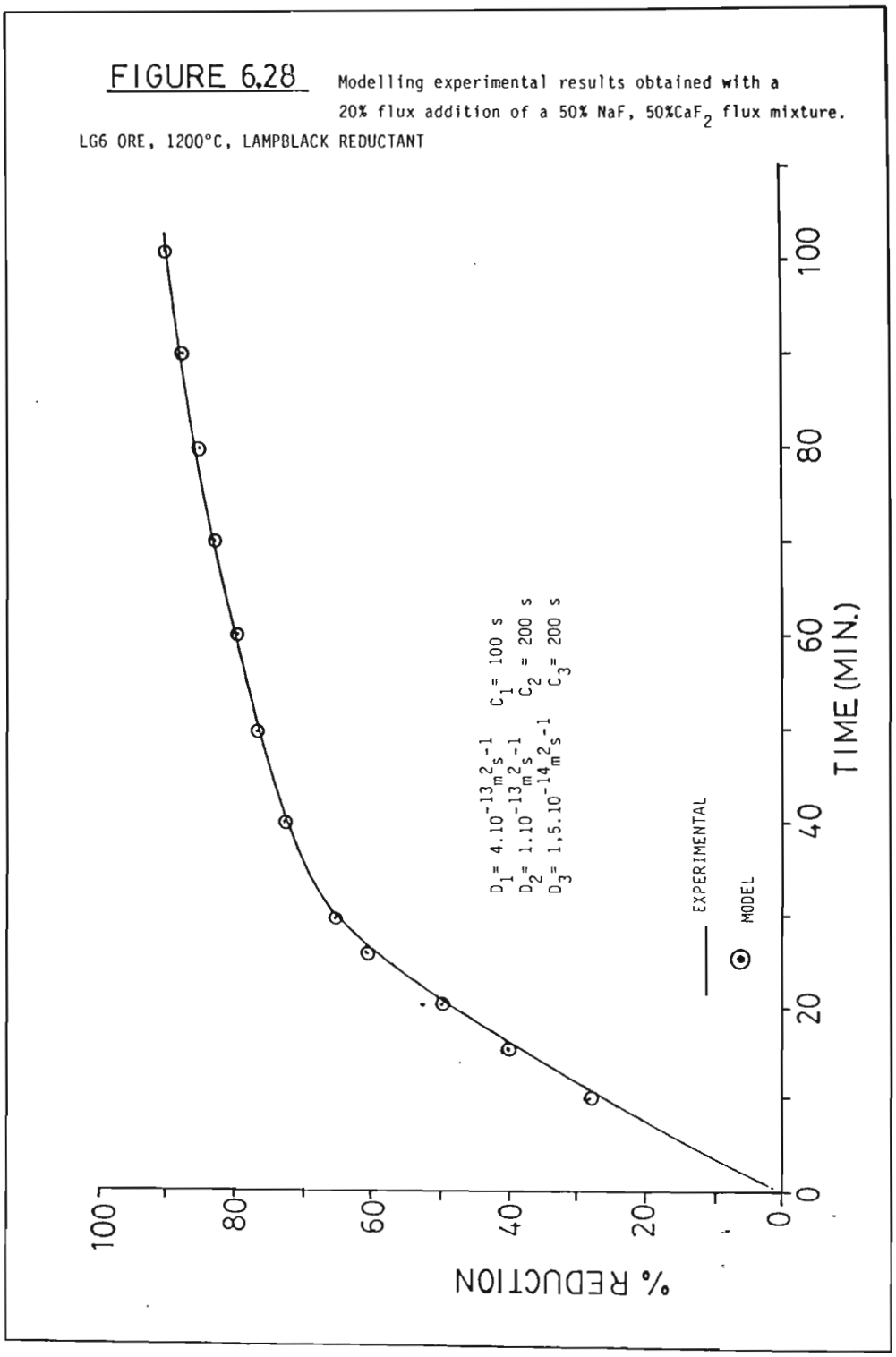

6.4 PRACTICAL APPLICATION OF SOLVENT FLUX ADDITION TO IMPROVE CHROMITE REDUCTION

6.4.1 INTRODUCTION

The ability of a solvent flux to promote the rate and extent of chromite reduction has obvious application in a commercial pre- reduction process. However the numerous constraints on any practical system have to be considered with respect to the nature and quantity of flux addition.

In practice the likely treatment of a coarser range of ore and reductant particle sizes (e.g. 10- 3000 micron), requires a flux with increased solubility for the spinel components. The necessity for this was shown by the very limited effect of the NaF- CaF_2 flux on chromite in this size range with a discrete carbon source.

In addition the costs associated with the use of NaF as a fluxing agent suggested that cheaper and more readily available alternatives be considered.

Accordingly the principal of a solvent flux addition was investigated over a wider range of particle sizes and flux compositions.

Considering the CaF_2 - spinel system, the work of Nafziger (124b) on the CaF_2 - CaO- MgO- Al_2O_3 system shows a low liquidus region in the quaternary system at the 20% Al_2O_3 join, and the region below the liquidus remaining near the CaF_2 join. Analysis of the quaternary system shows the eutectic valley to be faced with steep sloping sides, particularly on the MgO side, with low solubility of MgO in the eutectic melt phase.

This suggests the need for fluxing the MgO content to a greater degree. The CaF_2 - MgO- SiO_2 system (figure 6.29) shows a relatively large liquidus region at 1200°C, capable of accepting

at least 15% MgO. Accordingly SiO_2 was included in the flux system.

When considering the CaF_2 - (SiO_2,Al_2O_3) -(CaO,MgO) system, a liquidus region similar to that shown in figure 6.30 might be expected. From this it appears that a 20-30% addition of a flux containing 70% CaF_2 , 15% SiO_2,15% CaO would be capable of solubilizing most of the magnesia component of the spinel and remaining reasonably fluid at a temperature of 1300°C.

However as seen from figure 6.31, the inclusion of SiO_2 in the flux together with CaF_2 is likely to result in the formation of a two phase liquid system. Since this was not expected to be particularly beneficial, and because of the known beneficial effects of alkali components in the flux, including a miscibilising action (figure 6.32), a quantity of Na_2O was included (ref. 5a,65,51).

Initial investigation was thus based on a slag containing 60% CaF_2 , 15% CaO, 20% SiO_2 and 5% Na_2O (flux 1). Variations on this composition as shown in table 6.5 were also investigated.

6.5.2 SUMMARY OF RESULTS

Initial tests were conducted with relatively large quantities of slag (amounting to between 20 and 50% of the chromite mass), with the reactants agglomerated in the form of a pellet to ensure the greatest degree of homogeneity and carbon proximity possible.

Flux 1 was found to be relatively aggressive towards the spinel, resulting in rapid reduction rates.

The reduction product showed good slag penetration (plate 6.7). A feature evident from these tests however, was the significant recrystallization of a pure spinel at the grain surface. This suggests a lower than expected solubility of these components in the slag phase at 1200- 1240°C. The recrystallization appeared to retard the flux action, resulting in slower reduction rates and

FIGURE 6.29

The CaF_2 - MgO - SiO_2 system. (ref. 102)

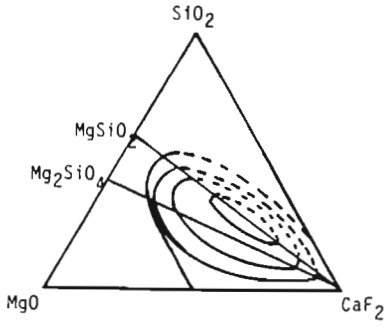

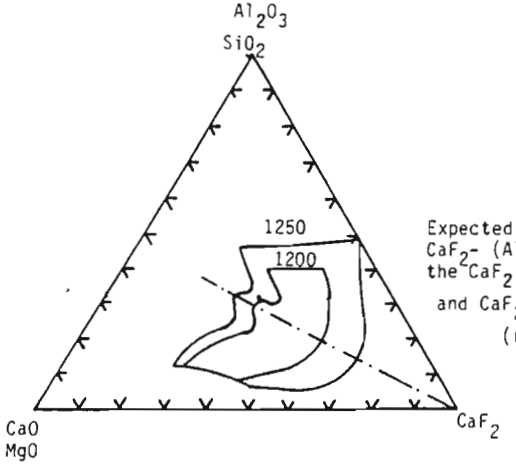

Expected liquidus region for the system CaF_2- (Al_2O_3,SiO_2)- (CaO,MgO), based on the CaF_2,SiO_2,CaO; SiO_2,Al_2O_3,MgO and CaF_2,SiO_2,MgO systems.
(ref. 102)

FIGURE 6.30

FIGURE 6.31

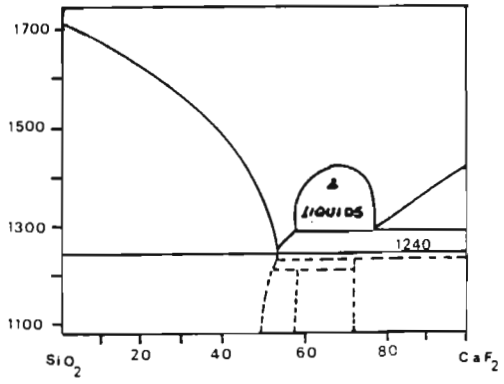

The CaF_2 - SiO_2 system showing eutectic point at 1240°C
(ref. 102)

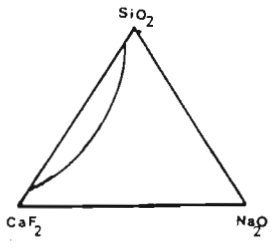

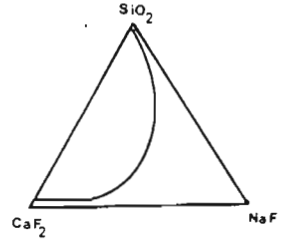

FIGURE 6.32

Two ternary systems showing the miscibilising effect of Na_2O and NaF on the binary liquid phases in the CaF_2-SiO_2 system.
(ref. 102)

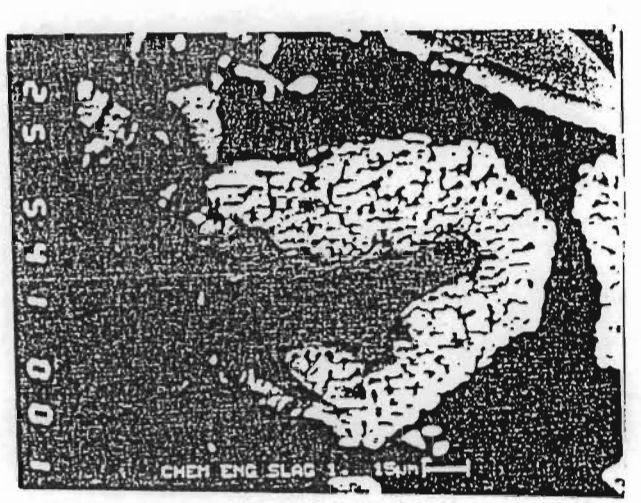

PLATE 6.7 Section through a chromite grain after reduction with a CaF -SiO -CaO flux and carbon in the size range 30- 90μm

PLATE 6.8 Metal phase morphology after reduction with surplus flux and carbon of a discrete particle sizing as above.

TABLE 6.5

STANDARD FLUX COMPOSITIONS.

FLUX	CaF_2	CaO	SiO_2	Na_2O
FLUX 1	60,00	15,00	20,00	5,00
FLUX 2	27,30	18,20	45,50	9,10
FLUX 3	27,27	9,09	54,55	9,09

reduced chromium recovery.

Metallization, absent at the chromite grain surface, but attached to the larger pieces of reductant (plate 6.10), suggested that the transport properties in the slag phases were playing a role in determining the overall kinetics of reduction.

The use of discretely sized reductant (30- 105 micron) resulted in improved metal phase growth. Comparison of the metal formation shown in plates 6.8 through 6.11 at similar extents of reduction, clearly shows the benefit of discrete reductant sizing on metal phase growth. However, increased reductant sizing and resultant increased transport distances for dissolved species were found to result in a decreased reduction rates.

Fluxes with higher SiO_2 content (fluxes 2 and 3) were found to be more capable of sustaining a reasonable reduction rate for the duration of the reaction. The resulting slags were found to have a distinct two phase structure on cooling, the minor phase in such cases being silica rich, and containing most of the magnesia and alumina dissolved from the spinel, as shown by the E.D.S. spectra in figure 6.33 (resulting from a 50% addition of flux type 2).

In contrast, flux 1 with a lower silica content and proportionally more alkali, though not as effective at spinel dissolution, did not show any significant two phase character, confirming the miscibilising action of the alkali component.

With flux 1, the bulk slag phase was found to contain some magnesia, though most of the magnesia initially dissolved in the flux was found to have reprecipitated together with the alumina to form the recrystallized spinel phase, as shown by the E.D.S. spectra in figure 6.34.

The importance of avoiding precipitation of the spinel around the surface of the chromite grain prompted further consideration of flux systems capable of taking magnesia and alumina into

PLATE 6.9 (A)

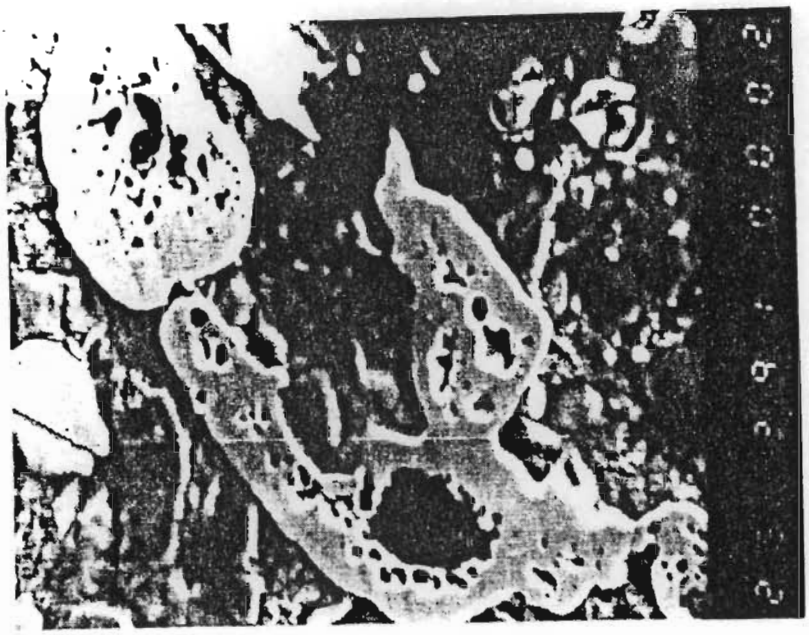

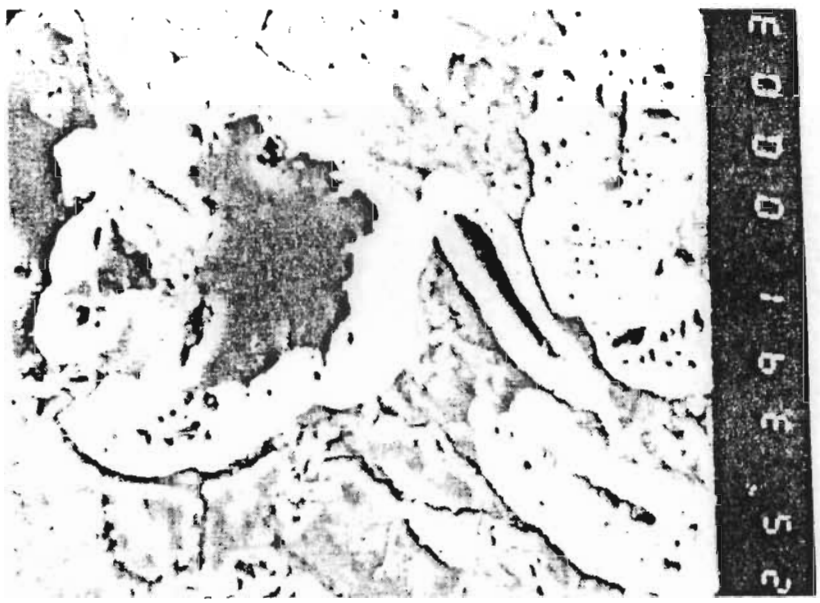

PLATE 6.9 (B) These plates are typical of the metal phase after reduction with larger discrete carbon particles (30-150μm). The metal is seen to be located in association with the carbon particles rather than with the chromite grain. In most cases this represents a considerable separation of residual chromite and metal phases.

PLATE 6.10 (A) Metal sizing with the use of carbon black as reductant. The fine particle size of the metal is typical.

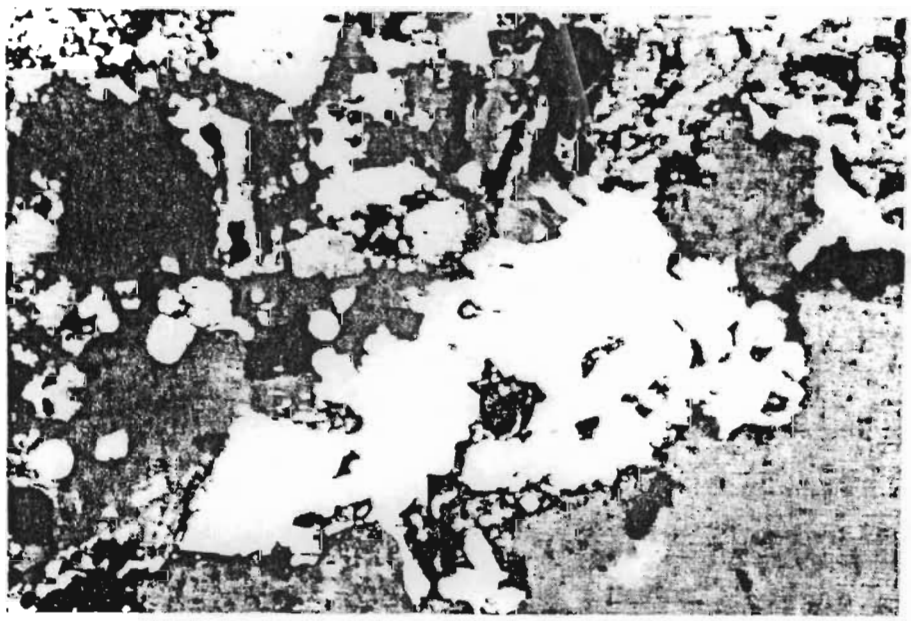

PLATE 6.10 (B) Metal phase formation adjacent to a large piece of carbon when using a discrete carbon sized between 50-200μm.

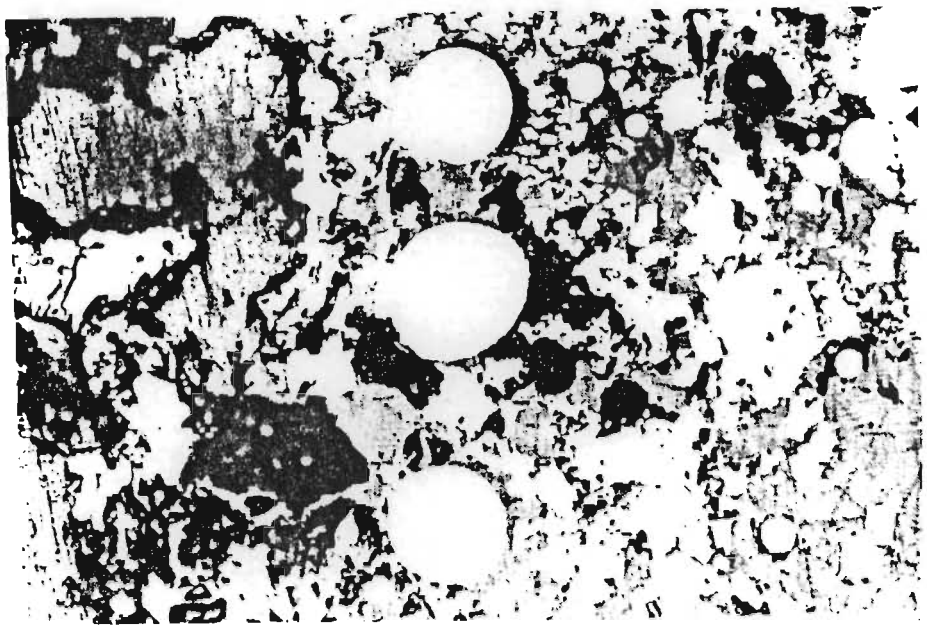

PLATE 6.11 Metal phase morphology typical of reduction in the presence of large carbon particles.

PLATE 6.12 The resultant slag phase after reduction with a feldspar-fluorspar-silica flux. No residual chromite grains are found implying that complete dissolution of the residual chromite has occurred resulting in the formation of a micaceous slag phase.

FIGURE 6.34 E.D.S. Spectrum of slag phasesresulting from fluxes with low silica content.

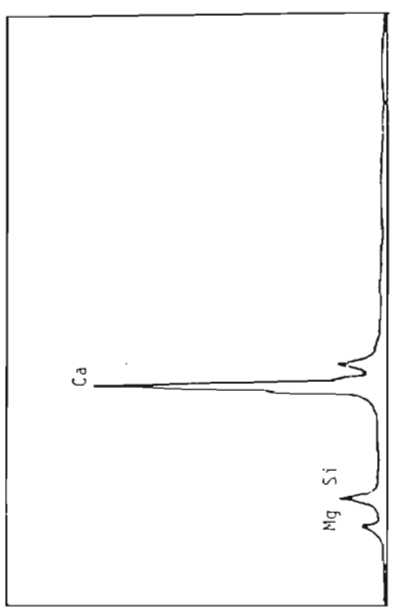

Bulk slag phase near metal and residual chromite showing very minor quantities of dissolved magnesia and alumina.

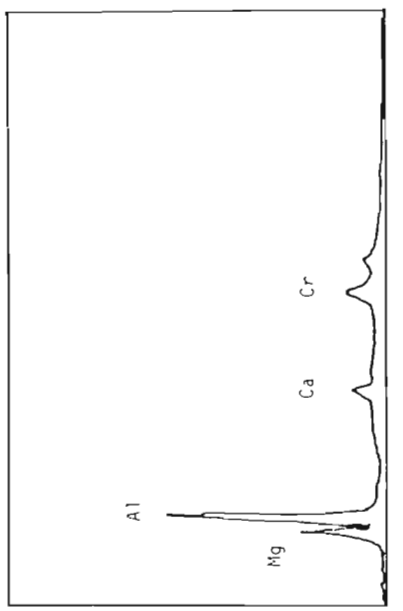

Recrystallized spinel at grain edge showing no slag contamination.

FIGURE 6.34

FIGURE 6.33 E.D.S. Spectra of slag phases resulting from fluxes rich in silica.

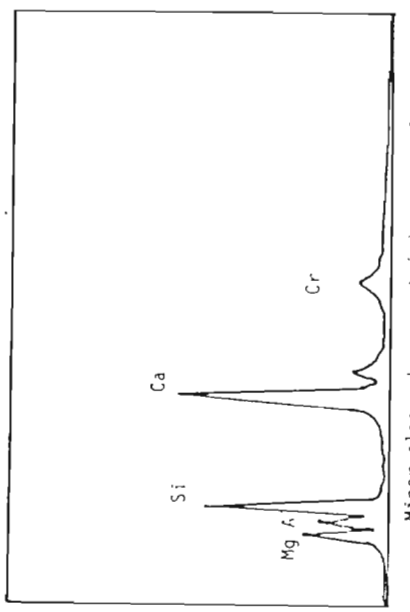

Minor slag phase containing most of the magnesium and aluminium dissolved from the spinel

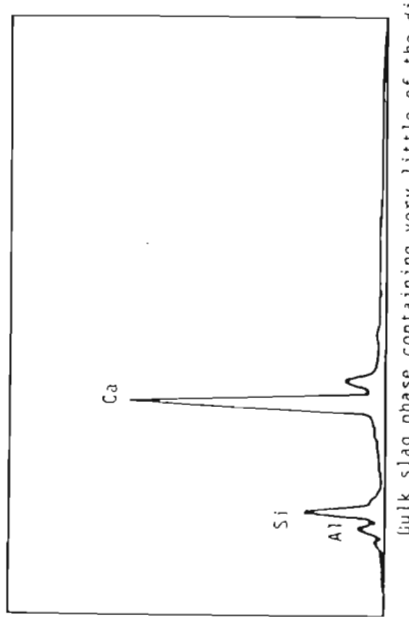

Bulk slag phase containing very little of the dissolved magnesia and alumina.

FIGURE 6.33

FIGURE 6.35

The Ca_2SiO_4 - $MgAl_2O_4$ - $MgCr_2O_4$ system (Ca_2SiO_4 rich region, ref. 102)

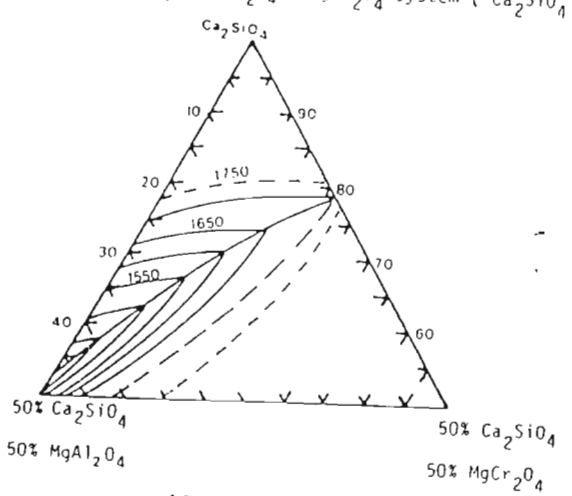

solution with the least possible change occurring to the physical properties of the slag.

Considering the $MgAl_2O_4$ - $MgCr_2O_4$ - Ca_2SiO_4 system shown in figure 6.35 (the Ca_2SiO_4 rich region), it is found that the temperature of the binary eutectic formed between the silicate and the continuous series of spinel solid solutions decreases steadily from 1700°C to 1418°C as Cr_2O_3 is replaced by Al_2O_3. This suggests that additional alumina could improve flux performance, and underlines the importance of maintaining a low chromium concentration in solution. It is expected that a build-up of chromium in the slag, resulting from substoichiometric carbon addition or removal of carbon to a relatively remote location, would result in a rapid increase in liquidus temperature and viscosity of the liquid phase, possibly resulting in precipitation of a chromium rich phase (probably a $(Cr,Al)_2O_3$ sesquioxide).

It was decided to attempt reduction with a fluorspar containing alkali silicate type flux with relatively fine reductant (30- 106 micron).

Initial tests using a 60% feldspar, 20% fluorspar, 20% silica flux showed that this type of flux was effective in promoting the rate of reduction. However higher temperatures of the order of 1250- 1350°C were required in order to gain maximum benefit from the flux addition.

Calculation showed that approximately 20% flux addition was required in order to form a micaceous slag (a type of phlogopite), with the residual magnesium from the spinel.

Tests conducted with this flux mixture at additions up to 50% of the chromite mass at temperatures between 1300 and 1400°C, showed that complete chromite dissolution occurred in under two hours. The uptake of magnesia and alumina into the slag phase resulted in a slag which when cool had a very pale colour and

flaky micaceous texture.

Investigation of this slag under the S.E.M. showed spinel recrystallization as dark euhedral crystals. The slag matrix was found to have a composition corresponding approximately to that of mica as suggested above, and an additional phase crystallized in fine needle form as shown in plate 6.12.

Analysis of these needles showed them to be rich in silica, with an approximate equal concentration of magnesium, aluminium, calcium and potassium as shown by the E.D.S. spectra (figure 6.36).

The similarity in composition between some granites and the feldspar- silica mixture found to be effective in promoting the reduction rate, prompted the use of a granite fluorspar flux mixture, with the granite having a composition approximately equivalent to 75% feldspar 25% silica.

Composite pellets containing a 20% addition of a granite-fluorspar flux (3:1 ratio) were found to perform well at between 1200 and 1300°C, giving a significant improvement in reduction rate (figure 6.37).

In general, dissolution of the chromite grain was found to occur, with migration of the dissolved chromium and iron species to the carbon particles where reduction took place. The dissolved magnesia and alumina were accepted into solution, resulting in a change in physical character of the slag.

As expected, carbon proximity was found to be very important in ensuring a high degree of reduction. In cases where the carbon located near a chromite grain had been consumed by reduction before completion of the reaction, grain dissolution was found to halt, leaving a refractory chromium rich core as shown in plate 6.13. In this case dissolution has continued to the point at which the carbon supply has been exhausted. At this point, the flux character has changed, resulting in precipitation of spinel

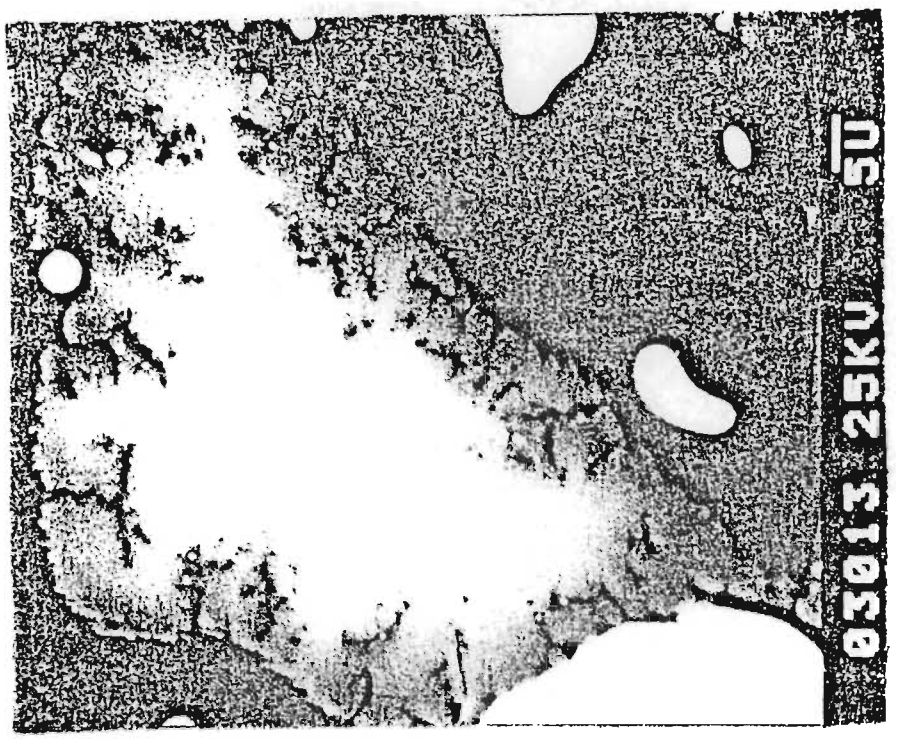

PLATE 6.13 (A) Section through a chromite grain showing the limited degree of flux penetration in the absence of sufficient reductant in close proximity to the grain.

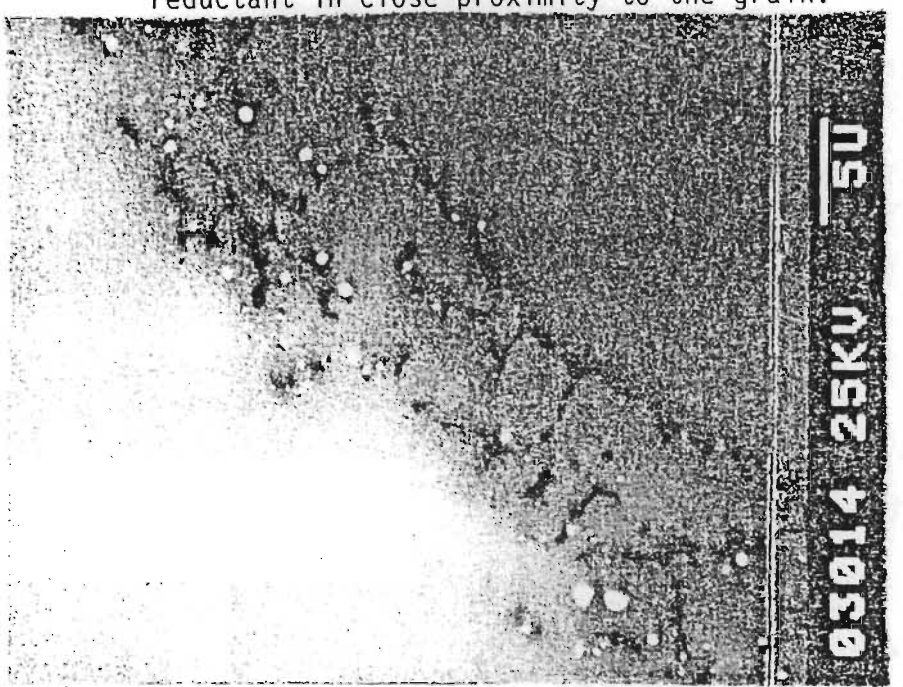

PLATE 6.13 (B) Detail of the grain edge showing recrystallization of a spinel phase at the surface (similar to that seen in plate 6.6) and a minor amount of metallizationat the-interface between residual grain and the recrysallized surface

Euhedral grains of recrystallized spinel.

Bulk slag phase containing fair amount of Mg and Al dissolved from the spinel.

Dark needle form in the slag phase.

Spectrum from a large dark needle in the slag phase

FIGURE 6.36 E.D.S. Spectra of slag phases after reduction with a fluorspar- feldspar -silica flux phase at 1300°C.

FIGURE 6.38

The effect of sub-stoiciometric carbon addition on the reduction rate in the presence of a flux phase.

CONDITIONS:
TEMPERATURE: 1300°C (isothermal)
CHROMITE : LG-6, 75% - 75 micron (pelletized)
REDUCTANT : metallurgical graphite 75% -75 micron
FLUX : 75% granite - 25% fluorspar.

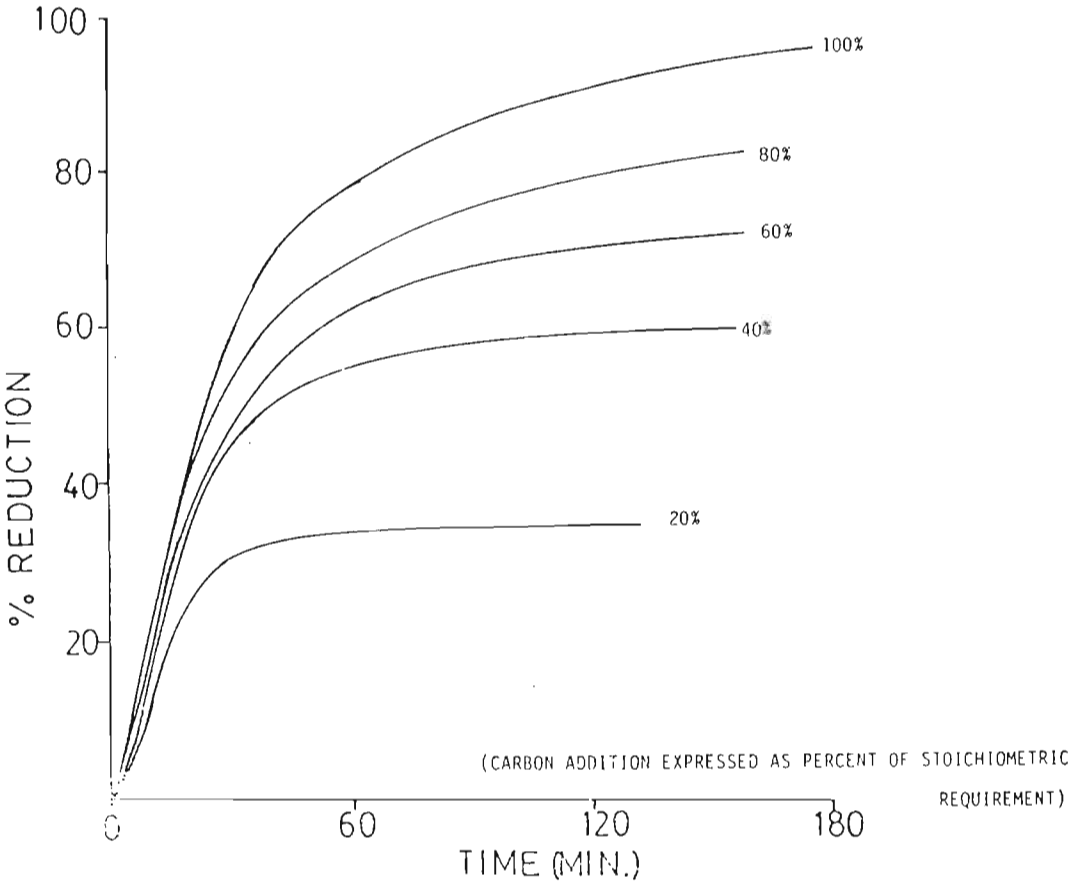

FIGURE 6.37

The effect of a commercially viable flux on the reduction process.

CONDITIONS:
CHROMITE: LG-6, 75% -75 micron size range
TEMPERATURE: 1300°C (isothermal) and 1200°C (isothermal)
FLUX : 20% addition of a granite (75%)- fluorspar (25%) flux

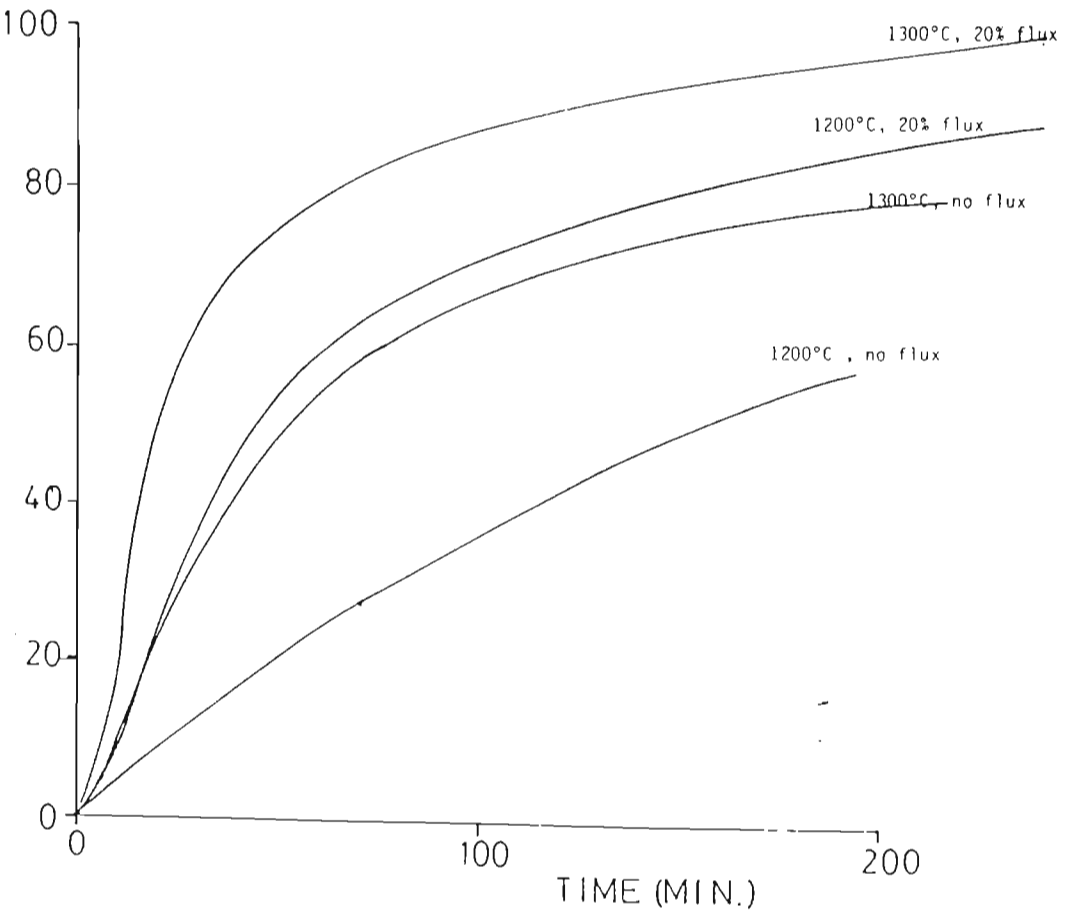

at the grain edge and the general cessation of the dissolution reaction.

Sub-stoichiometric carbon addition with a standard 20% addition of fluorspar- granite flux (1:3 ratio) resulted in a proportional limiting of the degree of reduction (figure 6.38), and an average metal composition in accordance with the metallization curve shown earlier.

Limiting the carbon addition to between 40 and 80% of the stoichiometric requirement for total reduction, resulted in the precipitation of varying quantities of sesquioxide phase, in a distinctive crystalline needle form. Analysis of this phase showed it to have a fairly constant composition of approximately 66% Cr_2O_3; 34% Al_2O_3.

The quantity of sesquioxide phase was found to be largely dependent on reaction extent. Very little sesquioxide was evident below 40% reduction, compared to a massive appearance of sesquioxide phase at between 50 and 65% reduction (plate 6.14 typical of the product at the point where sesquioxide is starting to crystallize and plate 6.15 at a later stage).

These results indicate the importance of adequate carbon supply and proximity in ensuring the maximum reaction extent and kinetics.

6.6 CONCLUSIONS REGARDING THE PRACTICAL APPLICATION OF SOLVENT FLUX ADDITION

The success of minor additions of CaF_2 - NaF type fluxes in promoting the reduction rate and increasing the degree of chromium reduction have obvious limitations in terms of any commercial process.

However, the effectiveness of fluorspar- feldspar- silica or fluorspar granite fluxes in this respect has considerable potential for a commercial process.

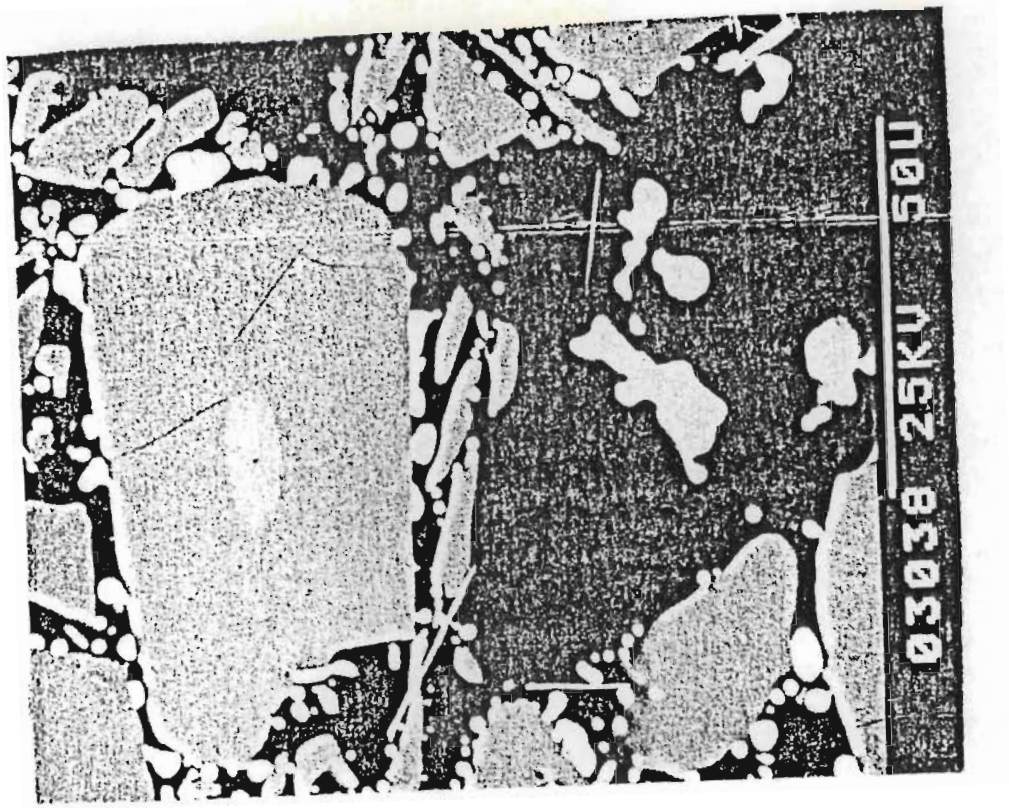

PLATE 6.14 The reduction product appearance at a low state of reduction (approx 20%) when limited by carbon starvation.

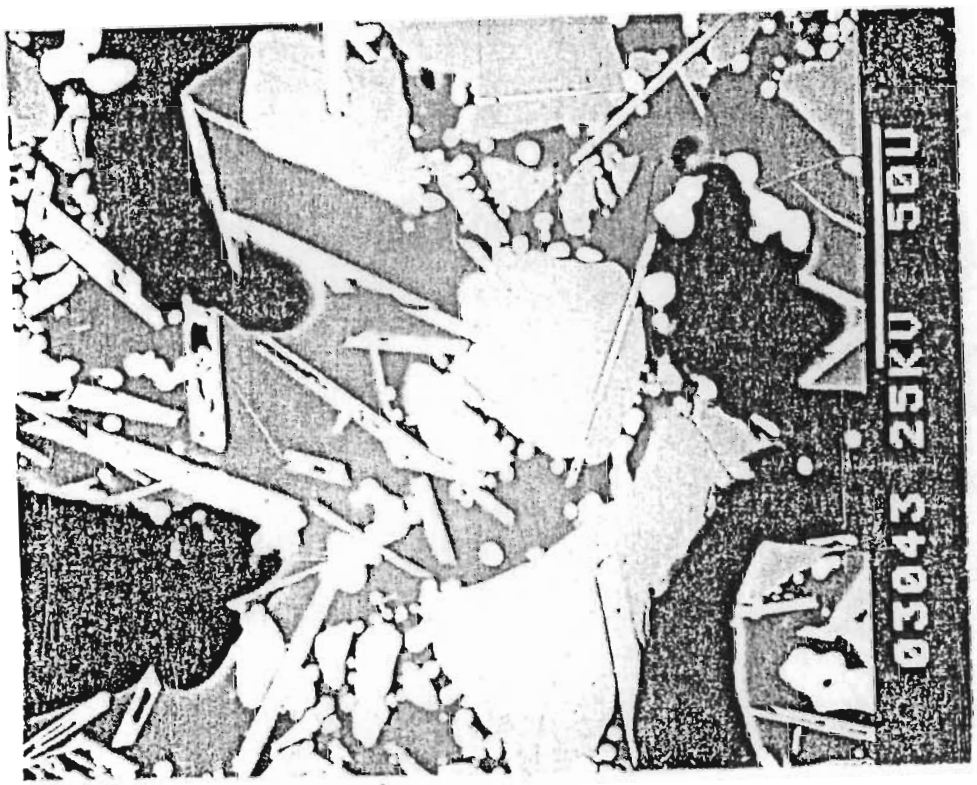

PLATE 6.15 The reduction product after approx. 50% reduction, the reduction being limited by carbon addition . The needle like phase is a chromium rich sesquioxide phase.

It would appear that maximum benefit may be derived from the addition of between 5 and 15% of such a flux to a mixture of fine chromite and carbon (preferably not exceeding 200 micron) in a pre-reduction operation at temperatures of 1300- 1350°C.

Low flux additions (~5%) appear to be suitable for use in pre-reduction processes as practiced at present. Such a limited addition would not significantly affect the behaviour of pellets in the kiln but would produce a significant increase in the degree of metallization achieved in these operations. It is also expected that the resulting low level of fluoride and alkali in the smelter slag would not upset current operations.

However, it would appear that maximum benefit could be achieved with higher flux additions (10- 15%) in a small, highly integrated plant configuration. The design of the plant would have to cater for the far lower slag levels, and higher degrees of metallization obtained from the pre- reduction operation. Such a plant, including hot metal transfer could enable net electrical energy savings of approximately 1000 KW.h/t compared with conventional pre-reduction and smelting operations (136,157,98).

CHAPTER SEVEN: SUMMARY AND CONCLUSIONS

7.1 SUMMARY OF FINDINGS

The limited information available concerning chromite reduction and the factors limiting the rate and extent of the reduction reactions in the region 1100- 1300°C prompted the investigation presented in this work.

Analysis of the thermodynamics of the reduction reaction indicated that the reaction should go to virtual completion for an LG6 type ore in the temperature range 1250- 1300°C. This is contrary to experimental results which indicate the presence of a reaction ceiling at approximately 76% reduction, a limit that is found to persist even at temperatures of 1400°C (Algie, 3).

Comparison of the compositional changes taking place within the chromite grain, calculated using a thermodynamic model based on the assumption of equilibrium between metal and spinel phases, was found to give results very similar to those found experimentally. However marked concentration profiles found across chromite grains while undergoing reduction indicated that the metal and spinel phases were not in equilibrium. This contradicts the conclusion drawn by Kucukkaragoz (93) that a near equilibrium state existed between metal and spinel throughout the reduction.

The presence of concentration profiles across the grain has the added implication that the reduction reaction is a kinetic process, largely controlled by factors internal to the chromite grain.

Analysis of the grains at various stages of reduction showed the formation of a distinct shrinking core of unaltered chromite surrounded by a growing shell of spinel with decreasing iron and chromium content.

It was concluded that reduction kinetics were limited by the independent rates of iron and chromium diffusion through the expanding shell of partly altered spinel. The continued removal of iron and chromium species from the spinel was found to result in the development of a thin robust film of refractory picrochromite- spinel solid solution at the surface of the chromite grain. The reduced vacancy concentration in this layer and its refractory nature resulted in the effective isolation of the grain from the reduction environment and the cessation of the reduction reaction.

Analysis of the reduction kinetics using a shrinking core model with independent diffusion coefficients for iron and chromium species, and allowing for an additional limitation due to the formation of the refractory surface layer, was found to closely simulate actual experimental results. The accuracy of this model in simulating experimental results provided further support for the proposed mechanism of chromite reduction.

It was concluded that an increase in reaction kinetics and extent could be achieved by the introduction into the reaction system of a component capable of disrupting the thin refractory layer responsible for limiting the reaction extent.

Investigations using a range of fluoride based fluxes showed that disruption of the surface of the chromite grain was highly effective in promoting the rate and extent of reduction. Eutectic mixtures of NaF and CaF_2 were found to be particularly effective even in very small quantities (5%).

Examination of the reduction products showed the action of the flux to be that of a solvent, capable of accepting small quantities of spinel components into solution. Removal of species from the solution through reduction and recrystallization resulted in relatively small quantities of flux (3-10%) remaining effective for prolonged reaction times.

Analysis of the reaction kinetics showed that diffusion of iron and chromium species still dominated the reaction. However the removal of the refractory surface layer resulted in an increase in particularly the effective diffusion coefficient of the chromium species, and the removal of the substantial film limitation on this species.

Several flux compositions were investigated over a range of ore and reductant particle sizes and temperatures. This led ultimately to the investigation of granite fluorspar fluxes.

These fluxes were found to be effective in promoting the reduction reaction, and particularly attractive in terms of an industrial process having the benefits of being cheap and readily obtainable. In addition, the phase changes within the granite-fluorspar slag, resulting from dissolution of the chromite spinel, resulted in the fixing of the fluoride component in a micaceous phlogopite type phase. The fixing of the fluoride component of the flux in this way effectively neutralises the aggressiveness of the slag, thus minimizing the refractory wear likely to otherwise be encountered in a downstream melting operation.

7.2 CONCLUSIONS

The development of a refractory film at the surface of the chromite grain under normal reduction circumstances has been shown to cause the typical slow and limited degree of chromite reduction.

It has further been shown that the disruption or removal of this refractory film will result in an increase in the rate and extent of reaction.

The addition of minor quantities of eutectic fluoride fluxes was found to be highly effective in achieving the desired

disruption of the grain surface.

The principles outlined in this work were used in the development of a granite- fluorspar flux , with potential benefits in terms of a commercial pre- reduction operation .

However, effective implementation of these principles to obtain a viable process requires careful matching of equipment and process capabilities to minimise energy consumption and maximise throughput.

It is believed that such a process could reduce the electrical energy consumption in the manufacture of ferrochromium to less than 30% of that required for normal arc furnace smelting.

However further work is required in order to fully establish the feasibility of a commercial process utilizing a solvent flux to enhance the pre- reduction process. The high temperature strength capabilities of composite flux containing pellets and the final smelting performance of the highly pre- reduced material has to be established.

Once these aspects have been resolved, a systematic approach may be adopted in the design and optimization of a process utilizing the flux enhanced reduction technology. In particular the results obtained suggest the need for equipment having good heat transfer capabilities. In addition care has to be taken in ensuring efficient utilisation of fuel energy while maintaining highly reducing conditions in the vicinity of the chromite reduction process.

In this respect a commercial process may ultimately differ from that outlined above, though it is believed that the fundamental principles outlined in this work, both in terms of the standard reduction reaction and the reaction promoted by the presence of a solvent flux are generally applicable.

7.3 RECOMMENDATIONS

In view of the potential cost savings of an enhanced pre-reduction operation, it is recommended that further work be performed to establish the commercial feasibility of such a process. This work should aim at establishing:

i) The high temperature strength capabilities of the pelletised material.

ii) The smelting performance of the reduced product, effectively assessing the compatibility of the product with operation of either plasma, open arc or coal- oxygen type furnaces for performing the final melting operation.

iii) The atmosphere isolation potential of the slag, enabling a greater efficiency of operation of a fuel fired reduction operation.

Once these aspects have been resolved, an optimum means of integrating a flux promoted pre- reduction process with available plant equipment can be found.

NOTE:

The abbreviation MINTEK has been used for The Council for Mineral Technology (formally The National Institute for Metallurgy or N.I.M.), Randburg, South Africa.

8. LIST OF REFERENCES

1) Abeland,P. and Baumard, J.F.
"A new graphical representation for a systematic study of the defect structure in ternary oxides with a specific application to Forsterite, Mg2SiO4 "
J.Phys. Chem. Solids, vol. 43, no. 7 pp617-625, 1982.

2) Alcock, C.B.
"Principles of Pyrometallurgy."
Academic press, London, 1976.

3) Algie, S.H. and Finn, C.W.P.
"Reaction mechinisms in the reduction of Winterveld chrome spinel with graphite and carbon."
Mintek report M157, December 1984.

4) Agren, J.
"Diffusion in phases with several components and sublattices
J. Phys. Chem. Solids vol 43 no.5 pp421-430, 1982

5a) Alper, A.M. (ed.)
"Phase diagrams "
Materials science and technology, Vol i;ii;iii; Academic press, New York,1970 .

5b) Alper, A.M.; McNally,R.N.; Ribbe,P.H. and Doman,R.C.
"The system MgO-MgAl2O4"
J. Am. Ceram. Soc. vol. 45,no.6;1962. pp263-268

6) Akerman,K. ; Hoffman, P.and Zablotny,W.
"Mechanism and rate of passage of materials in rotary kilns."
Br. Chem. Engng. 1966, vol.11 (no.1). pp.26-19.

7) Armbruster,T.H. and Lager,G.A
"Defect structure of the spinel."
J.Phys.Chem.Solids vol 42 no.9 pp725-728, 1981.

8) Arlet, R.H.
"Behaviour of chromium in the system MgAl2O4-Al2O3."
J.Am. Ceram. Soc. vol 45. no11,1962. pp523-527.

9) Athawale,A.S. and Altekar,V.A.
"Chemical beneficiation of chromite by selective chlorination

in a fluidised bed."
Trans. Ind. Inst.of Metals. June 1960, pp 29-37.

10) Ball,D.F. ; Dawson, P.R., Fitton,J.T.
"Additives in iron ore pelletising."
Inst. Mining and Met. C vol() sep. 1970. pp.C189-196

11) Barnes,A.R.
"The pre-reduction and smelting of UG2 chromite concentrates."
M.Sc Thesis, University of the Witwatersrand, Johannesburg, 1981.

12a) Barnes,A.R. and Finn,C.W.P.
"The prereduction of chromites from the UG-2 reef."
N.I.M. Report no.2070, 30 October 1980.

12b) Barnes,A.R. and Finn,C.W.P.
"The behaviour of UG-2 chromite concentrates during smelting ."
N.I.M. report no.2112, 15 July 1981.

12c) Barnes, A.R. Finn,C.W.P. and Algie,S.H.
"The pre-reduction and smelting of chromite concentrate of 1 chromium - to - iron ratio ."
J. S.A.I.M.M., vol.83, no.3, March 1983.

13) Barksdale,J.
"Titanium, its occurance,chemistry and technology."
The Ronald press co. New York. 1949.

14) Barcza,N.A.; Jochens,P.R. and Howat,D.D.
"The mechanism and kinetics of reduction of Transvaal chromite ores"
Electric Furnace Proceedings,1971.

15) Barcza, N.A.
"Studies of incipient fusion in the system : chromite - MgO Al2O3 - C ."
N.I.M. report 1365, January 1972.

16) Barcza,N.A. Curr,T.R. and Maske,K.U.
"The application of thermal plasma technology to large scale pyrometallurgical processes ."
EXTRACTION METALLURGY '85; I.M.M. Sept 1985

17) Baretka,J.et al.
"The kinetics of the reaction between magnesium oxide and iron(iii)oxide:The effect of particle size."
Reactivity of solids. -Proc. of 8th Int. Symp. Plenum press, N.Y. 1977, pp743- 757.

18) Benz,R. ;Elliott,J.F. and Chipman,J.
"Thermodynamics of carbides in the system Fe-Cr-C."
Metall. Trans. vol5 1974, pp 2235-2240.

19) Benedict,R.P.
"Fundamentals of temperature, pressure and flow measurements 2nd edition."
John Willey and Sons ; 1977.

20) Bibb,M.
"A comparison between the reactivity of coke and anthracite with regard to Winterveld chromite ore and prereduced winterveld

chromite"
Discussions on project 005791, MINTEK, January 1982.

21) Blazek,A. (trans. editor Tyson,J.F.)
"Thermal analysis"
van Nostrand Riennhold co. London. 1973. (Original print in Czechoslovakia)

22) Boerike, F.S. and Bangert,W.M.
"Effect of variables in chemical beneficiation of chromite ores."
U.S.Bureau of Mines R.I. 3817. July 1945.

23) Boericke,F.S.
"Selective reduction of iron in chromite by methane-hydroge and similar gas mixtures."
U.S. Bueau of Mines R.I 3847, February 1946.

24) Branstatter,H.G.
"Production and recovery of metallic carbides from ores and concentrates"
U.S. Patent 3,999,981, December 28,1976.

25) Brittan,M.I. and Liebenberg, R.R.
"A kinetic study of the TORCO copper segregation process."
I.M.M. sec C vol(). Sep 1971.; C156-168.

26) Chadwick,G.A. and Smith, D.A. (Ed.)
"Grain boundary structure and properties."
Academic press London,1976.

27) Chipman, J.
a) "Atomic interaction in molten alloy steels."
J. Iron and Steel Inst. vol 180. June 1955, pp97-106.

b) "Thermodynamics of binary and ternary solutions containing one interstitial solute."
Metall. Trans vol3 April 1972. pp879-885

c) "Thermodynamics and phase diagrams of the Fe-C system."
Met. Trans. 3.n 1972. pp55-63.

28) Chipman, J.
"Thermodynamics of the transformation in Fe-Cr alloys."
Metallurgical Transactions vol 5. Feb.1974. pp521-523.

29) Chinje, U.F. and Jeffes, J.H.E.
"Evidence of the formation of liquid phase during gaseous reduction of Fe2O3-Cr2O3 solid solutions at low oxygen potentials and relatively low temperatures."

30) Crank, J.
"The mathematics of diffusion."
Oxford University Press, 2nd ed. 1957

31) Cunliff, J. de. B; Edwards, R.I. and Dawson, M.F.
Discussions on a plant for the production of ferro-chrome and chromic oxide.
Project 18061, Hydrometallurgy division, MINTEK, 1983.

32) Chu,W.F. and Ramel,A.
"Kinetics of the reduction of chromium oxide by hydrogen"
Metall. Trans. B. vol 10B, no. 3, September 1979, pp401-407.

33) Cohen,E. and Ng,W.K.
"Process of pelletizing and leaching chromite ore concentrates."
Symposium on advances in extractive metallurgy, London, 1967

34) Cohen,E. and Yalcin,T.
"The chromothermic reduction of chromite."
paper presented at the Royal School of Mines, London, 1971.

35) Coetzee, C.B.(Ed).
"Mineral Resources of the Republic of South Africa - 5th.Ed."
S.A. Dept. of Mines, Geological Survey, Pretoria, 1976.

36) Crawford,G.A.
"Segregation of nickel in laterites: The Falconbridge Experience."
The Metallurgical Society of A.I.M.E. ;T.M.S. paper selection paper no. A72-89

37) Chepeleva,V.P.;Delevi,V.G.;Tkachenko,R.K.; Trunevich,L.V. and Svinolobova,I.N.
"Reaction of refactory compounds of titanium and chromium with some transition metals."
Sverktverd. Mater. 1980,(2),12-15 (Russ)

38) C.R.C. HANDBOOK, Weast,R.C. (Ed.)
C.R.C. press,62nd. edition.
The Chemical Rubber Co. Cleveland,Ohio. 1982.

39) Dawson,M.F. et al.
Discussions on the preparation of chromite and lime stone for the production of chrome chemicals.
MINTEK, December 1982.

40) Dawson, M.F. and Edwards, R.I.
"An alternative route for the production of chromium chemicals from chromite " MINTEK 50, Proceedings of the International Symposium on Advances in the Minerals Industry, H. Glen (ed.)
Council for Mineral Technology, Randburg, South Africa. 1985 pp735-742.

41) Deer, W.A.; Howie,R.A. and Zussman,J.
"Rock-forming minerals, vol 5, Non-Silicates."
Longmans,Green and Co. Ltd. 1962.

42) Dennis, W.E. and Richardson,F.D.
"The equilibrium controlling the decarburization of Iron-Chromium-Carbon melts."
J Iron and Steel Inst. vol 175, November 1953.

43) den Hoed,P.
Research conducted at Univ. of Natal, private communication, 1984.

44) den Hoed,P.
Discussions on the construction and operation of a computer based data gathering system on a themobalance.
MINTEK project 24382, February 1984.

45) de Waal, S.A.
a)"The chromites of the Bushveld Igneous Complex. An assessment of published information."
N.I.M. report 1203, 1 March 1971.

b)"The interrelation of the chemical,physical and certain metallurgical properties of chrome spinels from the bushveld igneous complex."
N.I.M. report 1415, 17 April 1972.

c)"The chromite from the Marico occurence, Western Transvaal, its alteration,and possible reasons for its refractory nature
N.I.M. repert 1730, 18 April 1975.

46) Dewar,K. and See,J.B.
"The influence of carbonaceous reducing agents on the rate of reduction of representative manganese and chromium ores."
N.I.M. report 1968, December 1978.

47) Doerner,H.A.
"Roasting of chromite ores to produce chromates."
(A study of the effects of various impurities and reagents on the oxidation reaction.)
U.S. Bureau of Mines R.I. 2999, June 1930.

48) Dollimore, D.(Ed).
"Proceedings of the first European Symposium on thermal analysis."
Univ. of Salford, U.K. 20-24 Sept. 1976.
Pub. HEYDEN. LONDON 1976.

49) Downes, K.W. and Morgan D.W.
"The utilisation of low grade domestic chromite."
Dept. of Mines and Technical Surveys, Mines Branch. Ottawa, Canada.
Memorandum series no. 116. October 1951.

50) Duclos,R.;Doukhan,N. and Escaig,B.
"Study of the origin of the composition influence on the mechanical properties of MgO.Al2O3 spinels."
Acta Mettalurgica, 30,pp.1381 to 1388
Pergamon G.B. 1982.

51) Duckworth and Hoyle
"Electro-slag refining."
Chapman and Hall, London, 1969.

52) Eadie, R.L; Wilkinson, D.S. and Weatherley, G.C.
"Rate of shrinkage during the initial stage of sintering"
Acta Met. 22,pp.1185-1194.(1974)

53) Edwards, R.I. and Bompas,G.
Communications concerning the thermodynamics and kinetics of the lime-chromite roast reaction and a technical and economic assessment of the conventional process for the production of sodium dichromate in South Africa.
MINTEK Hydromet Div. May 1982.

54) Eliezer,I. and Howald,R.A.
"A systematic treatment of the three component system Fe-Ni-C."
High Temp. Science 9, pp119-130. (1977)

55) Eyring, H; Henderson, D and Jost, W.
"Physical Chemistry - An Advanced Treatise. vol.X Solid State."
Academic Press, New York. 1970.; LCCCN 66-29951.

56) Fremont-Lamouranne,R.;Grillet,Y. and Guerin,H.

"The reactivity of carbons with respect to solid oxides ."
Bulletin de la Societe Chimique de France, 1972, no.10, pp3675-3681.
(N.I.M. translation, T.R.-522)

57) Frost,H.J.
Over view #17 "Cavities in dense random packings."
Acta. Mettalurgica 30,pp889 to 904,1982
Pergamon Press. 1982

58) Gailey, A.J.
"Ore treatment."
U.S. patent 2,277,220 patented Mar 24, 1942
Abs. J. 3071,p225 ref 60,text p217.

59) Gaskell,D.R.
"Introduction to metallurgical thermodynamics."
McGraw-Hill,New York 1973.

60) Gilchrist, J.D.
"Extraction metallurgy, " 2nd edition
Pergamon press, Oxford 1980.

61) Goken,N.A.
"Activity coefficients of solutes in binary solvents."
High Temp. Science 15, pp293-300 (1982)

62) Gregs,S.J.
"The surface chemistry of solids."(2nd Ed.)
Rienhold publishing corp. New York. 1961.

63) Griffing, N.R.; Forgeng,W.D. and Healy, G.W.
"C - Cr - Fe liquidus surface."
Trans. Metall. soc. A.I.M.E. vol.224, February 1962.

64) Grieve,A.; Jennings,R.F.; Nelson,P.H. and Kato, K.
"A new technique for burden preparation for ferro-alloy production."
Proceedings of the First International Ferro-Alloys Conference- INFACON 74, H. Glen (Ed.),Council for Mineral Technology, 1974.

65) Gokhale,A.A. and Johnson,D.L.
"Recomputation of phase equilibria in the sodium-carbon-oxygen system: effect of oxygen."
Metallurgical Transactions (A), 13A, June 1982, pp1101-1102.

66) Golde, E.
"The K.R. process. - New Technology in steel making".
Proceeding of the International conference on Recent Advanc in Mineral Science and Technology, L.F. Haughton (Ed). MINTEK, April 1984.

67) Goldschmidt,J.H.
"The structure of carbides in alloy steels -part I general survey."
J.I.S.I. 160, December 1948, pp 345-362.

68) Gullberg, R.
"Kinetics of dissolution of M23C6-Carbides in Austenite."
J. Iron and Steel Inst. Jan. 1973 . pp 59-65.

69) Halton, T.A.; Lewellen, P.C.; and Lightfoot, E.N.
"Transient diffusion and reaction in solids immersed in poorly

- stirred fluids. - i.
Chem. Eng. Sci. 37, (9), pp.1315-1324., 1982
Pergamon Press.

70) Harris, D.L.
"Chemical upgrading of Stillwater chromite."
Trans. Soc. of Min. Eng., September 1964, pp 267-281.

71) Hannay, N.B. (Ed).
"Treatise on Solid State Chemistry, vol 4.- Reactivity of Solids."
Plenum Press. New York 1976. ISBN 0-306-35054-8.

72) Hawkins,R.J. and Davies M.W.
"Thermodynamics of FeO Bearing CaF2 -based slags."
J. Iron and Steel Inst., March 1971, pp226-230.

73) Hill, C.G.
"An Introduction to Chemical Engineering Kinetics and Reactor Design."
Wiley, New York, 1972.

74) Hohmann,H.H.; Muller,W.; Schmalzried,H. and Tretjakow,J.D.
"Dissorder in ferrites."
Max Planck Institut fur Physicalische Chemie, Gottingen, Germany, 1967.

75) Himmel, L; Mehl, R.F. and Birchenall, C.E.
"Self diffusion of Iron in iron oxides and the Wagner theory of oxidation."
J. Metals Trans. AIME. 1953. pp827-843.

76) Hunter,W.L and Banning,L.H.
"Pyrometallurgical beneficiation of offgrade chromite and production of ferrochromium."
U.S.Bureau of Mines, R.I.16010.

77) Hunter,W.L. and Paulson,D.L.
"Carbon reduction of chromite."
R.I. 6755, U.S. Bureau of Mines (1966).U.S. Dept. of the Int.library

78) Healy, G.W.
"The thermodynamics of chromite ore smelting."
Iron and Steel maker, vol14, no 12, Dec 1987. pp 51-59.

79a) Hussein, M.K. and El-Barawi,K.
"Study of the chlorination and beneficiation of Egyptian chromite ores."
Trans. I.M.M.; March 1971.

79b) Hussein, M.K.;Winterhager, H.;Kammel, R. and El-Barawi, K.
"Chlorination behaviour of the main oxide components of chromite ores."
Trans. I.M.M. Sept. 1974.

80) Harris,D.L.
"Chemical upgrading of stillwater chromite."
Trans. A.I.M.E. vol 229. 1964. pp 167-281

81) Harber,J. and Piekarska-Sadowska,H.
"Mechanism and kinetics of solid state reaction in the system $CuCr_2O_4$- $Cu_2Cr_2O_4$-CuO."
Proc. 8th Int. Symp. React. Solids, Plenum Press, 1977, pp

409-417.

82) Hulbert S.F.; Bosnan,D.A. and Smoak,R.H.
"Kinetics and mechanism of the reaction between MgO and Cr2O3."
Proc. 8th Int. Symp. Reactivity of Solids, Plenum Press, 1977 pp573-584.

83) Ishii, M.; Hiraishi, J. and Yamanaka, T.
"Structure and lattice vibrations of Mg- Al spinel solid solutions."
Phys. Chem. Minerals, vol 8, 1982. pp. 64- 68.

84) Ichikawa, K.
"High carbon ferrochromium route slashes power use."
Chem. Eng. 81 (7),1974. pp36-37.

85) Jochens, P.R.

a)DIMECA PATENT . S.A.patent no. 72/6389, in conjunction with the Council for Mineral Technology, 1974.

b) Communications concerning the attendance at INFACON 83 and technical visits in Japan.
MINTEK, July,1983.

86) Jost,W.
"Diffusion - in solids,liquids,gases" Academic press . London - Transport phenomena in solids and gases.

87) Katayama, H.G.; Tokuda, M. and Ohtani, M.
"Promotion of carbothermic reduction of chromium ore by the addition of borates"
Transact. Iron and Steel institute Japan, vol 22. no.3. 1982

88) Kingery, W.D; Bowen, H.K. and Uhlmann, D.R.
"Introduction to Ceramics." 2nd ed
John Wiley and Sons. 1976. ISBN 0471-47860-1.

89) Kolchin, O.P.
"The mechanism of reduction of metals from their oxides by carbon."
Mekh. Kinet. Vosstanov, Met. Mater. Simp. 1968. pp.40-48 (N.I.M. translation no.244.)

90) Kirchner, G.; Nishizawa, T. and Uhrenius, B.
"The distribution of chromium between ferrite and austinite and the thermodynamics of the equilibrium in the Fe-Cr and Fe-Mn Systems."
Metallurgical Transactions vol 4.;Jan. 1973. pp167-174.

91) Koursaris,A. and See,J.B.
"The resistivity of mixtures of Mamatwan manganese ore and reducing agents ."
N.I.M. Report 1982, 31 August,1978.

92) Kubaschewski, O and Alcock,C.B.
"Metallurgical thermo-chemistry. 5th ed."
Pergamon press, Oxford, 1979.

93) Kucukkaragoz, C.S.; Algie, S.M. and Finn, C.W.P.
"The Reduction of Winterveld Chrome Spinel at 1300°C under an Argon atmosphere in the presence of Carbon."
Mintek Report M154, October 1984.

94) Kucukkarazog, C.S.
"The mechanism and kinetics of reduction of Winterveld chromite fines."
Ph.D.Thesis, Univ. of the Witwatersrand, 1983.

95) Kouri, S., Morita, K. and Sano, N.
"Smelting reduction of Composite Chromite pellets by Plasma."
Proceedings of the international Conference on Mineral Science and Technology; L.F. Haughton (Ed), MINTEK, March 1984.

96) Krupkowski,A. and Koperski,S.
"Reduction of metal oxides by carbon and carbon monoxide."
Rudy i Metale Niezelazne, vol.7. no. 3 pp101-106. (N.I.M. translation,tr 809)

97) Krupp patent:
Process for the production of ferrochromium."
Application for S.A. Patent, 8 410 101; Fried. Krupp Gesellschaft mit bechankter Haftung, 1984.

98) Radke, D., Ulrich, K.H. and Jansen, W.
"Iron containing chromium ore reduction process with part of the coal requirement fed through the rotary furnace burner"
Patent Assignee, Krupp, F. GmbH. SA patent ZA 86/03819.

99) Kawasaki Steel Corp. (Hamad, T. et al.)
"A pre-reduction method for powdery ore in a fluidized bed pre-reduction furnace."
Application for patent: SHOWA 57-192117, November 1, 1982. Hamad, T. et al., KAWASAKI STEEL CORP.

100) Laidler,K.J.
"Theories of chemical reaction rates." McGraw-Hill book Co. New York, 1969.

101) Langer,J.S. and Turski,L.A.
"Studies in the theory of interfacial stability -I. stationary symmetric model."
ACTA METALLURGICA,25, pp 1113-1119.

102) Levin,E.M.;Robbins, C.R. and McMurdie,H.F. (Eds.)
"Phase diagrams for ceramicists."
The American Ceramic Society. 1964.

103) Levenspiel, O.
"Chemical Reaction Engineering, 2nd ed."
Wiley, New York, 1972.

104) Lindner,R.
"Use of radioisotopes for the study of self diffusion in oxide systems."
Proc. 2nd Int. Conf. Peaceful uses of Atomic Energy vol20 p116, 1958

105) Lisnyak,S.S. ; Belikov,A.M. and Morosov, A.N.
"Kinetics and mechanism of chromite reduction by means of solid carbon."
SBORNIK NAUCH. TECKHN TR. NAUCHN-ISSLFD.
INST. MET. CHEELYAB SOVNAREHOSA 1961 No. 4. (N.I.M. translation TR. 78).

106) Lloyd,R.P. ; Garst, O.C. Rawles, W.T. et al.
"Beneficiation of Montana chromite concentrates by roasting and leaching."
U.S. Bureau of Mines R.I. 3834. February 1946.

107) Lovering, D.G. (Ed).
" Molten salt technology."
Plenum press. New York. 1982.

108) Lyubinov,V.D.; Shveikin,G.P.; Afonin,Yu.D.; Timoshchuk,T.A. Shalaginov,V.N. et al.
"Study of the gaseous reaction products of the carbon reduction of the oxides of transition metals."
Izvestiya Akademii Nauk sssr. METALLY,No.2 pp57-66,1984 .

109) Lichter,J.K.H.
"A study of fine grinding of chromite ore in a Palla vibration mill."
M.Sc thesis, University of Natal, Durban,1985.

110) Maier,C.G.
"Sponge chromium."
U.S. Bureau of Mines, Bulletin 436.(1942)

111) Maske,K.U.
"The reduction of chromite in a transferred-arc plasma furnace."
MINTEK report, M178, Jan. 1985 .

112) Maude,C.R. and Sale,F.R.
"Hydrochlorination of chromite with in- situ generation of HCl."
Trans I.M.M. June 1977. (669.094.4:669.263.1:661.419)

113) McColm, I.J.
"Ceramic Science for Material Technologists."
Leonard Hill; Blackie and Sons ltd. 1983.

114) McKie, D. and C.
"Crystalline solids."
Nelson, London; 1974.

115a) McRae,L.B.
"The upgrading of chromite ore from Moreesburg."
N.I.M. Report 1513, 1974.

115b) McRae,L.B. and Selmer-Olsen,S.S.
"An investigation into the pelletising and pre-reduction of Transvaal chromites."
2nd INTERNATIONAL SYMPOSIUM ON AGGLOMERATION, Atlanta, Georgia. 1977.

116) McRae, L.B. and Siebrits,F.K.
"Preparation and reduction of chromite pellets containing a reducing agent."
N.I.M. report 1724, 14 April 1975, (reissue, March 1977)

117) Mao, H.K. and Bell, P.M.
"Crystal field effects in spinel: oxidation states of iron a chromium."
Geochem et Cosmochimica Acta vol.39, 1975. pp. 865- 874.

118) METALS HANDBOOK, 8th Ed. V8.
Metallography and phase diagrams.

A.S.M., Ohio, 1973.

119) Mitchell,T.E.; Hobbs, L.W; Heuer, J. and Castaing, J.; Cadoz,J and Philibert,J. -OVERVIEW NO.6
"Interaction between point defects and dislocation in oxides
ACTA METALLURGICA 27, pp1677 - 1691

120) Morning, J.L.
"CHROMIUM .";Mineral Commodity Profiles, MCP - 1 May 1977.
U.S. Bureau of Mines, May 1977.

121) Moore,J.J. ; Ried, K.J. and Tylko,J.K.
"In flight plasma reduction of domestic chromites."
J. METALS. Aug. 1981, pp.43-49.

122) Muan, A.
a)"Slag-metal equilibria involving chromium as a component."
Proceedings of the International Conference on Mineral Science and Technology; L.F. Haughton (Ed.); RANDBURG, March,1984.

b)"Phase relationships in chromium oxide- containing systems a elevated temperatures."
Geochimica et Cosmochimica Acta, vol. 39; 1975, pp791-802.

123) Murhammer, D.; Davis, D. and Levenspiel, O.
"Shrinking core model/reaction control for a wide size distribution of solids."
Chem. Eng. Jour. vol. 32, 1986; pp87-91.

124) Nafziger, R.H.
a) "A review of the deposits and beneficiation of lower-grade chromite."
J. S.A.I.M.M., August 1982; pp205-226.

b) "Liquidus phase relationships in portions of the system CaF2-CaO-MgO-Al2O3 in an inert atmosphere."
High Temp. Sci. vol. 7,1975; pp179-188

125) Nafziger, R.H.; Trees, J.E. and Page, J.T.
"Carbothermic reduction of domestic chromites."
Metall. Trans. B. ,vol. 10B, Met. Soc. of A.I.M.E, March 1979; pp5-14.

126) Nafziger, R.H.; Sanker, P.E.; Trees, J.E. and McCune, R.A.
"Prereduction of domestic chromites."
Twin Cities Research Centre; U.S. Bureau of Mines.

127a) Navrotsky, A. and Kleppa, O.J.
"Thermodynamics of cation distributions in simple spinels."
J. Inorg. Nucl. Chem., vol. 29, 1967; pp2701-2714.

127b) Navrotsky, A.
"Thermochemistry of chromium compounds, especially oxides at high temperature."
Geochimica et Cosmochimica Acta, vol. 39, 1975; pp819- 832.

128) Narayan, J. and Washburn
"Self diffusion in magnesium oxide."
Acta Metallurgica, vol. 21, May 1973; pp533-538.

129) Novokhatskii, I.A. and Lenev, E.M.
"Thermodynamic properties of Cr2O3 and FeCr2O4 at high temperature."
Russ. J. inorg. Chem., vol.11, no.9. Sep. 1966. pp 1078- 1081.

130) Negasawa, S.; Aoki, N. and Iwabuchi, H.
"Operation of chrome ore pelletising plant for large electric furnaces."
Technical report, Nippon Kokkan k.k. steel co. Japan; 1980.

131) Ossin, D.I. and Fletcher, G.
"The production of stainless steel in South Africa."
N.I.M. report no. 1899; July 1977.

132) Ossin,D.I.
"The production of medium - carbon ferrochromium alloys by solid state reduction."
N.I.M. report no. 1650; August 1974.

133) Ossin ,D.I.
"Liquidus temperatures, viscosities and electrical conductivities of lime containing slags produced during the smelting of high carbon ferrochromium and ferrochromium-silicide alloys."
N.I.M. report no. 1366; October, 1971.

134) Omofoma, M.A. and Taylor, P.R.
"The kinetics of chromite ore reaction in a SO2 - air mixture."
Presented at the symposium on kinetics I.
Oxidation/ reduction Processes. T.M.S. Physical Chem. Committee and I.S.S. Process technology Div. Atlanta. 8th March 1983.

135) Ossin, D.I. and Bibb, M.
"The effect of hydrogen on the reduction of chromite ore wit caron."
N.I.M report 2031; October 1979.

136) Otani, Y and Ichikawa, K.
"Manufacture and use of prereduced chromium ore pellets."
Proceedings of the First Ferro-Alloys Conference, Johannesburg, South Africa; H.Glen (Ed.), MINTEK; 1974.

137) Poole,K.R. et al.
"Mixing of powders to fine-scale homogeneity - studies of batch mixing."
Trans. Inst. Chem. Eng., vol. 42, 1964; pp305-315.

138) Paynter et al.
"The Pyrometallurgical Research Group's current research programme on ferro alloys."
N.I.M. Pyro. Met. group, Univ. Witwatersrand, 1974.

139) Pelton, A.D.; Schmalzried, H. and Sticher, J.
"Computer assisted analysis and calculation of phase diagram of the Fe-Cr-O , Fe-Ni-O and Cr-Ni-O systems"
J. Phys. Chem. Solids, vol. 41, 1980; pp1053-1063.

140) Peiser, H.S.; Rooksby, H.P. and Wilson,A.J.C. (Tech. Eds.)
"X-ray diffraction by polycrystalline materials." - Ch. 14 15."
Pub. on behalf of the Institute of Phsics.
Chapman and Hall Ltd. London.1960.

141) Pelton, A.D. and Etsell, T.H.
"Analytical solution of Fick's second law when the diffusion coefficient varies directly as concentration."
Acta. Met. vol 20. Nov 1972.; pp1269-1274.

142) Puddington,I.E. and Sparks ,B.D.
"Spherical agglomeration processes."
Minerals Sci. Engng,vol 7,no 3, Oct. 1975

143) Quayyum, M.A. and Reeve, D.A.
"Reduction of chromites to sponge ferrochromium in methane hydrogen mixtures."
Canadian Met. Quarterly 15, (1976)

144) Ramdohr, P.
"The ore minerals and their intergrowths 2nd ed."
Pergamon press,Frankfurt,1980.

145a) Rao, Y.K.
"A physico-chemical model for reactions between particulate solids occuring through gaseous intermediates -I. Reduction of hematite by carbon."
Chem. Eng. Sci., vol.29. 1974. pp1435-1445.

145b) Rao, Y.K. and Chuang, Y.K.
"A physico-chemical model for reactions between particulate solids occuring through gaseous intermediates - II general solutions."
Chem. Eng. Sci. 29,(1974).pp1933-1938.

146) Reed-Hill, R.E.
"Physical Metallurgy Principles. 2nd Ed."
D. van Nostrand, New York; 1973.

147) Richardson ,F.D.
"Physical chemistry of melts in metallurgy. - vol I."
Academic press (London); 1974.

148) Richardson, F.D. and Jeffes, J.H.E.
"The thermodynamics of substances of interest in iron and steel making from 0C to 2400C."
J. Iron and Steel Inst., vol. 160, November, 1948; pp 261-27

149) Rankin, W.J.
"Solid state reduction by graphite and carbon of chromite from the Bushveld Igneous Complex."
N.I.M. report no.1975, September, 1978.

150) Read,P.J.; Reeve,D.A.; Walsh,J.H. and Rehder,J.
"Reduction of chromites in methane -hydrogen mixtures of chromium sesquioxide."
Can. Met. Quart., vol. 13, no. 4, 1974; pp587-595.

151) Rao, Y.K. and Jalan, B.P.
"A study of the rates of carbon- carbon dioxide reaction in the temperature range 839- 1050C."
Met. Trans. vol.3 1972. pp.2465- 2472.

152) Rao, C.N.R. and Rao, K.J.
"Phase transition in solids - an approach to the study of the chemistry and physics of solids."
McGraw-Hill 1978 (ISBN 0-07-051185-3)

153) Richardson,F.D.
"The thermodynamics of metallurgical carbides of carbon in iron."
J.Iron and Steel Inst. Sep. 1953 . pp 33-51.

154) Rankin,W.J.
"The composition and structure of chromite during reduction with carbon."
Report of the dept. of Chem. and Metall. Eng. Univ. of Stellenbosch, South Africa; 1979.
arc. Eisenhuttenwes. 50.(1979) nr 9, Sept. pp373-378.

155) Rankin, J.W. and Biswas, A.K.
"Oxidation states of chromium in slag and chromium distribution in slag-metal systems at 1600 C."
I.M.M. Trans., vol. 87;1978.

156) Rankin,W.J.
"Reduction of chromite by graphite and carbon monoxide."
J.S.A.I.M.M. June 1979; ppC107-C113.

157) Roberts ,F.; Taylor ,R.F. and Jenkins ,T.R. (ed.)
"High temperature chemical reaction engineering."
- a report of a working party of the institute of Chemical Engineers.
Inst. Chem. Eng.;1971.

158) Reese, R.B.; Rapp, R.A. and st. Pierre, G.R.
"The chemical activities of iron and chromium in binary Fe-alloys."
Trans. Met. Soc. AIME. vol. 242, Aug. 1968. pp. 1719- 1726.

159) Sack, R.O.
"Spinels as petrogenic indicators: activity - composition relations at low pressures."
Contrib. Mineral. Petrol.(1982) 79:169-186.

160) Searle ,M.J. and Finn ,C.W.P.
"The mathematical modelling of the reduction behaviour of chromite from the upper chromite layer of the Bushveld Complex
MINTEK report M96; July 1983.

161) Sato, H.; Machida, Y.; Sekita, Y. and Shoji, T.
"Evaluation method for chromium ore for solid state reduction processes (SRC)."
Showa Denko K.K. publication, Tokyo , 1984

162) See,J.B.
"The work of the pyrometallurgy research group at the University of the Witwatersrand."
N.I.M. report no. 1707., May 1975.

163) Sangster, M.J.L. and Stoneham, A.M.
"Calculation of absolute diffusion rates in oxides."
J. Phys.C: Solid State Phys., 17, 1984.pp. 6093-6104.

164) Stanton, R.L.
"Ore Petrology."
McGraw-hill, New York; 1972.

165) Stanko, J.S.
a) "A literature survey on the manufacture of ferro-chrome.
N.I.M. report 378, September 1968.
b) "Chemical beneficiation and agglomeration of low grade chromite ores - a literature survey."
N.I.M. report 447. January 1969.

166) Small, M. and Ryba, E.
"Calculation and evaluation of the Gibbs energies of formation

of Cr3C2 ;Cr7C3 and Cr23C6."
Metal. Trans. A., vol. 12A, August 1981; pp1389-1396.

167) Sun, R.
"Diffusion of cobalt and chromium in chromite spinel."
J. Chem. Phys., vol. 28, no. 2, February 1938; pp 290-293.

168) Sudzuki,R.
"Extraction of Nickel from oxidised Nickel ores by segregation roasting and magnetic separation."
TSVETNYE METALLY - Soviet non ferrous metals p10-12;U.D.C. 669.243 (3081)

169) Soykan, O.
"The solid state reduction characteristics of the Bushveld Complex chromites."
Ph. D. Thesis, University of the Witwatersrand, 1988.

170) Stubican, V.S. and Greskovich, C.
"Trivalent and divalent chromium ions in spinels."
Geochimica et Cosmochimica Acta, vol. 39, 1975; pp875-881.

171) Smalzried,H.
"Solid State Reactions."
Verlog Chemie Wienheim/Bergstr.
Acadmeic press inc. New York, 1974.

172) Smellie ,A.M. and Brandstatter,H.G.
"Metal carbides and metals from ores and alloys."
CANADIAN PATENT 1,053,910; 8th may 1979; pp 173-178.

173) Taylor, J.R.
"An introduction to Error analysis - The study of uncertainties in Physical Measurements".
University Science Books; California, 1982.

174) Taylor, J.L. and Grieve, A.
"Pellet firing in an annular kiln."
Symposium on advances in extractive metallurgy, London; 1967

175) Themelis, N.J. and Gauvin, W.H.
"A generalized rate equation for the reduction of iron oxides."
Trans. Met. Soc. A.I.M.E. vol. 227, April 1963; pp290-300.

176) Perry, K.P.D.
"The determination of the Gibbs Free energies of formation of chromite spinels."
Ph. D. Thesis, University of the Witwatersrand, 1986.

177) Tu, C.m.; Davis, M. & Hottel, H.C.
"Combustion rate of carbon - combustion of spheres in flowing gas streams."
Int. com. Heat mass transfer vol 11, pp15-23; 1984.

178) Toker, N. and Darken, L.S.
"Preparation of Cr2O3 crucibles and the defect structure of Cr2O3."
Geochem. et Cosmochem. Acta, vol.39, 1975. pp.847- 852.

179) Turkdogan ,E.T.
"Chromium- Oxygen equilibrium in liquid iron ."
J. Iron and Steel Inst., November 1954, pp278-283.

180) Turkdogan, E.T.
a) "Phyical chemistry of high temperature technology."
Academic press, New York, 1970.

b) "Rate Phenomena in smelting and refining processes."
Minerals Sci. Engng, vol. 8, no. 2, April 1976.

181) Tien, R.H. and Turdugan, E.T.
a) "Mathematical analysis of reactions in metal oxide/carbon mixtures."

b) "Mathematical analysis of non isothermal mass transfer process - application to oxidaation of carbon with CO2-CO mixtures."
Carbon 1972, vol. 10, Pergamon press; pp35-49.

c) "Incomplete pore diffusion effect on internal burning of carbon."
Carbon, vol. 8, Pergamon press, 1970; pp607-621.

182) Turkdogan, E.T.,Koump, V.,Vinters, J.V. and Perzak, T.F.
"Rate of oxidation of graphite in carbon dioxide."
Carbon, vol. 6, Pergamon Press, 1968; pp467-48.

183) Turkdogan, E.T. and Vinters, J.V.
"Kinetics of oxidation of graphite and charcoal in carbon dioxide."
Carbon, vol. 7, Pergamon Press, 1969; pp101-117.

184) Treffner, W.S.
"Changes in microstructure of chromite spinel during service
J.Am. Ceram. Soc., vol. 45, no. 10, October 1962.

185a) Ulmer, G.C. and White, W.B.
"Existence of chromous ion in the spinel solid solution series FeCr2O4- MgCr2O4."
J. Am. Ceram. Soc., vol. 49, 1966; pp50- 51.

185b) Ulmer, G.C.
"Experimental investigations of chrome spinels."
Magmatic ore deposits; Monograph 4, H.D.B. Wilson (Ed.), The Economic Geology Pub. Co., 1969.

186) Urquhart,R.C.
"Reactions occuring during the smelting of high carbon ferrochromium from Transvaal chromite ores."
N.I.M. report 1482; 1975.

187) Urquhart,R.C.; Jochens,P.R. and Howat,D.D.
"A laboratory investigation of the smelting mechanisms associated with the production of high carbon ferrochromium"
Proceedings of the first International Ferro- Alloys Conference (INFACON 74), Johannesburg, South African, H. Glen (Ed.), MINTEK, 1974.

188) Verhoven ,J.D.
"Fundamentals of physical metallurgy."
John Wiley and sons. New York, 1975.

189) Visnapu ,A. and Dressel ,W.M.
Symp. Process Minerology: Application to Metallurgy TMS/SME-AIME. Joint Process Mineralogy Comm. , Atlanta , 8 Mar. 1983.

190) von Bogdandy, L.; Chitil, M.; Innes, J.A. and Jonker, C.C.
"The direct use of coal in iron and steel making operations.
Proceedings of the International Conference on Mineral Science and Technology, L.F. Haughton (Ed.); MINTEK, 1984.

191) Wada, T.;Wada, H.; Elliott, J.F. and Chipman ,J.
"Activity of carbon and solubility of carbides in the F.C.C. Fe-Mo-C , Fe-Cr-C and Fe-V-C alloys.
Metall. Trans. vol. 3, November 1972; pp 2865-2872.

192) Wagner, C.
"Contributions to the thermodynamics of interstitial solid solutions."
Acta Mellurgica. vol. 19, August 1971; pp843-849.

193) Walsted, J.P.
"Electric smelting of low grade chromite concentrates."
U.S. Bureau of Mines R.I. 5268, October 1956.

194) Weber, G.W; Bitler W.B. and Stubican, V.S.
"Diffusion of Cr in Cr-Doped MgO."
J. phys. Chem. Solids, vol. 41, pp 1355-1359.

195a) Wedepohl, A.
"The mineralogy of the reduction of chromium ore in a plasma furnace."
Proceedings of the International Conference on Mineral Science and Technology, L.F. Haughton (Ed.); MINTEK, 1984.

195b) Wedepohl, A. and Barcza, N.A.
"The dig-out of a Ferrochromium furnace."
Spec. Publ. Geol. Soc. S.Afr. 7(1983) pp351-363.

196) Warshaw, I. and Keith, M.L.
"Solid solution and chromium oxide loss in part of the system MgO- Al2O3- Cr2O3- SiO2."
J. Am. Ceram. Soc., vol. 37, no. 4, April 1954; pp161- 168.

197) Wilde, W.T. and Reese, W.J.
"The ternary system MgO- Al2O3- Cr2O3."
Original from Ph.D. thesis by W.T. Wilde, University of Sheffield, 1939.

198) Whalley,L.
"Chromium substitution."
Trans. I.M.M. sec. C, pp 107-113

199) Williams, R.O.
"Interface formation during spinodal decomposition."
Acta Metallurgica 29. pp 95-100; Pergamon Press 1981.

200) Hausler, W.D., Ulrich, K.H. and Jansen, W.
"Reduction of ore in rotary kilns using precise temperature regulation features."
Patent Assignee, Krupp, F. GmbH. S.A. patent ZA 84/07639.

201) Wagoner ,R.H.
"Calculating dislocation spacing in pile-ups at grain boundaries."
Metallurgical Transactions A. 12A 1981. pp 2015-2023.

202) Wolf, D.
"Diffusion and correlation effects in non-stoichiometric crystals."

J. Phys. Chem. Solids, vol. 41, pp1053- 1063; 1980.

203) Wollacott, N.L. and See ,J.B.
"Factors affecting the carbon contents of alloys formed during the pre- reduction of chromite ores."
N.I.M. Report #1950. , 31 March 1978.

204) Worrell, W.L.
"A thermodynamic analysis of the Cr-C-O, Mo-C-O and W-C-O system."
Trans. Met. Soc. of A.I.M.E. 233 . June 1965.pp 1173-1177.

205) Woodhouse, D. and White, J.
"Phase relationships of iron oxide containing spinels."
Research paper 275, British Ceram. Research Assoc., December 1954.

206) Yoon, H.; Wei, J. and Denn, M.M.
"A model for moving- bed coal gasification reactors."
A.I.ChE. Journal, vol. 24,no.5, Sep. 1978. pp.885- 903.

207) The Minerals Bureau of South Africa, 60 Juta Street, Braamfontein, Johannesburg, 2001.

208) Freuhan, R.I.
"Activities in the liquid Fe- Cr- O system."
Trans. Met. Soc. A.I.M.E., vol.245, June 1969. pp. 1215- 121

209) Slatter, D.; Barcza, N.A.; Curr, T.R., Maske, K.U.; McRae, L.B
"Technology for the production of new grades and types of ferro- alloys using thermal plasma."
Proceedings of the 4th International Ferro- Alloys Conference (ABRAFE), Rio de Janeiro, 1986.

210) Sciaroni, M.
Production manager, C.M.I. Lydenburg, Transvaal.
Private communication, 1986.

Dv = vacancy diffusion coefficient

Da = apparent diffusion coefficient

D_i = effective diffusion coefficient for diferent cation species i

D_1 = effective diffusion coefficient for Fe3+

D_2 = effective diffusion coefficient for Fe2+

D_3 = effective diffusion coefficient for Cr3+

e_i = extent of reaction completion for reaction i

S.E.I. = secondary electron image

B.E.I. = backscattered electron image

A site = octahedral lattice site in a spinel structure

B site = tetrahedral lattice site in a spinel structure

Mi = metallization of species i

Rf = fractional reduction of species i

h' = electron hole

V = vacancy

c_i = concentration of species i

R = hydraulic mean particle radius

dp = hydraulic mean particle diameter

n_i = number of moles of species i

x_i = mole fraction of species i

a_i = activity of species i

γ_i = geometrical factor related to the optimum reduction path for a species through the spinel (taking site preferences into consideration)

λ_i = appropriate jump length for species i

υ_i = resonant vibrational frequency for species i at temperature T

G* = the free energy change associated with the formation of a transitional state during the diffusion

COMPARISON OF MEAN ORE COMPOSITIONS USED IN VARIOUS INVESTIGATIONS

COMPONENT	OXIDE MASS %		
	UG2(1)	LG6(2)	LG6(3)
Cr_2O_3	41,3	46,92	46,7
FeO	21,0	18,46	18,9
Fe_2O_3	10,79	8,36	7,9
Al_2O_3	17,81	14,20	15,5
MgO	9,87	10,10	10,9
SiO_2	1,24	0,84	0,34
TiO_2	---	0,57	0,61
CaO	0,089	0,16	0,08
Cr/Fe	1,18	1,60	1,58

NOTES

1) UG2 ore as used by Searle and Finn (160).

2) LG6 ore used in this investigation.

3) LG6 ore used by Algie and Finn (3).

TABLE A1.2

SUMMARY OF COMPOSITIONAL AVERAGE AND VARIATIONS FOR THE CHROMITE SPINELS OF THE BUSHVELD IGNEOUS COMPLEX.

Average taken over analyses of the lower group of chromite seams across both Eastern and Western sectors of the complex (ref. de Waal, 45).

OXIDE COMPONENT	MASS % OF COMPONENT	
	AVERAGE VALUE	STANDARD DEVIATION
SiO_2	0,71	0,48
Al_2O_3	14,41	1,59
Fe_2O_3	7,41	2,23
FeO	17,23	4,07
MgO	10,29	1,40
CaO	0,08	0,03
TiO_2	0,51	0,16
Cr_2O_3	48,49	2,89
MnO	0,17	0,028
ZnO	0,076	0,021
NiO	0,086	0,009
V_2O_3	0,258	0,071
CoO	0,075	0,012

APPENDIX 2 GENERAL MASS BALANCES AND COMPONENT DATA

A2.1 Calculation of stoichiometric carbon requirement.

Based on the reduction reactions:

$Fe_2O_3 + 3C = 2Fe + 3CO$

$FeO + C = Fe + CO$

$Cr_2O_3 + 3C = 2Fe + 3CO$

and the reactions for carbide formation

$3Fe + C = Fe_3C$

$7Cr + 3C = Cr_7C_3$

The carbon requirement for reduction (basis = 100g ore)

for iron : $\left[\frac{18,46.12}{71,847}\right] + \left[\frac{8,36.3.12}{159,69}\right]$ = 4,968g

for chromium $\left[\frac{46,92.3.12}{151,992}\right]$ = 11,113g

total carbon required for reduction = 16,081g

Carbon requirement for carbide formation

$Fe_3C = \left[\frac{0,36.12}{3}\right]$ = 1,447g

$Cr_7C_3 = \left[\frac{0,617.3.12}{7}\right]$ = 3,173g

total for carbide = 4,620g

total carbon requirement = 20,701g (i.e. 20,7% of chromite mass)

Thus 25% carbon addition allows 20,8% excess compared to stoichiometric carbon requirements.

maximum possible mass loss (assuming all carbon is lost as CO =

2,333.16,081 = 37,522g (i.e. 37,52% of chromite mass)

2.2 Sample mass balance over reduction reaction.

Definition of terms:

a) REDUCTION = removal of oxygen from oxide species

$$\% \text{ REDUCTION} = \frac{[\text{mass of oxygen removed from oxide}]}{[\text{total mass of oxygen after complete reduction of chromium and iron}]}$$

b) METALLIZATION = conversion of oxide to metal

$$\% \text{ METALLIZATION of i} = \frac{[\text{mass of i in metal phase}]}{[\text{mass of i initially present}]}$$

Input: 16g chromite, 4g carbon

COMPONENT	ADDITION (g)	METAL	ADDITION (g)
MgO	1,616	Mg	0,975
Al2O3	2,272	Al	1,203
Cr2O3	7,507	Cr	5,136
FeO	2,954	Fe	3,232
Fe2O3	1,338		
C	4,000		

Mass loss recorded during reduction = 4,45g = 27,81% mass loss

in terms of reduction extent = 74,13% reduction

Sample was taken and leached, and fusion performed on acid leach residue.

TABLE A2.1 MASS BALANCE ACROSS SAMPLE AFTER REDUCTION

COMPONENT	RECOVERED IN LEACH g	RECOVERED IN FUSION g	MISSING g
Mg	---	0,972	0,003
Al	---	1,198	0,005
Cr	3,12	2,011	0,02
Fe	3,230	0,000	0,002

Extents of metallization calculated from leach results :

Cr: (3.12/5.136) Fe: (3.23/3.232)

Net : (6.35/8.37)

TABLE A2.2 SUMMARY OF MEASURED REACTION EXTENTS

measured mass loss (T.G.A.)	= 4,45g
implied extent of reduction	= 74,13%
extent of metallization Cr	= 60,75%
Fe	= 99,94%
total extent of metallization	= 75,88%
implied degree of reduction	= 72,85%
difference	= 1,28%

The difference between the measure degree of reduction and that calculated from the extent of metallization of 1,28% is typical of the T.G.A. results, and is largely attributed to inaccuracies in weighing the sample during reduction.

2.3 Charge agglomeration - pelletization information

particle size distribution of components for pelletizing was as follows:

TABLE A2.3

SIZE DISTRIBUTION OF COMPONENTS FOR PELLETIZING

size (micron)	mass % passing			
	chromite	reductant	feldspar	fluorspar
+300	99,98	99,67	99,98	99,93
+212	99,83	97,79	99,82	99,38
+150	93,71	88,89	97,57	96,90
+106	80,58	76,12	86,22	89,47
+ 75	71,60	67,70	75,27	78,28
+ 53	57,60	54,76	60,49	47,59
+ 38	50,94	47,89	52,20	33,66

The size distribution selected as shown above is based on various results published in the literature as being suitable for pelletizing (ref. 142,161,64,115b,174).

FIGURE A 2.1

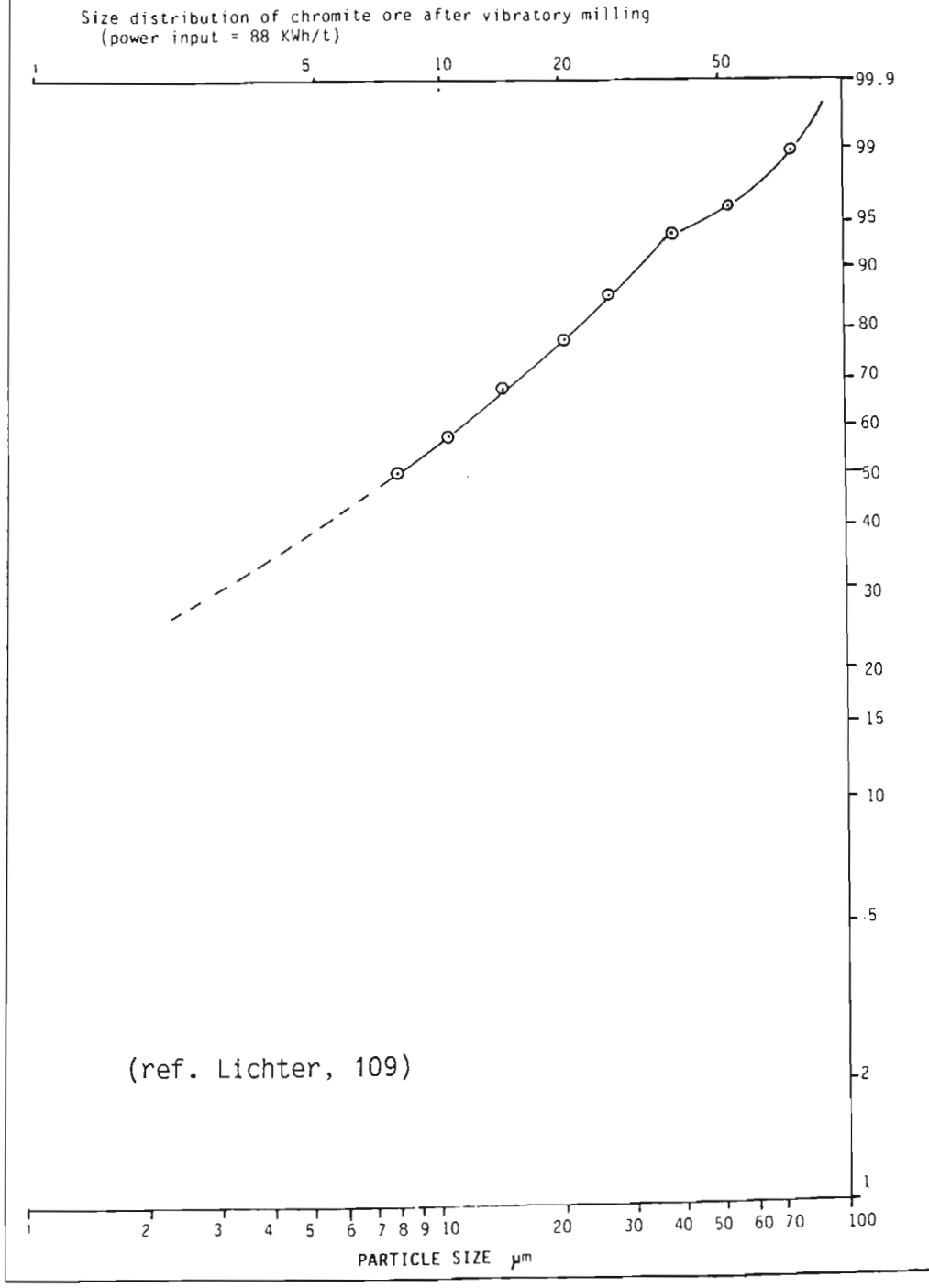

(ref. Lichter, 109)

APPENDIX 3: DESCRIPTION OF CHROMITE REDUCTION IN TERMS OF A THERMODYNAMIC MODEL

A 3.1 General approach

As stated in chapter 3, the reduction of chromite may be regarded as a kinetic process, proceeding along a particular composition coordinate pathway towards an end point, representing a final state of thermodynamic equilibrium between the reaction phases present.

Because of the importance not only of the end point, but also of the approach to the end point, a method is adopted in which particular attention is paid to the progress of the reactants and intermediate products towards the final reaction end point. Analysis of the progress of the reaction is performed in terms of a thermodynamic pathway from a point where the initial reactants represent the only stable species, to a point representing complete reduction of both iron and chromium species.

In order to perform such an analysis, the reaction system has to be comprehensively described in terms of a set of equilibrium reactions, together with a description of the activity behaviour of the component species during the course of the reaction. In addition a means has to be established for conveniently describing the progress of the reaction from initial to final points. This should also serve as a means of defining intermediate or "pseudo equilibrium" points where the relative composition of each phase can be established.

Chromite reduction, encompassing numerous reactions between a complex composite metal oxide and various carbonaceous reductants can be considered in numerous ways (Kolchin,89; 78,146,147,2,186).

In general terms, a set of four rigorous equations, namely :

$FeO = Fe + 1/2O_2$ --------- 3.1.1

$Cr_2O_3 = Cr + 3/2\ O_2$ ------ 3.1.2

$C(m) + CO_2(g) = 2CO(g)$------ 3.1.3

$CO + 1/2O_2 = CO_2$ ---------- 3.1.4

could be used to describe the reduction of a spinel composed of the phases FeOM2O3; MOCr2O3 and MOAl2O3.

The thermodynamic "pathway" could then be considered in terms of the equilibrium between metal (carbide), oxide (spinel) and gas atmosphere at specific oxygen potentials (or interms of CO/CO_2 ratio, where $Pco + PCO_2 = 1atm$ is a general constraint applied), ranging from relatively mildly reducing ($Po_2 \sim 10^{-8}$ atm), to highly reducing ($Po_2 \sim 10^{-20}$ atm).

In this way the pseudo-equilibrium between changing metal and oxide compositions can be examined from the point where unaltered spinel can exist to the point where the equilibrium gas atmosphere is limited by the presence of solid carbon.

The results obtained from such an analysis are represented in terms of the iron- chromium metallization profile, which provides a convenient way of assessing the calculated progress of the reaction and comparing this with experimental results in a non time-dependent reference frame.

However, accurate description of the activity relationships for the above system, in the complex metal and oxide phases is not possible, and thus in order to simplify the system and enable ready computation, various simplifying assumptions have to be made as will be considered below.

A 3.2 Component activity models

(a) Oxide phases

As a result of the complexity of the chromite spinel, various alternative means of describing the activity of species within the spinel were investigated. Complete homogeneity throughout the spinel structure was assumed, the existence of concentration profiles as described in chapters 5 and 6 was ignored and attention was focused on the changes experienced in a small homogeneous region of spinel. In addition, in the absence of sufficient thermodynamic data, the possible existence of divalent chromium ions in the spinel structure, particularly towards the end of the reduction reaction was not considered.

Models for the activity of species in a spinel phase are usually described in terms of the activity of various end member species, which are assumed to interact or mix in a particular way. Complex models such as those described by Spilane and subsequently Sack (159), describe the activity of end member species using a Tempkin type model for the configurational entropy of the system, together with a polynomial expression to describe the free energy of mixing.

While such models are obviously accurate within the relatively confined domain of naturally occuring spinel compositions, the results obtained using such a model are not meaningful where extrapolation is performed well beyond the field of typical spinel occurrence, such as is the case during the latter part of the reduction reaction. Thus simpler, less accurate, though more general models were sought to describe the activity of species

throughout the reduction reaction.

Description of the activity of species in the spinel phase was first considered in terms of individual cation species. The activity of species was determined in terms of the atom ratio of a particular species to the total number of lattice sites that could be occupied by that cation. Implicit in this model are the assumptions of ideality in mixing of Fe2+ and Mg2+ cations on tetrahedral lattice sites and of Fe3+, Al3+ and Cr3+ on octahedral lattice sites. It was also assumed that there was no intermixing of cations on octahedral and tetrahedral lattice sites, and that no specific ratio of octahedral to tetrahedral lattice sites was maintained throughout the reaction.

The assumptions made in such a model obviously limit the applicability of the model, placing unrealistic constraints on the solutions obtained, particularly near the end of the reduction reaction. It was generally found that this type of model could reasonably describe the behaviour of the spinel during the early stages of reduction, but could not adequately describe spinel behaviour towards the end of the reduction reaction. This type of model can thus only be successfully used to describe spinel behaviour during the initial stages of reduction.

More in keeping with the nature of chromite spinels, a modified varsion of the Sack type model was considered next. Chromite was considered as a composite of end member spinels Fe_3O_4, $FeCr_2O_4$ $MgCr_2O_4$ and $MgAl_2O_4$, with reactions based on these components. It was initially assumed that these species mix ideally in all proportions, and that any MgO surplus to that

required for spinel formation (as is the case during the latter part of the reduction reaction), would result in the exsolution of a separate periclase phase.

Susequently allowance was made for possible non-ideal behaviour of spinel end member components using a method similar to that of Sack (159). However, while the results obtained for the first half of the reduction reaction were found to be similar to the previous model and to experimental results, it was found that this type of model could still not accurately describe spinel behaviour during the latter stages of the reduction reaction.

An alternative description of the activities of components in the spinel phase particularly during the latter stages of the reduction) was investigated based on consideration of the spinel in terms of an ideal mixture of two spinel components, namely $FeO(Cr,Al)_2O_3$ and $MgO(Cr,Al)_2O_3$. It was assumed that any M_2O_3 formed as a result of reduction of FeO from $FeO(Cr,Al)_2O_3$, surplus to that required for a balanced spinel, would result in the formation of sesquioxide (M_2O_3), which was assumed to mix ideally with the remaining spinel.

This type of model, being less constrained, was found to be more suited to describing the behaviour of the spinel during the latter part of the reduction reaction. Thus a combination of the earlier models, describing the initial stages of reduction, together with the last model, describing spinel behaviour towards the end of the reduction reaction, was found to be most appropriate.

b) Alloy phase

Numerous models exist decribing the activity of components within limited regions of the Fe-Cr-C system, though none are particularly applicable over the wide range of compositions encountered over the duration of the reduction reaction. In this context, the prime consideration must be a means whereby account can be taken of the effect of carbon in the alloy phase on the activity of the iron and chromium species.

In the method employed by Healy (78), use is made of a general expression for the activity coefficient of carbon in the liquid phase, expressed as a series of terms catering for both concentrated and dilute solutions of chromium in iron. The system is then treated using the Gibbs-Schuhmann integration technique applied to a ternary system. This however is not applicable in the solid state where the formation of various carbides in particular M_7C_3, is not catered for.

The work of Wada et al., Banya and Chipman (27c), enable carbon activity and hence iron activity to be calculated over a limited range at low chromium concentration. The methods employed assume Raoultian behaviour in the Fe-Cr system, with a depression in the activityies of Fe and Cr due to the presence of carbon according to various empirical relationships based on experimental data. However the range of available data and hence region of applicability is very narrow and does not adequately cater for M_7C_3 formation.

However, use was made of this model to gauge the effect of carbon in the alloy phase on the activity of Fe and Cr during

the initial stages of the reduction reaction. It was found that the impact of carbon was most noticable in terms of the Po_2-metallization curve and hence the final extent of reduction achievable, though little effect in terms of the iron chromium metallization curve was found. However, this method is obviously not accurate in the latter stages of the reduction reaction.

In the light of these models, the initial assumption made was that the alloy phase could be represented as as ideal solution of iron and chromium carbide (Fe- Cr_7C_3). This is obviously not accurate since the equilibrium carbon content of various alloy phases across the metallization curve shows that only about half of the measured carbon content of the alloy phase can be attributed to a pure Cr_7C_3 phase. Accordingly the remainder of the carbon in the alloy phase must be associated with iron, either in the mixed $(Cr,Fe)_7C_3$ phase, or with Fe in the Fe rich, Fe,Fe_3C phase.

Thus the initial assumption of an ideal mixture of Fe and Cr_7C_3 was modified to include the effect of additional carbon, the activity of which was not assumed to be greater than that of Cr_7C_3. It was believed that this was a reasonable assumption within the region of interest.

A3.3 Calculation of the metallization and Po2 curves.

As discussed in section A3.2, various different models can be used to describe the behaviour of the different species in the spinel and metal phases. Three of these models are considered

below, starting with the simplest, most constrained model only applicable near the start of the reaction , to the more advanced model treating spinel behaviour near the end of the reduction reaction.

Chromite reduction can be described in terms of the reactions shown below.

$$\langle \overline{Fe_2O_3} \rangle = 2\langle \overline{FeO} \rangle + 1/2\ (O_2)$$

$$\Delta G1 = 69\ 620 - 31{,}14T \text{ cal/mol.} \quad \text{-------} \quad (3.3.1)$$

$$Kp1 = \left[\frac{(PO_2)^{1/2}\ (aFeO)^2}{(aFe_2O_3)} \right]$$

The molar extent for this reaction being defined as e1, with maximum extent ME(1).

$$\langle \overline{FeO} \rangle = \langle \underline{Fe} \rangle + 1/2(O_2)$$

$$\Delta G2 = 62\ 050 - 14{,}95T \text{ cal/mol} \quad \text{----------} \quad (3.3.2)$$

$$Kp2 = \left[\frac{(PO_2)^{1/2}\ (aFe)}{(aFeO)} \right]$$

The molar extent for this reaction is defined as e2, with maximum extent ME(2).

$$\langle \overline{Cr_2O_3} \rangle = 2\langle \underline{Cr} \rangle + 3/2(O_2)$$

$$\Delta G3 = 267\ 750 - 62{,}10T \text{ cal/mol} \quad \text{---------} \quad (3.3.3)$$

$$Kp3 = \left[\frac{(PO_2)^{3/2}\ (aCr)}{(aCr_2O_3)} \right]$$

The molar extent for this reaction is defined as ê3, with maximum extent ME(3).

(< > denotes in spinel phase solution, < > denotes in alloy phase solution).

From an initially defined spinel composition, the relative molar quantities of the various oxides can be calculated as shown below.

Defining the quantities of oxides as:

M(1) = moles of MgO
M(2) = moles of Al_2O_3
M(3) = moles of Cr_2O_3
M(4) = moles of FeO
M(5) = moles of Fe_2O_3

---------- (3.3.4)

and NN as the total number of moles in the oxide (spinel) phase = M(1)+M(2)+M(3)+M(4)+M(5), the effect of reactions 3.1.1 through 3.1.3 can be accounted for as follows:

M(1) = moles of MgO
M(2) = moles of Al_2O_3
M(3)-e3 = moles of Cr_2O_3
M(4)-e2+2e1 = moles of FeO
M(5)-e1 = moles of Fe_2O_3,

---------- (3.3.5)

with NN being adjusted accordingly.

The activities of the various species can now be defined (using the assumptions discussed in A3.2(a) and (b)) as shown below.

$$a1 = aFe_2O_3 = \left[\frac{(M(5)-e1)}{(M(2)+M(3)+M(5)-e1-e3)}\right] \text{ --- (3.3.6)}$$

$$a2 = aFeO = \left[\frac{(M(4)-e2+2e1)}{(M(4)-e2+2e1+M(1))}\right] \text{ ------- (3.3.7)}$$

$$a3 = aCr\ O = \left[\frac{(M(3)-e3)}{(M(2)+M(3)+M(5)-e1-e3)}\right] \text{ --- (3.3.8)}$$

$$a4 = aMgO = \left[\frac{(M(1))}{(M(1)+M(4)+2e1-e2)}\right] \text{ ------- (3.3.9)}$$

$$a5 = aAl_2O_3 = \left[\frac{(M(2))}{(M(2)+M(3)+M(5)-e1-e3)}\right] \text{ --- (3.3.10)}$$

$$a6 = aFe = \left[\frac{(e2)}{(e2 + e3 + XC)}\right] \text{ --------- (3.3.11)}$$

$$a7 = aCr = \left[\frac{(e3)}{(e2 + e3 + XC)}\right] \text{ --------- (3.3.12)}$$

(Where XC represents an adjusment made to the activities of iron and chromium in the metal to account for the presence of carbon after the method of Chipman (27c)).

Using the above expressions for the activities of the various species in the equilibrium expressions defined in equations 3.3.1 through 3.3.3, expressions for each equilibrium constant in terms of the individual extents of reactions 3.3.1, 3.3.2 and 3.3.3 can be obtained and solved for as shown below.

From 3.3.1

$$\frac{Kp1}{PO_2^{1/2}} = \left[\frac{(M(4)-e2+2e1)2(M(2)+M(3)+M(5)-e1-e3)}{(M(4)-e2+2e1+M(1))2(M(3)-e1)}\right] \text{ ------ (3.3.13)}$$

From 3.3.2

$$\frac{Kp2}{PO_2^{1/2}} = \left[\frac{((e2)(M(4)+M(1)+2e1-e2)}{((e2+e3+XC)(M(4)+2e1-e2)}\right] \text{ -------- (3.3.14)}$$

From 3.3.3

$$\frac{Kp3}{PO_2^{2/3}} = \left[\frac{((e3)(M(2)+M(3)+M(5)-e1-e3)}{((e2+e3+XC)(M(3)-e3)}\right] \text{ -------- (3.3.15)}$$

Solutions to these three non linear equations can be obtained in various ways, in this case the equations were simplified and rewritten in terms of a cubic and two quadratic equations as shown below. A simplified Newton- Raphson technique was used to solve the cubic equation, while standard solutions to the quadratic equation were sought within the well defined regions $0<e(i)<ME(i)$. This technique was applied iteratively until the desired convergence had been obtained on all three e(i) values.

Defining the terms :

$N1 = (M(4)-e2)$

$N2 = (M(2)+M(3)+M(5)-e3)$

$N3 = (M(4)-e2+M(1))$

$k1 = Kp1/PO_2^{1/2}$

equation 3.3.13 can be rewritten as

$$k1 = \left[\frac{(N1+2e1)^2 (N2-e1)}{(N3+2e1)^2 (M(5)-e1)}\right] \quad \text{---------- (3.3.16)}$$

which can be rewritten as

$$e1^3 (4-4k1) + e1^2 (4k1(M(5)-4k1N3-4N2+4N1) + e1(k14N3M(5)-k1N3^2-4nN1N2+N1^2) + (k1N3^2 M(5)-N1N2) = 0$$

---------- (3.3.17)

Then if $A1 = (4-4k1)$; $B1 = (4k1M(5)-4k1N3-4N2+4N1)$; $C1 = (4k1N3M(5) - k1N3^2 - 4N1N2 + N1^2)$ and $D1 = (K1N3^2 M(5)-N1^2 N2)$, equation 3.3.17 can be simplified to

$A1e1^3 + B1e1^2 + C1e1 + D1 = 0$ ---------- (3.3.18)

Similarly equations 3.3.14 and 3.3.15 can be simplified to cubic equations and solutions to the set of three simultaneous equations sought as described above.

However, as stated in section 3.2(a), this model is not suited to describing the reduction reaction during the latter stages of the reduction reaction. Thus alternative ways were sought for describing the behaviour of species, particularly in the spinel phase.

In the second model the chromite spinel is considered in terms of specific spinel end members $MgOAl_2O_3$, $MgOCr_2O_3$, $FeOCr_2O_3$ and $FeOFe_2O_3$. The overall reduction reaction is then described in terms of a set of three basic reactions involving these spinel end members as shown below.

$$Fe_3O_4 + 4CO = 3Fe + 4CO_2$$

$$\Delta G = -9230 + 8,25T \text{ cal/mol} \quad \text{---------} \quad (3.3.19)$$

$$Kp1 = \left[\frac{(PCO_2)^4 \, aFe^3}{(PCO)^4 \, aFe_3O_4}\right]$$

The molar extent for this reaction is defined as e1 with a maximum extent ME(1).

$$2FeCr_3O_4 + 80/7CO = 2Fe + 4/7Cr_7C_3 + 68/7CO_2$$

$$\Delta G = 33\ 323 + 85,57T \text{ cal/mol} \quad \text{--------} \quad (3.3.20)$$

$$Kp2 = \left[\frac{(PCO_2)^{68/7} . \, aFe2 . aCr_7C_3^{4/7}}{(PCO)^{80/7} \, aMgCr_2O_4}\right]$$

The molar extent for this reaction is defined as e2, with a maximum extent ME(2).

$$7MgCr_2O_4 + 33CO = 7MgO + 2Cr_7C_3 + 27\ CO_2$$

$$\Delta G = 251\ 006 + 200,5T \text{ cal/mol} \quad \text{-------} \quad (3.3.21)$$

$$Kp3 = \left[\frac{(PCO_2)^{27} . aMgO^7 . aCr_7C_3^2}{(PCO)^{33} \, aMgCr_2O_4^{\,7}}\right]$$

The molar extent for this reaction is defined as e3, with maximum extent ME(3).

Again from an initially defined spinel composition, the relative molar quantities of the various oxides can be calculated and hence the relative quantities of spinel end members defined as shown below.

M(1) = moles $MgAl_2O_4$
M(2) = moles Fe_3O_4
M(3) = moles $FeCr_2O_4$
M(4) = moles $MgCr_2O_4$

---------- (3.3.22)

NN = total number of moles of all end member spinels in that phase.

Accounting for the effect of reactions 3.3.19 through 3.3.21 in terms of the extents of reaction (e(i)), and making the

assumptions regarding the activities of the various species as discussed in section A3.2, the activities of the various species can be described as shown below.

$$a_{Fe_3O_4} = \frac{n1}{d1} = \left[\frac{M(2) - e1}{NN - e1 - 2e2 - 7e3}\right] \quad \text{-------} \quad (3.3.23)$$

$$a_{FeCr_2O_4} = \frac{n2}{d1} = \left[\frac{M(3) - 2e2}{NN - e1 - 2e2 - 7e3}\right] \quad \text{-------} \quad (3.3.24)$$

$$a_{MgCr_2O_4} = \frac{n3}{d1} = \left[\frac{M(4) - 7e3}{NN - e1 - 2e2 - 7e3}\right] \quad \text{-------} \quad (3.3.25)$$

$$a_{Fe} = \frac{n4}{d2} = \left[\frac{3e1 + 2e2}{3e1 + 2e2 + 4/7e2 + 2e3}\right] \quad \text{-------} \quad (3.3.26)$$

$$a_{Cr_7C_3} = \frac{n5}{d2} = \left[\frac{4/7e2 + 2e3}{3e1 + 2e2 + 4/7e2 + 2e3}\right] \quad \text{-------} \quad (3.3.27)$$

(ei being the molar extent of reactions 3.3.19,3.3.20 and 3.3.21 respectively).

Rewriting the equilibrium expressions in equations 3.3.19 through 3.3.21 using the activity relationships defined above, the results can be expressed in terms of logarithmic equations as shown below (for simplicity use is made of the ni/di notation defined above).

From 3.3.19:

$$\ln(Kp1) = 4\ln(PCO_2) - 4\ln(PCO) + 3\ln(n4/d2) - \ln(n1/d1)$$

and putting $cc1 = (-\Delta G/RT - 4\ln(PCO_2) + 4\ln(PCO))$, we get:

$$\ln(n1) = 3\ln(n4) - 3\ln(d2) + \ln(d1) - cc1 \quad \text{--------} \quad (3.3.28)$$

From 3.3.20:

$$\ln(KP2) = 68/7\ln(PCO_2) - 80/7\ln(PCO) + 4/7\ln(n5/d2) + 2\ln(n4/d2) - 2\ln(n2/d1) \quad \text{--- (11)}$$

and putting $cc2 = (34/7\ln(PCO_2) - 40/7\ln(PCO) - 1/2(-\Delta G/RT))$, we get:

$$\ln(n2) = \ln(n4) - 9/7\ln(d2) + \ln(d1) + 2/7\ln(n5) + cc2 \quad \text{---------- (3.3.29)}$$

From 3.3.21:

$$\ln(kp3) = 27\ln(PCO_2) - 33\ln(PCO) + 2\ln(n5/d2) - 7\ln(n3/d1)$$

and putting $cc3 = (1/7(\Delta G/RT) + 27/7\ln(Pco_2) - 33/7\ln(PCO)$, we get:

$$\ln(n3) = 2/7\ln(n5) - 2/7\ln(d2) + \ln(d1) + cc3 \quad \text{------ (3.3.30)}$$

Solutions to these three non linear equations (3.3.28 through 3.3.30) were obtained using an iterative technique to solve for e1,e2 and e3 in turn and repeat the sequence of calculations using the previously estimated ei values until convergence had been achieved in terms of all three ei values.

A standard Newton-Raphson technique was used to solve for e(i) values within the constrained interval $0<ei<ME(i)$.

This method was found to be suitable provided small increments in Pco/Pco_2 ratio were considered, and the previous ei values could be used as the initial point for the iterative solution.

However this technique was still not found to be generally applicable over the whole chromite reduction reaction. Only solutions representing spinel behaviour during the earlier stages, and not during the latter part of the reduction were found to be meaningful and bear close correspondence to experimental values. Thus a third model was investigated specifically for application to the latter stages of the reduction reaction.

In the third model, the assumption is made that the spinel may be considered as an ideal mixture of two sinel components i.e. $FeO(Cr,Al)_2O_3$ and $MgO(Cr,Al)_2O_3$ or $FeO(M_2O_3)$ and $MO(Cr_2O_3)$. The latter part of the reduction reaction can then be described in terms of the three reactions shown below.

$$FeCr_2O_4 = Fe + 1/2\ O_2 + Cr_2O_3$$

$$\Delta G = 65\ 800 - 12,1T \text{ cal/mol} \quad \text{---------- (3.3.31)}$$

$$Kp14 = \left[\frac{(Po_2)^{1/2} \cdot aCr_2O_3 \cdot aFe}{aFeCr_2O_4}\right]$$

The molar extent for this reaction is defined as e1, with maximum extent ME(1).

$$Cr_2O_3 + 6/7C = 2/7\ Cr_7C_3 + 3/2\ O_2$$

$$\Delta G = 255\ 834 - 63,86T \text{ cal/mol} \quad \text{--------- (3.3.32)}$$

$$Kp15 = \left[\frac{(Po_2)^{3/2} \cdot (acr_7C_3)^{2/7}}{acr_2O_3}\right]$$

The molar extent for this reaction is defined as e2, with a maximum extent of ME(2).

$$MgOCr_2O_3 + 6/7\ C = MgO + 2/7\ Cr_7C_3 + 3/2\ O_2$$

$$\Delta G = 266\ 084 - 65,56T \text{ cal/mol} \quad \text{---------- (3.3.33)}$$

$$Kp16 = \left[\frac{(Po_2)^{3/2} \cdot (aCr_7C_3)^{2/7} \cdot aMgO}{aMgOCr_2O_3}\right]$$

The molar extent of this reaction is defined as e3, with a maximum extent of ME(3).

here are three independent equations in three unknowns. It is possible to solve for these unknowns, though the accuracy of the solution will depend on the assumptions and relations used to

define the activity of each species.

From an initially defined spinel composition, the relative molar quantities of various oxides and hence spinel end members can be calculated.

M(1) = moles of MgO

M(2) = moles of Al_2O_3

M(3) = moles of Cr_2O_3 ---------- (3.3.34)

M(4) = moles of FeO

M(5) = moles of Fe_2O_3

NN = total numuber of moles = $\sum_{i=1}^{i=5}(M(i))$

Chromite is then defined in terms of the spinel end members ($CM(1)=FeCr_2O_4$, $CM(2)= MgCr_2O_4$, $CM(3)= MgAl_2O_4$), from most to least stable,

$CM(3)= M(2)$ (all Al_2O_3 associated as $MgAl_2O_4$)

$CM(2)= M(1)-M(2)$ (all MgO not associated with Al_2O_3 will be associated with Cr_2O_3)

$CM(1)= M(3)- (M(1)-M(2))$ (all Cr_2O_3 not associated with Mg will be associated with Fe).

This defines the initial molar quantities present after Fe3+ reduction has taken place. At subsequent stages of reduction the molar quantities of each phase present can be described in terms of the extents of reactions 3.3.31 through 3.3.33 as shown below.

molar quantity of $MgAl_2O_4$ = CM(3) (unchanged)

molar quantity of $MgCr_2O_4$ = CM(2)- e3

molar quantity of $FeCr_2O_4$ = CM(1) - e1

molar quantity of Cr_2O_3 = e1-e2

molar quantity of MgO = e3

molar quantity of Fe = f3 + e1 (where f3 is a factor corresponding to the fraction of iron reduced during the initial stages of the reduction)

molar quantity of Cr_7C_3 = 2/7(e2+ e3)

The activities of the various species may then be defined (using the assummptions discussed in A3.2(a) and (b)) as shown below.

$$aFe = \left[\frac{f3 + e1}{(f3 + E1 + 2/7(e2+e3))}\right] \quad \text{---------- (3.3.37)}$$

$$aCr_7C_3 = \left[\frac{2/7(e2+e3)}{(f3 + e1 + 2/7(e2+e3))}\right] \quad \text{---------- (3.3.38)}$$

$$aFeCr_2O_4 = \left[\frac{(CM(1)-e1)}{(CM(1)+CM(2)+CM(3)-e2)}\right] \quad \text{--------- (3.3.39)}$$

$$aCr_2O_3 = \left[\frac{(e1-e2)}{(CM(1)+CM(2)+CM(3)-e2)}\right] \quad \text{--------- (3.3.40)}$$

$$aMgCr_2O_4 = \left[\frac{(CM(2) - e1)}{(CM(1) + CM(2) + CM(3) - e2)}\right] \quad \text{---- (3.3.41)}$$

The above set of equations can then be written in the form f(e1,e2,e3) = 0 as follows (converting the expressions first to logarithmic terms):

f1(e1,e2,e3)

ln(f3+e1) + ln(e1-e2) + 1/2ln(Po2) - ln(f3-e1+2/7(e2-e3) - ln(CM(1) - e1) ln(Kp17) = 0 ---------- (3.3.42)

f2(e1,e2,e3)

3/2ln(Po2)+ 2/7ln(2/7(e2+e3))+ ln(CM(1)+ CM(2)+CM(3)- e2) - 2/7ln(f3+e1+2/7(e2+e3))- ln(e1-e2)- ln(Kp18) = 0 ---- (3.3.43)

f3(e1,e2,e3):

3/2ln(Po2) + 2/7ln(2/7(e2+e3)) + ln(CM(1) + CM(2)+CM(3)-e2) - 2/7ln(f3+e1+2/7(e2+e3))- ln(CM(2)-e3) - ln(Kp19) --- (3.3.44)

The above equations were solved using a modified, sequential iterative, Newton- Raphson technique with numerical differentiation to solve for e(i) on the constrained interval 0<e(i)<ME(i).

This model was found to be reasonably applicable to the spinel duriing the final stages of reduction.

APPENDIX 4.1 : DETAILS OF THE THERMOBALANCE ASSEMBLY

Details of the thermobalance assembly are shown below in figure A4.1. This apparatus was used for the bulk of the experimental investigation.

FIGURE A4.1

DETAILS OF THE THERMOBALANCE SYSTEM

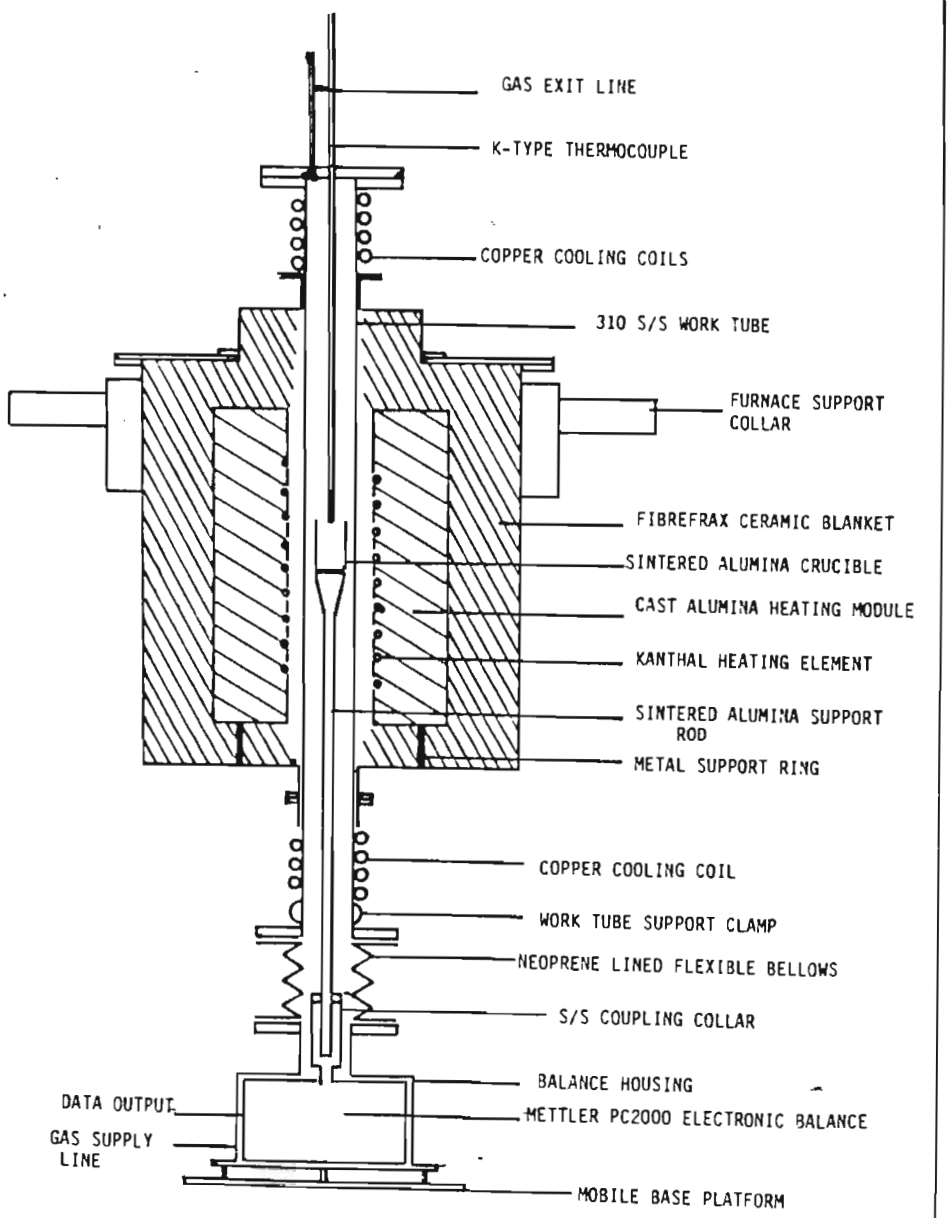

APPENDIX 4.2

COMPUTERISED DATA GATHERING AND MANIPULATION

Continuous monitoring of the reduction reaction was performed using an Apple IIC computer. An outline of the programmes used for data logging and manipulation are given below.

APPENDIX 4.3 DATA PRESENTATION

In order to facilitate the comparison and interpretation of results, the data gathered on disk was retrieved and plotted as indicated (figure A4.3).

The extent of reduction was calculated as the fractional mass loss recorded compared to the maximum theoretical mass loss obtainable at 100% chromium and iron reduction.

The rate of reduction was calculated as either the slope of a line segment passing through the average data points for a short period of time (this tended to give an erratic curve); or as the derivative of a cubic spline fitted to data points covering a short period of time. The latter was found to agree closely with the tangent method but provide a much smoother curve (ref. 44).

APPENDIX 4.4 CONDITIONS USED FOR E.D.S. ANALYSIS

a) Beam current 200pA +/- 10pA.

b) Accelerating voltage = 24,8KV.

c) Effective detection limit at element number 10 (Na).

d) Take- off angle=18.

e) Spot size 2- 3 micron, maximum penetration 5 micron (oxides).

f) Correction routine: standardised ZAF correction, using MAGIC 5 routine with oxidation states of oxides:

Fe=2+; Cr=3+;Mg=2+;Al=3+;Si=4+;Ca=2+

spinel generalised formula used i.e. oxygen/ cation ratio = $4/3$.

FLOW SHEET FOR DATA PLOTTING

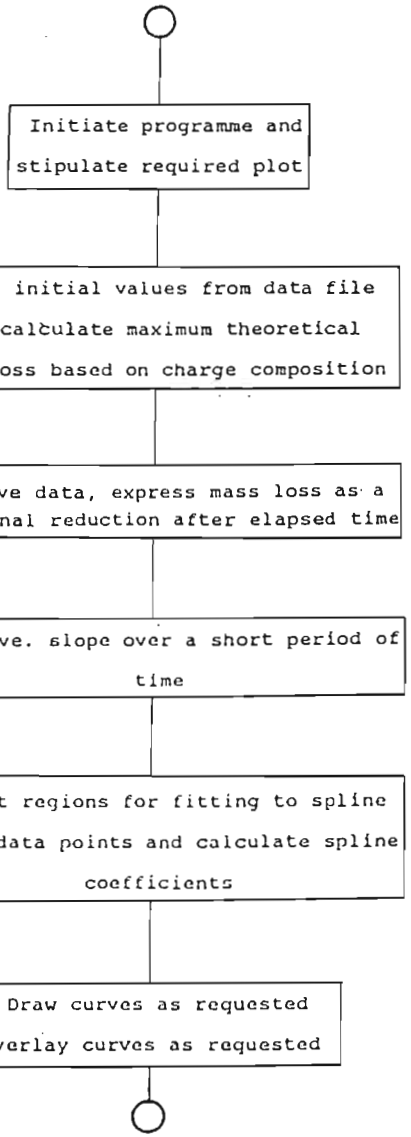

FIGURE A4.3

DATA GATHERING: PROGRAMME STRUCTURE

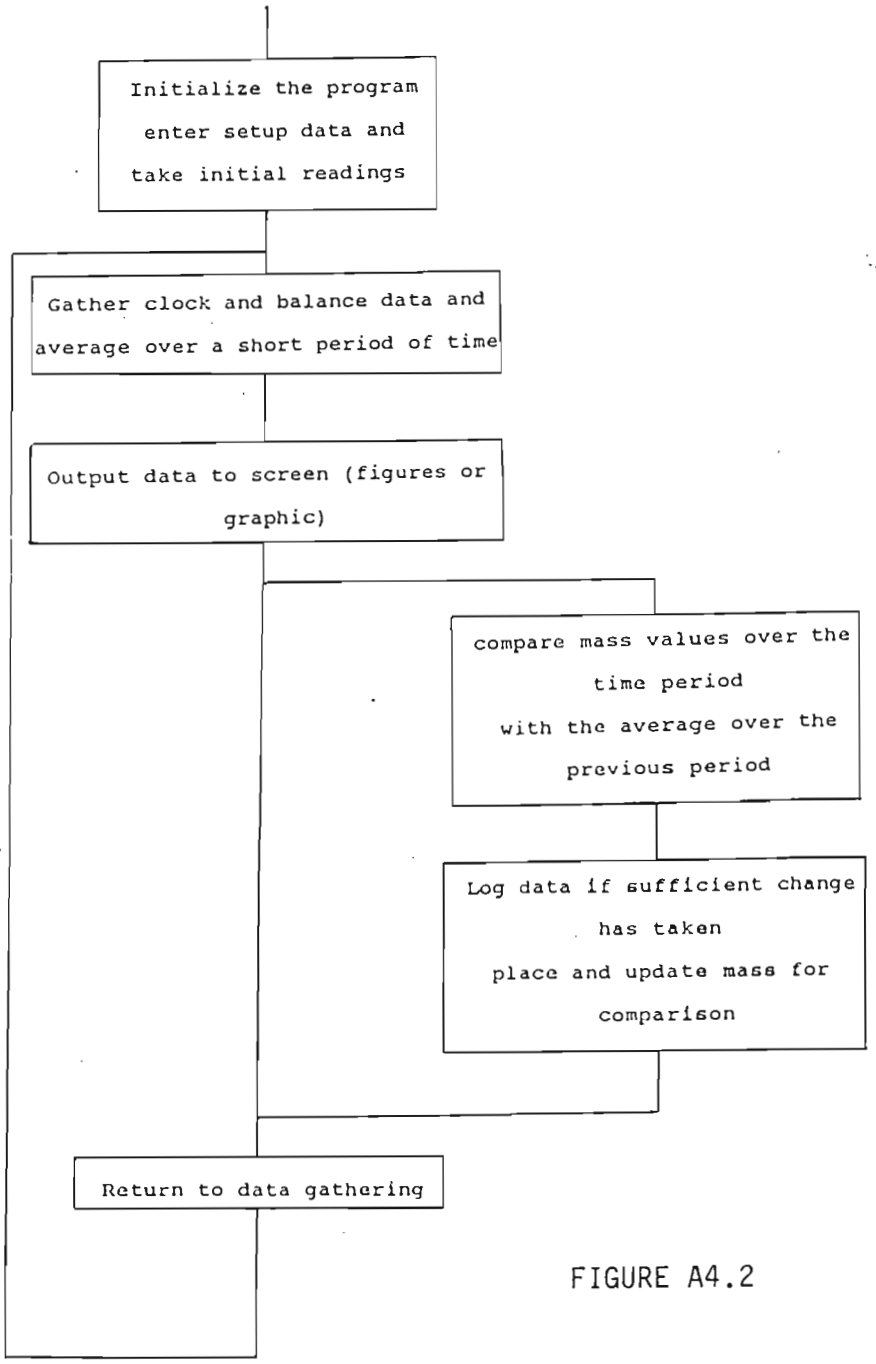

FIGURE A4.2

LG6 chromite: CR8 standard, ex BEESON, U.S.G.S. (similar composition to LG6), and refined samples of LG6 ore grains with detailed wet chemical analysis.

ANALYSIS OF THE REPRODUCIBILITY OF T.G.A. RESULTS.

It must be clearly stated that all results, particularly such as the thermogravimetric results discussed in this work have a small amount of inherent variability (Taylor, 173). This aspect was thus considered in some detail and the following conclusions drawn for this work:

i) Every effort had to be made to ensure the maximum degree of mixing and homogeneity in the sample.

ii) Reduction reactions involving relatively coarse particle sizes (+100 Micron) of both oxide and reductant were found to be inherently variable because of poor mixing properties and hence sample inhomogeneity.

iii) Where very fine reductant (such as lampblack) was used with a varying ore size, and well mixed, relatively good reproducibility was obtained as shown by the narrow spread of results obtained on repeat tests as shown in figure A4.4.

iv) Such reproducibility suggests that meaningful comment can be offered on the effects of parameters such as particle size and temperature.

STATISTICAL ANALYSIS OF SIMILARITY IN T.G.A. RESULTS

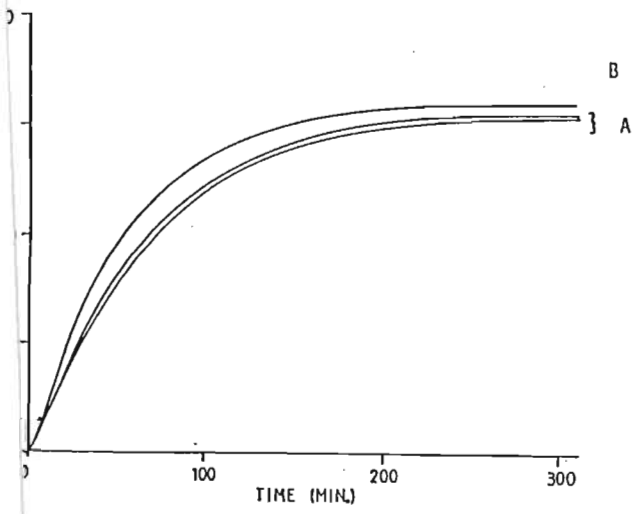

FIGURE A4.4

Statisical analysis of the similarity and difference between T.G.A. reduction curves.

Using a chi-square goodness-of-fit test over 8 to 10 cells over the length of the reduction curve, analysis of the difference between T.G.A. test results was performed. Analysis of the difference in time taken to achieve a specific degree of metallization (based on a normalized starting time) was performed for both identical repeat tests, as well as tests where a specific parameter such as particle size had been varied by the least amount as described in the test work above.

A) Analysis of repeat tests: The spread in time taken to reach various degrees of metallization (sample of 3-5 repeat tests).

$H_0: \mu_D = 0$; $H_1 = \mu_D \neq 0$; level of significance, $= 0{,}01, \nu = 7$

$\chi^2 = 1{,}239$; $X^2 = 0{,}979$ $\therefore$ accept H_0, i.e. curves are the same at the 99% confidence level.

B) Analysis of the effect of particle size, $\bar{d}_{p1} = 30{,}82\mu m$ $\bar{d}_{p2} = 41{,}43\mu m$ taken as the closest set of particle sizes analysed.

$H_0: \mu_D = 0$; $H_1: \mu_D \neq 0$; level of significance $= 0{,}01$; $\nu = 7$

$X^2 = 2{,}17$ $\therefore$ reject H_0, accept H_1 i.e. the curves established experimentally can not be taken as the same (the test was repeated and showed that even at the 95% confidence level, the curves could not be taken as being similar)

Thus it was concluded that the smallest effective change in particle size as examined in chapters 5 and 6, was sufficiently different in terms of resultant reduction curve, from the normal variation obtained in repeat tests, as to make the analysis of the effect of particle size valid.

APPENDIX 5: CONSIDERATION OF THE DIFFUSION OF CATIONIC SPECIES IN THE CHROMITE SPINEL LATTICE.

A5.1 CALCULATION OF THE CHANGES IN TRIVALENT/ DIVALENT CATION BALANCE WITHIN THE SPINEL DURING REDUCTION

As an initial step in investigating the changes taking place within the spinel, consideration was given to the ratio of trivalent to divalent cationic species in the spinel.

Data from the standard iron- chromium metallization curve was used together with the assumption of a static magnesium and aluminium component in the spinel to calculate the composition of the residual spinel. The balance was performed assuming initial reduction and removal of the Fe3+ content of the spinel.

TABLE A5.1 SUMMARY OF THE CATION COMPOSITION OF THE SPINEL

INITIAL COMPOSITION	normalised composition	cation contents (mols)
MgO = 10,10g	10,3	0,255
Al_2O_3 = 14,20g	14,5	0,285
Cr_2O_3 = 46,92g	47,9	0,631
FeO = 18,46g	18,8	0,256
Fe_2O_3 = 8,36g	8,5	0,106
total = 98,04g	100,0	2,09

After 20% reduction, 44,72% of the iron has been removed and 4,4% of the chromium has been removed, thus the residual spinel has the composition:

A5.2 Cation balance in LG6 spinel after 20% reduction has occurred

cation	mols
Mg2+	= 0,255
Al3+	= 0,285
Cr3+	= 0,6032
Fe2+	= 0,2001
Fe3+	= 0,000
Σ3+/Σ2+	= 1,9517

The final results over the reduction are summarised in figure 5.18.

A5.2 DERIVATION OF SPECIFIC DIFFUSION COEFFICIENTS FOR INDIVIDUAL SPECIES IN THE SPINEL WHILE UNDERGOING REDUCTION.

In this work an attempt was made to calculate approximate diffusion coefficients for each of the cation species undergoing reduction during the reduction reaction, thereby gaining insite into the fundamental reaction rate for the process.

Diffusion of ionic species within a solid spinel lattice may be considered as a thermally activated process, with the energy requirement for atoms to pass through the intermediate high energy state experienced between specific lattice sites being equivalent to the activation energy for the jump and hence the diffusion process (ref. 86,88,71,55,7,128,163,202).

The fraction of atoms capable of surmounting this barrier is exponentially related to temperature and the effective diffusion

coefficient for such a process is commonly expressed as:

$$Di = Do.\exp(-DG^*/kT) \text{----------} 5.1.1$$

This expression can be expanded to yield an expression for the diffusion coefficient in terms of more fundamental parameters. From a consideration of statistical mechanics, an expression of the form:

$$Di = \nu_v \lambda^2.\exp(DS/k) \text{ ----------} 5.1.2$$

Where the exponential term refers to the entropy associated with vacancy formation (ref Kingery et al. 88; Hannay, 71 and Schmalzried, 171 , Verhoven,188; Laidler, 100).

With a knowledge of specific site reactions within the lattice, this expression can be rearranged to include the vacancy concentration of a specific defect type as:

$$Di = \nu_v \lambda^2.(Vi).\exp(-DG^*/kT) \text{ -------} 5.1.3$$

(after Eyring , 55; Hannay, 71 and Schmalzried 171).

The application of such an expression in the determination of individual diffusion coefficients for the chromium and iron species leaves many unknowns. However certain simplifying assumptions may be made in the case under consideration: (ref 101,62,201 152,26,52,69)

(i) Although a composite of Chromium, Iron, Aluminium and Magnesium, it is assumed that only the chromium and iron content of the spinel are significantly affected during the reduction reaction. Accordingly the changes taking place during the reduction are based on consideration of a simple pseudoternary compound AB2O4, with the the nonreducing cations simply acting as inert species merely reducing the activity of the chromium and iron component in an ideal way.

(ii) In the pseudoternary compound postulated, the thermodynamic state is assumed to be specified by four independent variables choosen as P,T, pO_2 and the activity of one of the iron or chromium species.

(iii) The above parameters (P,T,pO_2 and ai) are taken as

defining a configaration space. In this case consisting of 3 regions, each of which has a specific, dominant, defect pair, on which any diffusion process relying on the density and mobility of these defects is dependent.

(iv) Having P and T fixed for a particular reaction, the thermodynamic analysis performed earlier provides an indication of the relationship between pO2 and ai, and what remains is to define a set of dominant or majority defect pairs over each region of the configuration space.

(v) In defining a set of majority defects it was assumed that interstitial location of cationic species was relatively unlikely because of the close-packed structure of the chromite spinel and the size of the cations relative to the interstitial volume available (ref. 113,119,57,4).

(vi) The strong temperature dependence of defects (judging from their high thermal activation (Sangster, 163), suggests that only two terms corresponding to majority defects of opposite charge need be considered (ref. 4).

(vii) In any one region of the configuration space, only one pair of majority defects need be considered (as discussed by Abeland et al., 1).

Based on theses assumptions, a simple reaction scheme was proposed as in the thermodynamic analysis, an a set of reactions formulated relating the concentration of an assumed majority defect with corresponding material, charge and site balances.

The equilibrium expression from each of these reactions can the be rewritten to give an explicit relationship between the thermodynamic parameters defining the area of the configuration space and the diffusion coefficient for that particular species.

The following reactions were formulated (using Kroger- Vink notation):

(i) for the Fe3+ species:

$$Feb + Fea + Oo = Fea + Fe + 1/2\ O_2 + Vo + Vb$$

--------5.1.3

(this includes the intermediate jump from octahedral to tetrahedral lattice site as proposed by Sun, 167).

Assuming (Fea) ~(Vb)~(Vo)

$$Ke1 = \frac{[(Vb)^3 . aFe . pO_2]}{[a1 . a2]} \qquad \text{---------- 5.1.5}$$

(ii) For the Fe2+ species:

$$Fea + Oo = Fe + 1/2O_2 + Va + Vo \text{ ------ 5.1.6}$$

$$Ke2 = \frac{[Po_2^{1/2} . a4 . (Va)^2]}{[a2]} \qquad \text{---------- 5.1.7}$$

(iii) Two separate reactions may be formulated for the chromium species; firstly if a relatively high vacancy concentration is assumed on octahedral lattice sites stemming from the removal of the trivalent iron speciecs. Such a reaction might take the form:

$$Crb + 3/2Oo + Feb + Va = Cr + 3/4O_2 + 2Vb + 3/2\ Vo + Fea$$

---5.1.7

Alternatively, if a net reduction in number of vacant sites occurs through rearrangement of atoms within the lattice, equivalent to a healing out of defects, the smaller concentration of defects on octahedral lattice sites might lead to a reaction of the form:

$$Crb + 3/2Oo = Cr + 3/4O_2 + Vb + 3/2Vo \text{ ---- 5.1.8}$$

The equilibrium expressions from equations 5.1.5 trough 5.1.8 can then be rewritten to give an explicit expression for the assumed majority defect type in each part of the configuration space.

Assuming in the case of Fe3+ diffusion that (Fea) = (Vb) = (Vo) from 5.1.5:

$$(Vb) = \frac{\left[Ke1/3 pO2^{-1/6}.(a1.a2)^{1/3}\right]}{\left[(a4)\right]} \quad \text{---------- 5.1.9}$$

Similarly in the case of Fe2+ diffusion, assuming that (Va) = (Vo), then from 5.1.6

$$(Va) = Ke1/2.pO2^{-1/4}(a2/a4)^{1/2} \quad \text{---------- 5.1.10}$$

(ref. 74,75,104)

In the case of Cr3+ diffusion, assuming (Vo) = 3/4(Vb) and (Fea) = (Va), from 5.1.7:

$$(Vb) = \frac{\left[1.0563.Ke2/7.pO2^{-6/28}.(a2.a1)^{2/7}\right]}{\left[(a5)\right]} \quad \text{------ 5.1.11}$$

During the latter stages of the reaction, assuming (Vb) = 2/3(Vo)

$$(Vb) = (.782)Ke2/5.pO2^{-3/10}.(a3/a5)^{2/5} \quad \text{------ 5.1.12}$$

Interpollating from the data of Sangster, Stoneham 163;(and 83,127a,b 128,129,50,194) estimates of Ke can be made and the following values were assumed:

DG1 = 427521,3 - 167,21T Cal/mol

DG2 = 551643.1 - 187,85T Cal/mol

DG3 = 553474,3 - 161,47T Cal/mol

DG4 = 623589,0 - 181,00T Cal/mol ---------- 5.1.13

Using the values in the above expressions, a generalized set of equations was formulated describing diffusion coefficients for each species as a function of the parameters that define the configuration space during that part of the reduction reaction, as:

D1 = 4.153.10-8.pO2-1/6(a1.a2/a4)1/3.exp(20112 - 51421.8/T)

D2 = 4.153.10-8.pO2-1/4.(a2/a4)1/2exp(22.59 - 66351/T)

D3 = 6.44.10-10.pO2-3/8(a5)-1/2exp(19.42 - 66571/T)

D4 = 5.21.10-8.pO2-0.3(a3/.54.a5)0.4exp(21.77 - 75005/T)

-------- 5.1.14

These equations indicate that substantial changes in the actual diffusion coefficient must be expected over the duration of the

reduction reaction as shown in figure A5.1.

Though this is a very crude approach, and hardly accurate, two aspects are evident from the results. Firstly the diffusion coefficient of the Cr3+ species is expected to drop significantly during the final stages of reduction- possibly by several orders of magnitude. It is thus possible that a well reacted surface layer on the chromite particle would effectively inhibit further reaction.

Secondly, though only very approximate, some indication has been gained of the range of effective diffusion coefficients that might be expected for the different species during the reaction.

APPENDIX 5.3 CONSIDERATION OF THE CHANGES IN UNIT CELL DIMENTION OF THE SPINEL

Use was made of the X.R.D. trace to determine the unit cell dimension of the residual chromite spinel after acid leaching. The method used is briefly shown below.

A5.3 The determination of unit cell dimentions from X-Ray diffraction measurements :

(ref. 114, 164, 140).

1) Bragg law used to establish the value of d :

$$n\lambda = 2d \sin\theta \qquad 5.1.15$$

n = order of diffraction, an integer taken as unity in this case.

$$\text{from (1)} \quad d = \frac{\lambda}{2 \sin\theta} \qquad 5.1.16$$

For work with chromite ores, using Cu lamp; with $\lambda\, CuK_{\alpha} = 1{,}5418$ Å

for the particular radiation we are interested in

$$d = \frac{0{,}7709}{\sin\theta}$$

FIGURE A 5.1(a)

Calculated variation in the diffusion coefficients of the chromium and iron species in LG-6 chromite during the reduction reaction at 1200°C.

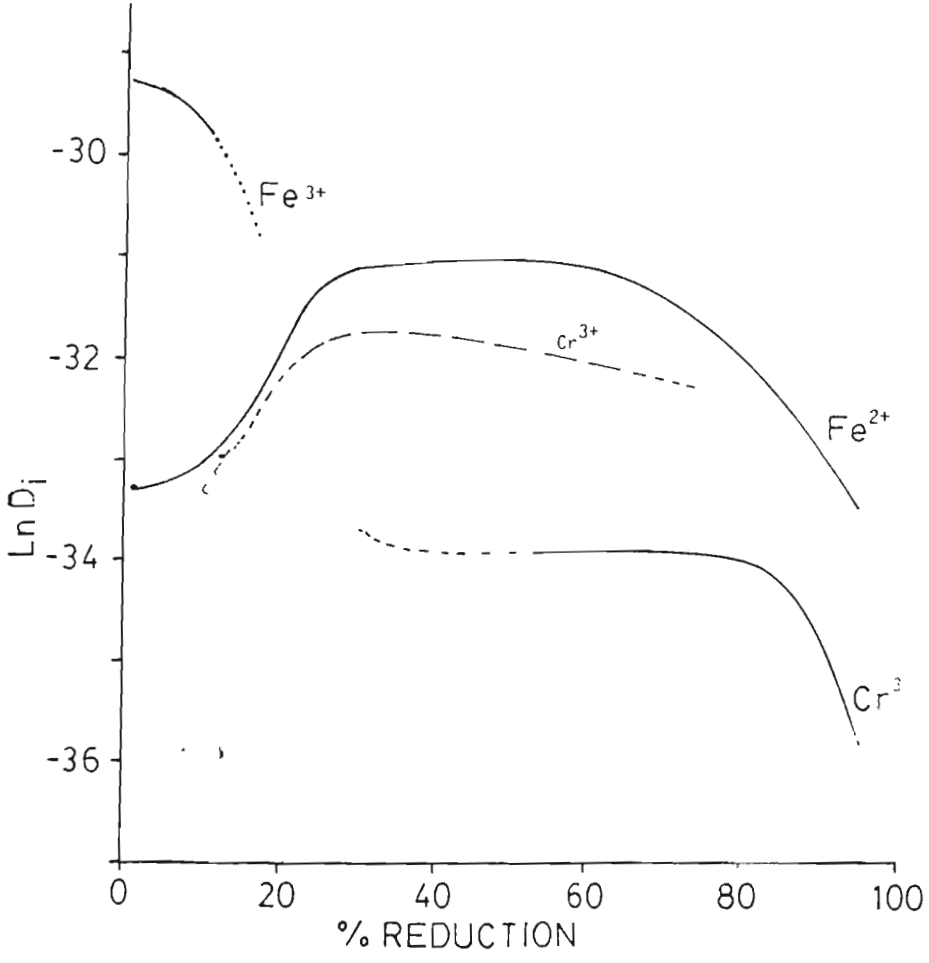

FIGURE A 5.1(b)

Calculated variation in the diffusion coefficients for the iron and chromium species in LG-6 chromite during reduction at 1300°C.

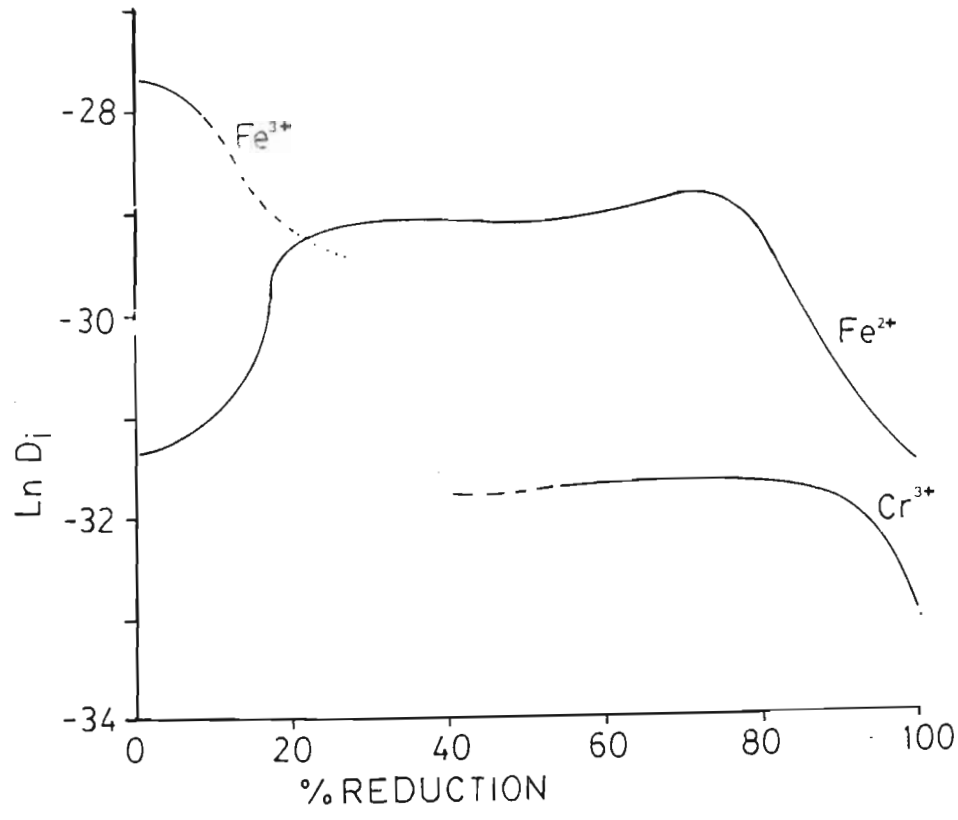

2) It has been established that for each crystal system there is a relationship between the spacing d, the Miller indices of the scattering planes and the size and shape of the unit cell, i.e.

$$1/d^2 = f(h, k, l, a, b, c, \alpha, \beta, \gamma)$$

For the cubic spinel system :

$$\frac{1}{d^2} = \frac{h^2 + k^2 + l^2}{a^2}$$

$$\lambda = 2d \sin\theta$$

$$\lambda^2 = 4d^2 \sin^2\theta$$

$$d = \sqrt{\frac{\lambda^2}{4 \sin^2\theta}} \qquad \text{5.1.17}$$

$$\sin^2\theta = \frac{2(h^2 + k^2 + l^2)}{4a^2}$$

equation of the form :

$$\sin^2\theta = A.\ (h^2 + k^2 + l^2) \qquad \text{5.1.18}$$

Where $A = \frac{\lambda^2}{4a^2}$ and let $(h^2 + k^2 + l^2) = N.$ 5.1.19

$$\sin^2\theta = A.N$$

plotting $\sin^2\theta$ vs. N gives a straight line, with slope

$$A = \frac{\sin^2\theta}{N}$$

$$\frac{\lambda^2}{4a^2} = A \qquad a = \frac{\lambda}{2\sqrt{A}} \qquad \text{5.1.20}$$

Having established a means of determining approximate cell dimension from the X.R.D. trace a means was sought to estimate cell dimension from the composition of the spinel (i.e. as a function of trivalent and divalent ionic radii).

Using the ionic radii listed (table A5.3) and the known cell dimensions for pure spinel end members (table A5.4), a formula was derived giving spinel unit cell dimension as a function of reaction extent as:

$$a0 = 6,765 + 0,45r^{2} + 2,03r^{3} \quad \text{------ a5.1.21}$$

where a0 is unit cell dimesion in angstrom units, and r2+ and r3+ the weighted average of divalent and trivalent cationic radii that constitute the spinel.

This formula fits the measured data well as shown in table A5.4 , and provides a means of predicting unit cell dimension as a function of reaction extent.

Considering the compositional changes taking place during the reduction reaction, the accompanying change in unit cell dimension can be calculated using the data from the iron-chromium metallization curve to establish the composition of the residual spinel and hence unit cell dimension.

This was performed using data from figure 5.13 and the results found to agree very well with unit cell dimensions measured on samples at various stages of reduction (figure A5.2).

This result further confirms the reaction path suggested by the metallization curve, and the shape of the curve in figure A5.2 suggests that radical structural change occurs in the spinel only near the end on the reduction, when a noticeable decrease in unit cell size is noted. Such change might be expected to infer increased diffusional resistance, and the possible development of a diffusion barrier, and hence kinetic limit.

FIGURE A 5.1

Measured and predicted change in spinel unit cell dimension as a fuction of reaction extent.

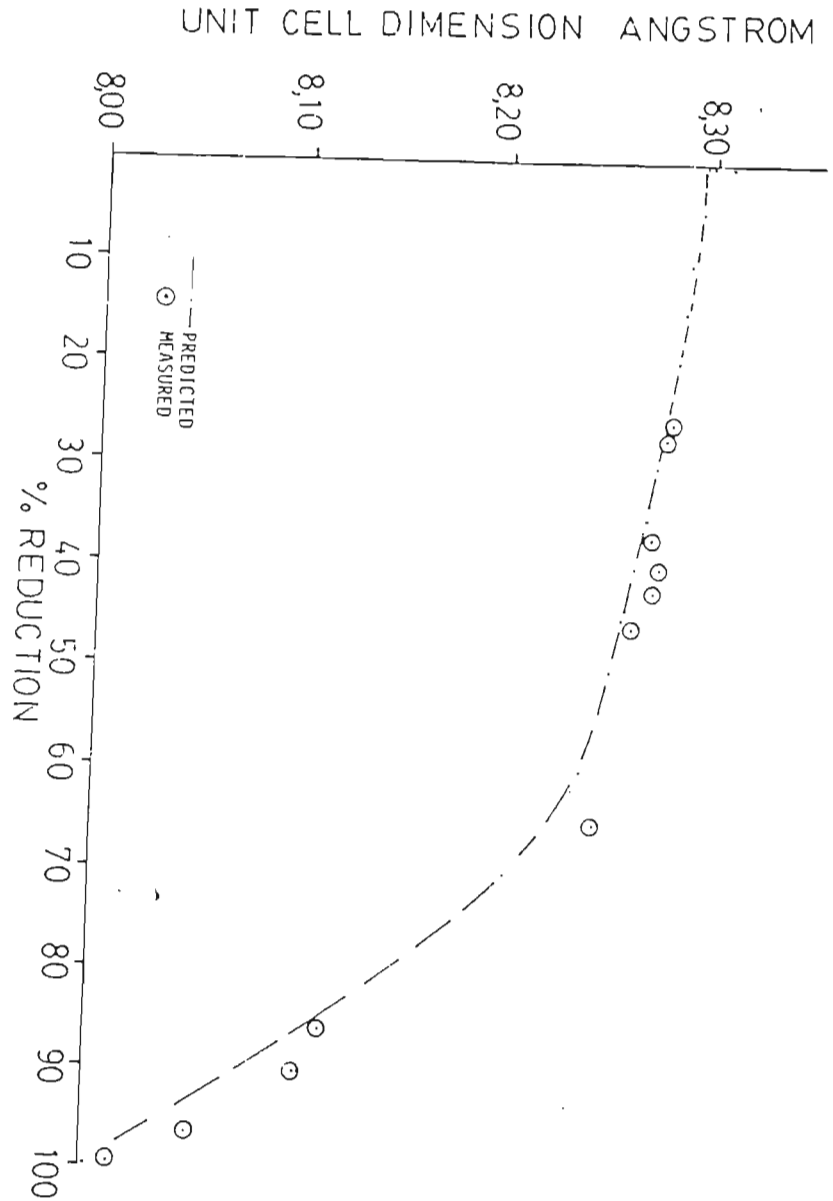

TABLE A 5.4

SPINEL END MEMBER UNIT CELL DIMENTIONS

Spinel type	Measured A	Ref.	Mikeev pred. A	Predicted A
$FeOCr_2O_3$	8,378	DHZ	8,23	
	8,36	PDF		8,360
$MgOCr_2O_3$	8,334	DHZ	8,150	8,334
	8,333	PDF		
$Mg\ Al_2O_4$	8,075	DHZ	7,82	
	8,0831	PDF		8,0831

PDF = powder diffraction files, DHZ= ref 41

TABLE A 5.3

Species	r/Å	Ref.
Cr^{3+}	0,63	CRC
Al^{3+}	0,51	CRC
Fe^{3+}	0,64	CRC
Fe^{2+}	0,74	CRC
O^{2-}	1,32	CRC
Cr^{2+}	0,89	CRC

CRC= ref 38

APPENDIX 6

A6.1 DERIVATION OF A SHRINKING CORE MODEL FOR THE REDUCTION OF CHROMITE

Using as a basis, the Shrinking core model, with diffusion through the ash layer as rate controlling (ref. 73,123, 206, 103).

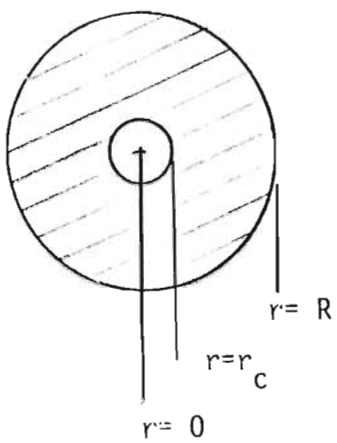

If QA = flux of A through the surface of any radius; with the nomenclature :

outwards is positive

inwards is negative

Considering the outward migration of some species A, initially unif. distance

At steady state : $\frac{-dNA}{dt} = 4\pi\ ^2 QA \qquad 4\pi R^2\ Q_{AS} = 4\pi r_c^2\ Q_{AC}$ ..... (1)

Let the flux of A within the 'ash' be expressed by Ficks' law :

$$Q_A = -Da \frac{dC_A}{dr} \quad .... \quad (2)$$ note Q_A and dC_A/dr are of opposite sign

combining these we have :

$$-\frac{dNA}{dt} = -4\pi\ r^2 Da \frac{dC_A}{dr} = \text{constant at steady state.} \quad ..... \quad (2)$$

Integrating across the ash layer from R to rc

$$-\frac{dNA}{dt} \int_R^{r_c} \frac{dr}{r^2} = 4\pi\ Da \int_{C_{AS=o}}^{C_{AC}=C_{Fe}} dC_A$$

$$- \frac{dNA}{dt}\left[\frac{1}{r_c} - \frac{1}{R}\right] = 4\pi\ Da\ .\ C_{Fe} \quad \ldots\ldots\ (3)$$

net ρ_A molar density of A in the solid and V = volume of the particle

$$N_A = \rho_A V \qquad dNA = \rho_A dV$$

$$= \rho_A \cdot \frac{4}{3}\pi(dr_c^3)$$

$$= \rho_A . 4\pi\ r_c^2 . dr_c \quad \ldots\ldots\ (4)$$

which in (3) gives :

$$- \rho_A\ 4\pi \frac{r_c^2}{dt} \cdot \left[\frac{1}{r_c} - \frac{1}{R}\right] dr_c = 4\pi . DaC_A \quad \ldots\ldots\ (5)$$

Separating variables and integrating :

$$- \rho_A \int_R^{r_c} \left(r_c - \frac{r_c^2}{R} \right) dr_c = DaC_A \int_{t=o}^{t} dt \quad \ldots\ldots\ (6)$$

$$- \frac{\rho_A}{6} \left[3\ r_c - 2\ \frac{r_c^3}{R} \right]_R^{r_c} = DaC_A . t$$

$$- \frac{\rho_A}{6} \left[3\ r_c^2 - 3R^2 - 2\ \frac{r_c^3}{R} + 2\ R^2 \right] = DaC_A . t$$

$$\frac{R^2 \rho_A}{6} \left[1 - 3\left(\frac{r_c}{R}\right)^2 + 2\left(\frac{r_c}{R}\right)^3 \right] = DaC_A . t$$

$$t = \frac{\rho_A R^2}{6\,Da C_A}\left[1 - 3\left(\frac{r_c}{R}\right)^2 + 2\left(\frac{r_c}{R}\right)^3\right] \quad \ldots\ldots (7)$$

But: ρ_A = moles A / unit volome.

C = moles A / unit volume.

Thus we have

$$t = \frac{R^2}{6\,Da}\left[1 - 3\left(\frac{r_c}{R}\right)^2 + 2\left(\frac{r_c}{R}\right)^3\right] \quad \ldots\ldots (8)$$

let $\tau = \frac{R^2}{6Da}$

$t_{complete} = \tau\,[1]$

$(r_c = 0)$

then $\tau = t_{complete}$

$$\frac{t}{\tau} = 1 - 3\left(\frac{r_c}{R}\right)^2 + 2\left(\frac{r_c}{R}\right)^3 \quad \ldots\ldots (9)$$

However (rc/R) may be expressed in terms of the remaining fraction of component i (xi) as

$(rc/R) = (1-xi)1/3$

thus equation 6.1.9 may be expressed as

$t/\tau = (1 - 3(1-xi)^{2/3} + 2(1-xi))$ ---- (6.1.10)

Alternatively the extent of metallization of species i can be solved for after a certain time interval (t) as the solution xi to: $f(x_i) = 0$

$f(x_i) = \tau - 3(1-xi)^{2/3}\,\tau + 2(1-xi)\tau - t$ --------- (6.1.11)

The value of T being established either from experimental ....

A6.2 ESTABLISHING VALUES OF T FROM EXPERIMENTAL RESULTS

In order to establish τ, a set of reduction results is required over a range of particle sizes. Since $\tau = R^2/6D$; a linear relationship is expected between τ and R^2, with a slope of $1/6D$.

In order to establish τ, the following assumptions are made:

i) Reduction and removal of Fe3+ takes place before any significant reduction of Fe2+.

ii) Each species has its own distinct diffusion characteristic and hence diffusion coefficient.

Taking as example the data of Searle and Finn (93), from the metallization curve Fe3+ reduction is approximately complete at an extent of 15% reduction, thus t15 can be taken as T1.

Because of the limited reaction extent achieved the approximate time for completion of the reduction reaction for Fe2+ and Cr3+can only be approximated.

Fe2+ is approximately 75% reduced at 55% net reduction, and Cr3+ approximately 55% reduced by 75% net reduction. This does introduce considerable error into the calculation, and must be bourne in mind when evaluating the accuracy of the model.

Taking the time required to reach each of the prescribed degrees of reduction as defined above, acroos a particle size range will give the relationship between τ and R.

From Searle and Finn (93), the following information was obtained at 1300°C:

TABLE A6.1 Estimatedreaction times for Fe3+, Fe2+ and Cr3+ cations at 1300°C

dp (micron)	dp^2 ($m^2 * 10^{-10}$)	τ_1 (sec)	τ_2 (sec)	τ_3 (sec)
17	2,89	289	1061	7103
30,8	9,49	323	1259	8619

		τ_1	τ_2	τ_3
41,4	17,10	364	1385	10429
48,8	23,8	394	1779	14054
63	39,7	606	2725	
82	67,6	660	2725	
98,7	97,4	849		

Using linear regression the straight line coefficients are:

Fe3+: a= 277, b= $5,99.10^{10}$ $D_1 = 6,69.10^{-13}$ m^2s^{-1} (r= 0,96)

Fe2+: a= 929, b= $3,68.10^{11}$ $D_2 = 1,13.10^{-13}$ m^2s^{-1} (r= 0,96)

Cr3+: a= 5800, b= $3,22.10^{12}$ $D_3 = 1,3.10^{-14}$ m^2s^{-1}

(The linear nature of these relationships is shown in figure 5.20)

The diffusion coefficients obtained can then be used to calculate x_i for any specified particle size by solving equation 5.1.

Further analysis of the additional delay time or C_i requires a large amount of very accurate data. If for example, this delay is attributed to a film mass transfer limitation, C_i would be expected to some relationship to particle size. No such relationship was found. Accordingly the value of τ_i obtained from equation 5.2 was used directly in equation 5.1.

Where data was available over a wider range of particle sizes (such as Seale and Finn) a slightly modified formulation:

$t/\tau_T = (1-3(1-x)^{2/3} + 2(1-x)).\tau_p/\tau_T + x(\tau_f/\tau_T)$

was found to give slightly improved results where $\tau_f = C_i/(Dp\ ave.)$.

This indicates that a film limitation is operative, however in the case of Searle and Finn, analysis of this film limitation is clouded by the fact that larger carbon particles were used with larger chromite particles, thus introducing the carbon proximity

problem. In contrast a large reduction in C_i value was experienced in tests with massive addition of ultra fine carbon.

However these results are not sufficiently conclusive to define the nature of C_i.

A6.4 ANALYSIS OF REACTION KINETICS IN THE PRESENCE OF A FLUX PHASE

As discussed in chapter 6 a similar approach was used in establishing values of D_i and C_i from experimental results with flux to that described above without flux.

The most significant aspect appart from the increase in D_i values was the noticeable drop in C_i value caused by flux addition.

In general a C_i value of 100- 300 seconds was found to be standard for all three species. This remarkable reduction in C_i value lend further support to the conclusion that C_i is principally associated with a form of film limitation. This limitation is obviously removed by the fluxing action.